

Nottingham Geospatial Institute

ROBUST COOPERATIVE POSITIONING USING DGPS AND UWB FOR V2X APPLICATIONS

By

YANG GAO

B.Sc., M.Sc.

Thesis submitted to the University of Nottingham for the degree of Doctor of Philosophy

May 2017

Abstract

Road transportation injuries, environmental pollution, and traffic congestion have resulted in a considerable cost to society annually. They have led to an increasing demand for a new generation of Intelligent Transportation Systems (ITS) road applications, which promise to tackle these widespread issues. A common element of such applications is the positioning system, and its performance has been highlighted as one of the key enablers. With the rapid expansion of Global Navigation Satellite Systems (GNSS), satellite-based positioning and navigation will continue to be the predominant positioning solution for most of ITS road applications. GNSS positioning systems offer global coverage, they are primarily free of charge, operate in all weather conditions, and are available all day, every day. However, there are challenges for GNSS-based positioning for ITS applications; in particular, the limited availability and degraded performance of GNSS signals in urban canyons. These challenges could impede the adoption of ITS applications, such as collision avoidance systems, lane departure warning systems, connected and autonomous vehicles. There is a gap between the positioning performance of GNSS-based systems and the positioning performance demanded by ITS applications.

To bridge this gap, this research considers multi-sensor integration and cooperative positioning based on vehicle-to-vehicle, vehicle-to-infrastructure, and vehicle-to-pedestrian communications (collectively known as V2X communication). In comparison to other radio frequency augmentation techniques, Ultra-Wideband (UWB) is of particular interest for multi-sensor integration due to its fine time resolution and robust performance in high signal multipath environments. In addition to this benefit, Dedicated Short Range Communication (DSRC), as a key enabling communication component in V2X communication, not only allows vehicles to exchange their position information but also to share traffic safety-related information such as real-time congestion, accident and incident details, and variable speed limits. By taking

advantage of DSRC, a vehicle in a GNSS hostile environment can calculate its position based on data shared from surrounding road users.

This thesis utilises Global Positioning System (GPS) as a representative of GNSS and proposes to augment Differential GPS (DGPS) with UWB ranging observations attained from surrounding vehicles and infrastructure. It is accomplished by tightly integrating double-difference (DD) code pseudo-range GPS observations and UWB ranging observations using a Robust Kalman Filter. The performance of the proposed Robust Cooperative Positioning (RCP) method is evaluated using real and simulated GPS code pseudo-range and UWB ranging observations supported by assumed DSRC transmission.

This thesis carries out a thorough assessment of the ranging performance, error sources and positioning performance of the Thales UWB Lock-on Model LD2. The assessment is completed by conducting a series of tests in different static and dynamic situations.

In addition to this in-field assessment of the UWB device, the positioning performance of the proposed RCP method is demonstrated in both favourable and hostile GPS environments. The proposed RCP method effectively eliminates the impact of observed outliers, and the integrated RCP solution outperforms the DGPS-only solution, especially when the GPS signal is partially or fully obstructed.

The results based on simulated UWB ranging observations and real GPS code pseudo-range observations on the roof of the Nottingham Geospatial Building achieve sub-metre three-dimensional accuracies when three DD code pseudo-ranges and four UWB ranging observations are available.

Acknowledgements

I would like to express my greatest gratitude to my supervisors, Dr Xiaolin Meng and Dr Craig, M. Hancock, for their guidance and support during my research study to make this work possible. I would like to thank Prof Terry Moore for his valuable advice on my annual assessments.

The partially financial support from the Sino-UK Geospatial Engineering Centre, the University of Nottingham is acknowledged.

I would like to thank Dr Lukasz Bonenberg and Mr Sean Ince for their technical support for data collection of practical experiments. The thanks also go to visiting scholars, Prof Jian Wang, Dr Qiuzhao Zhang, Dr Guoliang Chen, Dr Zhiqin Zhu, Mr Denghui Wang and Mr Qusen Chen, for their knowledge sharing.

My friends here, Ms Jessica Shi, Dr Scott Stephenson, Dr Hao Jing, Ms Jialin Xiao, Mr Penghe Zhang, Mr Asyran Muhammad Che Amat, Mr George Filip, Mr Hasan Jaafar, and all members of the Nottingham Geospatial Institute, are thanked for their discussion and help, and for making the life here joyful during my last year of study.

Most importantly, this work is dedicated to my father, Xirui Gao, without his encouragement and financial support, I could not have the opportunity to go this far from my hometown to the big world; to my beloved mother, Yiwei Zhou, for her love and effort for supporting the family; and my wife, Xuan Pu, for her selfless love, support and comforting when I am facing difficulty during study.

I dedicate this work to my grandmother, Rurong Zhai, who raised me up and passed away during my PhD study and I will miss her forever.

Contents

Abstract ..... **i**

Acknowledgements ..... **iii**

Contents ..... **iv**

List of Figures ..... **viii**

List of Tables ..... **xii**

List of Abbreviations ..... **xiv**

Chapter 1 Introduction **1**

1.1 Overview 1

1.1.1 The Role of Positioning Technologies in Intelligent Transportation Systems 1

1.1.2 Cooperative Positioning Based on Multi-sensor Integration 5

1.2 Problem Statements 9

1.3 Aims and Objectives 9

1.4 Contributions 11

1.5 Thesis Outline 12

Chapter 2 Emerging ITS Applications **14**

2.1 Overview 14

2.2 Intelligent Transportation Systems 14

2.2.1 Definition and History of ITS 14

2.2.2 Benefits of ITS 15

2.3 Connected and Autonomous Vehicles 24

2.3.1 Autonomous Vehicles 26

2.3.2 Connected Vehicles 39

2.4 Required Positioning Performance 51

2.4.1 Performance Evaluation Metrics 51

2.4.2 Required Positioning Performance for the V2X Applications 53

2.5 Summary 55

Chapter 3 Positioning Technologies Supporting to the V2X Applications 57

3.1 Overview 57

3.2 Positioning Techniques for Multi-sensor Integration 57

3.3 Global Navigation Satellite Systems (GNSS) 60

3.3.1 The Expanding GNSS Landscape 60

3.3.2 Reference System 66

3.3.3 Observations and Performance 68

3.4 UWB Positioning System 75

3.4.1 An Overview of UWB 75

3.4.2 UWB Positioning System Based on Different Positioning Techniques 80

3.5 Summary 85

Chapter 4 Robust Cooperative Positioning in the V2X Environment ... 86

4.1 Overview 86

4.2 Position Estimation 86

4.2.1 Least Squares Estimation (LSE) 87

4.2.2 Kalman Filter (KF) 90

4.2.3 Extended Kalman Filter (EKF) 94

4.2.4 Robust Kalman Filter (RKF) 96

4.3 Multi-sensor Cooperative Positioning 99

4.3.1 Multi-sensor Integration 100

4.3.2 Tightly Integrated GPS/UWB Cooperative Positioning Supported by V2X Communication 102

4.3.3 Robust Cooperative Positioning 105

4.4 Summary 116

Chapter 5 UWB Ranging Assessment 117

5.1 Overview 117
5.2 The Thales UWB System 117
5.3 Ranging Data Collection and Analysis 120
5.3.1 Indoor Static Test 121
5.3.2 Outdoor Dynamic Test 124
5.3.3 Locomotive Test 128
5.4 UWB Positioning Assessment 146
5.4.1 Indoor Static Positioning 146
5.4.2 Outdoor Static Positioning Based on Dynamic Ranging Observations 151
5.4.3 Kinematic Positioning Based on Dynamic Ranging Observations 156
5.5 Summary 164
Chapter 6 Robust Cooperative Positioning with DD Code Pseudo-range and UWB Ranging Integration Supported by V2X Communication 166
6.1 Overview 166
6.2 Robust Cooperative Positioning Based on DGPS/UWB Integration 166
6.2.1 Data Collection of the Roof Trial 166
6.2.2 UWB Ranging Observations Assessment of the Roof Trial 169
6.2.3 Positioning Performance Evaluation of the Roof Trial Applied the RCP Method 172
6.3 Positioning Performance Assessment Using Simulated UWB Ranging Observations 181
6.3.1 The Robustness Assessment of the Proposed RCP Method (Scenario 1) 183
6.3.2 The Urban Canyon Scenario (Scenario 2) 185
6.3.3 The Approaching Tunnel Scenario (Scenario 3) 187
6.3.4 Mobile Reference Station (Scenario 4) 189

6.4 Summary 191

Chapter 7 Conclusions and Recommendations 192

7.1 Conclusions 192

7.2 Recommendations and Future Work 196

References 198

List of Figures

Fig.1.1 Real-Time Bus Arrival Service (left) and Smart Motorway (right).. 3
Fig.1.2 An Illustration of the Connected Vehicles 5
Fig.2.1 Fatalities in Reported Road Accidents: GB, 2005-2015 16
Fig.2.2 Fatality Composition Caused by Vehicle Occupants in the U.S..... 17
Fig.2.3 Vehicle Miles Travelled in U.K. Since 1949 21
Fig.2.4 Average Statistics of Emission Levels by the Member States 23
Fig.2.5 Google's Lexus RX Self-driving Vehicle 30
Fig.2.6 Visual Representation of V2X Technology 41
Fig.2.7 Estimated Market for CV Technology, 2016-2021 44
Fig.2.8 The Pyramid of Performance Metrics 51
Fig.3.1 UWB Emission Mask as Defined by FCC 77
Fig.3.2 UWB Emission Mask as Defined by ECC 78
Fig.3.3 RSS Positioning Technique 81
Fig.3.4 AOA Positioning Technique 82
Fig.3.5 TOA Positioning Technique 83
Fig.3.6 TDOA Positioning Technique 85
Fig.4.1 Procedure of the Kalman Filter Algorithm 94
Fig.4.2 Procedure of the Extended Kalman Filter Algorithm 96
Fig.4.3 The Schematic of GPS/UWB Cooperative Positioning Method Supported by V2X 104
Fig.4.4 Data Flow Chart for Robust Cooperative Positioning (RCP) Method 113
Fig.5.1 Thales Lock-on Model LD2 UWB Unit 118
Fig.5.2 Thales TDOA Positioning 119
Fig.5.3 The Accuracy of the Laptop System Time 120
Fig.5.4 UWB System Setup in Static Test 121
Fig.5.5 UWB Ranging Sampling Rate in Static Test 122
Fig.5.6 UWB Ranging Error in Static Test 123
Fig.5.7 Setup Environment in Dynamic Test 125
Fig.5.8 UWB Ranging Error in Open Environment 126
Fig.5.9 UWB Ranging Error under the Dynamic Condition 127

Fig.5.10 BUs Distribution in Locomotive Test 129
Fig.5.11 Setup Environment in Locomotive Test 130
Fig.5.12 The Plan of the Roof of NGB 130
Fig.5.13 Two MU Carried by the Locomotive and a Person in Locomotive Test 131
Fig.5.14 The Comparison between Raw UWB Ranging and Ground Truth in Locomotive Test 132
Fig.5.15 Raw UWB Ranging Error in Locomotive Test 133
Fig.5.16 The Histogram of Raw UWB Ranging Error in Locomotive Test 134
Fig.5.17 The Outlier Distribution in Locomotive Test 136
Fig.5.18 UWB Ranging Error (Outlier Excluded) in Locomotive Test 138
Fig.5.19 UWB MU92 Ranging Error (Outlier Excluded) in Locomotive Test and Its Corresponding Histogram 139
Fig.5.20 Raw Ranging Error (Outlier Excluded) with Linear Fit in Locomotive Test 142
Fig.5.21 Ranging Errors Histogram (Outlier Excluded) without Linear Fit Scale Factor and Bias Compensation 144
Fig.5.22 Ranging Error Histogram (Outlier Excluded) with Linear Fit Scale Factor and Bias Compensation 144
Fig.5.23 Raw Ranging Error (Outlier Excluded) in Dual-moving Situation Versus Reference Distance and with Linear Fit (Left); Raw Ranging Error with Normal Distribution Fit (Right) 145
Fig.5.24 Ranging Error (Outlier Excluded) in Dual-moving Situation Versus Reference Distance and with Compensation (Left); Compensated Ranging Error with Normal Distribution Fit 146
Fig.5.25 UWB Positioning Accuracy in a Static Test (6 BUs) 147
Fig.5.26 Ranging Error of BU80 and Number of BUs for Positioning 148
Fig.5.27 UWB Positioning Accuracy in the Static Test (5 BUs) 149
Fig.5.28 Combined 5 Ranging Errors in the Static Test 149
Fig.5.29 DOP Comparison between six and five Ranging Observations in the Static Test 151
Fig.5.30 UWB Static Positioning Accuracy Using the Dynamic Ranging Observations (5 BUs) 152
Fig.5.31 Combined 5 Ranging Errors in the Dynamic Test 152

Fig.5.32 UWB Static Positioning Accuracy (4 BUs) 153
Fig.5.33 UWB Static Positioning Accuracy Using Dynamic Ranging Observations (5 BUs and Applying WLSE Method)..... 154
Fig.5.34 DOP Comparison between Five- and Four-Unit Scenarios in the Dynamic Test 156
Fig.5.35 Positioning Result in Height Direction (Applying Standard KF Method) in the Locomotive Test..... 157
Fig.5.36 Measured Heights of 4 BUs and MU26 against the ZDOP Values in the Locomotive Test..... 157
Fig.5.37 Positioning Result in Easting and Northing Directions (Applying Standard KF Method) in Locomotive Test 158
Fig.5.38 Position Error in Easting and Northing Directions (Applying Standard KF Method) in Locomotive Test 159
Fig.5.39 Combined 6 Ranging Errors in the Locomotive Test 159
Fig.5.40 Positioning Result in Easting and Northing Directions (Applying Robust KF Method) in the Locomotive Test 161
Fig.5.41 Position Error in Easting and Northing Directions (Applying Robust KF Method) in the Locomotive Test..... 161
Fig.5.42 XDOP and YDOP in the Locomotive Test..... 162
Fig.5.43 A Sample Lap Position Error in Locomotive Test..... 162
Fig.5.44 Velocity of the Target Unit in the Locomotive Test..... 163
Fig.6.1 The GPS Reference Station and the Bundles of UWB and GPS Units..... 167
Fig.6.2 System Deployment in the Roof Trial 169
Fig.6.3 Comparison between UWB Raw Ranging Observations and Ground Truth Distances in the Roof Trial..... 170
Fig.6.4 Examples of NLOS Situations Induced Ranging Outliers in the Roof Trial..... 171
Fig.6.5 Positioning Result in Three Directions Based on the Pure UWB Ranging Observations in the Roof Trial (Applying the RCP Method) 173
Fig.6.6 Position Errors in Three Directions Based on the Pure UWB Ranging Observations in the Roof Trial (Applying the RCP Method) 173

Fig.6.7 BUs Height Changes and ZDOP in the Roof Trial 174
Fig.6.8 XDOP and YDOP in the Roof Trial 175
Fig.6.9 The Positioning Result Comparison between Pure DD Code Pseudo-range and DD Code Pseudo-range/UWB Ranging Combination in the Roof Trial (Applying the RCP Method) 177
Fig.6.10 The GPS Sky Plot for the Roof Trial 178
Fig.6.11 The Numbers of SVs and BUs in the Roof Trial 179
Fig.6.12 The DOP Comparison between Pure DD Code Pseudo-range and DD Code Pseudo-range/UWB Ranging Combination in the Roof Trial 179
Fig.6.13 The Histogram of Collected and Simulated Kinematic Ranging Observation 182
Fig.6.14 Position Error Based on Selected GPS Pseudo-range and Contaminated UWB Ranging Observations Using Standard KF Method 184
Fig.6.15 Position Error Based on Selected GPS Pseudo-range and Contaminated UWB Ranging Observations Using RKF Method. 184
Fig.6.16 The GPS Sky Plot with Cut-off Angle of 40 Degrees 186
Fig.6.17 Positioning CDF Using Different Numbers of Simulated UWB Ranging Observations with Three DD Code Pseudo-range Observations..... 187
Fig.6.18 Positioning CDF Using Different Numbers of DD Code Pseudo-range Observations with Four Simulated UWB Ranging Observations..... 188
Fig.6.19 Position Error Comparison with or without Simulated UWB Ranging Observations Based on the MRS02 190
Fig.6.20 Position Error Comparison with or without UWB Simulated Ranging Observations Based on the MRS04 191

List of Tables

Table 1.1 The Generations of Intelligent Transportation Systems 2

Table 2.1 Country Level Economy-wide Direct and Indirect Costs (Millions of U.S. Dollar) 20

Table 2.2 Summary of Levels of Driving Automation for On-Road Vehicles (SAE, NHTSA and BASt) 28

Table 2.3 The Cross-Correlation between Vehicle Safety Technologies and Crash Types 34

Table 2.4 The V2X Applications Based on DSRC..... 47

Table 2.5 Positioning Requirements for SafeTRIP Services..... 54

Table 3.1 Candidate Sensors Used in Integrated Positioning Solutions..... 58

Table 3.2 GPS UERE for A Single-Frequency C/A Code Receiver 74

Table 3.3 UWB Emission Limits for Indoor and Outdoor Systems as Defined by FCC..... 77

Table 3.4 UWB Emission Limits as Defined by Electronic Communications Committee (ECC) 78

Table 5.1 The BU and MU Coordinates in Static Test..... 122

Table 5.2 UWB Ranging Error in Static Test..... 124

Table 5.3 The Stationary BU and MU Coordinates in Dynamic Test..... 125

Table 5.4 UWB Ranging Error in Dynamic Test 128

Table 5.5 The Static BU Coordinates in Locomotive Test..... 129

Table 5.6 UWB Ranging Error (Outlier Excluded) in Locomotive Test... 138

Table 5.7 UWB MU92 Ranging Error (Outlier Excluded) in Locomotive Test 140

Table 5.8 Scale factor and Bias of Each Unit in Locomotive Test..... 143

Table 5.9 UWB Static Positioning Performance in the Indoor Static Test 150

Table 5.10 UWB Static Positioning Performance in the Outdoor Dynamic Test 156

Table 5.11 UWB Kinematic Positioning Performance in the Locomotive Test 164

Table 6.1 Coordinates of the Static BUs and GPS Reference Station..... 168

Table 6.2 UWB Ranging Evaluation (Outlier Removed) in the Roof Trial 172

Table 6.3 Pure UWB Positioning Performance in the Roof Trial (Applying the RCP Method) 176
Table 6.4 The Positioning Performance Comparison between Pure DD Code Pseudo-range and DD code pseudo-range/UWB Ranging Combination in the Roof Trial (Applying the RCP Method) 181
Table 6.5 The Positioning Performance Comparison Using Different Numbers of Simulated UWB Ranging Observations with Three DD Code Pseudo-range Observations 187
Table 6.6 The Positioning Performance Comparison Using Different Numbers of DD Code Pseudo-range Observations with Four Simulated UWB Ranging Observations 189
Table 6.7 The Positioning Performance Comparison with or without Simulated UWB Ranging Observations Using Different MRS 191

List of Abbreviations

2D	2 Dimensional
3D	3 Dimensional
3G	The 3rd Generation Telecommunication
4G	The 4th Generation Telecommunication
5G	The 5th Generation Telecommunication
5GPPP	5G Infrastructure Public Private Partnership
ABS	Anti-lock Braking System
ACC	Adaptive Cruise Control
AHS	Automated Highway System
AOA	Angle of Arrival
AV	Autonomous Vehicle
BASt	Germany Federal Highway Research Institute
BDS	BeiDou Navigation Satellite System
BLOS	Beyond Line-of-Sight
BSM	Basic Safety Message
BU	Base Unit
CAGR	Compound Annual Growth Rate
CAM	Cooperative Awareness Messages
CAVs	Connected and Autonomous Vehicles
CDMA	Code Division Multiple Access
CEPT	European Conference of Postal and Telecommunications Administration
CLOS	Clear Line-of-Sight
CP	Cooperative Positioning
CS	Commercial Service
CV	Connected Vehicle
DARPA	Defence Advanced Research Projects Agency
DD	Double Differencing
DENM	Decentralised Environmental Notification Messages
DfT	U.K. Department for Transport
DGPS	Differential Global Positioning System

DOP	Dilution of Precision
DoT	U.S. Department of Transportation
DR	Dead Reckoning
DSRC	Dedicated Short Range Communication
EC	European Commission
ECC	Electronic Communications Committee
ECEF	Earth-centred, Earth-fixed
EEA	European Environment Agency
EGNOS	European Geostationary Navigation Overlay Service
EKF	Extended Kalman Filter
ERTICO	European Road Transport Telematics Implementation Coordination Organization
ETRS89	European Terrestrial Reference System 1989
ESA	European Space Agency
ESTEC	European Space Research and Technology Centre
ETSC	European Transport Safety Council
ETSI	European Telecommunications Standards Institute
EU	European Union
FCC	Federal Communication Commission
FDMA	Frequency Division Multiple Access
FOC	Full Operational Capability
GAO	U.S. Government Accountability Office
GDP	Gross Domestic Product
GEO	Geostationary Orbit
GNSS	Global Navigation Satellite Systems
GPS	Global Positioning System
GSM	Global System for Mobile Communications
ICCT	International Council on Clean Transportation
ICT	Information and Communications Technology
IEEE	Institute of Electrical and Electronic Engineers
IGSO	Inclined Geosynchronous Orbit
IMechE	Institution of Mechanical Engineers
IMU	Inertial Measurement Unit

INS	Inertial Navigation System
IOV	In-Orbit Validation
IR	Impulse Radio
IRTAD	International Road Traffic and Accident Database
ITF	International Transport Forum
ITRF	International Terrestrial Reference Frame
ITS	Intelligent Transportation Systems
IVI	Intelligent Vehicle Initiative
JPO	U.S. Joint Program Office
KF	Kalman Filters
KPI	Key Performance Indicator
LiDAR	Light Detection and Ranging
LOS	Line-of-Sight
LSE	Least Squares Estimation
MANETs	Mobile Ad-hoc Networks
MC	Multi-Carrier
MEO	Medium Earth Orbit
MRS	Mobile Reference Station
MU	Mobile Unit
NGB	Nottingham Geospatial Building
NHTSA	U.S. National Highway Traffic Safety Administration
NLOS	Non-Line-of-Sight
OECD	Organisation for Economic Co-operation and Development
OS	Open Service
OSGB36	Ordnance Survey Great Britain 1936
PRS	Public Regulated Service
QZSS	Quasi-Zenith Satellite System
RCP	Robust Cooperative Positioning
RF	Radio Frequency
RITA	U.S. Research and Innovative Technology Administration
RKF	Robust Kalman Filter
RNP	Required Navigation Performance

RPP	Required Positioning Performance
RSS	Received Signal Strength
RSU	Road Side Unit
RTK	Real-Time Kinematic
RTTT	Road Transport and Traffic Telematics
SA	Selective Availability
SAE	Society of Automotive Engineers
SAR	Search and Rescue Service
SBAS	Satellite-Based Augmentation System
SD	Single Differencing
SIS	Signal-in-Space
SoL	Safety of Life Service
SPP	Single Point Positioning
SV	Space Vehicle
TDOA	Time Difference of Arrival
TOA	Time of Arrival
UERE	User Equivalent Range Error
UN	United Nations
UNECE	United Nations Economic Commission for Europe
URE	User Range Error
USSR	Union of Soviet Socialist Republics
UTC	Coordinated Universal Time
UVEK	Federal Department of Environment, Transport, Energy and Communications in Switzerland
UWB	Ultra-Wideband
V2I	Vehicle-to-Infrastructure
V2P	Vehicle-to-Pedestrian
V2V	Vehicle-to-Vehicle
V2X	The cumulative term for V2V, V2I, V2P, etc.
VANETs	Vehicular Ad-hoc Networks
VIAC	VisLAB Intercontinental Autonomous Challenge
VII	Vehicle Infrastructure Integration
VMT	Vehicle Miles Travelled

WGS	World Geodetic System
WHO	World Health Organization
WLAN	Wireless Local Area Network

Chapter 1 Introduction

1.1 Overview

1.1.1 The Role of Positioning Technologies in Intelligent Transportation Systems

Intelligent Transportation Systems (ITS) are increasingly being considered to be the solution to road transportation congestion, safety improvement and emission reduction (RITA, 2009). For example, applying real-time traffic data to the U.S. traffic signal lights can improve mobility significantly by reducing stops as much as 40% which is equivalent as 25% travel time-saving. Meanwhile, it lowers gas consumption by 10% (1.1 million gallons of gas annually) and further cuts emissions by 22% (9,600 tonnes of carbon dioxide emissions daily) (Ezell, 2010). From the economic perspective, according to Ezell (2010), ITS offer superior benefit-cost return compared to traditional investment and the overall benefit-cost ratio has been estimated as high as about 25 to 1 if the U.S. were to implement a national real-time traffic information program. Also, this report points many countries are making increasing investment in ITS. For example, Japan invests $690 million annually, ahead of the South Korea with about $230 million a year from 2008 to 2020 and the U.S. with $110 million per annum. In the U.K., £100 million Intelligent Mobility Fund has been announced by the Chancellor in the spring 2015 budget (U.K. DfT, 2015b). Moreover, £20 million has been awarded to develop next generation of Autonomous Vehicles (AV) which is a vital part of new generation ITS applications (U.K. DfT, 2016a). This becomes the first motivation to define the aim of this research that the enhancement of vehicular positioning will ultimately improve the performance of a variety of ITS road applications.

Day to day popularity of ITS and the development of relevant technologies divided ITS into generations as listed in Table 1.1 (Bunch et al., 2012). No matter which generation, the position of vehicles is the fundamental parameter

in many ITS applications (Drane and Rizos, 1998). The 1st generation ITS road applications focus on traffic management and traffic-related information publishing. Two examples of ITS road applications are demonstrated in Fig.1.1 (NCC, 2016, TRL, 2013). The real-time bus arrival service tells the waiting passengers the exact time of bus arrival relying on the GPS device embedded on the bus. Moreover, the Smart Motorway manages the traffic flow on motorway basing on the real-time traffic volume which is obtained from the positions of vehicles.

Table 1.1 The Generations of Intelligent Transportation Systems, based on source: (Bunch et al., 2012)

Generation	**Time of Occurrence**	**Technology**
1st Generation (ITS 1.0)	Prior to 2000	One way communication technology and primarily based on infrastructure
2nd Generation (ITS 2.0)	Around 2000	Collaborative or two-way communication technology
3rd Generation (ITS 3.0)	2004/2005	Partially Automated vehicle operations and automated, interactive system operations and system management
4th Generation (ITS 4.0)	Now	Connected systems incorporating personal mobile devices, vehicles, infrastructure and information networks for multi-modal system operations as well as personal contextual mobility solutions



Fig.1.1 Real-Time Bus Arrival Service (left) and Smart Motorway (right), based on sources:(NCC, 2016, TRL, 2013)

The 2nd generation ITS road applications crystallise the application areas to enable more personalised services. For example, The SafeTRIP was an integrated project of the EU that integrates satellite positioning technologies (GPS/EGNOS/GALILEO) and two-way satellite communication technology (S-band Eutelsat 10A satellite) to provide on-board communication solution for the transport stakeholders (SafeTRIP, 2013). SafeTRIP established a platform that offers wild opportunities to developers and third parties to build new services. The platform established in the SafeTRIP has been utilised for future connected vehicle applications by the project in the Horizon 2020 which is the biggest EU research and innovation programme ever from 2014 to 2020 (EC, 2014).

Along with the multi-sensor and multi-user integration for systems operations and use of big data for systems monitoring, the 3rd and 4th generations ITS road applications are shifting towards the connected vehicles (Bunch et al., 2012). The Connected Vehicle (CV) allows a vehicle to connect to other vehicles, infrastructure and even the pedestrians within Vehicular Ad-hoc Networks (VANETs[1]) which is a variation of Mobile Ad-hoc Networks (MANETs). Lane departure warning, cooperative adaptive cruise control and intersection movement assist warning are just a few of the connected vehicle applications,

[1] The VANETs is supported by V2X (short for Vehicle-to-Vehicle, Vehicle-to-Infrastructure and Vehicle-to-Pedestrian) communication technology. In this thesis, the V2X communication technology is an interchangeable concept with the CV technology.

and more details of the connected vehicle will be further discussed in Section 2.3.2.

To support the demands of a variety of ITS road applications, Global Navigation Satellite Systems (GNSS) is a general technique to provide position information due to its worldwide coverage and free of charge. Therefore, GNSS is the most suitable choice to support those ITS road applications. The required positioning performance of the 1st and 2nd generations ITS road applications aim at metre level accuracy and a mass market Global Positioning System (GPS) receiver is qualified for those applications which enable users to solve for their positions at a global scale with achievable accuracy around 10 metres (Hofmann-Wellenhof et al., 2007). Furthermore, the Single Point Positioning (SPP) using the combination of GPS, GLONASS and BeiDou satellites could improve the positioning accuracy to 5 metres (Santerre et al., 2014). This is also believed by the findings of the SafeTRIP project that most of the SafeTRIP services can be supported by the widely used, inexpensive GNSS receivers and there is no need for applying geodetic and Real-Time Kinematic (RTK) receivers for such ITS applications (Lovas et al., 2011). However, the positioning performance requirement of many 3rd and 4th generation ITS road applications such as collision avoidance and lane level traffic navigation which need sub-metre level accuracy has exceeded the capability of the GNSS SPP solution. Some advanced techniques are required to improve the performance of GNSS, such as Differential Global Positioning System (DGPS) and RTK (Shladover and Tan, 2006). Furthermore, the inherent limit of the Line-of-Sight (LOS) technology of GNSS normally results in problems for any ITS road applications in an urban area, especially in an urban canyon. As shown in Fig.1.2, the erection of tall constructions and skyscrapers obstructs the GNSS signal which may lead to the insufficient GNSS observations and further the failure of GNSS positioning (Basnayake, 2011). For instance, the applications like intersection movement assist warning and blind spot warning which need the locations of each vehicle at the level of where in the lane when GNSS positioning is unavailable. The gap between the required positioning performances for such ITS road applications and what

GNSS provides must be bridged to make GNSS-based positioning applicable. It is also one of the objectives to conduct this research to fill up this gap. Thus the multi-sensor integration plus Cooperative Positioning (CP) based on V2X communication technology are considered for this purpose.

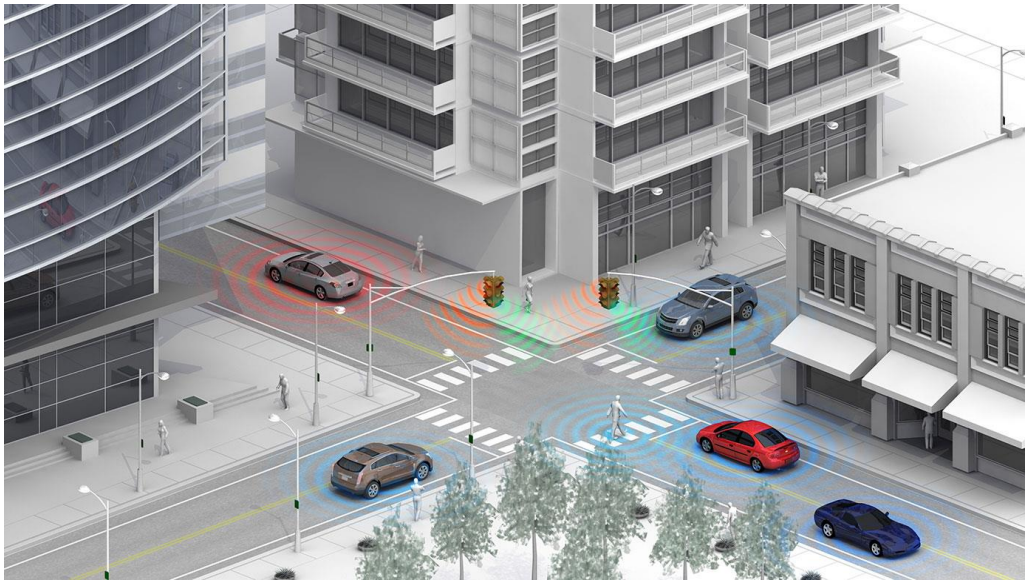


Fig.1.2An Illustration of the Connected Vehicles, based on source: (Basnayake, 2011)

1.1.2 Cooperative Positioning Based on Multi-sensor Integration

As discussed in lots of other literature, the poor performance of GNSS user equipment in urban canyon is a well-known problem due to its clear Line-of-Sight (LOS) requirement, GNSS alone solution is, therefore, unable to provide position with required performance such as, accuracy, availability, integrity, continuity and reliability (Ballester-Gurpide et al., 2000, Ji et al., 2010, Lachapelle et al., 1997, Tsakiri et al., 1998, Groves, 2011). To improve the GNSS-based positioning solution, Cooperative Positioning (CP) is valued with an increasing importance and improvement of positioning accuracy and robustness (Thompson and Buehrer, 2012). As one of the key implementation techniques for the ITS application, CP has become an area of research interest in recent years. Cooperative positioning, also called collaborative positioning, is a positioning approach in which a number of participants contribute their position-related information. To explain the advantage of cooperative

positioning, 'the whole is greater than the sum of its parts' may be the best way to interpret its benefits of sharing information. In a CP system, two or more participants are allowed to work cooperatively to improve their position performance by sharing relevant location information (Garello et al., 2012).

Conventionally, Differential GPS (DGPS) could be thought as a CP approach to improve the positioning performance of rover receiver by using the correction information transmitted from reference station via radio, GSM or 3G (Stephenson et al., 2014). Nowadays, not only the correction but also position-related information of rover receivers, such as the distance between the rover and reference and received pseudo-ranges, is communicated via Dedicated Short Range Communication (DSRC), 4G, even 5G (Alam and Dempster, 2013).

To compensate for the shortcomings of the GNSS signals, additional observations transmitted from other transportation participants and sensors are desired. Aiming to improve traffic safety and enhance transportation efficiency, the U.S. Federal Communication Commission allocated 75 MHz of DSRC spectrum between 5.85 GHz and 5.925 GHz to be used exclusively for Vehicle to Vehicle (V2V) and Vehicle to Infrastructure (V2I) communication (generically referred to as V2X communication). Bridging the communication gaps among transportation participants, they can cooperatively pinpoint themselves by talking to surrounding participants for information exchange via V2X communication. Since V2X technology can be used to bridge the communication gap between road users, their exact location and status can be cooperatively obtained and transferred to each other.

Furthermore, the multi-sensor integration approach is another way to be an augmentation in GNSS-challenged environments and holds promises of delivering reliable positioning solution. The Ultra-Wideband (UWB) technology is one of the leading technology to compensate GNSS because it

not only has the abilities of multipath influence mitigation and suppression of signal reflection but also tackle Non-Line-of-Sight (NLOS) situations with its superior penetration characteristics (Meng et al., 2012, Gao et al., 2014b). Besides, UWB can achieve decimetre or even millimetre level positioning accuracy with its range observations (Zhang et al., 2010). In other words, the distances between UWB-equipped road users or infrastructure can be measured with high accuracy. If there are enough range measurements (at least two for 2D positioning) from other objects with known coordinates, a vehicle can compute its coordinates. All these make UWB become a suitable candidate sensor to integrate with GNSS.

The author believed the adoption of V2X technology is due to the urgent need to improve the efficiency and safety of road transportation systems (Lu et al., 2014). The authors also discuss the challenges of the V2V technology, and one of them is how to aid GPS to achieve few metres level positioning accuracy in hostile environments, such as an urban intersection. Similarly, the lack of GNSS signals is the biggest challenge in such an environment. Researchers proposed a positioning technique which can produce positioning solution with fewer than four GNSS satellites (Tan et al., 2009). Utilising the difference of the pseudo-range between two satellites, this technique could provide approximately 15-metre positioning accuracy. The feasibility of using cooperative positioning as a key implementation of position acquisition under V2X scenarios has also been investigated (Tang et al., 2015, Yao et al., 2011a, Richter et al., 2009, Yao et al., 2011b, Tsai et al., 2015, Liu and Lim, 2012). By transmitting GNSS positions to each other in different driving environments, the positioning quality has been significantly improved. However, the benefit of V2X communication can only be maximised when vehicles are able to compute its position based on a sufficient number of visible GNSS satellites.

The authors proposed a method to collect enough GNSS signals by combining two GNSS receivers' observations (Zhang et al., 2014). It resolves the problem caused by the lack of GNSS signals, but the pre-measurement of the baseline

between two static receivers limits its implantation in transport. A novel method has been raised to transmit RTK corrections in the V2X environment (Stephenson et al., 2014). It is feasible for transportation applications due to the outstanding performance of RTK technology. However, the monopoly of GNSS positioning cannot provide enough reliability and continuity for traffic safety applications.

To improve the robustness and stability of the positioning solution, multi-sensor integration needs to be considered. A loosely-coupled integration of low-cost GPS, Inertial Navigation System (INS) and UWB solution is proposed. This method implements seamless indoor and outdoor positioning, and it can achieve 20 cm accuracy with observable UWB measurements in the indoor environment (Tanigawa et al., 2004). My previous research has proposed a tightly-coupled integration of GPS, INS and UWB solution, which indicated that the employment of INS and UWB onto GPS could improve the positioning accuracy to around 50 cm in 2D (Wang et al., 2016). Abandoning the INS, a tightly-coupled Kalman filter-based solution that provides 2D precision mobile tracking is proposed (Johnson and Dewberry, 2011). Moreover, a Particle filter-based solution is proposed by combining an odometer, GPS and Dead Reckoning (DR) to achieve 20 cm accuracy (Gonzalez et al., 2007). And a peer-to-peer cooperative positioning has been introduced, and the capability of terrestrial ranging has been assessed RITA, 2009. To further exploit the excellence of UWB, its ranging observations are employed in tightly integration system. Initially, single or multiple UWB devices are only used as static base stations to assist GPS receivers to resolve the integer ambiguity, by combining the UWB ranging observations with GPS measurements in a tightly-coupled integration to compute the position of a rover device (Jiang et al., 2012, Chiu and O'Keefe, 2008, MacGougan and Klukas, 2009, MacGougan et al., 2008, MacGougan et al., 2010). In further research, UWB ranging observation from mobile base stations and simulated bearing measurements are employed to improve the positioning accuracy in a V2V scenario (Petovello et al., 2012, Amirloo Abolfathi, 2015, Wang et al., 2013, Wang, 2015).

1.2 Problem Statements

The emerging modern ITS road applications bring up the higher requirement for positioning solution on availability, integrity, accuracy, etc. Due to the inherent LOS limit, GNSS-only solution cannot always meet the new positioning requirement, especially for those applications in the urban area. Although the mature multi-sensor integration approach can make up for deficiencies and some automotive manufacturers have developed partially autonomous vehicles based on it, the expensiveness of some sensors, such as INS, Light Detection and Ranging (LiDAR), shuts down the opportunity for mass market application. Basing on the recent development of V2X communications technology, CP approach has been extensively used in vehicle positioning. By employing both multi-sensor integration and CP, it is possible to find solutions for vehicle positioning in GNSS hostile environment with acceptable cost and performance which will further enable a variety of ITS road applications. This thesis will address the following problems with multi-sensor integration CP for ITS road applications in an urban area:

- GNSS signal obstruction;
- The selection of sensors that integrates with GNSS;
- GNSS correction message outage.

1.3 Aims and Objectives

The primary aim of this thesis is to develop a cooperative positioning algorithm by fusing the Double Differential (DD) GPS pseudo-range and Ultra-Wideband (UWB) range observations for V2X ITS applications.

To achieve the aim, the following objectives are formulated:

1. To explore positioning requirements of emerging ITS applications (the positioning accuracy and precision are mainly concentrated in this thesis)

2. To review the state-of-the-art positioning technologies to support V2X ITS services
3. To investigate the ranging and positioning performance of UWB sensors by examining different sources of errors
4. To develop a cooperative positioning algorithm by integrating of GPS DD code pseudo-range and UWB ranging observations
5. To evaluate the performance of the developed algorithm via simulated V2X communications under different scenarios

The research design of this thesis is listed below:

Objective	Method	Data	Outcome	Chapter
1	Literature review	Journals, conferences, books, reports	Positioning requirements for different V2X ITS applications	2
2	Literature review	Journals, conferences, books, reports	Identification of positioning technologies to support the positioning requirements of V2X ITS applications	3
3	Field experiments	Leica GNSS receivers & Thales UWB sensors	Characterisation of Thales UWB sensors regarding ranging and positioning under different scenarios	5, 6

4	Least Squares Estimation (LSE) & Robust Kalman Filter (RKF)	Journals, conferences, books	Developed cooperative positioning algorithm for V2X ITS applications	4
5	Field experiments & Simulation	Leica GNSS receivers & Thales UWB sensors	Performance assessment of the developed algorithm under different scenarios	6

1.4 Contributions

Based on the above objectives, the contributions of this research can be itemised as follows:

- With the assumed DSRC device, a multi-sensor cooperative positioning method that tightly integrates DD code pseudo-range and UWB ranging observations has been proposed, which dedicates to vehicle positioning in GNSS hostile environment;
- The ranging and positioning performance of UWB technology have been comprehensively evaluated. The major error source of UWB ranging observations, Non-Line-of-Sight (NLOS) situation, has been identified and the Robust Kalman Filter (RKF) approach has been applied to minimise the impact of these outliers;
- The UWB-only positioning solution and the UWB and partially GPS pseudo-range integration solution have been implemented under the simulative lack of GPS scenario. And the positioning results demonstrate the feasibility and reliability of the UWB augmentation; and

- Taking advantage of the V2X communications, the Mobile Reference Station (MRS) concept has been proved, which offers an alternative way to broadcast DGPS correction.

The findings presented in this thesis have been published in two conference papers and one peer-reviewed journal paper. Also, one more peer-reviewed journal paper is in preparation.

- Meng, X., Gao, Y., Zhao, H. & Ryding, J. Comprehensive Assessment of UWB for Indoor Positioning and Navigation. European Navigation Conference, 2012. 25-27.
- Gao, Y., Meng, X., Hancock, C. M., Stephenson, S., Zhang, Q., "UWB/GNSS-Based Cooperative Positioning Method for V2X Applications," Proceedings of the 27th International Technical Meeting of The Satellite Division of the Institute of Navigation (ION GNSS+ 2014), Tampa, Florida, September 2014, pp. 3212-3221.
- Wang, J., Gao, Y., Li, Z., Meng, X., Hancock, C.M. A Tightly-Coupled GPS/INS/UWB Cooperative Positioning Sensors System Supported by V2I Communication. Sensors 2016, 16, 944.

1.5 Thesis Outline

Each remainder chapter has individual overview and summary for a better understanding of the context. The content of this thesis is outlined as follows.

Chapter 2 discusses the motivation and development of ITS. This includes an introduction to today and future ITS road applications especially supported by V2X communications technology, such as Connected Vehicle (CV) and Autonomous Vehicle (AV). Then it follows the main challenges of CV and AV and some of them will be tackled in this thesis. This chapter finishes by reviewing and discussing the current required positioning performance for the V2X applications

Chapter 3 takes a look at the positioning technique that could be utilised for the V2X applications and demonstrates the selection criteria. Then it focuses on two positioning technologies that will be used in this thesis from the theoretical background, including positioning technique, error sources, type of observations, etc.

Chapter 4 proposes the Robust Cooperative Positioning (RCP) method that integrates DD code pseudo-range and UWB ranging observations for the V2X applications. The chapter covers the estimation algorithm, design of state and measurement models, the information transmitted by the assumed DSRC device and parameter selection.

Chapter 5 assesses the ranging and positioning performance of Thales UWB units by carrying out three tests, i.e., indoor static test, outdoor dynamic test and the locomotive test. The UWB ranging observations collected in the different situation are compared to the ground truth, which is derived from accurate GPS RTK post processing results.

Chapter 6 examines the performance of the proposed RCP method by conducting the roof trial and simulating four application scenarios, including the robustness, availability and the concept of the Mobile Reference Station (MRS).

Chapter 7 finishes this thesis with concluding remarks on the primary results and findings during the development and demonstration of the proposed RCP method. Several recommendations on potential future work are also briefly discussed.

Chapter 2 Emerging ITS Applications

2.1 Overview

Intelligent Transportation Systems (ITS) assemble information technology, communication technology, sensor technology, positioning technology, etc., to provide safety, mobility and environmental benefits (Chen and Miles, 2004). The new millennium has witnessed the explosion of ITS applications along with the evolutions on ITS underlying technologies. ITS safety applications are of paramount importance to save millions of lives from traffic accidents. The conventional ITS safety applications concentrated on public transport operators and traffic managers gather and disseminate traffic-related information to all road users via transport infrastructure. The concerns of conventional ITS safety applications include the difficulties to collect information from all relevant road users and reflect the up-to-date state of the traffic. In recent decades, the flourish of Connected and Autonomous Vehicles (CAVs) technologies led to a variety of new generation ITS safety applications and also witnessed the transition that is from passive to active ITS safety application. CAVs technologies radically change traffic information flow from the manner of the one-way broadcast to two-way exchange. To be benefited from CAVs technologies, road users alter their safety strategies from damage mitigation to crash prevention. To obtain benefits from emerging ITS applications, people's attentions have also been turned on corresponding required positioning performance.

2.2 Intelligent Transportation Systems

2.2.1 Definition and History of ITS

According to the definition of the directive 2010/40/EU, ITS is defined as (EU, 2010):

> *"Advanced applications which without embodying intelligence as such aim to provide innovative services relating to different modes of transport and traffic management and enable various users to be better informed and make safer, more coordinated and 'smarter' use of transport networks."*

ITS cover all transportation modes, such as air, rail, water, etc. but only road transportation is discussed in this thesis. The origin of ITS dates back to the development of Electronic Route Guidance System in the U.S. in the 1960s which provided drivers with route guidance based on real-time traffic analysis (Vanajakshi et al., 2010). Then the same era saw the sprouting of ITS in the U.S., Europe and Japan at the end of 20th century.

2.2.2 Benefits of ITS

The Intelligent Transportation Society of America (ITS America) has estimated in its report that the revenues of 3,000 U.S. ITS companies have reached $48 billion for end-use ITS manufacturing products and services in 2009 and is projected to exceed $67 billion in 2015 (ITS America, 2011). In addition to the enormous economic benefits by providing various services to road users, the benefits of ITS are also typically considered in safety, mobility, environmental benefits, etc. (Chen and Miles, 2004).

2.2.2.1 Safety Improvement

Safety is always the paramount objective as an accident could lead to casualties and fatalities. Given in a report from the Department for Transport (DfT), Great Britain (U.K. DfT, 2016b), a total of 1,732 people were killed in reported road traffic accidents in 2015 (see Fig.2.1) (U.K. DfT, 2016b). There was a 2% decrease compared to 2014, and this is the second lowest annual total on record after 2013. To compare with the number in 2005, it nearly dropped by 50%. In addition to the fatalities, there were 186,209 casualties of all severities in reported road traffic accidents in 2015. More specifically, car occupants have

contributed the largest share in each casualty severity, e.g. 755 (44% out of 1,732) deaths and 111,708 (60% out of 186,209) overall casualties.



Fig.2.1Fatalities in Reported Road Accidents: GB, 2005-2015, based on source: (U.K. DfT, 2016b)

With regard to the United States, 35,092 people died in motor vehicle traffic crashes in 2015 and increased 7.2% compared to 2014, which is the largest percentage increase in nearly 50 years. Moreover, an estimated 2.34 million people were injured in motor vehicle traffic crashes in 2015 which increased 100,000 by 2014 (NHTSA, 2016). However, the reason for such increase in numbers of fatality and casualty does not explain in this statistic report. The pie chart in Fig.**2.2** shows that 68% fatality is caused by vehicle occupants, including light truck, passenger car, bus, etc. (NHTSA, 2016). Looking at the U.K. case, vehicle occupants account for the vast majority of the traffic fatalities and the similarity has also been detected in most of the motorised countries, such as Australia, France and German where motorcar occupants make up more than half of all traffic fatalities (WHO, 2009).

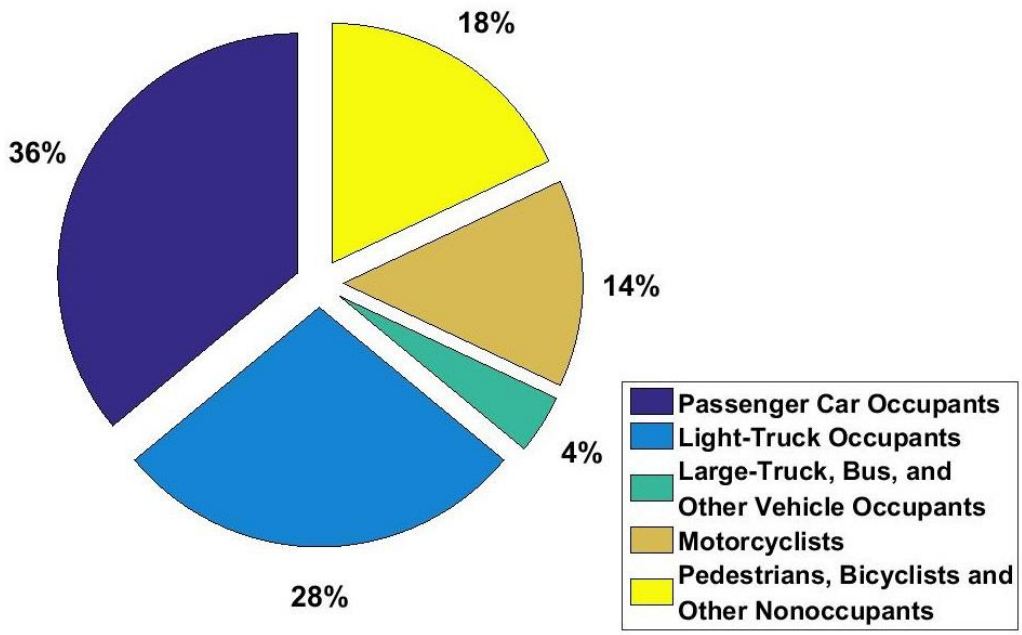


Fig.2.2 Fatality Composition Caused by Vehicle Occupants in the U.S., based on source: (NHTSA, 2016)

The fatalities caused by traffic accident have been becoming a global issue. Looking at the longer-term trend, the number of road fatalities in 32 International Road Traffic and Accident Database (IRTAD) countries dropped by 42% between 2000 and 2014 which is a dramatic decrease within a relative short period according to the report released by the International Transport Forum (ITF). Though many IRTAD countries have made an indisputable progress, the results achieved in those countries only represent a small share (6%) of global figure that 1.3 million people are killed, and tens of millions are injured on the road, in which ninety percent of casualties occur in low and middle-income countries (OECD/ITF, 2016). The World Health Organisation (WHO) has predicted that road traffic injuries will become the fifth leading cause of death by 2030 including a wide range of diseases (WHO, 2009). In 2010, the United Nations took action to proclaimed the launch of "The Decade of Action for Road Safety 2011-2020" which was aiming to save millions of lives by 2020 (UN, 2010).

ITS applications are expected to cut down the fatalities caused by traffic accidents. The European Transport Safety Council (ETSC) concluded that the

most safety beneficial systems, such as collision avoidance systems, driver and vehicle monitoring systems and automated speed enforcement, could potentially reduce fatalities and injuries by more than 10% (ETSC, 1999). For instance, an automatic collision detection and prevention system was estimated to save 45% of road fatalities in Japan (Hiramatsu et al., 1997). Also, similar collision avoidance systems were optimistically predicted with an 80 percent reduction in fatalities (Perrett, 1996). More recently, an increasing number of new ITS safety technologies, e.g. eCall, Intelligent Speed Adaptation, In-vehicle Driver Assistance and Warning Technologies, have been demonstrated successfully and shown promising potential for accident reduction (Parliamentary Office of Science and Technology, 2009).

2.2.2.2 Congestion Relief

Transport problems are not limited to traffic accidents, and congestion is another thorny issue that is expected to be remedied by ITS. Goodwin (2004) has estimated the economic costs of road traffic congestion in London (Goodwin, 2004). It is estimated that £20 billion was wasted annually in 2000 and the figure would be increased to £30 billion in 2010. Later on, Eddington (2006) estimated in his advice to government that the cost of existing congestion on the U.K. road network would be worth some £7 to £8 billion of GDP per annum. Due to the rapid growth of travel demand, by 2025 the rising cost of congestion will lead to an extra £22 billion worth of time in England alone, and 13% of traffic will suffer from stop-start travel conditions (Eddington, 2006). Recently, Department for Transport (DfT) announced the action for roads for the 21st century in 2013. They are concerned that almost a quarter of all travel time could be wasted on stuck in traffic by 2040. This amounts to at least 70 hours per year for every household which is equivalent to 100 million working days lost. To monetise it, £14 billion will be spent by the freight industry which results in higher prices in the shops (U.K. DfT, 2013).

Congestion is not unique in the U.K. but throughout the world. The joint study by Texas A&M Transportation Institute and INRIX, a traffic information provider, provides a comprehensive analysis of the U.S. traffic conditions in 471 urban areas. It shows that each auto commuter wasted 42 hours and 19 gallons fuel yearly which is equivalent to $960 in 2014. The corresponding cost in country level generates a total of $160 billion and it almost four-fold of the congestion cost in 1982 (Texas A&M Transportation Institute and INRIX, 2015). According to a comparative report on the cost of road traffic congestion generated by INRIX collaborated with the Centre for Economics and Business Research, a London-based consultancy. Based in the U.K., France, Germany and the U.S. data, the study reveals that 36 hours are spent, on average, in gridlock every year in metropolitan areas. This significantly influences the economies of these countries as urban areas to generate a considerable proportion of GDP but encompass an incommensurate size of territory. For example, urban areas in the U.S. account for 1.5% of the total landmass but contribute 50% of GDP. Table 2.1 lists the costs in four countries imposed by congestion. The aggregate cost is forecasted to rise from $200.7 billion in 2013 to $293.1 billion by 2030 which is a 46% increase. The U.K. is going to experience the most severe deterioration of traffic condition as there is predicted to be a 66% increase in annual cost of congestion from 2013 to 2030. Meanwhile, the U.S. is expected to incur the highest overall annual cost persistently from 2013 to 2030 (Cebr, 2014).

Table 2.1 Country Level Economy-wide Direct and Indirect Costs (Millions of U.S. Dollar), based on source: (Cebr, 2014)

Country	Sector	2013	2020	2025	2030	2013-30 %change
U.K.	Direct costs[2]	12,649	15,865	18,264	20,937	66
	Indirect costs[3]	7,883	9,565	10,928	12,473	58
	Total	**20,532**	**25,430**	**29,191**	**33,410**	**63**
France	Direct costs	12,881	14,780	15,984	17,158	33
	Indirect costs	9,630	10,668	11,517	12,430	29
	Total	**22,510**	**25,448**	**27,501**	**29,589**	**31**
Germany	Direct costs	21,684	24,224	25,929	27,702	28
	Indirect costs	11,796	13,116	14,517	16,137	37
	Total	**33,480**	**37,341**	**40,446**	**43,838**	**31**
The U.S.	Direct costs	78,519	97,099	109,550	120,695	54
	Indirect costs	45,639	54,157	60,151	65,526	44
	Total	**124,158**	**151,257**	**169,701**	**186,221**	**50**
Total		**200,681**	**239,474**	**266,838**	**293,058**	**46**

The scale of the problem is enormous, and congestion has been bringing severe consequences for national economies. The ITS services are profitable for cities and maximise the capacity of the road network. For example, the ITS-based electronic road pricing tolls in Singapore increase average car speeds to 27 km/hour compare to 16 km/hour in London and 11 km/hour in Tokyo (KPMG, 2014). ITS-based Active Traffic Management pilot on the M42 road in the U.K. has also shown success in reducing congestion and increasing the capacity. An average 27% reduction in journey time during weekdays and a 7% to 10% increase in road capacity were successfully achieved (SDG, 2008). ITS-enabled road pricing schemes have been implemented across the world, for instance, in the EU and the U.S. that revealed promising effects on reducing congestion (Ezell, 2010).

2.2.2.3 Emission Reduction

Considering the high correlation between congestion and emissions, the worsening traffic congestion often results in an increase in fuel consumption

[2] Direct costs indicate the value of fuel and time spent in congestion rather than being productive

[3] Indirect costs point to extra freighting and business fees from vehicle idling in traffic

and emissions (Barth and Boriboonsomsin, 2009). The tremendous amount of emissions from vehicles has significant impacts on the environment and public health. By the end of 2015, there were 36.5 million vehicles licensed for use on the road in U.K., of which 30.3 million were cars (U.K. DfT, 2016d). According to the latest Road Traffic Estimates released by DfT in 2016, road transport continues to be the dominant transport mode for individuals and businesses. To be specific, road transport covered 89% of passenger kilometres and 73% of freight goods in 2014, respectively. Fig.**2**.**3** reveals that 316.7 billion Vehicle Miles Travelled (VMT)[4] in 2015, a 1.1% increase from 2014. It is also found that the growth of annual VMT is slowing and saturated and the 316.7 billion VMT in 2015 is nearly 1% more than the previous peak compared to 314.1 billion in 2007 (U.K. DfT, 2016c).

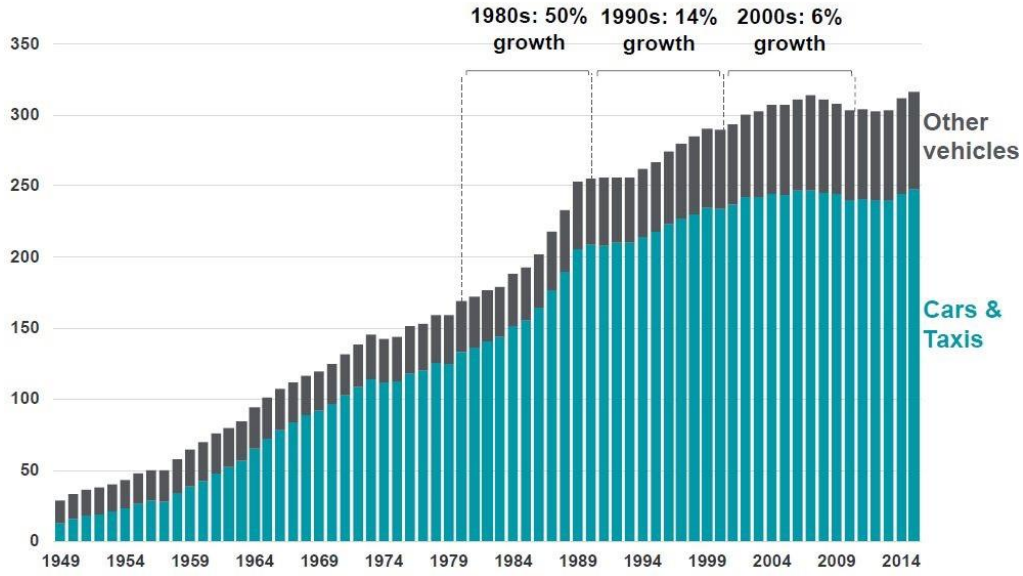


Fig.2.3 Vehicle Miles Travelled in U.K. Since 1949, based on source: (U.K. DfT, 2016c)

Owing to the increasing number of licensed vehicles and an enormous amount of VMT on a globe scale, the corresponding emission and congestion problems have brought along incredible health, environmental and economic costs. The report published by the Royal Automobile Club Foundation in June 2014 has

[4] Vehicle Miles Travelled is a measurement of miles travelled by vehicles in a specified region for a specified time period

demonstrated that around 95% of national air pollution is a result of transport activity which was worth an estimation health cost between £4.5 and £10 billion (Hitchcock et al., 2014). Findings from the research based on public health data in Austria, France and Switzerland demonstrated that road traffic-related air pollution has contributed to about 3% of total mortality and also brought more than a half million new cases of respiratory disease. Moreover, € 26,700 million of health cost are generated by road traffic-related air pollution in those three countries (Sommer et al., 2000, Künzli et al., 2000). It is in light of the research that has been done by Organisation for Economic Co-operation and Development (OECD) that $864,144 million of health cost, including mortality costs, are attributed to road traffic-related air pollution in OECD countries in 2010 (OECD, 2014).

Under European Commission (EC) Regulation No 433/2009, a target of average emission of 95g CO_2/km has been set for the new car fleet from 2020 onwards to reduce the greenhouse gas emission (EC, 2009). A briefing came out from the International Council on Clean Transportation (ICCT) has summarised that all car manufacturers achieved their 2015 targets ahead of time with the average emission of 123.3g CO_2/km and stayed on the right track to reach their 2020 target (Nikiforos et al., 2015). Unfortunately, findings from European Environment Agency (EEA) have shown that only 17 out of 28 member states' average emission levels in 2014 were below 130g CO_2/km in Fig.**2.4**. Particularly, Netherlands (107g CO_2/km), Greece (108g CO_2/km) and Portugal (109g CO_2/km) ranked top three on the leaderboard whereas Estonia (141g CO_2/km), Latvia (140g CO_2/km) and Bulgaria (136g CO_2/km) dragged the EU average emission, because they have bought the least efficient cars (EEA, 2015).

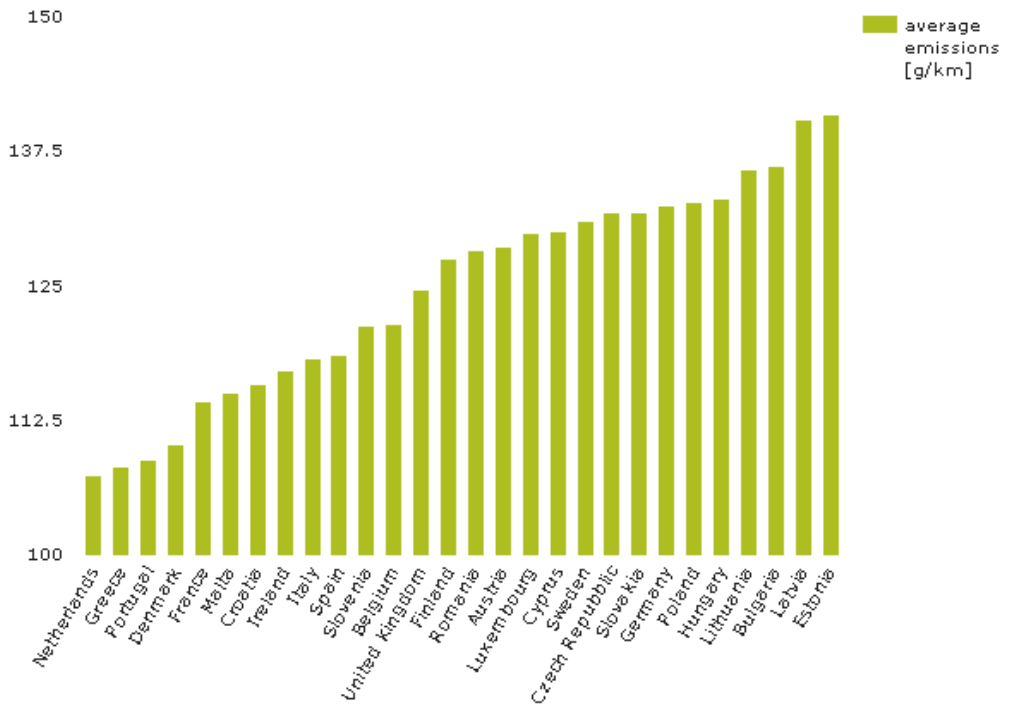


Fig.2.4 Average Statistics of Emission Levels by the Member States, based on source: (EEA, 2015)

A comprehensive review by Bell has demonstrated how ITS can play a major role in alleviating emissions by traffic management (Bell, 2006). Also, the authors believed that ITS could tackle the environmental problem by reducing fuel consumption and CO_2 emissions. ITS strategies, such as traffic signal control, electronic toll collection and automated speed enforcement, are verified for fuel saving and CO_2 emission cutting down (Shaheen and Lipman, 2007). The findings from Webb has also shown that Information and Communications Technology (ICT), which is a key technology for the deployment of ITS services, would save 1.52 Gt[5] CO_2 emission (worth € 280 billion) in 2020 in Europe through a host of efficiencies in transport and storage (Webb, 2008). More recent reports published by SE Consult, EU and ERTICO-ITS Europe[6] emphasise the promising future of ITS technology to save up to 30% fuel consumption and emissions through a variety of applications (EU, 2012, Jean-Charles and Andrew, 2015, SE Consult, 2009).

[5] 1 Gt = 1 gigatonnes

[6] ERTICO-ITS Europe is a partnership of around 100 companies and institutions involved in the production of Intelligent Transport Systems (ITS) in Europe.

2.3 Connected and Autonomous Vehicles

ITS can be categorised into infrastructure-based, in-vehicle and cooperative ITS. Traditionally, infrastructure-based ITS serve road users by spreading traffic information and managing traffic flow. The Institution of Mechanical Engineers (IMechE) believed that the boost of Connected and Autonomous Vehicles (CAVs) technologies have made ITS more interactive rather than the one-way reception mode of conventional ITS to facilitate the development of in-vehicle ITS and cooperative ITS (IMechE, 2012). Vehicles are the most dominant component in ITS and the evolution of vehicle technology, therefore, drives the fundamental transformation of ITS. To Improve traffic safety as the top priority of ITS, two approaches of vehicle technology are mainly applied. Firstly, Autonomous Vehicle (AV) technology, also considered as sensor-based solutions, has drawn lots of attention by automotive industries. The core of AV technologies is to fuse available sensors and artificial intelligence to "see" and understanding the vehicle's surroundings as accurately as a human being can. Secondly, Connected Vehicle (CV) technology, also classified as connectivity-based solutions, has received significant interests from governments and institutes. The key idea of CV technology is the use of wireless technologies to communicate in real-time with the vehicle and the outside environment. AV and CV technologies are not necessarily reliant on one another. However, the combining of CAV technologies could reduce the cost and adequately mimic human senses to deliver better safety (Silberg et al., 2012).

It is essential to examine the contributors to traffic accidents since the top motivation for developing ITS is casualty elimination. A series of researches have shown that the human error contributes an overwhelming majority of road accidents. A landmark analysis of crash causation published in 1979 found that human factors were a cause in at least 64% of accidents and were probably causes[7] in about 90%-93% of accidents (Treat et al., 1979). A U.K. study that followed in 1980 likewise identifies driver and pedestrian error and

[7] Probably cause is considered here to an 80% confidence level.

impairment[8] were main contributory factors in 1942 out of 2042 accidents (95%) (Sabey and Taylor, 1980). Another U.S. study released in 2001 concluded that driver behaviour errors accounted for the 96.8% of traffic crash investigated (Hendricks et al., 2001). Moreover, a report from the U.S. National Highway Traffic Safety Administration (NHTSA) stated that 5,096 out of 5,361 crashes attributed to driver factors compared to 130 to vehicles and 135 to the roadway and weather-related factors (NHTSA, 2008). The latest study released by NHTSA in 2015 shown that a 94% of crashes was assigned to driver-related critical reasons in a total number of 2,189,000 crashes (Singh, 2015). Due to the fact that human errors cause most of the traffic crashes, it is considerable to find an alternative to driving where CAV technologies could play a major role.

In addition to enhanced road safety, CAV technologies could reinforce ITS to construct a transportation system with maximised mobility, limited energy consumption and cutting down environmental pollution (Patrick, 2015, GSMA, 2015b, Lynne and Marcus, 2014). As an innovative and cutting-edge field, the development and implementation of CAV technologies have been assigned as top priorities in ITS Strategic Plan (2015-2019) released by the U.S. Department of Transportation (DoT) (Barbaresso et al., 2014). Besides, the U.K. government announced a £100 million fund in the Chancellor's Spring Budget in March 2015, which will be match-funded by industry to total £200 million, to enhance the development of CAVs, including numbers of road trials (SMMT, 2015). CAVs bring safety and environmental benefits as well as enormous economic opportunities. It is predicted that CAVs could create an additional 320,000 jobs in the U.K. by 2030 which contributes £51 billion to the overall economic and social benefit per year. It also predicted that the market share of connected vehicles could reach 50% in 2015 standing on 1.7 million automotive sales; in contrast, autonomous vehicles (including vehicles with autonomous features) will emerge on auto market in 2017 at a 4% share.

[8] Impairment factors include alcohol, fatigue, drugs, illness and emotional distress.

By 2030, CAVs will monopolise the auto market of 2.3 million in sales volume (KPMG, 2015).

2.3.1 Autonomous Vehicles

Autonomous Vehicles (AVs), are also known as a driverless vehicle or self-driving vehicle, are vehicles that can make decisions without human intervention. The first example of exposition of a self-driving car was at the 1939 World's Fair in New York by General Motors' Futurama exhibit (Ozguner et al., 2011). The extensive foundational researches on AVs have been conducted from approximately 1980 to 2003. Then the U.S. Defence Advanced Research Projects Agency (DARPA) stimulated advancements in AV technology by holding three "Grand Challenges" between 2003 and 2007. Based on the solidified partnerships between the auto manufacturer and the education sector during the DARPA Challenges, AV has gone out from the laboratory to commercial applications. For instance, the most notable and prevalent AV, Google's Driverless Car, was exposed by conducting road tests in 2012, Audi and Toyota both to unveil their AV visions in following year and more details will be given in Section 2.3.1.2 (Anderson et al., 2014).

2.3.1.1 Levels of Automation

Today, vehicles with partial autonomy are already becoming available in the marketplace, such as emergency braking systems, self-parking and lane departure warning. To specify the automation level of AVs, the U.S. National Highway Traffic Safety Administration (NHTSA) and the Germany Federal Highway Research Institute (BASt) has individually published their hierarchies of vehicle automation level. To unify the standards, Society of Automotive Engineers (SAE) has issued international's new standard J3016 in 2014 to harmonise classification system of AVs. Table 2.2 lists the definitions of SAE standard on automation level for on-road vehicle alongside the hierarchies from NHTSA and BASt. The automation level could be roughly classified into two sub-groups depending on either human driver or automated driving system takes more responsibility for monitoring the driving environment. Level 0 –

level 2 in all three standards are labelled with human driver domination while the rest refers to the mode under the charge of an automated system. Also, it is important to clarify between “autonomous” and “automation”. “Autonomous” generally refers to acting independently; whereas “automation” points to some driving behaviours are conducted automatically and not manually. In another word, “autonomous vehicle” in this thesis always tends to the second sub-group (SAE level 3–level 5) (Gasser and Westhoff, 2012, NHTSA, 2013, SAE, 2014).

Table 2.2 Summary of Levels of Driving Automation for On-Road Vehicles (SAE, NHTSA and BASt), based on sources: (Gasser and Westhoff, 2012, NHTSA, 2013, SAE, 2014)

SAE Level	Name	Definition	NHTSA Level	BASt Level
0	No Automation	The vehicle is completely controlled by the human driver sometimes warning, or intervention systems may help the driver	No Automation (Level 0)	Driver Only (Level 0)
1	Driver Assistance	The vehicle is controlled by the human driver most of the time, but a driver assistance system may execute few driving tasks using information from the driving environment (for example, steering or acceleration)	Function-specific Automation (Level 1)	Driver Assistance (Level 1)
2	Partial Automation	More than one driving tasks are executed by the system (for example, steering and acceleration) while the human driver perform all remaining aspects	Combined Function Automation (Level 2)	Partial Automation (Level 2)
3	Conditional Automation	An automated driving system performs all aspects of the dynamic driving task, but a human driver is required to intervene sometime	Limited Self-Driving Automation (Level 3)	High Automation (Level 3)
4	High Automation	An automated driving system performs all aspects of the dynamic driving task even if a human driver does not respond appropriately to a request to intervene		Full Automation (Level 4)
5	Full Automation	The vehicle is full-time automated driven under all environmental and road conditions that can be managed by a human driver	Full Self-Driving Automation (Level 4)	

2.3.1.2 Technology Advances in AV Technology

Although AV technology is complex, the questions that an autonomous vehicle needs to answer are simple: "where am I?", "what is around me?" and "what does it mean?" (Google, 2015). To figure out those answers, AV technology can be divided into four basic component categories: sensors, mapping, perception and communication. Sensor technology includes a variety of hardware such as camera, radar, GPS, LiDAR and IMU. Mapping technology is typically comprised coordinate files of points and line segments and establishes a basic platform for navigation. Perception technology involves the set of software that processes data from sensors, compares with stored mapping and determines how the vehicle will react under current circumstance. Communication technology enables the vehicle to share information with other vehicles or infrastructure in the vicinity (Lutin et al., 2013). Reconsidering three questions raised in the beginning, sensor and mapping technologies help to locate the vehicle itself and to detect objects all around the vehicle which resolve the first two questions. Perception technology gives the vehicle orders based on analysis of sensor input and preloaded map data which answers the third question. Communication technology exchanges information about positions and movement intentions with other vehicles to allow every vehicle to anticipate and respond to manoeuvres which explain the second and third questions.

AV is a sunrise industry. Numerous organisations, auto manufacturers and services companies are racing to develop their prototypes, and some of them use the milestone of the year 2020 for the product launch of fully automated AV, for instance, Google, Nissan and Volvo. Meanwhile, some car makers have released semi-automated vehicles, and some are still in the development phase. To better understand the state-of-the-art of AV technology, more detailed examples are given below based on the levels of automation defined by NHTSA. Today, most automakers offer Level 1 technology, and some have advanced to Level 2, such as adaptive cruise control, lane-keeping systems and parking assistant. More specifically, BMW's Traffic Jam Assistant automatically maintains the desired distance from the vehicle ahead at a speed

of up to 60 km/h (BMW, 2015b); Mercedes-Benz's DISTRONIC PLUS enables Adaptive Cruise Control (ACC), and active lane-keep assist features at a speed of up to 200 km/h (Mercedes-Benz, 2015); General Motors expect semi-autonomous vehicles to be available to customers before 2020 while Cadillac and Ford are also working on integrating ACC feature into their future models (GM, 2015a, KPMG, 2013). Represented by Google cars, several companies have been one step ahead of the rest to release AV prototypes or future strategies on AV, which fits Level 3, and some activities list as follows. Level 4 depicts the ultimate stage of AV development, and more lessons are still needed.

Google Self-Driving Car Project

As one of the most exposed companies studying on autonomous vehicles, technology giant Google has been working on this project and retrofitted lots of vehicles into AVs since 2009 (shown in Fig.**2.5**). According to its monthly report for October 2015, their AVs have covered a distance of nearly 1.3 million miles in autonomous mode (Google, 2015). They work toward a fully self-driving vehicle that can take anyone from point A to point B by only pushing a button and expect to have a commercialised AV by 2020. With regards to their latest prototype vehicle released in December 2014, steering wheel and pedals were removed and instead on-board sensors (lasers, radars and cameras) will detect objects in all directions.

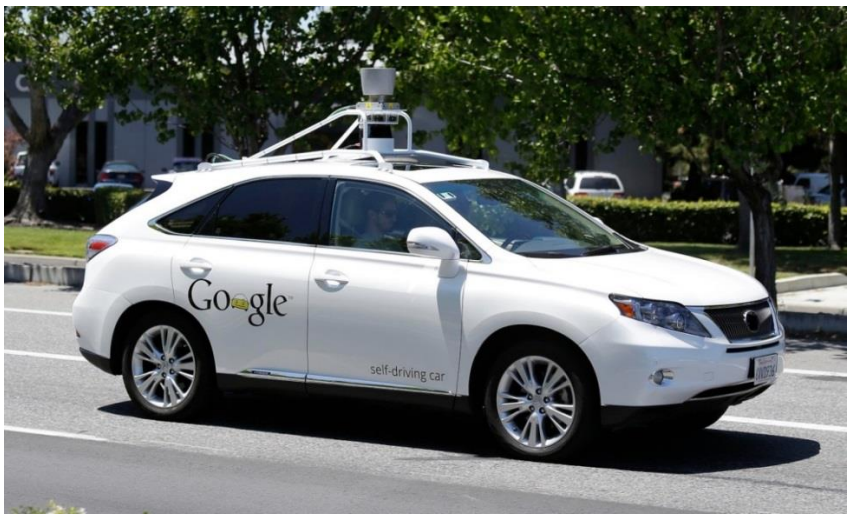


Fig.2.5 Google's Lexus RX Self-driving Vehicle

Volvo Drive Me Project

Looking forward to achieving the goal that no one will be seriously injured or killed in a new Volvo by 2020, the Drive Me project, a partnership between Volvo Car Group and Swedish Government, will start in 2017 by developing 100 self-driving vehicles on public roads. Currently, some autonomous driving features already exist in Volvo cars, such as automatic braking and adaptive cruise control. It is more encouraging that President of the Volvo Car Group has announced that "Volvo will accept full liability for the actions of its autonomous cars when in autopilot mode". It makes Volvo one of the first auto manufacturers in the world to make such a promise (Volvo, 2015).

Audi Piloted Driving

Bobby, the nickname of an Audi RS7, completed a lap on the Grand Prix track in Hockenheim without a driver in racing speed (top speed at 240 km/h). His brother Jack, An Audi A7, drove 550 miles from Silicon Valley to Las Vegas in autonomous driving mode. In addition to those exciting news, more road tests have also been conducted in Beijing and Shanghai, China by Audi autonomous driving cars. To complete those performances, radars, cameras, LiDAR units and ultrasonic sensors have to be installed on-board. Having evaluated this piloted driving technology, Audi aims to put it to use in next generation A8 Sedan (Audi, 2015).

Delphi

Delphi, an automotive technology supplier, has outfitted their technology into an Audi SQ5 to make it autonomous. This upgraded vehicle has successfully completed a 3,400 miles trip in 2015 from San Francisco to New York with 99% of the drive in fully automated mode. The realisation of hand free journey benefited from equipped long-range and short-range radars, three vision-based cameras, a localisation system, a full suite of Advanced Drive Assistance Systems (ADAS), etc. (Delphi, 2015).

VisLAB SRL

As a spinout company from the University of Parma, VisLAB tried to commercialise the results of their researches. VisLAB Intercontinental Autonomous Challenge (VIAC) is launched in 2010, a 13,000 km road test for autonomous vehicles. A convoy of eleven vehicles (four autonomous vans) drove from Parma in Italy to Shanghai in China. Later on, VisLAB has tested its BRAiVE autonomous vehicle in downtown Parma with 20 minutes run without any human interventions in 2013. In 2014 VisLAB unveiled the new autonomous vehicle prototype, DEEVA, which is equipped with fully integrated sensors (cameras, lasers, GPS and IMU) to enable covering a very detailed 360-degree view of the surroundings (Bertozzi et al., 2013, Broggi et al., 2013, VisLAB, 2014).

2.3.1.3 Market of AV Technology and Traffic Safety Applications

Automakers are targeting autonomous vehicles as the fastest growing market for the next ten years and upgrading autonomous features for their mid-range and luxury models. It is estimated that the number of total cars sold globally could exceed 90 million units in 2014 which contain 15 million autonomous vehicles or 17% market share and the market share is predicted to pass 50% by 2030. It is also estimated that autonomous features could bring in $30 billion in additional revenue in 2014 and is expected to expand to $250 billion by 2030, which leads to a growth of 15% in Compound Annual Growth Rate (CAGR)[9]. Taking the pioneer Google as an example, its AVs are projected to bring additional revenue of $80 billion by 2030 (Jiang et al., 2015).

The core of traffic safety improvement is accident damage control, and vehicle safety applications are changing radically from passive manner to active manner. The passive safety applications focus on crash mitigation and minimisation that enhance the safety of the driver or other road users by

[9] CAGR is the mean annual growth rate of an investment over a specified period of time longer than one year.

reducing the severity when an accident occurred. The classic example of passive safety applications is an airbag. By comparison, active safety applications concentrate on collision avoidance that warns the driver about an imminent accident by continuously monitoring the surrounding environment and transport network. For example, Anti-lock Braking System (ABS), adaptive cruise control (ACC), lane-departure warning (IMechE, 2012). In recent decades, vehicle safety applications have been more preventative rather than protective. Table 2.3 reviews and envisions some typical active safety applications that are adopted to crash preventing (Gao et al., 2014a). An autonomous vehicle may contain all listed applications as it is expected to take the place of the driver to keep eyes on ambient traffic environment even blind spots. Moreover, Vehicle-to-Vehicle (V2V) and Vehicle-to-Infrastructure (V2I) communications appear in future vehicle safety applications, and the details will be given in Section 2.3.2.

Table 2.3 The Cross-Correlation between Vehicle Safety Technologies and Crash Types, based on source: (Gao et al., 2014a)

	From 1971 to 2013												Today	Future			
Vehicle crash type	A	B	C	D	E	F	G	H	I	J	K	L	M	N	O	P	Q
Off-roadway	■	■		■			■			■	■		■	■	■	■	■
Rear end	■		■		■	■						■	■	■	■	■	■
Lane change							■		■		■		■	■	■	■	■
Opposite direction							■		■	■			■	■	■	■	■
Bicyclist											■	■			■		■
Crossing paths													■	■		■	■
Pedestrian								■				■			■		■
Animal	■													■	■		
Opposite								■								■	■
Other																■	■

A. Anti-lock Brakes B. Traction Control C. 3rd Brake Light D. Electronic Stability Control E. Forward Collision Warning
F. Adaptive Cruise Control G. Lane-departure Warning H. Park Assist and Backover Prevention I. Adaptive Headlights
J. Lane-departure Prevention K. Blind-spot Detection L. Forward-collision Avoidance M. Fatigue Warning N. Evasive manoeuvres
O. Exit-to-exit Highway Driving P. Vehicle-to-vehicle Communication (V2V) Q. Vehicle-to-infrastructure Communication (V2I)

2.3.1.4 Challenges of AV technology

To enhance the transport safety and mobility, a fully autonomous vehicle is the ultimate goal. Numerous technological breakthroughs have made AVs driving on the road, but there are many difficult challenges to overcome. The most burning technical barrier is making sense of the complex and dynamic driving environment as the driving environment is constantly changing and affected by many elements. Chris Urmson, the team leader of the winner of DARPA Grand Challenges in 2007, has concluded that a rich representation of driving environment would allow AV interacting better with other road users. After he joined in Google to lead the Google car team in 2007, Google cars are keeping running on the roads as much as they can. Hence, cars can continuously learn about the real driving environment (Urmson et al., 2008). On the one hand, independent behaviours of other road users, daily weather conditions, infrastructure conditions and congestions or crashes are out of AV's control. For example, AV may not be able to dodge jaywalking pedestrians or cyclists. The collapse of the road surface may lead to a loss of vehicle control. A heavy rain or fog could cause AV to collect insufficient information since all on-board sensors are calibrated and developed under normal environmental conditions (Sivak and Schoettle, 2015).

On the other hand, with regards to the four core technologies in AV sector, a few examples of the limitations of particular sensors are as follows:

- Camera: changes in ambient conditions (e.g., fog or rainstorms) pose challenges as camera systems calibrated to certain conditions
- LiDAR: less useful at long ranges and poor reflection of certain kinds of materials
- Radar: pedestrians are essentially invisible to a radar sensor
- GPS: severe obstruction in urban canyons
- INS: significant drift even over very short periods

Secondly, the challenge of mapping technology mainly comes from the difficulty to construct and maintain highly accurate maps. Roads change over time about revising speed limits, construction, etc. and it can be frustrating to a human. It is even severe to a car that relies on this data to safely interact with the outside world. For perception technology, the huge amount of data fed from dozens of sensors could bring lots of burdens to computation and decision making. For example, if a ball were to roll onto a road, a human driver might slow down since he expected that a child could follow. However, an AV cannot yet provide that level of inferential thinking. Finally, the challenges of communication technology could be a prohibitive investment on public infrastructure and cyber security and will be further discussed in next section. Each sensor has its limitations and sensor combination could cover some individual shortages. Also, integrated sensors can perceive more about the environment that can be learned purely from the sum of individual sensors' data (Anderson et al., 2014).

System integration also poses challenges in hardware, software and algorithm perspectives. As AVs use many sensors for full coverage, a challenge for the future is to figure out how AVs can be accomplished with fewer, cheaper and conformal mounted sensors. From the software integration point of view, the hurdle is to ensure sufficient robustness to component failures. For algorithmic integration, future work is to determine what information is relevant and how to display it to users (Campbell et al., 2010).

Rather than technical limitations, there are more non-technical hurdles to tackle. Tough autonomous vehicles have been technically implemented by sensor integration; the price is still one of the key constraints to the mass market. According to research conducted by J.D. Power and Associates in 2014, only 24 percent of consumers surveyed were interested in fully autonomous driving feature in their next vehicle when they were telling that the market price for such a feature is around $3,000 and that percentage rose slightly compared with 21% in 2013 and 20% in 2012 (Youngs, 2014). Nonetheless, the harsh

reality is that LiDAR alone costs Google car around $75,000 and the price for whole sensor suite could be $150,000 which is unaffordable to most of the drivers. Another challenge is the liability, i.e., who should be responsible when an AV crashes. For instance, Joshua Brown died on the 7th of May 2016 after his Tesla Model S crash while the Autopilot was activated, which is the first known death involving a self-driving car (Woolf, 2016). Even Volvo has announced to accept full liability; we cannot place the same expectation on all other automakers (Volvo, 2015). Additionally, legislation has become an inevitable issue since technological innovation often moves faster than legal or regulatory systems. Previous to 2011, the words like "self-driving car" or "autonomous vehicle" didn't exist in any state or federal legislation in the U.S. To fill in the legislative gaps and pave the way for the development of autonomous vehicles, Google has successfully lobbied for a change in the law in the U.S. state of Nevada to allow the passage of driverless cars on state roads in 2011. Nevada bill SB 140 explicitly permitted the use of handheld wireless communications devices for persons in a legally operating autonomous vehicle. Following the example of Nevada, California (in 2012), Florida (in 2012), Michigan (in 2013), Washington, D.C. (in 2013), North Dakota (in 2015) and Tennessee (in 2015) have enacted autonomous vehicles legislation in succession that an autonomous vehicle could run on state roads just under the circumstance that a licenced driver sit in the driver's seat and prepare to take control of the autonomous vehicle at any moment. Oppositely, nine states decided to prohibit the road test of AVs. The rest of the states are either considering or waiting to see the development of AV technology (Weiner and Smith, 2015). In Europe, some governments have taken actions to amend regulations for AV technology. For example, 4 U.K. cities Greenwich, Bristol, Milton Keynes and Coventry have get green light for AVs trial that allows testing AVs on public road and the government made clear that the test driver will be considered responsible for the safe operation of the test vehicle whether the vehicle is operating in autonomous mode or manual mode (U.K. DfT, 2015a). In Germany, the Federal Highway Research Institute (BASt) published a report to clarify the legal consequences of emerging AV technology. It demonstrated that each federal state could grant exemptions allowing the tests of AVs on a public road but the driver in the driver's seat

will have full legal responsibility for the safe operation of the vehicle (Gasser et al., 2013). The Federal Department of Environment, Transport, Energy and Communications in Switzerland (UVEK) allowed Swisscom's driverless car testing on specified routes in Zurich (Swisscom, 2015). Moreover, few more European countries, such as Netherlands, Finland, France, etc., have also amended their regulatory frameworks to facilitate the road tests of AVs (Smith, 2015).

Finally, the public acceptance of AV technology has to be analysed. Three focus groups conducted by KPMG in Los Angeles, Chicago and Iselin in 2013 showed positive attitude on using self-driving cars, and even passionate drivers[10] are open to self-driving cars. Candidates were asked about their likelihood to use self-driving cars using a 10 point interval scale, where 10 is equivalent to "most willing", and 1 is "not at all willing". Those who have a high passion for driving were initially resistant to use self-driving technology and gave a median score of 5.5. Nevertheless, their median score jumped to 8 when they were asked the same question again after the ensuing two-hour discussion about the pros and cons of self-driving cars. Not surprisingly, those who have a low passion for driving rated the highest initial score (the median score of 9) and even levelled up to full score after the discussion. Those who remain neutral on a passion for driving were also ambivalent about self-driving cars. Their initial median score was an 8 but ticked down slightly to a 7.5 after discussion (KPMG, 2013). Another survey conducted by University of Michigan Transportation Research Institute in 2014 comprehensively assessed public opinion about AVs in China, India, Japan, The U.S., The U.K. and Australia. Overall, the majority of respondents expressed a positive view regarding AVs except Japan gave a neutral opinion. More than 95 percent respondents of China and India were interested in owning or leasing a fully autonomous vehicle and also willing to pay extra for AV technology. Conversely, around 30 percent of respondents from other four countries did not

[10] The numerical ratings on passion for driving (10 point scale) are broke down into three categories: High (8-10), Medium (4-7) and Low (1-3).

have interests at all. Furthermore, more than 80 percent of respondents concerned about driving or riding in an AV and India showed strongest interests. However, most of the respondents expressed high levels of concern about safety issues, such as system failures and the self-driving vehicle cannot perform as well as human drivers. Particularly, the highest level of concern was given on "safety consequences of equipment/system failure" in China, India, The U.K. and Australia, while Japan and the U.S. considered more about "self-driving vehicles confused by unexpected situations" (Schoettle and Sivak, 2014a, Schoettle and Sivak, 2014b).

2.3.2 Connected Vehicles

Autonomous vehicles will eventually perceive an accurate driving environment from sensor systems. However, many researchers have suggested an alternative that the environment could communicate its state to the vehicle. Connected Vehicle (CV) technology uses wireless communications technology to establish connectivity between vehicles and other road users or infrastructure. So the notion of CV is not restricted to the vehicle but encompasses all traffic users and infrastructure. As mentioned before, poor weather conditions interfere with many on-board sensors of AVs that require line-of-sight. To supplement these sensors, CV technology is expected to supply roadway situational information (e.g., movement of nearby vehicles), reduce the cost and complexity of stand-alone AV solution, particularly in circumstances where weather compromises visibility. In doing so, there is no need to conjecture the next moves of surrounding vehicles; instead, they are willing to inform you directly.

On the other hand, CV technology (as the core of new generation ITS, i.e. cooperative ITS) pushes forward the evolution of ITS over last decades. CV technology is not limited to vehicles and leverage advanced information and communications technologies to enable communication among vehicles, infrastructure, pedestrians and portable devices. Promises held by CV

technology coincide with the capabilities of ITS described in the U.S. ITS Standards Program Strategic Plan (2011-2014) as follows (Sill et al., 2011):

> *"The application of advanced information and communications technology to surface transportation in order to achieve enhanced safety and mobility while reducing the environmental impact of transportation."*

2.3.2.1 The Development of V2X Technology

CV technology offers a powerful and transformative opportunity to establish connectivity that enables dynamic data exchange. CV technology could be categorised into Vehicle to Vehicle (V2V) technology, Vehicle to Infrastructure (V2I) technology as well as Vehicle to Pedestrian (V2P) technology and they are collectively called V2X technology. Hereafter V2X technology is equivalent to CV technology in this thesis. V2V technology transmits data between vehicles to enable applications that warn drivers about potential collisions. V2I technology transmits data between vehicles and the road infrastructure to enable a variety of safety, mobility and environmental applications. V2P technology transmits data among vehicles and pedestrians, cyclists, and other non-vehicle occupants equipped with portable devices. Fig.**2.6** gives a visual representation of V2X technology that vehicles, pedestrians and road infrastructure are linked one another (Sheldrick, 2014).

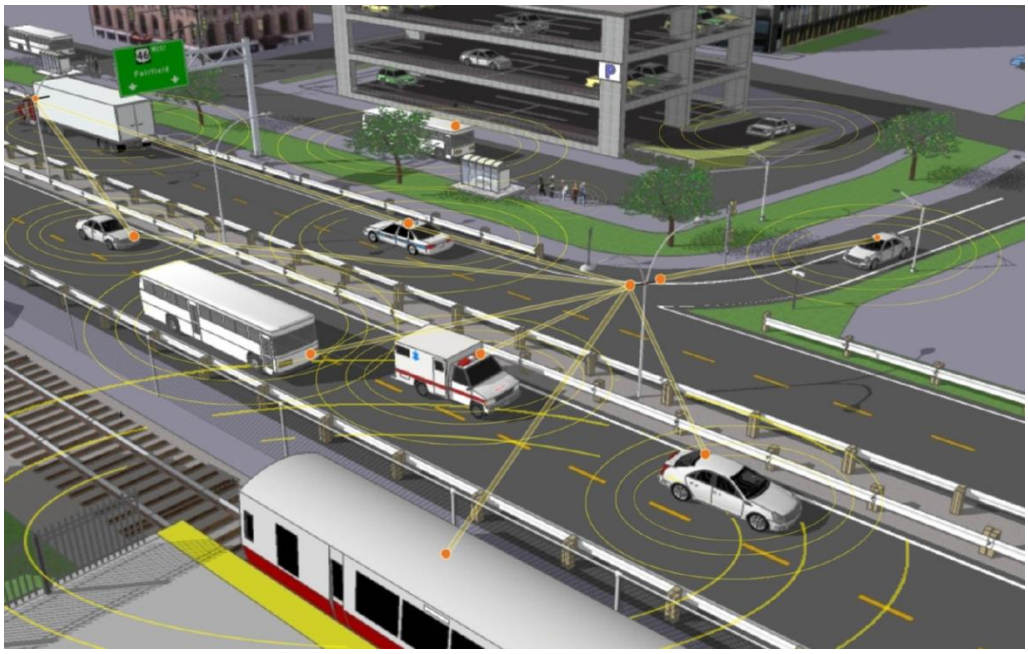


Fig.2.6Visual Representation of V2X Technology, based on source: (Sheldrick, 2014)

The origin of V2X research dates back the Automated Highway System (AHS) research which started in 1992 as part of the U.S. DoT's ITS initiative. The basic AHS concept was that the communication between sensors in the roadway and sensors on the vehicle enables partially automated systems and fully automated systems, and it was the first time that the roadway and the vehicle would be connected (Cheon, 2003). After AHS, DoT introduced the Intelligent Vehicle Initiative (IVI) in 1997 whose objectives were to prevent driver distraction and facilitate accelerated development of crash avoidance systems. IVI developed prototype crash avoidance systems using vehicle-based and infrastructure-based technologies which were supported by Dedicated Short Range Communication (DSRC), and it was the debut of DSRC applied to transportation (Hartman and Strasser, 2005). In 2003, the Vehicle Infrastructure Integration (VII) initiative was announced by DoT which represented the confluence of the result of IVI, an emphasis on improved traffic operations and the continuing evolution of telecommunication technology. The basic VII concept was that V2V and V2I communication could support safety and mobility applications and the success of the Proof of Concept provided the catalyst to create the connected vehicles initiative (Andrews and Cops, 2009). In 2009, DoT rebranded the VII program to

IntelliDrive to explore the potential applications of the newer wireless and computing technologies. The vision of the IntelliDrive program remained the same as the original vision of the VII program that to implement safety and mobility through wireless technology, but the approach to achieve the vision that revised to take advantage of new opportunities. Also, the IntelliDrive research comprised a major portion of the ITS Strategic Research Plan, 2010-2014 (U.S. DoT, 2010). To continue efforts on researching, testing and evaluating of V2X technology and ultimately transfer the next generation of ITS technology into the marketplace, DoT released the ITS Strategic Research Plan, 2010-2014 on December 8, 2009. The ITS Strategic Research Plan is designed to achieve a vision of:

> *"a national, multi-modal transportation system that features a connected transportation environment among vehicles of all types, the infrastructure, and portable devices that will serve the public good by leveraging technology to maximize safety, mobility, and environmental performance."*

In conclusion, the program intended to move the state-of-the-art of connected vehicle technology and applications forward with focuses on the highest priority of V2V and V2I communication for safety (RITA, 2009). Recently, the following ITS Strategic Plan, 2015-2019 was released in December 2014 and one of two primary strategic priorities has been defined as realising connected vehicle implementation which builds on the substantial progress made in recent years around design, testing, and planning for CVs to be nationally deployed (Barbaresso et al., 2014).

Not only in the U.S., the United Nations Economic Commission for Europe (UNECE) has also formulated their roadmap for promoting ITS that was summarised as 20 global actions between 2012 and 2020 of which V2V and

V2I communications are considered as key technical aspects of road transport (UNECE, 2012).

2.3.2.2 Market of CV Technology

In 2012, it was forecasted that more than 50% of vehicles sold worldwide in 2015 will be connected as well as more than 20% of sold vehicles will equip with embedded connectivity solutions. Moreover, the fitment rate of embedded connectivity features on new vehicles will rise rapidly to 90% and other new vehicles to be connected in multiple ways by 2025. In 2013, GSMA predicted that the global CV market will grow threefold from € 13 billion in 2012 to € 40 billion in 2018, among which there will be an almost sevenfold increase in the number of new vehicles equipped with connectivity features during that period. To be specific, the CV market will comprise € 24.5 billion from in-vehicle services (up from € 9.3 billion in 2012), € 6.9 billion from the sale of hardware (up from € 1.2 billion in 2012), € 4.5 billion from the delivery of telematics services (up from € 1.8 billion in 2012) and € 4.1 billion from the provision of connectivity (up from € 814 million in 2012) (GSMA, 2012, GSMA, 2013).

The studies conducted by PwC expected a 204 percent growth in overall revenue of CV technology, to € 122.6 billion between 2016 and 2021. Shown in Fig.**2.7**, the potential growth of CV technology could be categorised into seven aspects. Safety application, as always, will be the key selling point of CV technology that was projected to grow to € 49.3 billion by 2021 with 27 percent CAGR. Safety-related CV market will gain the largest market share at about 40 percent. To compensating the reliability of AV technology, the derived market of CV technology could grow to € 39.6 billion at the highest CAGR of 33 percent. Also, the entertainment applications will win the third biggest share of € 13.4 billion. What is more, well-being and vehicle management applications will have similar shares of € 7.6 billion and € 7.1

billion followed by €5.6 billion shares in mobility management application. Finally, the home integration applications would have the rest share of €66 million (Viereckl et al., 2015, Viereckl et al., 2014).

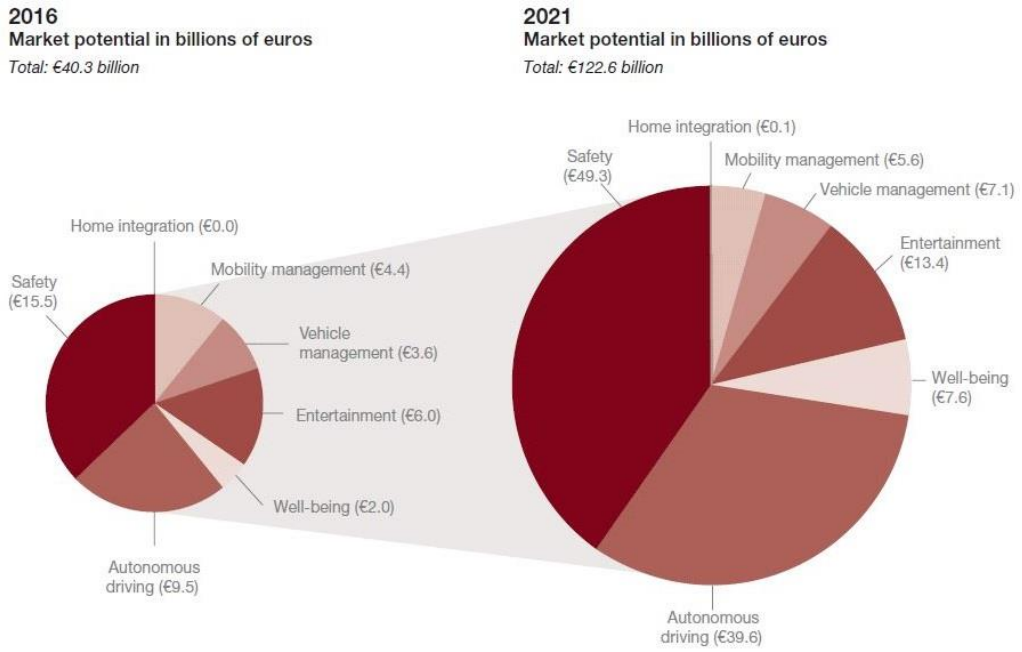


Fig.2.7 Estimated Market for CV Technology, 2016-2021, based on source: (Viereckl et al., 2015)

2.3.2.3 Communication Technology Support to the V2X Applications

Communication technology establishes a platform that allows vehicles to "talk" to each other and infrastructure in real-time, hence it is considered as the key enabling technology for the V2X applications. The DoT framed the definition of connectivity for the V2X applications to include both Dedicated Short Range Communication (DSRC) and non-DSRC technologies to provide an open platform which private industry can still be involved to exploit the potential of other technologies that may offer additional features. The research examined the potential of various communication technologies to support data delivery for the V2X applications. DSRC and cellular technologies were deemed as the most appropriate for such a purpose. Research led by DoT emphasises the need for DSRC communication for safety applications due to its low latency. Therefore, DSRC became the mainstream among those enabling communication technologies since key findings of VII program indicated the technical feasibility of DSRC for traffic safety application.

Meanwhile, the focus has broadened to cellular communication in recent years. As each technology has strengths and weaknesses, the future research will look at combinations of these techniques (Pina et al., 2012). In addition to above two supporting communication technologies, the Beyond Line-of-Sight (BLOS), a satellite communication technology that is previously mainly applied for military uses, has also been introduced in the ongoing i-Motors project to help vehicle remaining connected with sub-metre positioning accuracy, even when out of internet and GPS range (Meng, 2016).

2.3.2.3.1 DSRC Communications

DSRC technology could transmit information up to 27 Mbps[11] within 1,000 metres and was developed to support ITS safety and mobility applications through V2V and V2I communication technologies. The standard of DSRC is commonly referred as IEEE 802.11p which defines enhancements to IEEE 802.11a (Wi-Fi) for dedicated ITS applications by allocating unique operating frequency band, adjusting application environment and improving safety priority (Liu et al., 2005). Comparing with other technologies, DSRC could provide following main advantages (ITS JPO, 2015):

- **Low Latency:** Active safety applications must recognise surrounding vehicles and transmit messages in milliseconds without delay for collision avoidance.
- **Fast Network Acquisition:** Active safety applications require the immediate establishment of communication.
- **High Reliability:** Active safety applications require a high level of link reliability. DSRC performs well in high vehicle speed mobility conditions and immune to extreme weather conditions (e.g., rain, fog, snow).

[11] Mbps = Megabytes per second

Regarding the operation, the three major ITS research regions have different DSRC frequency allocation. In Report and Order FCC-99-305, the U.S. Federal Communications Commission (FCC) originally allocated 75 MHz of spectrum at 5.850-5.925 GHz for use by ITS vehicle safety and mobility applications in 1999 (FCC, 1999). In 2004, the FCC adopted DSRC to ensure interoperability in Report and Order FCC-03-324 (FCC, 2004). To compare with the U.S. DSRC standard, the European Telecommunications Standards Institute (ETSI) assigned 10 MHz at 5.795-5.805 GHz and 5. 805-5.815 GHz for pan-European and national Road Transport and Traffic Telematics (RTTT) applications respectively (ETSI, 2004). In Japan, 5.770-5.850 GHz has been allocated for V2V safety applications (Muller, 2009).

The development and implementation of V2X applications based on DSRC are primarily led by the U.S. DoT's Research and Innovative Technologies Administration (RITA) and the National Highway Traffic Safety Administration (NHTSA). As listed in Table 2.4, The continuous researches have enabled a large variety of V2X safety applications (Pina et al., 2012).

Table 2.4 The V2X Applications Based on DSRC, based on source: (Pina et al., 2012)

Category		Applications
Safety	V2V Communications for Safety	• Emergency electronic brake lights warning • Forward collision warning • Intersection movement assist warning • Blind spot warning • Lane change warning • Do not pass warning
	V2I Communications for Safety	• Intersection safety • Roadway departure prevention • Speed management • Transit safety and operations • Commercial vehicle enforcement and operations • At-grade rail crossing operations • Priority assignment for emergency vehicles
Mobility	Real-Time Data Capture and Management	• Prototype Data Environment • Research Data Exchange
	Dynamic Mobility Applications	• Freight Advanced Traveller Information System • Integrated Dynamic Transit Operations • Intelligent Network Flow Optimization • Multi-Modal Intelligent Traffic Signal System • Response, Emergency Staging and Communications, Uniform Management, and Evacuation • Enable Advanced Traveller Information System
Environment	Applications for the Environment: Real-Time Information Synthesis (AERIS)	• Eco-Signal Operations • Dynamic Eco-Lanes • Dynamic Low Emissions Zones • Support Alternative Fuel Vehicle Operations • Eco-Traveller Information • Eco-Integrated Corridor Management
Road Weather	Road Weather Connected Vehicle Applications	• Enhanced Maintenance Decision Support • Information for Maintenance and Fleet Management Systems • Traffic Signal Control and Variable Speed Limits for Weather-Responsive Traffic Management • Motorist Advisories and Warnings • Information for Freight Carriers • Information and Routeing Support for Emergency Responders

2.3.2.3.2 Cellular Communication

4G LTE (Fourth Generation Telecommunication, Long Term Evolution) cellular communication is the latest generation of wireless communication with much faster transmission speed. 4G LTE offers data rates of up to 100 Mbps and high mobility support of up to 500 km/h. The existing 4G LTE cellular infrastructure provides advantages for 4G-based V2X applications in comparison with the deployment of DSRC infrastructure. In December 2014, 4G network coverage was expanding rapidly and reached 26% of the world's population which included 90% of the population across developed countries and 15% in the developing countries. Furthermore, 4G coverage was expected to reach 95% of the population in developed countries while 60% in developing countries (GSMA, 2015a). In parallel with the U.S. DoT's effort on DSRC communication, cellular communication, especially 4G LTE, has been explored by the auto industry, IT companies and cellular carriers. More and more automakers have enabled 4G LTE connectivity in their new models, such as BMW ConnectedDrive services and GM OnStar 4G connection (GM, 2015b, BMW, 2015a). Furthermore, the higher communication requirements in the V2X application, such as higher frequency, a wider spectrum, drive the research of 5G. It is expected that 5G will be firstly deployed in 2020 and provide a number of benefits over the current 4G network which includes five times lower latencies, vastly improved network coverage and downloads speeds of up to 10 Gbps. By then, as low as 1 ms latencies provided by 5G will challenge the status of DSRC technology in the V2X applications (Kljai et al., 2016).

2.3.2.4 Challenges of CV technology

V2X technology holds enormous potential benefits on safety, mobility and environmental applications since NHTSA may mandate that future vehicles are equipped with DSRC devices. However, a variety of challenges slows down the deployment and implementation of V2X technology. The most challenge is the huge cost of deploying and maintaining the infrastructure. Researchers identify that DSRC field infrastructure deployment costs with an average of $17,600 per DSRC site (U.S. DoT, 2014b). Additionally, it was estimated

annual DSRC site operations, maintenance and replacement costs range from $1,950 to $3,050 (U.S. DoT, 2014a). As traffic safety is the overarching goal to apply V2X technology, it is a very great challenge to build up a reliable and trustworthy communication security system. The risk associated with cyber security can be categories into attacks on the users and attacks on the communication systems. Attacks on the users may cause users to make bad driving decisions resulting in an accident or congestion which will further reduce users' faith and acceptance of the V2X technology. On the other hand, attacks on the communication system lead to threats to user's privacy through tracking the location or driving route of a particular person (Kim et al., 2011).

Due to the fact that the essence of V2X technology is information sharing, the collection and sharing of location data also pose privacy risks. Firstly, the more devices and vehicles are connected, the more valuable the generated data is for advertisers, automakers, insurers, and so on. Consumers are generally unaware how their location data are shared with and used by third parties if there was not enough surveillance by law enforcement. Secondly, consumers could be at higher risk of theft or threats to personal safety with the lack of protection of shared data (U.S. GAO, 2012).

In response to requirements in the Middle-Class Tax Relief and Job Creation Act of 2012 (U.S. Congress, 2012), FCC allowed unlicensed devices to share the 5.9 GHz band of radio frequency spectrum that had been previously set aside for the use of DSRC-based V2X applications (FCC, 2013). Although existing FCC regulations are designed to ensure that unlicensed devices do not cause interference, intentional interference may jeopardise safety-related V2X applications.

Currently, DoT and various organisations have worked to standardise the message sets and associated performance requirements for DSRC which support a wide variety of V2X applications. However, there are different

DSRC standards in each country as discussed in Section 2.3.2.3.1. It is essential to develop technical standards to ensure interoperability of V2X technologies in different areas. Those standards should also define how a vehicle can connect and exchange data, in particular among various types of vehicles and devices. It should be noted that the definition of such standards was driven less by the technology but more by the need for multiple parties to work together (U.S. GAO, 2015).

Another challenge is manifested in liability issues. Because V2X technology offers warnings from surrounding vehicles, it could be harder to determine whether fault for a collision between vehicles equipped with V2X technology lies with one of the drivers, an automaker or a service provider. Furthermore, it is also difficult to determine liability if the V2X technology does not work appropriately, such as transmission delay, system hacker attack or inaccurate GPS readings (U.S. GAO, 2013).

Last but not least, public acceptance of CV technology should be evaluated as well which is important to promote and commercialise CV technology. A survey conducted by the University of Michigan Transportation Research Institute assessed public opinion about connected vehicles in the U.S., the U.K. and Australia. The majority of respondents (78.1% of total number) in all three countries had not heard of CVs, but more than half of the respondents had a positive impression of CV technology when they were introduced to CV technology, and approximately one-third of respondents had a neutral opinion. The vast majority of respondents (more than 80%) in all three countries thought that “safety” was the most important CV feature rather than “mobility” and “environment”. Therefore, they generally expressed higher level interests in safety-related benefits, such as fewer crashes and reduced severity of crashes. With regarding having CV technology in the own vehicle, more than 85% of respondents expressed either strong, moderate or slight interest. Moreover, 25% of respondents were willing to pay at least $500 for this technology in the U.S., and the corresponding amounts in the U.K. and Australia were $394 and $455,

respectively. However, more than 40% of respondents did not want to pay a penny.

2.4 Required Positioning Performance

2.4.1 Performance Evaluation Metrics

Various transportation applications pose variable requirements in positioning performance. The performance of a positioning system is characterised by a number of statistical quality parameters, i.e. accuracy, integrity, continuity and availability. Their hierarchy could be illustrated in Fig.2.8 (Hofmann-Wellenhof et al., 2007).

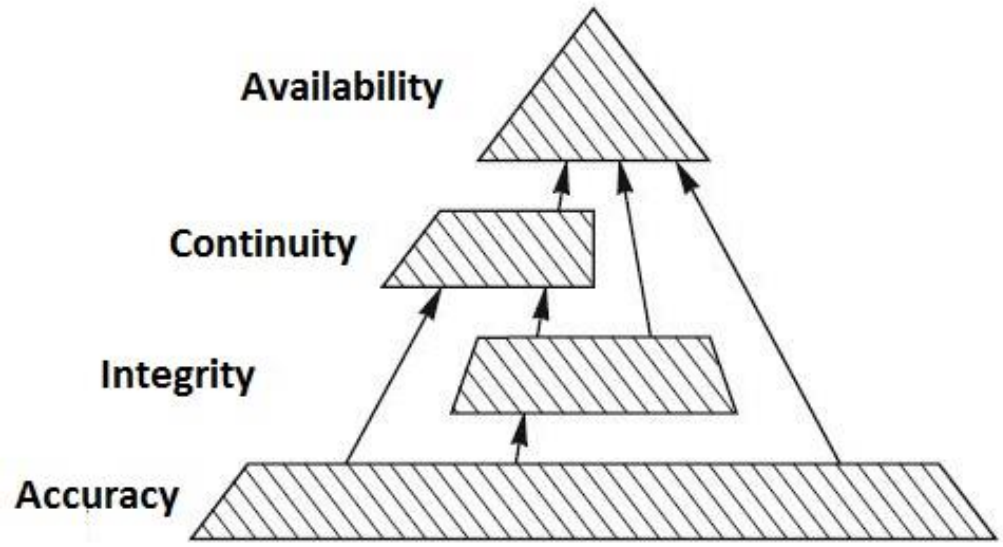


Fig.2.8 The Pyramid of Performance Metrics, based on source: (Hofmann-Wellenhof et al., 2007)

Accuracy

Accuracy is the most common parameter to evaluate the performance of a positioning system, and it is defined as the degree of conformance between an estimated or measured position and the reference value. Ideally, the reference value should be a known true value, but it is unable to get the absolute truth. Instead, the results from a positioning system that could achieve higher accuracy are regarded as the ground truth and used to assess the accuracy of the current positioning system. In civil applications, 1 σ and 2 σ error limits are

commonly used, which express the 63% and 95% percentages of errors, respectively, if the errors follow Gaussian distribution (Petovello, 2008).

Integrity

Integrity relates to the level of trust that can be placed on the information provided by the positioning system. It is also the ability of a system to provide timely and valid warnings to the users when the system should not be used. In practice, three sub-parameters are used to quantify the integrity. The first is integrity risk which expresses the probability that the system generates an unacceptable error without providing an alert. The second is an alert limit which defines the threshold of an unacceptable error that normally comes from requirements for particular applications. The third is time to alert which denotes the time gap between the occurrence of an unacceptable error and the activation of an alert (Petovello, 2008).

Continuity

Continuity is the ability of a positioning system to provide an output with the specified level of accuracy and integrity without non-scheduled interruptions during an intended period of operation. It should be noticed that the probability of false alert may affect continuity. A false alert is defined as the system issues an alert when there is no fault (Ochieng et al., 2003, Petovello, 2008).

Availability

Availability is an overall parameter of previous three parameters that expresses the ability of the system to provide a usable service to meet the requirement of an application. The service is available if all accuracy, integrity and continuity requirements are satisfied (Ochieng et al., 2003).

2.4.2 Required Positioning Performance for the V2X Applications

The Required Positioning or Navigation Performance (RPP or RNP) in transport domain has been well defined in aviation including limits on positioning availability, continuity, and integrity. However, the highest positioning accuracy is 185.2 metres which is far below some requirements of road transport applications (ICAO, 1999). There are currently no international agreements for positioning accuracy standards for ITS applications as the level of required positioning performance entirely depends on different V2X applications. Apparently, the pursuit of higher positioning performance can trigger various V2X applications which will eventually enable fully autonomous driving as an autonomous vehicle should support all V2X applications. However, it is important to identify the required positioning performance for each V2X application in order to obtain as many benefits as possible from existing V2X applications without taking the risk. The required positioning performance for a broad range of V2X applications varies a lot, and positioning accuracy requirements of different V2X applications are mainly reviewed in this thesis. Table 2.5 lists some applications involved in the SafeTRIP project (Lovas et al., 2011). Furthermore, the authors argue that 10 Hz of positioning solution with an accuracy of no worse than 50 cm is desirable for vehicular safety critical applications (Shladover and Tan, 2006). Other researchers state that the accuracy of 30 cm in each dimension will suit to the cooperative automated overtaking (Alieiev et al., 2015).

Table 2.5 Positioning Requirements for SafeTRIP Services, based on source: (Lovas et al., 2011)

Application	Description	Required Accuracy
Fleet Management	This service provides tracking of commercial vehicles such as coaches, trucks and patrol vehicles	50 m
Emergency Call	This service can trigger an emergency call if a collision is detected on a vehicle. By pressing a button, the vehicle position along with other information is then relayed to the authorities or a third party.	1-15 m
Stolen Vehicle Tracking	This service allows a stolen vehicle to be tracked when the theft is reported	1-15 m
Road Side Assistance	This service allows the occupant to request aid in case of breakdown or medical emergency	1-15 m
Coach Tracking	This service will provide the coach company to track its coaches across Europe	50 m

Moreover, another research generalises the positioning accuracy requirement of the V2X applications as following three categories: which road, which lane and where in the lane (Basnayake et al., 2010). In the case of which road, accuracy is only required to distinguish the road travelled. For instance, it is sufficient to know whether a vehicle is on the service road or the parallel freeway in road user charges application. The common accuracy requirement is better than 5 metres. In the case of which lane, the required accuracy should be able to identify entities with lane-level resolution. For example, blind spot warning application needs to know which lane the surrounding vehicle is in the blind spot. The common accuracy requirement is 1.5 metres or better which are approximately half of a lane width. In the case of where in the lane, the accuracy requirement should be better than 1 metre and even decimetre or centimetre which enable autonomous driving. A similar positioning accuracy requirement classification can be found in the report published by Austroads,

which presents road level, lane level, and where in the lane level accuracies corresponding to the above classification respectively (Ballingall, 2013). Although several studies have been conducted to explore the required positioning performance for the V2X application, no current standards and specifications have been established to define the requirement of positioning performance. In this thesis, where in the lane-level positioning accuracy, i.e. sub-metre level, has been set as the target to achieve.

As mentioned in the beginning in Section 1.1.2, the communication technology is an essential fundamental technology for vehicular cooperative positioning solution. Therefore the communication performance is also a part of the required positioning performance for the V2X application. In the whitepaper published by 5GPPP, few communication-related parameters have been designated as the Key Performance Indicator (KPI) for the V2X application, such as the latency, data rate and communication range (5GPPP, 2015). Moreover, the similar requirements have also been identified in (Papadimitratos et al., 2009), for example, the tolerable latency is between 50 ms to 500 ms, and the desired communication range is less than 250 m. Contrasting to the situation of lack of required positioning performance standards, some communication standards have been set to define the necessary message to be transmitted in the V2X applications. For instance, the Cooperative Awareness Messages (CAM) in (ETSI, 2014a), the Decentralised Environmental Notification Messages (DENM) in (ETSI, 2014b) and the Basic Safety Messages (BSM) in (SAE, 2016).

2.5 Summary

This chapter firstly explains three motivations to develop ITS application: safety improvement, congestion relief and emission reduction. The ITS safety applications are always given to top priority because life is precious. This chapter then introduces the new generation ITS applications based on AV and CV technologies. Both technologies apply to the same concept, i.e. transportation environment perception, and AV technology detects

environment through integrated sensors whereas CV technology learns surrounding road users' next moves via communications. Moreover, this chapter takes a glance at the huge market potential of both AV and CV technologies and lists several typical applications. Also, the underlying technologies of AV and CV technologies are introduced separately. Moreover, this chapter lists main challenges of both AV and CV technologies included both technical (such as positioning and communication difficulties) and non-technical (such as regulation and standardisation) limitations. In this thesis, the research focuses on the positioning difficulty due to obstruction, in particular for the Line-of-Sight (LOS) technology GPS. Therefore, the system integration for robustness improving is considered. Finally, the required positioning performance of the V2X applications has been discussed. Although the formulation of standards is behind the development of CAV technologies, academia has paid attentions on it and generates preliminary categories of required positioning performance according to the V2X applications.

Chapter 3 Positioning Technologies Supporting to the V2X Applications

3.1 Overview

As discussed in the previous chapter, positioning technology is one of the core technologies for the V2X applications. To achieve better positioning performance, multi-sensor integration is applied for maintaining the superior performance of the V2X applications. Hence, the selection of positioning sensor should be thought thoroughly including cost, accuracy, applying requirement, etc. With the global coverage and increasing constellations, GNSS have been implemented extensively in transportation application. On 17 July 1995, GPS became the first member of GNSS family by announcing its Full Operational Capability (FOC) by the Air Force, U.S. In recent decades, Russia, Europe and China have also joined in the GNSS family. Up to now, GNSS constellations are comprised four systems: GPS, GLONASS, Galileo and BeiDou. Compared with other positioning technologies GNSS hold the unbeatable advantages in transportation applications. However, GNSS do not usually perform well in urban areas since it is inherently a Line-of-Sight (LOS) technique. Other positioning technologies are therefore introduced to compensate GNSS for transportation applications in urban areas. Particularly, Ultra-Wideband (UWB) positioning system has been treated as a potential complementary due to its high accuracy and resistance to multipath.

3.2 Positioning Techniques for Multi-sensor Integration

In order to improve positioning performance for the V2X applications, an increasing number of positioning techniques can be integrated into a positioning system. Table 3.1 lists most of the relevant sensors which could be considered for sensor integration (Grejner-Brzezinska et al., 2016).

Table 3.1 Candidate Sensors Used in Integrated Positioning Solutions, based on source: (Grejner-Brzezinska et al., 2016)

Technique	Sensor	Operating Range	Typical Accuracy (m)	Requirement
Radio Frequency	GNSS	Long	10^{-2}-10^{1}	LOS
	Pseudolites	Medium	10^{-2}-10^{1}	LOS
	Signal strength-based WLAN	Short	10^{-1}-10^{1}	
	Fingerprinting WLAN	Short	10^{-1}-10^{1}	
	Ultra-Wideband	Medium	10^{-1}-10^{0}	
IMU	Accelerometers	N/A	10^{-2}-10^{3}	
	Gyroscopes	N/A		
Optical	2D image-based (mono)	Medium/short		LOS, light
	Multi 2D image-based (stereo and multi-ray)	Medium/short	10^{-2}-10^{1}	LOS, light
	3D image-based	Medium/short	10^{-2}-10^{1}	LOS
Others	Digital compass/magnetometer	N/A		No magnetic disturbance
	Acoustic	Short	10^{-1}-10^{1}	
	Digital barometer	Medium	10^{-1}-10^{0}	
	Odometer/step sensor	Short		

GNSS is an unarguably essential technique for transportation applications in order to provide position information and other candidate positioning techniques listed above could be integrated with GNSS for a more reliable and accurate position solution. Radio Frequency (RF) sensors are fundamental to positioning and navigation and usually classify into satellite-based and terrestrial-based categories. The RF sensor relies on a pre-deployed network of radio transmitter systems and supporting infrastructure for the purpose of providing the positioning solution in a global or local frame. Most RF sensors require Clear Line-of-Sight (CLOS) operations, such as GNSS. As mentioned

in Chapter 1, this is the main reason limit the positioning performance of GNSS in an urban canyon. Both Signal strength-based and fingerprinting Wireless Local Area Network (WLAN) focus on indoor positioning applications as its limited coverage which makes WLAN not applicable for the V2X applications.

In contrast to RF sensor, an Inertial Measurement Unit (IMU) sensor is based on physical measures so that it is infrastructureless. The IMU is becoming the primary sensor to be assisted by GNSS to provide more trustful position solutions. However, the price of an IMU sensor is usually not customer friendly and differs greatly depending on the required performance. For example, a tactical grade IMU cost tens of thousands of pounds which are same as a new family car.

Optical sensors have also been integrated with GNSS and IMU for positioning purpose. Light Detection and Ranging (LiDAR) and camera not only have the ability of positioning augmentation also provide rich information acquisition in the meantime. It is worth noting that the optical sensors are highly scene-dependent and are usually supported by matching pre-collected information at known coordinate for absolute positioning (Grejner-Brzezinska et al., 2016, Zsedrovits et al., 2014, Gao et al., 2015). It makes the weather condition, for instance, fog, rain, snow, etc., becoming a variable to affect final position output. Moreover, computation burden brought by image processing and exorbitant price of LiDAR are certain factors that have to been considered for the V2X applications.

As assessed above, the UWB positioning technique is selected to integrate with GNSS in this research. Firstly, UWB is an RF sensor which is same nature as the GNSS, and this makes the modelling of observations easier. Secondly, the achievable accuracy of UWB is centimetre level which is better than that of GNSS pseudo-range observations. Thirdly, the UWB signal owns the

capability of penetration and multipath suppression which is perfectly suitable for the NLOS situation and the urban canyon.

3.3 Global Navigation Satellite Systems (GNSS)

3.3.1 The Expanding GNSS Landscape

GNSS has been woven into nearly every application, especially involved in some hot topics, such as smart cities, big data, internet-of-things and machine-to-machine communications. GNSS bred an enormous downstream market that was forecasted to increase by a 7% CAGR from more than €200 billion in 2013 to almost €300 billion in 2023. By 2014, 260 million GNSS devices have been used for road applications which obtained a 38% market share (ESA, 2015a). GNSS became an essential element in the future of Intelligent Transportation Systems (ITS). "The promise of GPS technology for increasing safety and security, reducing congestion, and improving efficiency are limitless," said by Jeffrey N. Shane, Former Under Secretary for Policy, the U.S. Department of Transportation, "Quite simply, GPS has become the enabling technology for transportation." (National Coordination Office, 2015a). The U.S. Department of Transportation has taken the initiative and involved GPS into multiple applications as early as 1995, such as aviation, maritime and waterways and highway and construction, etc. (Pace et al., 1995). Recently, GPS was also employed as one of the essential underlying technologies in the latest V2X applications.

3.3.1.1 Global Positioning System (America)

On 17 July 1995, the Full Operational Capability (FOC) of GPS has been declared by the Air Force, U.S. Although the military applications are the initial purpose, the importance of civilian applications has appreciated especially since the U.S. government announced that Selective Availability (SA), which intentionally degrades the GPS signals availability to the public, has been discontinued since 2nd May 2000. Consequently, the civilian users of GPS will be able to pinpoint locations up to ten times more accurately than

before which stimulated the rapid growth of the market for civilian applications (Hofmann-Wellenhof et al., 2007).

To meet growing demands and stay competitive internationally, the GPS modernisation program is committed by the U.S. government since 2000. Lockheed Martin Corporation competed with the Boeing Company on signing Block IIR (M) ("Modernized"), Block IIF ("Follow-on"), and GPS III satellite contracts with the U.S. Air Force. As a result, the Block IIR (M) contract of 8 Space Vehicles (SVs) was awarded to Lockheed Martin, and the eighth satellite has been launched until 17 August 2009 (Los Angeles Air Force Base, 2015). On the other hand, the Block IIF contract has been won by the Boeing Company which includes the delivery of 12 SVs. The twelve launches began with the first launch on 27 May 2010 and had been completed with the final launch on 5 February 2016 (Boeing, 2016). Aiming to deliver signals three times more accurate than current GPS spacecraft and provide military users up to eight times improved anti-jamming capabilities, the U.S. Air Force has signed a series of GPS III satellite contracts with Lockheed Martin from 2008 to 2014 (Lockheed Martin, 2015). As of 27 September 2016, 12 legacy (12 IIR) and 19 modernised (7 IIR(M) and 12 IIF) operational satellites constitute the 31 satellites GPS constellation (Coast Guard Navigation Center, 2016). It is awkward that the main reason why few produced modernised satellites are still laid on the ground is the overage service of old GPS satellites. For example, 12 Block IIR satellites, launched before 2004 with 7.5 years design lifecycle, are still holding on their positions and providing proper service since they have been launched. It impedes the implementation of GPS modernisation as the old satellites cannot apply the new technology and transmit the new signals.(National Coordination Office, 2016).

As a major focus of the GPS modernisation program, new civilian signal transmitters are embedded into GPS modernisation satellites. The second civilian signal L2C is designed specifically to meet commercial needs and is featured with GPS Block IIR (M) satellite and every GPS satellite fielded since

the first launch of GPS IIR (M) in 2005 has included an L2C transmitter. Combining L1 C/A and L2C signal in a dual-frequency receiver, it enables ionospheric correction, a technique that boosts accuracy by eliminating the ionospheric error. As one of the major GNSS error sources, the ionospheric error will be discussed in Section 3.3.3.2. In addition, a higher effective power of L2C enlarges its capability to penetrate trees and even walls. The third civilian signal L5 is exclusively designed for aviation safety services and other high-performance applications and featured with GPS Block IIF satellite. Through a technique called trilaning, the combination of L1 C/A, L2C and L5 may enable sub-metre level accuracy without augmentations (National Coordination Office, 2015b). On 31 December 2014, the Air Force began broadcasting navigation messages on both L2C and L5 signals which allow user receiving. The latest generation civilian signal L1C is also designed to enable interoperability between GPS and other satellite navigation systems and will start to broadcast after the future launch of GPS III satellite in the spring of 2018 (Whitney, 2016). A problem still stands in the way of the launch of GPS III satellites that the GPS Next-Generation Operational Control System, known as GPS OCX, is years behind schedule and massively overspend. The OCX system will command all GPS satellites and manage all signals in order to provide more secured and resilient GPS operations. So the GPS III satellites would not be added to the constellation until OCX is activated (Chaplain et al., 2015).

3.3.1.2 GLONASS (Russia)

As a product of Soviet-American space race, the former Union of Soviet Socialist Republics (USSR) developed its GNSS, namely GLONASS. GLONASS officially declared operational on 24 September 1993, but the 24 satellites constellation was completed for the first time on 18 January 1996. Unfortunately, the number of available GLONASS satellites continuously dropped due to the financial pressures from 1996 when it just became the second full global coverage positioning and navigation system. The fall of the available number of satellites achieved its minimum in 2001 with around 7 satellites which led to the disability of global coverage. To revive the

GLONASS, a guaranteed funding was injected from 2002 to 2011, which is named as the Federal GLONASS Mission Oriented Program. It is worth to notice that GNSS equipment and technology implementation for transport is one of the six directions and subprograms of this GLONASS Mission Oriented Program (Hofmann-Wellenhof et al., 2007). By the end of 2011, GLONASS completed a long trek to regain FOC and followed up with an $11.81 billion budget approved for through 2020 for further development (Gibbons, 2012).

The GLONASS modernisation mission started with the launch of the first GLONASS-M satellite on 12 December 2003. Followed a series of launches of the GLONASS-M satellite from 2004 to 2011, GLONASS completed its second FOC. As a part of GLONASS modernisation, GLONASS started to transmit Code Division Multiple Access (CDMA) navigation signals, the way of GPS currently uses, coherently with existing Frequency Division Multiple Access (FDMA) signals. The first satellite of the third generation, GLONASS-K1, was successfully launched on 26 February 2011, which started to transmit CDMA signal while the second one was launched on 1 December 2014. As of 27 September 2016, there are 24 operational satellites in GLONASS constellation, including 22 GLONASS-M and 2 GLONASS-K1 satellites (Bonnor, 2012, Federal Space Agency, 2016).

3.3.1.3 GALILEO (Europe)

To develop European satellite positioning system and avoid the monopoly of GPS, the European Commission (EC) decided to develop its system in 1998. With the support of the European Space Agency (ESA), the release of the Communication “Galileo-Involving European a New Generation of Satellite Navigation Services” spelt the beginning of Galileo project (EC, 1999). Suffering from various delays to development, Galileo project took its step towards entering the In-Orbit Validation (IOV) phase by launching a pair of IOV-1 satellites on 21 October 2011 and the second pair of IOV-2 satellites on 12 October 2012. On 12 March 2013, the entire self-sufficient Galileo system officially showed its capability of positioning, where observed in the European

Space Research and Technology Centre (ESTEC) (ESA, 2015b). Following on the encouraging news, ten Galileo FOC satellites (FOC-1 to FOC-10) have been sent into the orbits, two at a time, on 22 August 2014, 28 March 2015, 11 September 2015, 17 December 2015 and latest 24 May 2016, respectively (EC, 2016). As of 10 January 2017, eleven operational satellites (3 IOV and 8 FOC satellites) in Galileo constellation (European GNSS Service Centre, 2017). Although it has a long way to go to fill the orbits up with 30 satellites according to the original plan, ESA expects to finish all launches by 2020. When fully operational Galileo will provide five services on a global base, including (Nurmi et al., 2015):

- Open Service (OS): provides position and timing services competitive with other GNSS systems (around 1 metre accuracy).
- Public Regulated Service (PRS): provides position and timing to government-authorised users for sensitive applications, e.g. energy, telecommunications and finance.
- Commercial Service (CS): provides access to two additional encrypted signals to allow for higher performance (sub-decimetre level accuracy).
- Search and Rescue Service (SAR): provides a global satellite-based search and rescue distress alert detection system.
- Safety of Life Service (SoL): improves the open service performance for safety-critical applications, such as running trains, guiding cars, navigation and aviation.

3.3.1.4 BeiDou Navigation Satellite System (BDS) or Compass (The People's Republic of China)

In the early 1980s, the People's Republic of China decided to develop its satellite positioning system. With three successful launches in October and December 2000 and May 2003, BeiDou-I has been established and further enhanced by sending up the fourth satellite in February 2007 (Bonnor, 2012). In 2003, China committed to invest $270 million for participating in the

development of Galileo project, but it has been forced out of the major decision-making role because of security concerns which led to the development of BeiDou-II (Gutierrez, 2012). Based on the predecessor of BeiDou-I, BeiDou-II is being extended to global coverage. Beginning with the first BeiDou-II satellite launch in April 2007, 23 BeiDou-II satellites are currently orbiting the earth with the latest successful launch on 12 June 2016. In December 2012, China Satellite Navigation Office released Interface Control Document (ICD) and declared the FOC for regional services later on at the end of that month. Since BDS was officially brought into service, its applications were progressively woven in the field of transportation, marine fisheries, weather forecasting, disaster relief and reduction, etc. In particular, BDS also played an important role in the Beijing Olympic Games in 2008 and the Shanghai World Expo in 2010 (China Satellite Navigation Office, 2015). China announced that the system would provide global coverage (a constellation consists of 35 satellites, which include 5 Geostationary Orbit (GEO), 3 Inclined Geosynchronous Orbit (IGSO) and 27 Medium Earth Orbit (MEO) satellites) by 2020, or even early (Murfin, 2015).

3.3.1.5 Quasi-Zenith Satellite System (QZSS) (Japan)

The Quasi-Zenith Satellite System (QZSS) is a Satellite-Based Augmentation System (SBAS) for the GPS that would be receivable in Japan. QZSS is utilised in an integrated fashion to complement GPS in Japan so that QZSS send signals of the same frequency and same timing as GPS. The first satellite 'Michibiki' was launched on 11 September 2010. The cabinet then decided in September 2011 that the government would establish a four-satellite constellation by 2018 and complete a seven-satellite constellation in the future (Office, 2017b). QZSS is primarily designed to increase the availability of GNSS as well as tackle the multipath errors in Japan's numerous urban canyons (Office, 2017a). The highly elliptical orbits of the quasi-zenith satellite allow the satellite to dwell for more than 12 hours a day with an elevation above 70 degree which helps to improve the situation of urban obstructions (Bonnor, 2012). The performance of GPS augmentation using QZSS have been

evaluated and particularly show accuracy improvement in the simulated urban canyon environment (Sato et al., 2011, Wu et al., 2004, Takasu et al., 2009)

3.3.2 Reference System

Due to the fact that all GNSS systems have a particular coordinate system and a time system, it is important to choose the correct systems when calculating the satellite and user coordinates, especially when we integrate GNSS system with other positioning technologies for cooperative positioning. In this thesis, only GPS system is integrated with other sensors. Thus, the following sections will focus on the characteristics of GPS as a representative and just give a brief summary of other three GNSS systems.

3.3.2.1 Coordinate System

The GPS terrestrial reference system is the World Geodetic System 1984 (WGS-84) which includes an Earth-centred, Earth-fixed (ECEF) reference frame that is originally bound by 1500 terrestrial sites and has been used for GPS since 1987. Then remarkable differences between WGS-84 and the International Terrestrial Reference Frame (ITRF) were revealed, where the accuracy of the GPS reference stations was in the range of 1 to 2 metres compared with the centimetre level accuracy of the ITRF (Malys and Slater, 1994). WGS-84 was unremittingly revised in 1994, 1996 and finally aligned to ITRF in 2002. With respect to ITRF2005, where the number specifies the release year, the refined WGS-84 (G1150), where the number 1150 refers to the GPS week number, shows insignificant systematic differences of 1 centimetre. Hence, both frames are virtually identical (Hofmann-Wellenhof et al., 2007).

GLONASS' coordinates are given in the Parametry Zemli 1990 (PZ-90) ECEF reference frame. According to the GLONASS modernisation plan, the updated version PZ-90.11 Geodetic Reference System aligned to the ITRF at the millimetre level (Lyskov, 2013). GALILEO relies on a geocentric Cartesian

reference frame as defined by the Galileo terrestrial reference frame (GTRF) which differs from the most recent ITRF by no more than 3 centimetres (2-sigma) (Hofmann-Wellenhof et al., 2007). BeiDou coordinate system, the China Geodetic Coordinate System 2000 (CGCS 2000), is realised by China Terrestrial Reference Frame 2000 (CTRF2000), which is referred to ITRF97 with the epoch of 2000.0. Although there is little difference with GPS WGS-84 because of different flattening of the defined ellipsoid, the caused biggest offset in the equator is within 1 millimetre which may be neglected. That is, the coordinate references of BeiDou system and GPS are consistent (Yuanxi et al., 2012).

3.3.2.2 Time System

GPS applies its time frame which relates to the atomic time scale implemented by the atomic clocks in the GPS satellites and the GPS ground control stations. GPS time has a constant offset with Temps Atomique International (TAI), where TAI is always ahead of GPS time by 19 seconds. Also, GPS time is coincident with Coordinated Universal Time (UTC), which we are using in daily life, at the GPS standard epoch 6 January 1980. It is worth to note that TAI and UTC differ by an integer number of seconds which is continually accumulated by an occasionally added leap second (Hofmann-Wellenhof et al., 2007). The most recent leap second inserted on 31 December 2016 at 23:59:60 UTC caused that TAI is ahead of UTC by 37 seconds. Hence, GPS time is ahead of UTC by 18 seconds.

Unlike other three GNSS systems, GLONASS time is periodically corrected to an integer number of seconds simultaneously with UTC corrections that are performed once a year (1.5 years). Consequently, there is no integer second difference between GLONASS time and UTC (Soviet Union), however, there is constant three-hour that GLONASS time is ahead of UTC (Soviet Union) due to GLONASS control segment-specific features. Moreover, the GLONASS time is now behind of TAI by 37 seconds (RISDE, 2008). The GALILEO System Time (GST) start epoch is 00:00:00 UTC on 22nd August 1999 and is

defined as 13 seconds before this start epoch. Therefore, GST is 19 seconds behind of TAI which is synchronised with GPS time within the nanoseconds order of magnitude (GSA, 2016). BDS time uses 00:00:00 UTC on 1st January 2006 as the start epoch, thence, BDS time is always 33 seconds behind of TAI and is now 4 seconds ahead of UTC (CSNO, 2013). In a nutshell, GPS, Galileo and Beidou systems adopt a continuous time scale starting at different epochs while GLONASS aligns with UTC by regularly calibrating.

3.3.3 Observations and Performance

3.3.3.1 GPS Observations

Most of the GNSS systems use one-way communication, e.g. satellite transmits a signal while millions of receivers passively receive it. In concept, GPS systems provide ranges between satellites and receivers which are deduced from the transmission time of a satellite generated signal from a satellite to a receiver. GPS offers two types of observations for location determination: code and phase pseudo-ranges.

The code pseudo-range and phase pseudo-range at epoch t between a satellite and a receiver, where indicate by superscript "s" and subscript "r", can be modelled respectively as Eq. 3.1 and Eq. 3.2:

$$PR_r^s(t) = \rho_r^s + c(\delta t_r - \delta t^s) + dion_r^s + dtrop_r^s + \varepsilon_r^s \tag{3.1}$$

$$\phi_r^s(t) = \frac{1}{\lambda}\rho_r^s + f(\delta t_r - \delta t^s) - N_r^s + \frac{1}{\lambda}dion_r^s + \frac{1}{\lambda}dtrop_r^s + \psi_r^s \tag{3.2}$$

Where c means the speed of light in a vacuum; δt_r and δt^s reflect receiver and satellite clock offsets; $dion_r^s$ and $dtrop_r^s$ point to the ionospheric and tropospheric errors associated with the transmission of the signal through the atmosphere; ε_r^s and ψ_r^s denote un-modelled effects and random errors in

pseudo-range and phase. f and λ denote the carrier frequency and wavelength; N_r^s is the integer ambiguity. ρ_r^s is the real geometry range between satellite and receiver and can be calculated as Eq. 3.3:

$$\rho_r^s = \sqrt{(X^s - X_r)^2 + (Y^s - Y_r)^2 + (Z^s - Z_r)^2} \tag{3.3}$$

Where the X, Y and Z coordinates of satellite and receiver are distinguished by superscript "s" and subscript "r".

In order to reduce and eliminate the effect of the error sources in both code and phase pseudo-ranges, observation differencing technique, known as Differential GPS (DGPS), is employed to improve the positioning accuracy. DGPS technique can be classified as Single Differencing (SD) and Double Differencing (DD). As only code pseudo-range observation is used in this thesis, any pseudo-range mentioned hereafter indicates code pseudo-range and just the code pseudo-range is discussed. For the SD technique, a reference station with known coordinate is required. Consider the observation equations for reference station a and rover receiver b observing same satellite i; the code pseudo-range can be expressed as Eq. 3.4:

$$\begin{aligned} PR_a^i(t) &= \rho_a^i + c(\delta t_a - \delta t^i) + dion_a^i + dtrop_a^i + \varepsilon_a^i \\ PR_b^i(t) &= \rho_b^i + c(\delta t_b - \delta t^i) + dion_b^i + dtrop_b^i + \varepsilon_b^i \end{aligned} \tag{3.4}$$

The SD observation is defined as the difference between two above pseudo-range observations as Eq. 3.5:

$$\Delta PR_{ab}^i(t) = \Delta\rho_{ab}^i + c\Delta\delta t_{ab} + \Delta dion_{ab}^i + \Delta dtrop_{ab}^i + \Delta\varepsilon_{ab}^i \tag{3.5}$$

As can be seen that it has one fewer parameter to deal with by forming SD equation, i.e. the satellite clock error is common to the two pseudo-ranges and cancelled out in the difference. Furthermore, the ionospheric and tropospheric errors are reduced and could be neglected in the case of short baseline.

The DD technique, consider the SD observation equations for reference station a and rover receiver b, observing satellite i and j:

$$\begin{aligned}\Delta PR_{ab}^{i}(t) &= \Delta\rho_{ab}^{i} + c\Delta\delta t_{ab} + \Delta dion_{ab}^{i} + \Delta dtrop_{ab}^{i} + \Delta\varepsilon_{ab}^{i} \\ \Delta PR_{ab}^{j}(t) &= \Delta\rho_{ab}^{j} + c\Delta\delta t_{ab} + \Delta dion_{ab}^{j} + \Delta dtrop_{ab}^{j} + \Delta\varepsilon_{ab}^{j}\end{aligned} \quad 3.6$$

And the DD observation is defined as the difference between two above SD observations as Eq. 3.7:

$$\nabla\Delta PR_{ab}^{ij}(t) = \nabla\Delta\rho_{ab}^{ij} + \nabla\Delta dion_{ab}^{ij} + \nabla\Delta dtrop_{ab}^{ij} + \nabla\Delta\varepsilon_{ab}^{ij} \quad 3.7$$

To compare with the SD observation, the receiver clock error is eliminated, which is common to the SD observations. However, a point worth mentioning is that unmodelled ionospheric and tropospheric errors are slightly increased by double differencing as compared to SD observation (similarly, it could be neglected in the case of short baseline). Moreover, the random errors are effectively doubled as compared with the original pseudo-range observation (Hofmann-Wellenhof et al., 2007, Li et al., 2012).

3.3.3.2 GPS Positioning Performance

The accuracy of a GPS position solution entirely depends on the quality of the GPS observations as well as satellite-user geometry. GPS utilise the concept of Time of Arrival (TOA) ranging to determine user's location. This concept

entails measuring the time it takes for a signal transmitted by a satellite at a known location to reach a user receiver. Therefore, it is important to find out any factors may affect the consuming time of signal transmission and the satellite-receiver ranging. Look at the journey of a GPS signal: firstly generated by satellite, then broadcasted through the atmosphere and finally arrived at a GPS receiver. Each step may create errors, and the ultimate goal is to minimise and even eliminate all of them to achieve a more accurate position. These errors can be classified into three groups, namely satellite-related errors, atmospheric propagation effects and receiver-related errors. Specifically, satellite-related errors include satellite clock offset and ephemerides error; atmospheric propagation effects could be subdivided into ionospheric and tropospheric errors; receiver-related errors contain multipath and receiver noises (Misra and Enge, 2006). Elaboration on the pseudo-range error source is provided as follows.

Ephemeris Error

Ephemeris contains important parameters for satellite position estimation and the errors in the ephemeris generate errors of the orbital position which further lead to the errors in the satellite position. The ephemeris error is usually decomposed into three orthogonal directions: radial (from the satellite toward the centre of the earth), along-track (the instantaneous direction of the travel of the satellite) and cross-track (perpendicular to the along-track and radial). The ephemeris error introduces satellite position error with typical magnitudes in the range of 1 m – 6 m which is translated to an effective pseudo-range error of 0.8 m (1σ probability) (Kaplan and Hegarty, 2005).

Satellite Clock Error

Although satellite carries very accurate and stable atomic clocks that control all on-board timing operations, including time of signal generation, there is still a deviation between satellite time and GPS time. The satellite clock offset is usually the smallest following the correction uploaded from a control segment

to a satellite, and it accumulates over time until the next upload (approximately 24 hours). At zero age of data, range errors due to the satellite clock error could be 0.8 m and up to 4 m before it is updated (Misra and Enge, 2006).

Ionospheric Error

The ionosphere is in the region of the atmosphere between about 70 km and 1,000 km above the earth's surface. Within this region, free electrons influence the GPS satellite signal broadcasts and cause delays in signal arrival time. For a signal arriving at vertical incidence, the ranging error due to ionospheric error is from 3 m at night to as much as 15 m during the day. Furthermore, ranging errors could be enlarged by up to three times when a signal observed at low satellite elevation angles (0° to 10), i.e. between 9 m to 45 m. The averaged ionospheric error over the globe and elevation angles is considered as 7 m (1σ probability) (Kaplan and Hegarty, 2005).

Tropospheric Error

The troposphere is the lower layer of the atmosphere and the site of day-to-day weather on earth. The tropospheric error is a function of the refractivity, which is dependent on the local temperature, pressure and relative humidity. The refractivity is often modelled as a dry component and a wet component. The dry component attributes to 90% of the tropospheric error but can be predicted accurately whereas the wet component is harder to predict due to uncertainties in the atmospheric distribution. Assuming a receiver is located at sea level, the ranging error caused by tropospheric error can vary from 2.4 m for a satellite at the zenith to about 25 m for a satellite at an elevation angle of approximately 5 degrees (Hofmann-Wellenhof et al., 2007).

Multipath Error

Multipath error varies significantly depending on the surrounding environment of the receiver, satellite elevation angle, antenna gain pattern, etc. Multipath typically contributes errors from 1 m in a benign environment to more than 5 m in the highly reflective environment (Misra and Enge, 2006). The maximum pseudo-range measurement error caused by multipath can be up to half a code chip (GPS C/A code chip is about 293 metres) (Paul, 2013). The research characterises the GPS multipath with tens metre level for passenger vehicles across urban environments (Le Marchand et al., 2009).

Receiver Noises

Dominant sources of receiver noises are antenna phase offset error, thermal noise jitter and inference. The receiver noises generated from a typical modern receiver are on the order of 10 cm or less without external interference (Kaplan and Hegarty, 2005).

To assess the overall accuracy of a receiver, errors discussed above can be categorised into two types. Firstly, the Signal-in-Space (SIS) User Range Error (URE) is defined as an estimation comprising satellite-related error and atmospheric propagation effect. The second is receiver-related errors, such as receiver clock offset error, multipath, etc. To combine URE and receiver-related error together, the User Equivalent Range Error (UERE) is obtained to indicate the sum of the contributions from each error source. Table 3.2 just gives an idea of the rough value of the GPS UERE[12] for a single frequency C/A code receiver in a good observation environment as there are too many variables should be taken into account in real situations, e.g., the elevation angle of the satellite influences the signal path length and meanwhile changes multipath environment (Hofmann-Wellenhof et al., 2007). It is worth noting

[12] This UERE computation is the 1σ probability level which amounts to 68.3%.

that the magnitude of multipath error in an urban canyon could be far beyond the value given in Table 3.2.

Table 3.2 GPS UERE for A Single-Frequency C/A Code Receiver, based on source: (Hofmann-Wellenhof et al., 2007)

Error Source	Bias (m)	Random (m)	Total[13] (m)
Ephemeris error	2.1	0.0	2.1
Satellite clock error	2.0	0.7	2.1
Ionospheric error	4.0	0.5	4.0
Tropospheric error	0.5	0.5	0.7
Multipath error	1.0	1.0	1.4
Receiver noises	0.5	0.2	0.5
UERE[14] (m)	5.1	1.4	5.3

As mentioned at the beginning of this section, the position error is a function of both UERE and user-satellite geometry. The Dilution of Precision (DOP) factor is used to quantify the instantaneous geometry since the geometry is constantly changing with time due to the relative motion of the receiver and the satellites. DOP factor can be calculated by following steps:

$$A=\begin{bmatrix} \frac{(X_1^s-X_r)}{\rho_1} & \frac{(Y_1^s-Y_r)}{\rho_1} & \frac{(Z_1^s-Z_r)}{\rho_1} & 1 \\ \frac{(X_2^s-X_r)}{\rho_2} & \frac{(Y_2^s-Y_r)}{\rho_2} & \frac{(Z_2^s-Z_r)}{\rho_2} & 1 \\ \vdots & \vdots & \vdots & \vdots \\ \frac{(X_n^s-X_r)}{\rho_n} & \frac{(Y_n^s-Y_r)}{\rho_n} & \frac{(Z_n^s-Z_r)}{\rho_n} & 1 \end{bmatrix} \quad 3.8$$

$$M=(A^TA)^{-1}=\begin{bmatrix} \sigma_x^2 & \sigma_{xy} & \sigma_{xz} & \sigma_{xt} \\ \sigma_{xy} & \sigma_y^2 & \sigma_{yz} & \sigma_{yt} \\ \sigma_{xz} & \sigma_{yz} & \sigma_z^2 & \sigma_{zt} \\ \sigma_{xt} & \sigma_{yt} & \sigma_{zt} & \sigma_t^2 \end{bmatrix} \quad 3.9$$

[13] The column headed by "Total" results from the square root of the sum of the squared bias and the squared random quantity.

[14] The UERE results from the square root of the sum of the squares of each constituent.

$$
\begin{aligned}
HDOP &= \sqrt{\sigma_x^2 + \sigma_y^2} \\
VDOP &= \sqrt{\sigma_z^2} \\
TDOP &= \sqrt{\sigma_t^2} \\
PDOP &= \sqrt{HDOP^2 + VDOP^2} \\
GDOP &= \sqrt{PDOP^2 + TDOP^2}
\end{aligned}
\qquad 3.10
$$

Where X_i^s, Y_i^s and Z_i^s denote the position of SV i ($i = 1, 2, \cdots n$) and X_r, Y_r and Z_r denote the position of the receiver; ρ_i indicates the distance between the satellite i and the receiver r and could be calculated according to Eq. 3.3. HDOP, VDOP, TDOP, PDOP and GDOP are horizontal, vertical, time, position and geometry DOPs respectively.

It could be found in the matrix A in Eq. 3.8 that DOP values are isolated from the satellite observations which are purely determined by both satellites and receiver's positions. In the case of 4 visible satellites, the combination that one satellite is at the zenith whereas the rest of satellites are equally spaced in azimuth at a low elevation angle could form a much better geometry. Practically, the observed satellites should be evenly distributed in horizontal and vertical which leads to better DOP values. Besides, the greater number of visible satellite, the better (lower) value of DOP. Consequently, the lower value of DOP results in a higher achievable positioning accuracy (Langley, 1999).

3.4 UWB Positioning System

3.4.1 An Overview of UWB

The application of Ultra-Wideband (UWB) technique could be dated back to the late 1960s and mainly focused on military purposes, particularly in communications and radar (Barrett, 2001). Interest in UWB for communications and civilian positioning applications has skyrocketed since the

First Report and Order FFC-02-48 was released by FCC in 2002. The FCC defined a UWB device as "any device has a -10 dB fractional bandwidth of at least 0.20 or a -10 dB bandwidth of at least 500 MHz". The fractional bandwidth B_f can be calculated from:

$$\begin{aligned} B_f &= \frac{B}{f_c} \\ B &= f_H - f_L \\ f_c &= \frac{f_H + f_L}{2} \end{aligned} \qquad 3.11$$

So

$$B_f = \frac{2(f_H - f_L)}{(f_H + f_L)} \qquad 3.12$$

Where f_c is the centre frequency; f_H and f_L are the higher and lower frequencies of the -10 dB emission point, respectively.

The UWB devices operate in a very broad bandwidth and sometimes have to share the spectrum with the existing communication systems where interferences may occur. Regulation of UWB radio spectrum is, therefore, necessary to establish a framework where UWB devices can peacefully coexist with legacy systems. In the U.S., the FCC allowed unlicensed UWB using in a 7.5 GHz frequency band between 3.1 GHz and 10.6 GHz at very low power, i.e. maximum of -41.3 dBm/MHz. The use of UWB devices in the U.S. is categorised into three types: imaging systems (including Ground Penetrating Radar Systems, Wall Imaging Systems, Surveillance Systems, etc.), vehicular radar systems and communications and measurement systems. Moreover, different standards have been specialised based on individual operating characteristics and potential for causing interference to the authorised radio services. Table 3.3 and Fig.3.1 demonstrate the emission limits for UWB

indoor and outdoor communications and measurement systems in the U.S. (FCC, 2002).

Table 3.3 UWB Emission Limits for Indoor and Outdoor Systems as Defined by FCC, based on source: (FCC, 2002)

Frequency (MHz)	**EIRP[15] limits for indoor communication and measurement system (dBm/MHz)**	**EIRP limits for outdoor communication and measurement system (dBm/MHz)**
960 – 1610	-75.3	-75.3
1610 – 1990	-53.3	-63.3
1990 – 3100	-51.3	-61.3
3100 – 10600	-41.3	-41.3
Above 10600	-51.3	-61.3

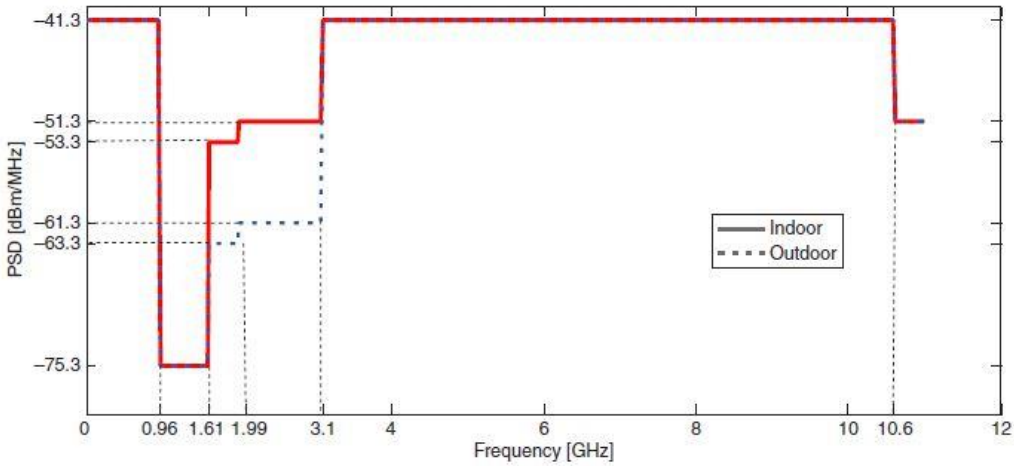


Fig.3.1 UWB Emission Mask as Defined by FCC[16], based on source: (FCC, 2002)

The UWB applications in Europe currently include communications applications, probing radar, precision location, and automotive radar. The organisations involved in the regulation of UWB in Europe are European Technical Standard Institute (ETSI) and European Conference of Postal and Telecommunications Administration (CEPT). The European regulations of

[15] EIRP is Equivalent Isotropic Radiated Power

[16] PSD in the vertical axis means Power Spectral Density, i.e. power over a specified reference bandwidth. It is equivalent to EIRP here.

UWB are more restrictive than the U.S. one and only have the same emission level as the FCC in the band 6 GHz – 8.5 GHz where is allocated for the operation of UWB locations tracking equipment. The details of European UWB emission limits are given in Table 3.4 and Fig.3.2 (Nikookar and Prasad, 2009, ETSI, 2008, Hirt, 2007). The UWB devices used in the trials discussed throughout this thesis is the Thales UWB system which complies with the standard UWB power density limit of -41.3 dBm/MHz, transmitting a signal between band 4760 MHz to 6200 MHz.

Table 3.4 UWB Emission Limits as Defined by Electronic Communications Committee (ECC), based on source: (ETSI, 2008)

Frequency (MHz)	EIRP limits (dBm/MHz)
Below 1600	-90
1600 – 3800	-85
3800 – 4200	-70
4200– 4800[17]	-70
4800 – 6000	-70
6000 – 8500	-41.3
8500 – 10600	-65
Above 10600	-85

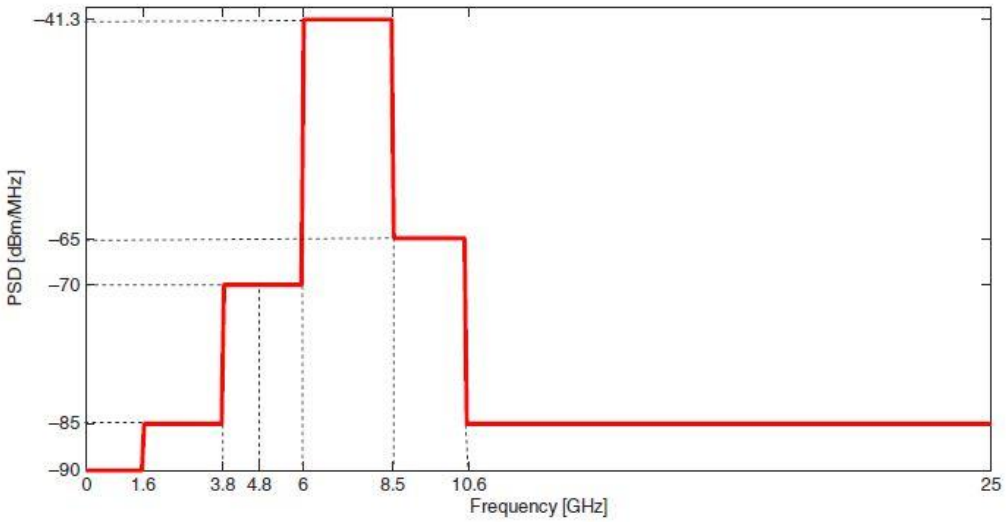


Fig.3.2 UWB Emission Mask as Defined by ECC, based on source: (ETSI, 2008)

[17] UWB devices placed on the market before 31st December 2010 are permitted to operate in the frequency band 4.2 GHz – 4.8 GHz with a maximum mean EIRP spectral density of -41.3 dBm/MHz.

There was a number of concerns about permitting the operation of UWB devices in the region of the spectrum below approximately 2 GHz before FCC released UWB regulations. Of particular concern is the impact of any potential interference to the GPS band at 1559 MHz – 1610 MHz (Akos et al., 2001). A series of studies were requested by FCC to determine the frequency bands and operational requirements for UWB devices to avoid such potential interference (Anderson et al., 2001, FCC, 2002). Also, more studies have reassured us that GPS can survive and maintain its position accuracy and coexist with UWB following careful design considerations (Hämäläinen et al., 2002, Isola et al., 2007, Van Slyke, 2009, Hamalainen et al., 2001). Due to the overlapped operation, a frequency between UWB and DSRC, a novel UWB antenna with a stop-band notch from 5 GHz to 6 GHz has been presented which paved the way to the V2X applications (Nadiah et al., 2014).

In the time-based ranging the ranging resolution d can be estimated by:

$$\mathrm{d} = \frac{c}{BW} \tag{3.13}$$

Where c denotes the light speed in a vacuum and BW is the bandwidth of the spread signal. It makes UWB technology especially suited for radio locating because of its very broad bandwidth. Although the ranging resolution estimation is calculated when a direct line-of-sight path is visible and can be affected by interference and multipath, UWB technology is still better than the narrowband technique (Ghavami et al., 2004).

There are two modulation schemes to implement the UWB system, namely: Impulse Radio (IR) and Multi-Carrier (MC). The conventional IR approach is formed by a series of very short discontinuous pulses, of the order of hundreds of picoseconds. IR-UWB has the significant advantages of being essentially baseband processing and fine time resolution. Also, the discontinuous pulses

lead to the resistance to severe multipath propagation. On the other hand, the MC-UWB approach divides the UWB frequency spectrum to multiple non-overlapping bands for transmitting signals. The biggest advantage of MC-UWB is the ability to utilise the entire 7.5 GHz of spectrum efficiently. Moreover, the separate bands may be treated independently and allow for coexistence with other communications systems (Oppermann et al., 2004, Nikookar and Prasad, 2009).

3.4.2 UWB Positioning System Based on Different Positioning Techniques

According to the observations used to estimate the position, UWB Positioning System can be classified as Received Signal Strength (RSS), Angle of Arrival (AOA), Time of Arrival (TOA) and Time Difference of Arrival (TDOA).

3.4.2.1 Received Signal Strength (RSS)

With the Received Signal Strength (RSS) technique, the signal strengths of the object to be pinpointed are measured at several stationary receivers. The path loss model is used to describe the signal power attenuation. The decay of the received signal strength (RSS) can be evaluated as Eq. 3.14:

$$P(f_g, d) = P(f_g, d_0) - 10\alpha \log_{10}(\frac{d}{d_0}) + \eta(0, \sigma_n) \qquad 3.14$$

Where $P(f_g, d)$ is the RSS at a distance d and $P(f_g, d_0)$ is the RSS at reference distance d_0; α is the path loss exponent and $\eta(0, \sigma_n)$ denotes a Gaussian distributed random variable with 0 dB average and standard deviation σ_n (Waadt et al., 2010, Gigl et al., 2007).

Ideally, each measurement will provide a set of points along the circumference of a circle with calculated distance d (derived from the RSS measurement), and the object position is then given by the intersection of these circles (shown on the left of Fig.3.3). However, an exact knowledge of the path loss is essential in order to get an accurate estimation of the RSS at the receivers. In practice, it is rare that all circles coincide exactly due to the multipath fading (shown on the right of Fig.3.3) (Ghavami et al., 2004, Sahinoglu et al., 2008, Nikookar and Prasad, 2009).

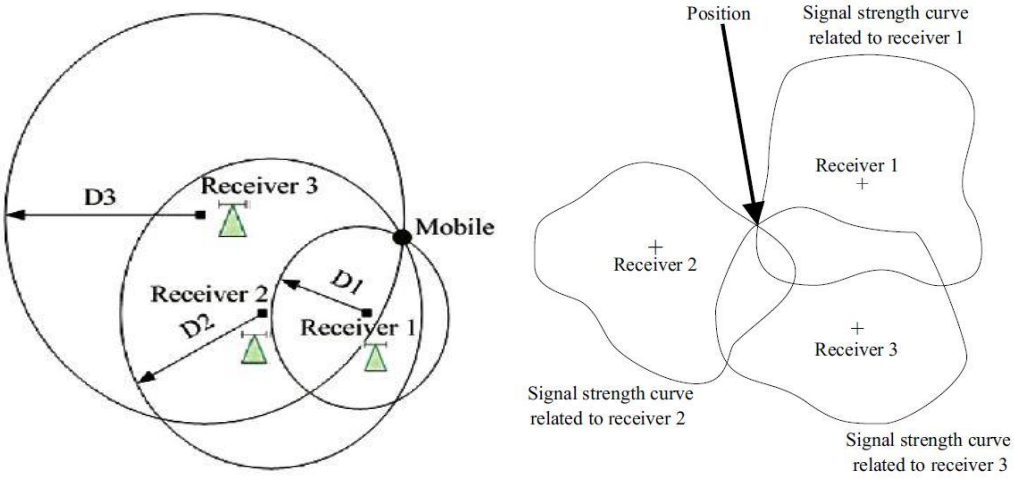


Fig.3.3 RSS Positioning Technique, based on source: (Sahinoglu et al., 2008)

3.4.2.2 Angle of Arrival (AOA)

In this method, the Angle of Arrival (AOA) of the signal sent by the transducer to be pinpointed is measured by receiving signals from several stationary transmitters, and each measurement forms a radial line from the transmitter to the transducer. The intersection of two directional lines will be defined as the location of the transducer. Therefore, only two reference transmitters are needed in theory for 2D positioning application (shown in Fig.3.4). However, additional transmitters are required because of the multipath effects in practice. This method has the advantages of not requiring synchronisation of the transmitters nor an accurate time reference. On the other hand, a complex hardware and regular calibration are required. It also suffers from Non-Line-of-Sight (NLOS) observations.

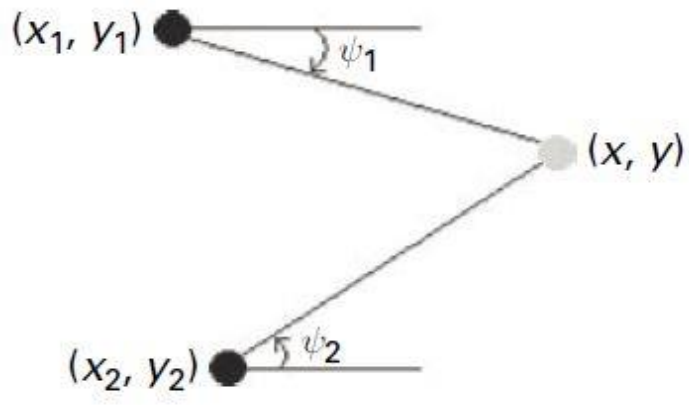


Fig.3.4 AOA Positioning Technique, based on source: (Sahinoglu et al., 2008)

(x_1, y_1) and (x_2, y_2) denote the known 2D coordinates of transmitters 1 and 2. Moreover, AOA ψ_1 and ψ_2 are measured by the transducer. Then, the position of the object can be solved from the following equations (Sahinoglu et al., 2008):

$$\tan\psi_i = \frac{y - y_i}{x - x_i}, i = 1, 2 \tag{3.15}$$

$$\begin{aligned} \mathrm{x} &= \frac{x_2 \tan\psi_2 - x_1 \tan\psi_1 + y_1 - y_2}{\tan\psi_2 - \tan\psi_1} \\ y &= \frac{(x_2 - x_1)\tan\psi_1 \tan\psi_2 + y_1 \tan\psi_2 - y_2 \tan\psi_1}{\tan\psi_2 - \tan\psi_1} \end{aligned} \tag{3.16}$$

3.4.2.3 Time of Arrival (TOA)

The Time of Arrival (TOA) technique measures the time that signal has taken to travel from the object to the reference receiver and then derives the distance between the object and the reference receiver. It is worth remembering that GPS also applies the TOA technique for positioning. As shown in Fig.3.5, three circles, centred at the reference receiver, are generated with the radius of measure distance and the intersection of the circles is the object location.

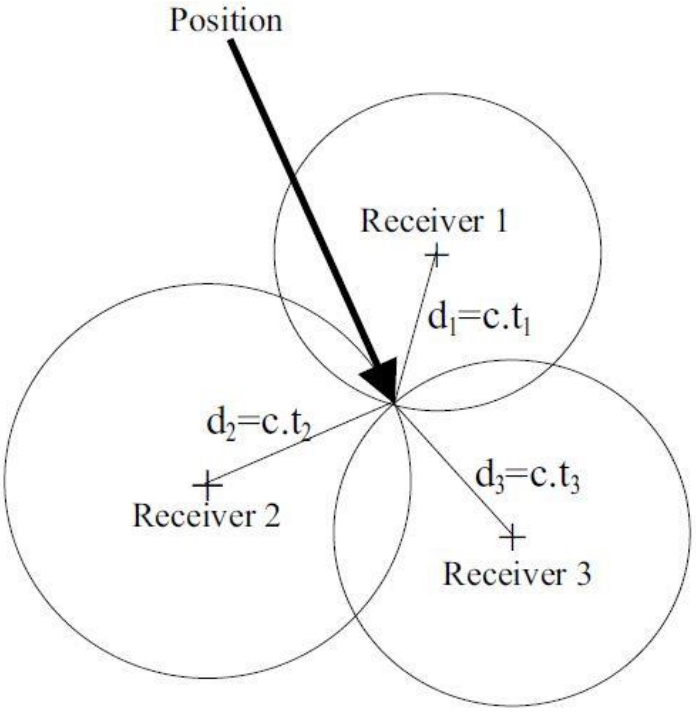


Fig.3.5 TOA Positioning Technique, based on source: (Sahinoglu et al., 2008)

For 2D positioning application, at least three reference receivers are needed as the transmission time t_0 at the object is unknown apart from the 2D coordinate of the object. Let d_i represent the range measurement obtained from three TOA or RSS[18] measurements as following:

$$d_i = c(t_i - t_0) = \sqrt{(x_i - x)^2 + (y_i - y)^2}, i = 1,2,3 \qquad 3.17$$

Where t_i is the TOA at ith reference receiver; (x_i, y_i) denotes the known coordinate of the ith reference receiver. (x, y) denotes the unknown coordinate of the object and can be solved from above equation as (Sahinoglu et al., 2008):

[18] Within the RSS positioning technique, the distance between the object and the reference receiver is derived from the RSS measurement. So it has the same procedure as the TOA for calculating the location of the object.

$$x = \frac{(y_2 - y_1)\gamma_1 + (y_2 - y_3)\gamma_2}{2[(x_2 - x_3)(y_2 - y_1) + (x_1 - x_2)(y_2 - y_3)]}$$
$$y = \frac{(x_2 - x_1)\gamma_1 + (x_2 - x_3)\gamma_2}{2[(x_2 - x_1)(y_2 - y_3) + (x_2 - x_3)(y_1 - y_2)]} \quad 3.18$$

Where

$$\gamma_1 = x_2^2 - x_3^2 + y_2^2 - y_3^2 + d_3^2 - d_2^2$$
$$\gamma_2 = x_1^2 - x_2^2 + y_1^2 - y_2^2 + d_2^2 - d_1^2 \quad 3.19$$

The TOA method is easy to implement; however, it requires high precise synchronisation at both the reference receiver and the object. Otherwise, large position errors can occur. For instance, even a 1-microsecond inaccuracy in the TOA estimation can lead to an error of up to 300 metres in ranging. In practice, the intersection of circles is always an area instead of a point due to errors. More ranging observations are required in order to improve positioning accuracy (Ghavami et al., 2004, Nikookar and Prasad, 2009).

3.4.2.4 Time Difference of Arrival (TDOA)

The Time Difference of Arrival (TDOA) approach is a variant of TOA. It calculates the object's location according to the time differences between two TOA at different reference receivers. For 2D positioning application, at least two pairs of reference receivers are needed, and the position is the intersection of the corresponding hyperboloids (shown in Fig.3.6). The merit of TDOA in comparison with TOA is that only the synchronisation among the reference receivers is required and there is no need for the transmission time at the object (Ghavami et al., 2004).

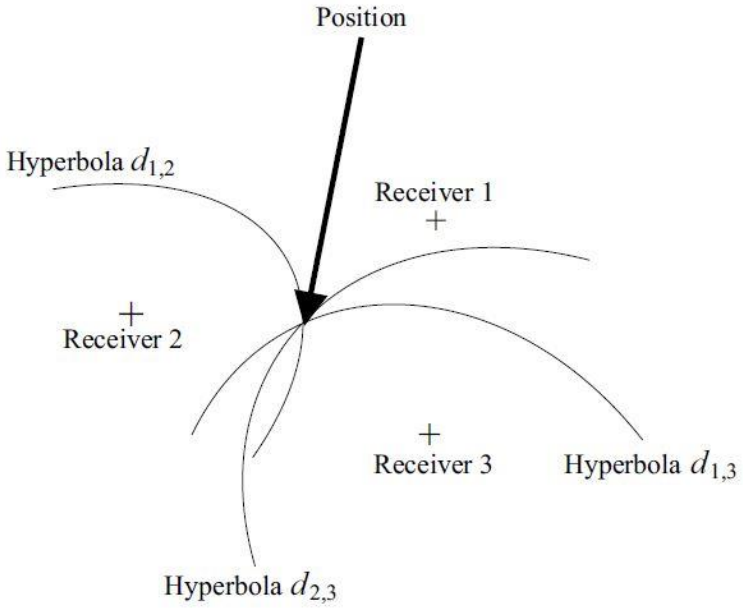


Fig.3.6 TDOA Positioning Technique, based on source: (Ghavami et al., 2004)

3.5 Summary

Based on the comprehensive selection criteria of positioning sensor, this chapter primarily explores two positioning systems which could be used to support the V2X applications, namely GPS and UWB. Firstly, the up-to-date GNSS landscape is reviewed. Then, GPS has been comprehensively discussed as the representative of GNSS from its coordinate system, time system, observations and performance. The parameters and error sources that influence GPS ultimate performance are introduced. Also, details of DGPS technique are explained through how to reduce and eliminate GPS errors that degrade performance. Secondly, UWB positioning system is recommended as a complementary system to GPS. The regulations and positioning techniques of UWB are represented. Due to the fact that both GPS and UWB adopt the TOA technique for positioning, the similarity of the observations makes the system integration easier, and the procedure of integration will be explicated in next chapter.

Chapter 4 Robust Cooperative Positioning in the V2X Environment

4.1 Overview

Chapter 3 reviews the fundamentals of GPS and UWB positioning technologies, the error characteristics and the corresponding derived observation equations. Chapter 4 further presents the positioning algorithm that fuses GPS and UWB measurements together. In the field of vehicle navigation and positioning, Least Squares Estimation (LSE) and Kalman Filters (KF) are frequently used as the estimator for sensor integration and provision of positioning solutions. The derivations of LSE and KF are given step by step. Also, two variants of KF, i.e., Extended Kalman Filter (EKF) and Robust Kalman Filter (RKF), are described for handling the non-linear systems and the systems that are contaminated by outliers, respectively. Furthermore, how the Cooperative Positioning (CP) could take advantage of the integration of GPS and UWB and V2X communication are explored. Finally, an integrated solution for vehicle positioning in the urban canyon is provided.

4.2 Position Estimation

Estimation is the process of calculating the value of a group of unknowns of interest from indirect, inaccurate and uncertain observations (Bar-Shalom et al., 2001). It refers in particular to the position and velocity in the V2X applications. To estimate the unknowns of interest, a mathematical model describing the current physical conditions of a system and its parameters is typically built, this is known as the state model. Besides, a functional relationship between the unknowns and the observations has to be created which is referred to as the measurement model. The measurement model requires a sufficient number of observations to determine the unknowns. The number of independent observations is at least equal to the number of the unknowns so that a unique solution would be obtained. In practical, it is expected that the observations are redundant (i.e. the number of observations is

in excess of the minimum number that is needed to determine the unknowns); hence the unknowns could be estimated in some optimal sense. First, the redundant observations are used to assess the size of the error in the observation can be made by examining the discrepancy between the observations. Second, the redundant observations permit an adjustment of the final values of the unknowns (Ghilani and Wolf, 2010). The Least Squares Estimation (LSE) and Kalman Filters (KF) are the most commonly used algorithms used in GNSS receivers for calculating their positions (Petovello, 2013).

4.2.1 Least Squares Estimation (LSE)

In the Least Squares Estimation (LSE), the state vector is purely based on the measurements. The measurement model at epoch t is usually expressed in the form of Eq. 4.1:

$$z_t = H_t x_t + v_t \tag{4.1}$$

Where z_t is the measurement vector. H_t is the design matrix. x_t is the state vector, containing all unknowns of interest. v_t is the vector of measurement errors which is the difference between the reference value and the measured value, referred to as residuals.

The LSE solution discussed in this section is based on a set of linear measurements, i.e. it is a linear relationship between design matrix and state vector. Due to the fact that both GPS and UWB provide non-linear measurements, the non-linear measurement model will be introduced in Section 4.2.3. In addition, the details of matrices in the measurement model and the linearization of measurement model will also be given.

The LSE seeks for the state vector that minimises the sum of the squares of the residuals (Bar-Shalom et al., 2001, Ghilani and Wolf, 2010, Blobel, 2005). The fundamental principle of LSE is expressed as Eq. 4.2:

$$\hat{x} = \arg\min\{\sum_{t=1}^{n} \hat{v}_t^{\,2}\} \tag{4.2}$$

From calculus, the minimum value of a function can be found by taking its first derivative and equating the resulting function with zero. Moreover, substituting Eq. 4.1 into Eq. 4.2 yields Eq. 4.3:

$$\begin{aligned}
&\frac{d(z_t - H_t\hat{x}_t)^2}{d\hat{x}_t} \\
&= \frac{d(z_t - H_t\hat{x}_t)^T(z_t - H_t\hat{x}_t)}{d\hat{x}_t} \\
&= \frac{d(z_t^T - \hat{x}_t^T H_t^T)(z_t - H_t\hat{x}_t)}{d\hat{x}_t} \\
&= \frac{d(z_t^T z_t - \hat{x}_t^T H_t^T z_t - z_t^T H_t\hat{x}_t + \hat{x}_t^T H_t^T H_t\hat{x}_t)}{d\hat{x}_t} \\
&= \frac{d(z_t^T z_t - 2\hat{x}_t^T H_t^T z_t + \hat{x}_t^T H_t^T H_t\hat{x}_t)}{d\hat{x}_t} \\
&= -2z_t^T H_t + 2\hat{x}_t^T H_t^T H_t
\end{aligned} \tag{4.3}$$

Where n is the number of observations.

The result of the LSE solution is obtained Eq. 4.4:

$$\begin{aligned} -2z_t^T H_t + 2\hat{x}_t^T H_t^T H_t &= 0 \\ 2\hat{x}_t^T H_t^T H_t &= 2z_t^T H_t \\ (\hat{x}_t^T H_t^T H_t)^T &= (z_t^T H_t)^T \\ H_t^T H_t \hat{x}_t &= H_t^T z_t \\ \hat{x}_t &= (H_t^T H_t)^{-1} H_t^T z_t \end{aligned} \quad 4.4$$

And the error covariance matrix of the LSE solution is Eq. 4.5:

$$C_{\hat{x}} = (H_t^T H_t)^{-1} H_t^T C_z H_t (H_t^T H_t)^{-1} \quad 4.5$$

Where C_z is the measurement covariance matrix.

In the ideal conditions of independent measurement errors, with zero mean and equal variance σ^2, the C_z becomes a diagonal matrix with equal values, and the error covariance matrix of the LSE solution $C_{\hat{x}}$ becomes:

$$C_{\hat{x}} = (H_t^T H_t)^{-1} \sigma^2 \quad 4.6$$

Taking into account the case that the measurements are characterised by different accuracies, the Weighted LSE (WLSE) can be performed. Eq. 4.3 is reformed as:

$$\frac{d(z_t - H_t \hat{x}_t)^T W (z_t - H_t \hat{x}_t)}{d\hat{x}_t} = 0 \quad 4.7$$

Where $W = C_z^{-1}$ is the weight matrix, referred to as the inverse of the covariance matrix of the measurements.

The result of WLSE solution and its error covariance matrix with independent measurements become:

$$\hat{x}_t = (H_t^T W H_t)^{-1} H_t^T W z_t \tag{4.8}$$

$$\begin{aligned} C_{\hat{x}} &= (H_t^T W H_t)^{-1} H_t^T W C_z W H_t (H_t^T W H_t)^{-1} \\ &= (H_t^T W H_t)^{-1} \end{aligned} \tag{4.9}$$

4.2.2 Kalman Filter (KF)

In 1960, Rudolf E. Kalman published the seminal Kalman Filter (KF) paper that describes a recursive solution to linear filtering problem of the discrete data (Kalman, 1960). The KF, named after him, has become a common technique used for positioning and navigation purposes. The KF uses knowledge of the state model as well as the measurement model rather than using a measurement model alone in LSE. The state model at epoch $t+1$ is derived from the prior state at epoch t according to the Eq. 4.10 (Faragher, 2012):

$$x_{t+1} = F_{t+1} x_t + B_{t+1} u_{t+1} + w_{t+1} \tag{4.10}$$

Where x_{t+1} and x_t are the state vectors containing the unknowns of interest for the system at epoch $t+1$ and t, respectively. F_{t+1} is the state transition matrix which is applied to the previous state. u_{t+1} is the vector containing any control inputs. B_{t+1} is the control input matrix which is applied to the control vector u_{t+1}. w_{t+1} is the process noise which is assumed as a zero-mean Gaussian distribution. The associated covariance matrix is given by:

$$Q_{t+1} = E(w_{t+1} w_{t+1}^T) \tag{4.11}$$

Where $E(\square)$ denotes the expectation. In addition, Q_{t+1} is a symmetric matrix and could become a diagonal matrix when all variables in state vector are uncorrelated.

It should be noticed that the KF has an identical measurement model to the measurement model used in the LSE (Eq. 4.1). v_t is the measurement noise that has zero mean Gaussian distribution. Similarly to the covariance matrix of process noise in the state model, the covariance matrix of the measurement noise at epoch $t+1$ is expressed by:

$$R_{t+1} = E(v_{t+1} v_{t+1}^T) \tag{4.12}$$

Where R_{t+1} is a diagonal matrix when all measurements are independent.

The KF is derived based on minimising the mean square error of the solution of unknowns whereas the LSE is based on the minimum value of measurement residual (Petovello, 2013, Bar-Shalom et al., 2001). It is worth noting that the KF is a linear estimator as well. Hence its variant, the Extended Kalman Filter (EKF) is developed to solve the nonlinear state estimation, especially in GPS and ITS applications (Groves, 2013).

The procedure of the KF is divided into two primary phases, i.e. prediction (also called time update) and update (also called measurement update). The prediction phase represents the system's evolution from the previous to the current epoch. The new state vector and associated covariance matrix are

predicted from the state at epoch t to the state at epoch $t+1$ based on the dynamic model:

$$\hat{x}_{t+1|t}^{-} = F_{t+1}\hat{x}_{t|t}^{+} + B_{t+1}u_{t+1} \tag{4.13}$$

$$P_{t+1|t}^{-} = F_{t+1}P_{t|t}^{+}F_{t+1}^{T} + Q_{t+1} \tag{4.14}$$

Where P is the covariance matrix of the state vector. Q_{t+1} is the associated process noise covariance matrix at epoch $t+1$. The superscript "-" indicates the priori quantity based on the updated quantity from the previous epoch and the superscript "+" indicates the posteriori quantity based on the fusion of measurements and predictions at current epoch.

In the update phase, the posteriori state estimation and covariance matrix are updated by combining the current measurements and the priori predictions. The equations of update phase are listed:

$$\hat{x}_{t+1|t+1}^{+} = \hat{x}_{t+1|t}^{-} + K_{t+1}V_{t+1} \tag{4.15}$$

$$P_{t+1|t+1}^{+} = P_{t+1|t}^{-} - K_{t+1}H_{t+1}P_{t+1|t}^{-} \tag{4.16}$$

Where K_{t+1} is the Kalman gain at epoch $t+1$ and V_{t+1} is the innovation vector at epoch $t+1$. The state update requires the Kalman gain which is obtained in the course of the covariance calculations and being used as weighting for prediction and the innovation vector. The innovation vector is defined as the difference between the predicted measurement vector and the actual measurement vector. Their equations are represented as follows.

$$V_{t+1} = z_{t+1} - H_{t+1}\hat{x}^{-}_{t+1|t} \quad 4.17$$

$$S_{t+1} = H_{t+1}P^{-}_{t+1|t}H^{T}_{t+1} + R_{t+1} \quad 4.18$$

$$K_{t+1} = P^{-}_{t+1|t}H^{T}_{t+1}S_{t+1}{}^{-1} \quad 4.19$$

Where Z_{t+1} is the inputted measurement at epoch $t+1$. H_{t+1} is the design matrix extracted from the measurement model. S_{t+1} is the innovation covariance associated with the innovation vector.

The Kalman gain is a weighting factor that indicates how much the measurements contained in the innovation vector could influence the final state vector estimate. When Kalman gain decreases, the contribution of the measurement to the final estimate also decreases and vice versa. Furthermore, it is worth noting that the process covariance matrix Q_{t+1} (in Eq. 4.14) and the measurement covariance matrix R_{t+1} are the two effective factors to adjust the magnitude of the Kalman gain as they are defined in the state model, and the measurement model and these two factors stay the same during the recursive procedure. Therefore, enlarged R_{t+1} leads to less affection from the measurement and more confidence from previous state estimate. This is directly opposite to the influence of Q_{t+1} (Kim and Huh, 2011). To substitute Eq. 4.17 and Eq. 4.18 into Eq. 4.19, the procedure of the KF algorithm can be summarised in Fig.4.1 below.

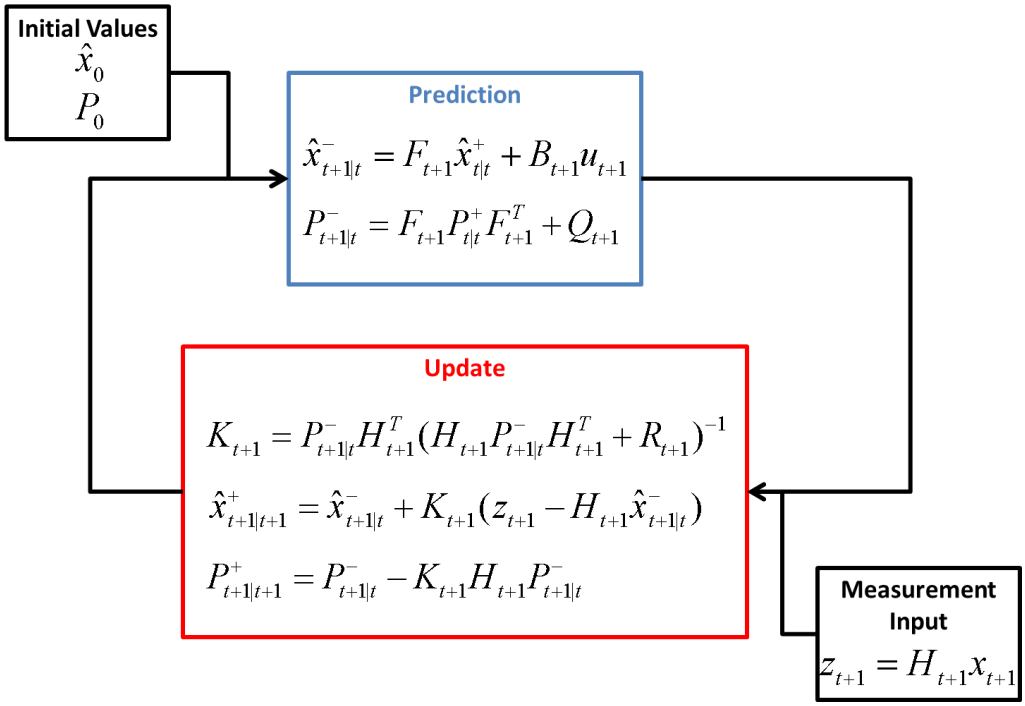


Fig.4.1 Procedure of the Kalman Filter Algorithm

4.2.3 Extended Kalman Filter (EKF)

As mentioned previously, the KF is essentially linear in nature. In most GPS and ITS applications, however, the state model and/or measurement model are non-linear. Therefore, the EKF extends the applications of the KF to the non-linear system by applying the linearization process based on Taylor series expansion (Chui and Chen, 2008).

The state and measurement models in a non-linear system at epoch $t+1$ are described as:

$$x_{t+1} = f(x_t, t) + w_{t+1} \tag{4.20}$$

$$z_{t+1} = h(x_{t+1}, t) + v_{t+1} \tag{4.21}$$

Where $f(\square)$ and $h(\square)$ are the non-linear function representing the temporal system states. For simplicity, it is assumed that there is no control factor in the state model.

To linearize the non-linear functions in Eq. 4.20 and Eq. 4.21, they are expanded in Taylor series with terms up to first order:

$$x_{t+1} \approx f(\dot{x}_{t|t}, t) + F_t^J (x_t - \dot{x}_{t|t}) + w_{t+1} \quad 4.22$$

$$z_{t+1} \approx h(\dot{x}_{t+1}, t) + H_{t+1}^J (x_t - \dot{x}_{t+1|t}) + v_{t+1} \quad 4.23$$

Where $\dot{x}$ is the nominal value of the state vector. The state transition matrix $F_t^J = \frac{\partial f(x_t, t)}{\partial x_t}|_{x_t = \dot{x}_{t|t}}$ and the design matrix $H_{t+1}^J = \frac{\partial f(x_t, t)}{\partial x_t}|_{x_t = \dot{x}_{t+1|t}}$ are Jacobian matrices of partial derivatives of $f(\square)$ and $h(\square)$ with respect to $\dot{x}$ respectively.

Due to the fact that the estimated state vector is composed of delta-quantities for the positioning and navigation purposes, the total estimate is formed by summing the nominal vector with the estimated state vector. Moreover, the priori state estimation is reset to zero before entering the next loop as the estimates of each epoch are uncorrelated. In practice, it is noted that a reasonable estimate of the trajectory is usually not available because we do not predefine an accurate trajectory and follow it when we are driving. Therefore, the EKF does not use a nominal value but the previous estimate as a reference point for linearization (Angrisano, 2010).

Fig.4.2 presents the flowchart of the EKF algorithm. The overall process of the EKF algorithm is same as the one for the KF. The equations for each step are slightly different, and the differences could be summarised as the following two contents. First, the EKF uses non-linear state and measurement models rather than the linear models. Second, the state transition and the design matrices are the Jacobian matrices of the non-linear models. All the remaining parts are identical to linear KF algorithm (Kim and Huh, 2011).

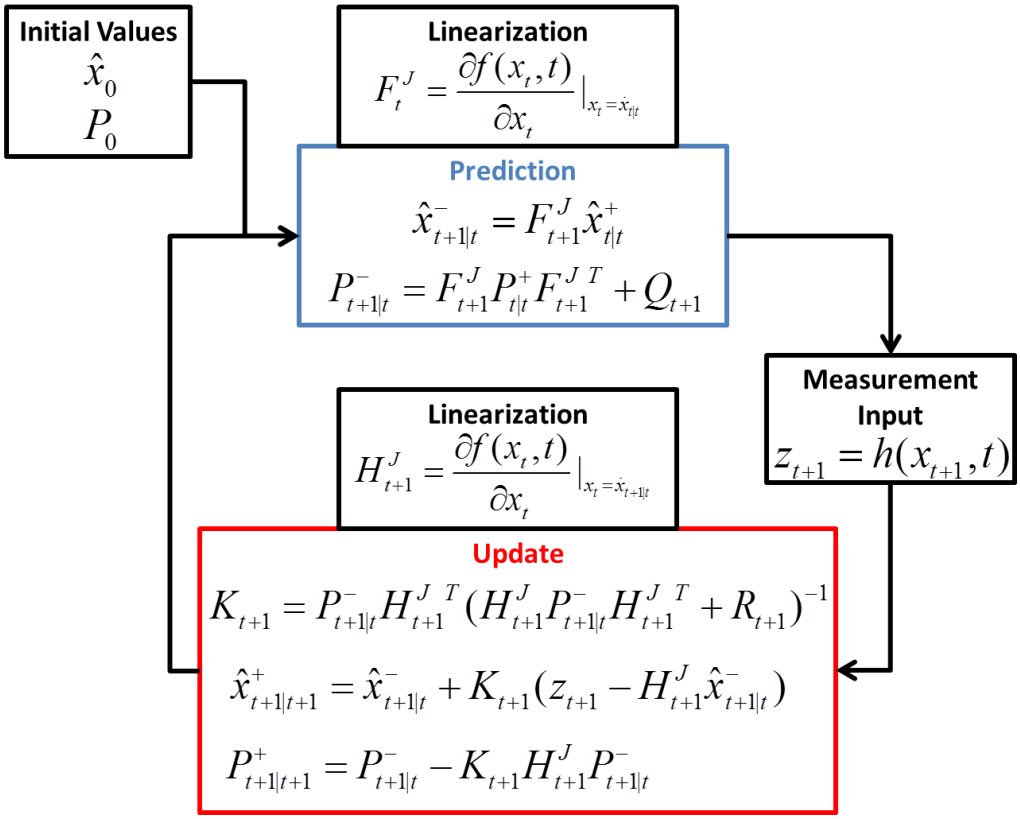


Fig.4.2 Procedure of the Extended Kalman Filter Algorithm

4.2.4 Robust Kalman Filter (RKF)

The KF has been applied extensively in the area of positioning and navigation. However, the reliability of the results is dropped when the models in the KF do not fit the actual situation accurately. These divergences can often be classified into three categories: (1) insufficient accuracy in state models: (2) insufficient accuracy in measurement models: (3) insufficient accuracy in stochastic models (Yang et al., 2001). In this thesis, the situation of insufficient accuracy in measurement models is particularly discussed and dealt. The insufficient accuracy is usually attributed to outliers from measurements. An outlier is defined as an observation that lies outside an overall pattern of distribution (Moore, 2007). Although the outlier occurs stochastically in any distributions, it often originates from unmodelled factors or anomalous causes. For instance, outliers may stem from transitory environmental disturbances, temporary sensor failure or incorrect measurements. To control the influences of the outliers, various outlier detection methods can be applied. Hodge and Austin have given a comprehensive survey of outlier detection methodologies and suggested that the two fundamental considerations to select an appropriate

outlier detection methodology are modelling the data distribution accurately and defining the outlier threshold suitably (Hodge and Austin, 2004). The outlier detection method normally classifies the measurements into two groups: one group is reliable, and the other is distrustful. Then the outlier detection rules are applied based on the reliable measurements for outlier screening. Alternatively, robust estimation can also be applied if the measurements are contaminated by outliers (Huber, 1964, Huber, 2011). The major advantage of the robust estimation over the outlier detection is that it can handle the outliers in a smoother way which is preferred in a kinematic estimation procedure. When using outlier detection, the measurement weights often jump from the original weight to the zero weight when the measurement errors fluctuate around the threshold, and the abandoning outlier may lead to insufficiency of effective measurements, especially when there is more than one outlier. When using the robust estimation, the measurement outliers are controlled by robust equivalent weights of the measurements (Yang, 1991, Yang, 1994, Zhu, 1996). Furthermore, the Robust Kalman Filter (RKF) was derived by using Bayesian statistics to deal with the outliers not only in the measurements but also in the updated parameters (Koch and Yang, 1998, Yang et al., 2001, Yang et al., 2010). In this thesis, only the outliers in the independent measurements are investigated. The robust estimator of the posterior state and corresponding covariance matrix then become:

$$\hat{x}^{+}_{t+1|t+1} = \hat{x}^{-}_{t+1|t} + \bar{K}_{t+1}(z_{t+1} - H_{t+1}\hat{x}^{-}_{t+1|t}) \tag{4.24}$$

$$P^{+}_{t+1|t+1} = P^{-}_{t+1|t} - \bar{K}_{t+1}H_{t+1}P^{-}_{t+1|t} \tag{4.25}$$

Where $\bar{K}_{t+1}$ is the Kalman gain matrix based on the equivalent weight matrix of observations at epoch $t+1$, specifying:

$$\bar{K}_{t+1} = P^{-}_{t+1|t}H^{T}_{t+1}(H_{t+1}P^{-}_{t+1|t}H^{T}_{t+1} + \bar{W}^{-1}_{t+1})^{-1} \tag{4.26}$$

In which $\bar{W}_{t+1}^{-1} = \bar{R}_{t+1}$ denotes the equivalent weight matrix of z_{t+1}.

$\bar{W}_{t+1}$ is a diagonal matrix with elements $\bar{w}_i (i = 1, 2, ..., n)$ in the independent case, and $\bar{w}_i$ can be defined by (Huber, 1964) and (Yang et al., 2002) as follows.

$$\bar{w}_i = \begin{cases} w_i & \left|V_i^{'}\right| \le c \\ w_i \cdot \dfrac{c}{\left|V_i^{'}\right|} & \left|V_i^{'}\right| > c \\ \dfrac{w_i}{10000} & \left|V_i^{'}\right| > 10 \end{cases} \qquad 4.27$$

Where $V_i^{'} = \dfrac{\mathrm{V}_i}{\sigma_i}$ is the standardised residual corresponding to V_i (the ith element of the innovation vector) and $\sigma_i = \sqrt{R_{i,i}}$ (the ith element on the diagonal of the measurement covariance matrix). c is a constant which is typically chosen between 1.0 and 1.5 based on the experience. Comparing to the method proposed by (Yang et al., 2002). c is selected as 3.0 in the proposed method in this thesis. Yang's method focuses on single observation type while our method is dealing with mixed DD code pseudo-range and UWB ranging observations. As the measurement noise of DD code pseudo-range is bigger than that of UWB ranging, the standardised residual of UWB ranging will be more sensitive and easily magnified which leads to observation over screening. Therefore, a bigger c is set to remain more valid observations.

If the measurement contains outliers and the standardised residual of the measurement is larger than c, then w_i is inflated. In this case, the contribution of the corresponding measurements to the state estimator will be reduced.

Apart from Yang's equivalent weight function, an additional screening criterion has been added to lessen further bad influence from outliers which the measurement gets a bigger than 10 standardised residual. The reason is elaborated below. This method scales the weight of observation based on the innovation vector which is the difference between raw observation and predicted estimate. The magnitude of UWB ranging outlier is bigger than the outlier of DD code pseudo-range. Meanwhile, the measurement noise of UWB ranging is smaller than that of DD code pseudo-range. According to the data analysis in Table 5.4 and

Table **5.7**, the measurement noise of UWB ranging is set as 0.2 metres, and the outlier screening criterion of 2 metres helps remaining more than 95% raw UWB ranging observations. Thus, an upper screening criterion of 10 has been calculated to diminish the impact of UWB ranging outlier.

Overall, $\bar{w}_i$ is a descending function with respect to the inflation factor, i.e. the standardised residual. When the standardised residual is less than c, the equivalent weight stays the same; the equivalent weight is set as a number by multiplying 10000 if the standardised residual is larger than the upper threshold, i.e. 60; and the equivalent weight is inflated linearly when the standardised residual is between c and 60.

4.3 Multi-sensor Cooperative Positioning

The positioning ability is based on the quantity and quality of the observations. The way that RKF could improve the quality of observation has been discussed in Section 4.2.4. The positioning procedure cannot be accomplished without adequate observations. The more observations received the higher possibility to solve the position. There are two ways to increase the number of observations, i.e., individual approach and cooperative approach. Firstly, a vehicle can equip with more sensors to receive additional observations on its own. Alternatively, it can borrow observations from other transportation participants in a cooperative approach.

4.3.1 Multi-sensor Integration

As mentioned in Section 3.2, GPS is undoubtedly the first choice for numerous V2X applications due to its global coverage, ease to use and being free of charge. However, GPS signals often suffer from interference, multipath and blockage, especially when a vehicle is running in an urban canyon. To cover the shortage of GPS, complementary sensors can be integrated together. Vehicles are generally equipped with lots of sensors for compensating GPS, for example, Inertial Navigation System (INS), radar, camera, etc. Particularly, the GPS/INS integration is most commonly used. However, the exorbitant price of INS is unacceptable for all vehicles. In this research, UWB is proposed to integrate with GPS.

With regard to integration strategy, several approaches can be used to integrate GPS and INS systems, and they are adopted to fuse the data of integrated GPS and UWB. Those approaches are differed by the "depth" of the interaction and the type of information that is shared between individual systems. The following four approaches are the most common (Petovello, 2003, Groves, 2013):

- Uncoupled Integration
- Loose Integration
- Tight Integration
- Ultra-Tight Integration (also called Deep Integration)

In the uncoupled integration, two systems work independently to provide positioning solutions, and the one that is typical of high accuracy is exploited to produce the final solution of the integrated system. In this way, both GPS and UWB have to receive sufficient observations to provide solutions on their own. According to the application scenario in this thesis, i.e., urban canyon, GPS and UWB may not get enough observations due to severe obstruction.

In contrast, GPS and UWB no longer work as independent systems in the deep integration. Instead, GPS and UWB help each other to track signals. Unfortunately, this approach requires access to the firmware level which is typically only implemented by equipment manufacturers.

The loose and tight integrations are the most common approaches in the literature. In both ways, the GPS and UWB operate separately and differ in the type of information shared between them. In the loose integration strategy, two stand-alone solutions of GPS and UWB are blended for a final solution whereas the raw GPS pseudo-ranges and UWB ranging observations are processed in one filter in the tight integration strategy. The two main advantages of the loose approach are simplicity and redundancy. As the GPS and UWB observations are processed separately, the dimension of the state vectors is generally smaller than the case of the tight approach. It leads to a short processing time. The redundancy stems from the independent positioning solutions from GPS-only or UWB-only (Groves, 2013). On the other hand, the loose integration has a disadvantage because separate KFs are used to perform the GPS-only and UWB-only positioning solutions. In this way, the processing noise will be added twice which affects the system performance (Petovello, 2003). By comparison, the tight integration has an advantage on a more accurate solution than loose integration because more observations are processed together. Another advantage it has over the loose integration is that useful observations can be continually extracted from GPS and UWB receivers in situations where fewer than minimal required number satellite and base unit are visible. Therefore, both GPS and UWB can still contribute information in case of partial availability (Wieser et al., 2007). That is the most important reason why tight integration of GPS and UWB has been chosen for this research because GPS receiver often has a bad visibility condition in an urban canyon.

4.3.2 Tightly Integrated GPS/UWB Cooperative Positioning Supported by V2X Communication

Although multi-sensor integration has achieved encouraging results in recent years, it cannot always meet the positioning requirements, e.g. where-in-the-lane level accuracy, particularly when we are talking about safety-related V2X applications. Basing on the multi-sensor integration, additional observations shared between transportation participants are able to enhance positioning capability further. On the strength of the development of V2X communication (e.g. DSRC), Cooperative Positioning (CP) opens another way to support numerous V2X applications. Cooperative positioning, also called collaborative positioning, is a positioning approach in which a number of participants contribute their position-related information (Garello et al., 2012). To explain the merits of the CP over the individually positioning, 'the whole is greater than the sum of its parts' maybe the best way to interpret its benefits of sharing information. In a CP system, two or more participants are allowed to work cooperatively to improve their position performance by sharing relevant location information. Bridging the communication gaps among transportation participants by V2X communication, vehicles are able to cooperatively position their locations by talking with surrounding participants for exchanging information.

With the assumption that V2X connectivity has been enabled for each vehicle, the protocols that how a vehicle resolves its position through the proposed CP are presented as follows: Individually, the positioning unit on each vehicle calculates its position using available data collected from both on-board sensors and surrounding vehicles or the Road Side Units (RSUs) via V2X communication, with respect to the current time. Simultaneously, the communication unit on each vehicle transmits its measurements and the calculated position of the neighbouring vehicles. Consequentially, each vehicle pinpoints and sends data recurrently when they are running on the road. By taking advantage of V2X communication, vehicles are able to share information with surrounding transportation participants for critical safety applications, such as lane change assistance, intersection collision warning,

overtaking vehicle warning, rear end collision warning, etc. (Karagiannis et al., 2011).

The schematic of the proposed Robust Cooperative Positioning (RCP) method supported by V2X communication is given in Fig.4.3. It is worth noting that the UWB technology is also capable of short range communication. The reason for assuming the DSRC unit rather than the UWB unit for communication is the coverage of UWB communication is usually up to 10 metres which are too small to build up the communication link between vehicles (Park and Rappaport, 2007). DSRC It is assumed that every vehicle and RSU is equipped with a set of a single frequency GPS receiver, a UWB unit, and a DSRC unit to communicate with each other for exchanging position-related information. Meanwhile, some vehicles are fitted with a dual-frequency GPS receiver which is able to receive high-grade GPS measurement (i.e. carrier phase) to provide real-time centimetre level position accuracy through Real-Time Kinematic (RTK) technique. These vehicles could be a speciality vehicle, for example, ambulance, police car, dangerous goods transport vehicle or perhaps just a premium car. On the other hand, the precise coordinate of the RSUs are pre-measured and broadcasted to the neighbouring vehicles. Moreover, some RSUs may be fitted with GPS receivers which allow them to provide real-time DGPS corrections.

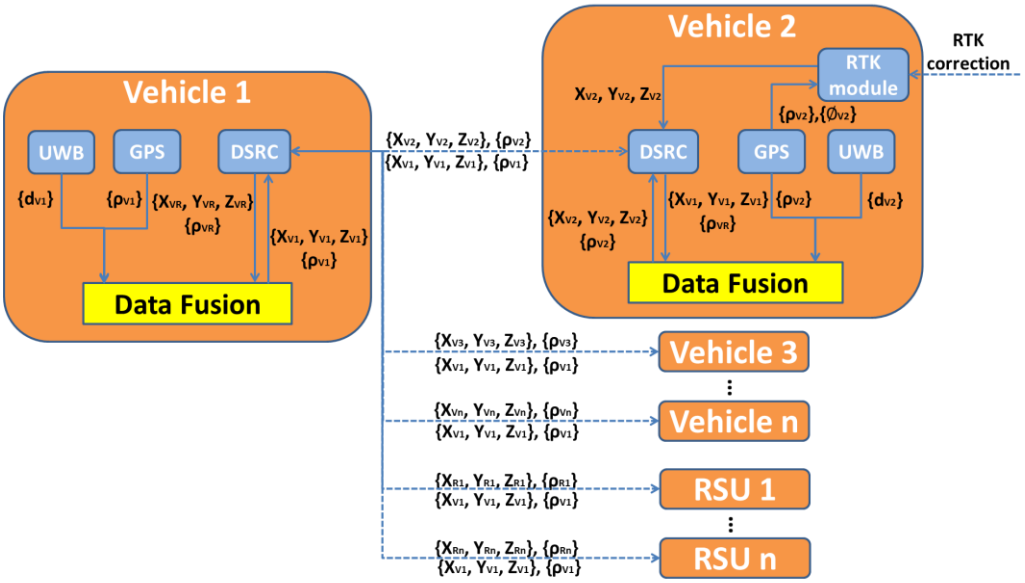


Fig.4.3 The Schematic of GPS/UWB Cooperative Positioning Method Supported by V2X

That solid line and dotted line arrows indicate the data flow inside an individual positioning unit and the communication link among transport participants, respectively. Supposing vehicle 1 is the target vehicle that needs to solve its location. It talks to other vehicles, which are fitted with the RTK module and the RSUs in the vicinity for trading information. The DSRC unit is used to exchange position-related information among the vehicles and RSUs at the beginning and the end of a positioning iteration. To solve the position of the target vehicle, the collected raw GPS pseudo-ranges $\{\rho_{V1}\}$ and UWB ranging observations $\{d_{V1}\}$ are fused together with a group of GPS pseudo-range measurements $\{\rho_{VR}\}$ and precise coordinates $\{X_{VR}, Y_{VR}, Z_{VR}\}$ of the nearby vehicles and RSUs. To simplify the computational process of coordinate transformation, the coordinates of all the UWB units installed on the RSUs will be set within the European Terrestrial Reference System 1989 (ETRS89) coordinate system which is in accordance with the GPS coordinate output.

4.3.3 Robust Cooperative Positioning

4.3.3.1 State Model

One of the keys to precise target positioning lies in the effective extraction of useful information about the targets state from the observations. This information extraction will be facilitated to a great extent by selecting a proper state model of the target that most accurately describes the target motion pattern (Li and Jilkov, 2003). In this proposed Robust Cooperative Positioning (RCP) method, the state model is a linear system and the discrete time Constant Velocity dynamic model has been chosen. Referring to Eq. 4.13 and Eq. 4.14, the state vector $\hat{x}$, the state transition matrix F and the process noise covariance matrix Q are defined as (Brown and Hwang, 2012):

$$\hat{x} = \begin{bmatrix} \Delta x & \Delta \dot{x} & \Delta y & \Delta \dot{y} & \Delta z & \Delta \dot{z} \end{bmatrix}^T \tag{4.28}$$

$$F = \begin{bmatrix} 1 & \Delta t & 0 & 0 & 0 & 0 \\ 0 & 1 & 0 & 0 & 0 & 0 \\ 0 & 0 & 1 & \Delta t & 0 & 0 \\ 0 & 0 & 0 & 1 & 0 & 0 \\ 0 & 0 & 0 & 0 & 1 & \Delta t \\ 0 & 0 & 0 & 0 & 0 & 1 \end{bmatrix} \tag{4.29}$$

$$Q = \begin{bmatrix} \frac{1}{3}s_p\Delta t^3 & \frac{1}{2}s_p\Delta t^2 & 0 & 0 & 0 & 0 \\ \frac{1}{2}s_p\Delta t^2 & s_p\Delta t & 0 & 0 & 0 & 0 \\ 0 & 0 & \frac{1}{3}s_p\Delta t^3 & \frac{1}{2}s_p\Delta t^2 & 0 & 0 \\ 0 & 0 & \frac{1}{2}s_p\Delta t^2 & s_p\Delta t & 0 & 0 \\ 0 & 0 & 0 & 0 & \frac{1}{3}s_p\Delta t^3 & \frac{1}{2}s_p\Delta t^2 \\ 0 & 0 & 0 & 0 & \frac{1}{2}s_p\Delta t^2 & s_p\Delta t \end{bmatrix} \tag{4.30}$$

Where $\hat{x}$ is comprised the correction of Cartesian coordinates in GPS coordinate system and corresponding velocities in three directions. Δt and s_p

denote the sampling time interval and the spectral density for position random process. In this proposed RCP method, Δt and s_p are chosen as 1 s and 0.05 m^2/s^3.

4.3.3.2 Measurement Model

The actual observation $X_{observed}$ could be written as the sum of a modelled observation $X_{modelled}$, plus an error term. The modelled observation is configured by the measurement model and split up into an estimated value $\tilde{X}$, a correction term ΔX and an error term v.

$$\begin{aligned} X_{observed} &= X_{modelled} + noise \\ &= \tilde{X} + \Delta X + v \end{aligned} \tag{4.31}$$

In this proposed RCP method, the measurement model is considered as a non-linear model and is composed of the DD code pseudo-range and UWB ranging observations. The measurement vector and the design matrix in Eq. 4.23 can be expressed as follows:

$$z = X_{observed} - X_{modelled} = \Delta X = \begin{bmatrix} \Delta\rho_1^{DGPS} \\ \Delta\rho_2^{DGPS} \\ \vdots \\ \Delta\rho_{m-1}^{DGPS} \\ \Delta d_1^{UWB} \\ \Delta d_2^{UWB} \\ \vdots \\ \Delta d_n^{UWB} \end{bmatrix} \tag{4.32}$$

$$H = \begin{bmatrix} \frac{\partial P}{\partial x} & \frac{\partial P}{\partial y} & \frac{\partial P}{\partial z} \end{bmatrix} \tag{4.33}$$

Where m and n are the numbers of GPS satellite and UWB base unit. The Δ term denotes the difference between the actual and modelled observations.

Furthermore, the observation equations of GPS pseudo-ranges and UWB ranging observations are shown as follows.

$$\rho_a^{S_m} = \sqrt{(X_a - X^{S_m})^2 + (Y_a - Y^{S_m})^2 + (Z_a - Z^{S_m})^2} \quad 4.34$$

$$d_a^{U_n} = \sqrt{(X_a - X^{U_n})^2 + (Y_a - Y^{U_n})^2 + (Z_a - Z^{U_n})^2} \quad 4.35$$

Where the superscripts "S" and "U" indicate the GPS satellites and the UWB base units, respectively. $\rho_a^{S_m}$ denotes the pseudo-range between receiver a and GPS satellite m. Moreover, $d_a^{U_n}$ denotes the ranging between receiver a and UWB base unit n.

Applying Taylor's theorem, the observation equations of GPS pseudo-range and UWB ranging are expanded at an estimated receiver position (X_0, Y_0, Z_0), and higher order terms are ignored. They are expressed in matrix form as:

$$\rho_a^{S_m} = \rho_{a_0}^{S_m} + \begin{bmatrix} \frac{X_0 - X^{S_m}}{\rho_{a_0}^{S_m}} & \frac{Y_0 - Y^{S_m}}{\rho_{a_0}^{S_m}} & \frac{Z_0 - Z^{S_m}}{\rho_{a_0}^{S_m}} & 1 \end{bmatrix} \begin{bmatrix} \Delta x \\ \Delta y \\ \Delta z \\ \Delta \tau \end{bmatrix} \quad 4.36$$

$$d_a^{U_n} = d_{a_0}^{U_n} + \begin{bmatrix} \frac{X_0 - X^{U_n}}{d_{a_0}^{U_n}} & \frac{Y_0 - Y^{U_n}}{d_{a_0}^{U_n}} & \frac{Z_0 - Z^{U_n}}{d_{a_0}^{U_n}} \end{bmatrix} \begin{bmatrix} \Delta x \\ \Delta y \\ \Delta z \end{bmatrix} \quad 4.37$$

Where $\Delta\tau$ is the clock bias correction.

As discussed in Section 3.3.3, both satellite and receiver clock offsets are eliminated by applying DD technique. So $\Delta\tau$ is removed from the unknown list. According to Eq. 3.7, the measurement model of RCP is particularly written as:

$$z = \begin{bmatrix} \nabla\Delta\rho_{ab}^{12} - \nabla\Delta\rho_{a_0b}^{12} \\ \nabla\Delta\rho_{ab}^{13} - \nabla\Delta\rho_{a_0b}^{13} \\ \vdots \\ \nabla\Delta\rho_{ab}^{1m} - \nabla\Delta\rho_{a_0b}^{1m} \\ d_a^1 - d_{a_0}^1 \\ d_a^2 - d_{a_0}^2 \\ \vdots \\ d_a^n - d_{a_0}^n \end{bmatrix} \tag{4.38}$$

$$H = \begin{bmatrix} \frac{X_0 - X^{S_1}}{\rho_{a_0}^{S_1}} - \frac{X_0 - X^{S_2}}{\rho_{a_0}^{S_2}} & 0 & \frac{Y_0 - Y^{S_1}}{\rho_{a_0}^{S_1}} - \frac{Y_0 - Y^{S_2}}{\rho_{a_0}^{S_2}} & 0 & \frac{Z_0 - Z^{S_1}}{\rho_{a_0}^{S_1}} - \frac{Z_0 - Z^{S_2}}{\rho_{a_0}^{S_2}} & 0 \\ \frac{X_0 - X^{S_1}}{\rho_{a_0}^{S_1}} - \frac{X_0 - X^{S_3}}{\rho_{a_0}^{S_3}} & 0 & \frac{Y_0 - Y^{S_1}}{\rho_{a_0}^{S_1}} - \frac{Y_0 - Y^{S_3}}{\rho_{a_0}^{S_3}} & 0 & \frac{Z_0 - Z^{S_1}}{\rho_{a_0}^{S_1}} - \frac{Z_0 - Z^{S_3}}{\rho_{a_0}^{S_3}} & 0 \\ \vdots & \vdots & \vdots & \vdots & \vdots & \vdots \\ \frac{X_0 - X^{S_1}}{\rho_{a_0}^{S_1}} - \frac{X_0 - X^{S_m}}{\rho_{a_0}^{S_m}} & 0 & \frac{Y_0 - Y^{S_1}}{\rho_{a_0}^{S_1}} - \frac{Y_0 - Y^{S_m}}{\rho_{a_0}^{S_m}} & 0 & \frac{Z_0 - Z^{S_1}}{\rho_{a_0}^{S_1}} - \frac{Z_0 - Z^{S_m}}{\rho_{a_0}^{S_m}} & 0 \\ \frac{X_0 - X^{U_1}}{d_{a_0}^{U_1}} & 0 & \frac{Y_0 - Y^{U_1}}{d_{a_0}^{U_1}} & 0 & \frac{Z_0 - Z^{U_1}}{d_{a_0}^{U_1}} & 0 \\ \frac{X_0 - X^{U_2}}{d_{a_0}^{U_2}} & 0 & \frac{Y_0 - Y^{U_2}}{d_{a_0}^{U_2}} & 0 & \frac{Z_0 - Z^{U_2}}{d_{a_0}^{U_2}} & 0 \\ \vdots & \vdots & \vdots & \vdots & \vdots & \vdots \\ \frac{X_0 - X^{U_n}}{d_{a_0}^{U_n}} & 0 & \frac{Y_0 - Y^{U_n}}{d_{a_0}^{U_n}} & 0 & \frac{Z_0 - Z^{U_n}}{d_{a_0}^{U_n}} & 0 \end{bmatrix} \tag{4.39}$$

Where S_1 is chosen as the reference satellite based on the maximal elevation angle. Also, the second, fourth and sixth columns are assigned to 0 as there is no velocity measurement input.

In Eq. 4.31, the error term v is turned into the covariance matrix of the measurement noise by applying Eq. 4.12. R is a $(m+n-1)\times(m+n-1)$ dimension diagonal matrix that is constitutive of the variances of the DD code pseudo-range and UWB ranging observations.

$$R=\begin{bmatrix} \sigma_{DGPS}^2 & & & 0_{(m-1)\times n} & \\ & \ddots & & & \\ & & \sigma_{DGPS}^2 & & \\ & & & \sigma_{UWB}^2 & \\ 0_{n\times(m-1)} & & & & \ddots \\ & & & & \sigma_{UWB}^2 \end{bmatrix} \quad 4.40$$

Where $\sigma_{DGPS}^2=0.25$ m^2 and $\sigma_{UWB}^2=0.04$ m^2 in this proposed RCP method, respectively. The measurement noise of GPS is chosen based on DD code pseudo-range accuracy in a good environment while the measurement noise of UWB is determined from the UWB ranging accuracy assessment in Section 5.3.2.

4.3.3.3 Initial Value Assignment

To carry out the RCP method, the initial value of the state vector $\hat{x}_0$ and the associated covariance matrix P_0 are assigned as follows.

$$\hat{x}_0=\begin{bmatrix}0 & 0 & 0 & 0 & 0 & 0\end{bmatrix}^T \quad 4.41$$

$$P_0 = \begin{bmatrix} 10 & & & & & \\ & 1 & & & 0 & \\ & & 10 & & & \\ & & & 1 & & \\ & 0 & & & 10 & \\ & & & & & 1 \end{bmatrix} \quad 4.42$$

Where P_0 is a diagonal matrix with initial variances of 10 m^2 for positions and 1 m^2/s^2 for velocities in three dimensions.

With regard to the estimated receiver position at the first epoch, it is recommended that an approximate coordinate should be employed rather than starting from 0. In doing so, the convergence period that the KF outputs a reasonable result could be largely reduced. The estimated coordinate either can directly receive the coordinate of surrounding vehicles or RSUs through V2X communication as long as they have clear Line-of-Sight (LOS) to the target vehicle or calculate by using the Single Point Positioning (SPP) technique. Firstly, the UWB ranging observation d is the sole criterion to select the nearest vehicle or RSU. On the other hand, if the user can observe sufficient visible satellites (at least 4 satellites) the WLSE method is utilised to generate the approximate receiver coordinate by applying Eq. 4.8. According to Eq. 4.36 and Eq. 4.37, the state vector, the design matrix, measurement vector and weight matrix for SPP WLSE method are shown as follows:

$$\hat{x} = \begin{bmatrix} \Delta x & \Delta y & \Delta z & \Delta \tau \end{bmatrix}^T \quad 4.43$$

$$H=\begin{bmatrix} \frac{X_0-X^{S_1}}{\rho_0^{S_1}} & \frac{Y_0-Y^{S_1}}{\rho_0^{S_1}} & \frac{Z_0-Z^{S_1}}{\rho_0^{S_1}} & 1 \\ \frac{X_0-X^{S_2}}{\rho_0^{S_2}} & \frac{Y_0-Y^{S_2}}{\rho_0^{S_2}} & \frac{Z_0-Z^{S_2}}{\rho_0^{S_2}} & 1 \\ \vdots & \vdots & \vdots & \vdots \\ \frac{X_0-X^{S_m}}{\rho_0^{S_m}} & \frac{Y_0-Y^{S_m}}{\rho_0^{S_m}} & \frac{Z_0-Z^{S_m}}{\rho_0^{S_m}} & 1 \\ \frac{X_0-X^{U_1}}{d_a^{U_1}} & \frac{Y_0-Y^{U_1}}{d_a^{U_1}} & \frac{Z_0-Z^{U_1}}{d_a^{U_1}} & 0 \\ \frac{X_0-X^{U_2}}{d_a^{U_2}} & \frac{Y_0-Y^{U_2}}{d_a^{U_2}} & \frac{Z_0-Z^{U_2}}{d_a^{U_2}} & 0 \\ \vdots & \vdots & \vdots & \vdots \\ \frac{X_0-X^{U_n}}{d_a^{U_n}} & \frac{Y_0-Y^{U_n}}{d_a^{U_n}} & \frac{Z_0-Z^{U_n}}{d_a^{U_n}} & 0 \end{bmatrix} \tag{4.44}$$

$$z=\begin{bmatrix} \rho_a^1-\rho_{a_0}^1 \\ \rho_a^2-\rho_{a_0}^2 \\ \vdots \\ \rho_a^m-\rho_{a_0}^m \\ d_a^1-d_{a_0}^1 \\ d_a^2-d_{a_0}^2 \\ \vdots \\ d_a^n-d_{a_0}^n \end{bmatrix} \tag{4.45}$$

$$W=\begin{bmatrix} 1/\sigma_{GPS}^2 & & & & & \\ & \ddots & & & 0 & \\ & & 1/\sigma_{GPS}^2 & & & \\ & & & 1/\sigma_{UWB}^2 & & \\ & 0 & & & \ddots & \\ & & & & & 1/\sigma_{UWB}^2 \end{bmatrix} \tag{4.46}$$

Where W is a diagonal matrix that is constitutive of the variances of the GPS pseudo-range $\sigma_{GPS}^2 = 10$ m^2 and UWB ranging $\sigma_{UWB}^2 = 0.04$ m^2 with the size of $(m+n)\times(m+n)$.

4.3.3.4 Implementation of RCP Method

A MATLAB script, GPS Easy, using C/A pseudo-ranges on L1 frequency for positioning of GPS receiver was developed by Kai Borre (Borre, 2003). The code is extended for DGPS and UWB integration implementation in the proposed RCP method which is fully programmed in MATLAB R2015a (version 8.5) environment. The data flow chart of the proposed RCP method is shown in Fig.4.4, including the equations used in each step. In addition, the coordinate system of the proposed RCP method is ETRS89. The coordinates of nearby vehicles and RSUs are obtained in ETRS89 in order to save the computation of coordinate conversion. Hence, the output positioning result will automatically stay in ETRS89.

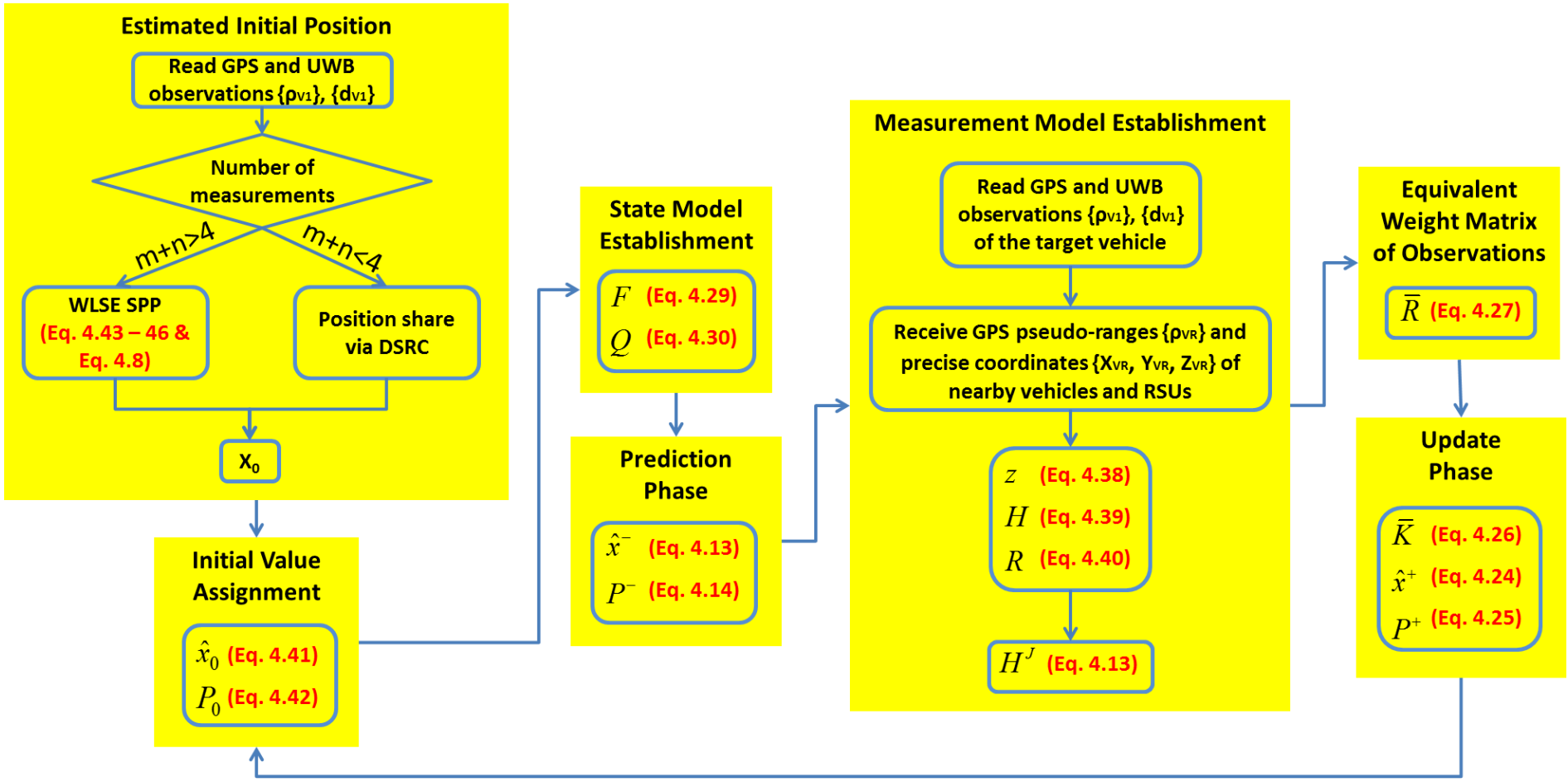


Fig.4.4 Data Flow Chart for Robust Cooperative Positioning (RCP) Method

The main features of RCP method are as follows:

1. **Estimated Initial Position**: The target vehicle (V1) collects GPS code pseudo-ranges $\{\rho_{V1}\}$ and UWB ranging $\{d_{V1}\}$ observations by the onboard sensor. The sum of the numbers of measurements (number of the visible satellite is m and the number of UWB base units is n) is the criterion that decides the way to obtain the estimated target vehicle initial position X_0. If the total number of measurements is more than 4, the WLSE SPP method is employed to solve its location based on collected GPS and UWB observations. Then the solution for target vehicle position can be provided. If there is not sufficient measurement, the approximate position is set as the location of the nearest vehicle or RSU is transmitted via DSRC.

2. **Initial Value Assignment**: To start the KF recursion, the initial value of state vector $\hat{x}_0$ and its associated covariance matrix P_0 need to be given. It is worth noting that the state vector should be reset as 0 when every time a new iteration begins as the states of adjacent epochs are independent.

3. **State Model Establishment**: The state vector of RCP method is composed of positions and velocities in three directions. The Constant Velocity dynamic model has been selected for RCP method, and the spectral density for position random process needs to be pre-set. Consequently, the state transition matrix F and the process noise covariance matrix Q are formed.

4. **Prediction Phase**: Substituting the estimated target vehicle position X_0 and initial values of the state vector $\hat{x}_0$ and corresponding covariance matrix P_0 into the state model, the priori predictions $\hat{x}^-$ and P^- are produced.

5. **Measurement Model Establishment**: GPS code pseudo-range $\{\rho_{V1}\}$ and UWB ranging $\{d_{V1}\}$ measurements of the target vehicle have been collected when we figure out the estimated position. Then the onboard DSRC unit talks to nearby vehicles and RSUs for position-related data exchange. The GPS code pseudo-range $\{\rho_{VR}\}$ measurements and precise coordinates $\{X_{VR}, Y_{VR}, Z_{VR}\}$ of the surrounding vehicles and RSUs are transmitted. The received data is combined with own observations of the target vehicle in order to structure the DGPS/UWB measurement vector z, the design matrix H and the measurement noise covariance matrix R. In addition, the components of R are determined by the variances of GPS code pseudo-range and UWB ranging observation. In the proposed RCP method, the measurement models of GPS and UWB are non-linear systems and linearization process based on Taylor expansion is applied to obtain the new design matrix H^J.

6. **Equivalent Weight Matrix of Observations**: In the case that GPS pseudo-ranges and UWB ranging observations contain outliers, an equivalent weight matrix of observations $\bar{R} = \bar{W}^{-1}$ must be generated by inflating the components of original measurement noise covariance matrix R based on the magnitude of the outlier. Thus the RKF can be applied to control the influence of outliers.

7. **Update phase**: The Kalman gain $\bar{K}$ is used to adjust the contributions of a priori predictions and measurements on the current state. The posteriori state estimation $\hat{x}^+$ and corresponding covariance matrix P^+ are solved by merging a priori prediction and measurement. Consequently, the position of the target vehicle can be obtained by adding posteriori state estimation $\hat{x}^+$ and estimated position X_0. Finally, the posteriori estimations are sent to next epoch as new priori estimation for further iteration.

4.4 Summary

This chapter firstly discusses the estimation from positioning algorithm perspective. The basic estimation approach LSE is explicated which is purely process the measurement information. Then another method, the KF, is introduced particularly on its beauty of fusing previous state information and current measurements. EKF is adopted because both GPS and UWB have a non-linear measurement model and RKF is further employed due to the outliers in raw observation. In consideration of the application scenario, i.e., the urban canyon, additional observations could alleviate the problem caused by building obstruction. The additional observations can either obtain from integrated sensors or receive from neighbouring transportation participants via V2X communication. Using the RKF algorithm, the Robust Cooperative Positioning (RCP) based on multi-sensor integration and V2X communication is finally proposed in this research. The details of model establishment and data flow are elaborated.

Chapter 5 UWB Ranging Assessment

5.1 Overview

As discussed in Chapter 4, the UWB technology is the sole augment positioning technology to GPS to implement cooperative positioning in this thesis. Therefore, the UWB positioning capability should be comprehensively assessed as well as the performance of UWB ranging observations. This chapter starts with the introduction of the particular UWB unit used in this thesis, produced by Thales Group U.K, on its technical parameters, including power density, communication mode and time synchronisation. Then three experiments have been conducted to evaluate the availability, accuracy and precision of UWB ranging observation and UWB-only positioning performance and ended with detailed analysis and discussion.

5.2 The Thales UWB System

As shown in Fig.5.1, the UWB unit used in the trials throughout this research is the Thales Lock-on Model LD2 UWB system which utilises a combination of Frequency Hopped and Direct Sequence Spread Spectrum signal covering 4760 MHz to 6200 MHz. The unit is supplied with external power and complies with the standard UWB power density limit of -41.3 dBm/MHz, which leads to a nominal output power of 100 μW. The unit size is 185 mm (height) × 80 mm (width) × 35 mm (depth), and the unit weight is 500g (Thales, 2010).



Fig.5.1 Thales Lock-on Model LD2 UWB Unit

A built-up UWB positioning network consists of two types of units: Base Unit (BU) and Mobile Unit (MU). Normally, a BU is stationary and set up over a known position where as an MU whose position is unknown and needs to be solved. With at least three non-collinear BUs, a local coordinate system can be built. In addition, one of the BUs (and only one) must be setup as a master BU in order to provide time synchronisation among the whole network. Fig.5.2 diagrammatically shows how the Thales UWB system positioning using TDOA technique. Immediately after switch on, the master BU will start transmitting to other BUs for synchronisation. Once the BUs have synchronised, the MUs can be powered up. Regarding the positioning, the master BU transmits a package to the next BU in a ring formation. In the meantime, the MU receives same packages and measures TDOA. With at least four TDOA observations, the MU's 3D position can be calculated.

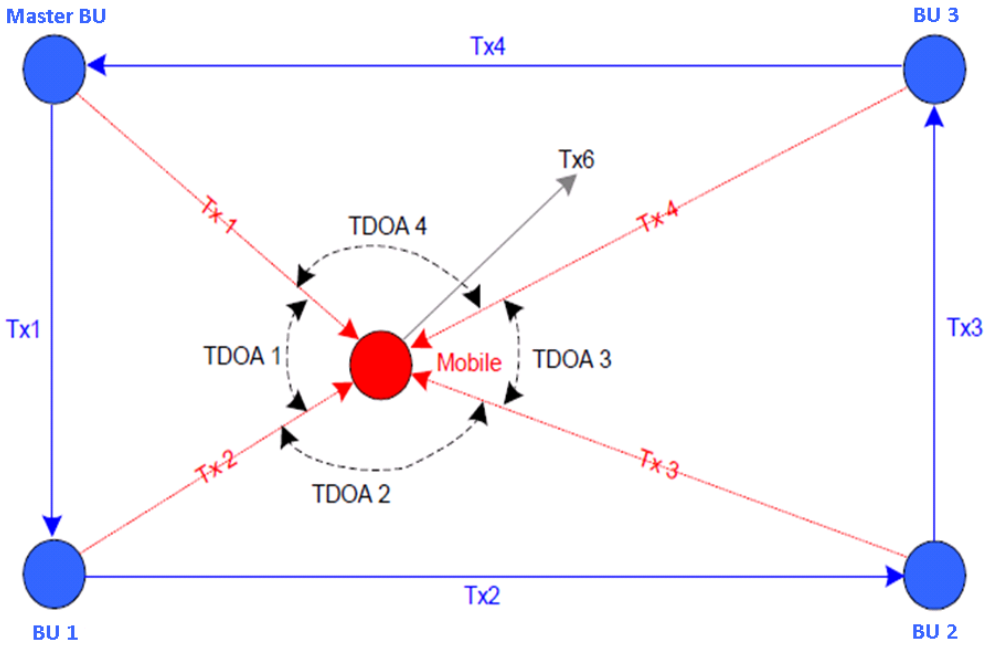


Fig.5.2 Thales TDOA Positioning

The Thales UWB system achieves positioning through TDOA technique. Meanwhile, an MU can provide distances to the BUs as long as a master BU is within the network. In this research, the UWB ranging observations are more meaningful than the Thales UWB positioning solution. The first reason is a target vehicle equipped with an MU cannot always stay in one positioning network in consideration of application area of this research. Secondly, it is realistic infeasible to set up a huge number of BUs alongside the road to form the UWB positioning network everywhere. Thirdly, a target vehicle equipped with an MU may not have sufficient BUs around to determine its position. Therefore, the Thales UWB positioning solution is not required in this research. And the TOA technique is replaced for positioning based on UWB ranging observations.

Before conducting any UWB ranging tests, two basic parameters of the Thales UWB unit should be determined, namely, sampling rate and time. For most of the tests, the sampling rates of UWB ranging were set as 1 Hz, although the Thales UWB units can provide a higher sampling rate and a high observation update frequency is desired for the V2X applications. The reason for choosing

low sampling rate is the Thales UWB units cannot give a precise decimal place in time, and an estimated or interpolated ranging may bring unexpected errors into the observation. With regard to the time system used in Thales UWB unit, the unit doesn't have an own clock and the time of ranging observations is stamped by the laptop that is connected to the unit. Therefore, the time accuracy of the UWB unit purely counts on the laptop's system time accuracy. The laptop system time was synchronised to the GPS time instead of UTC for all the tests so that we can get rid of dealing with GPS time offset. To check the accuracy of the laptop system time, a website (called time.is) offers a free online service that lets you compare your system time with an atomic clock, The displayed time on the laptop has a precision of 0.02 - 0.10 seconds, and this depends on the internet connection and how busy the computer is (TheWindowsClub, 2016, time.is, 2016). As an example shown in Fig.5.3, the laptop system time has a 0.041 seconds difference with 0.016 seconds precision according to the website service.



Fig.5.3 The Accuracy of the Laptop System Time, based on source: (time.is, 2016)

5.3 Ranging Data Collection and Analysis

The Thales UWB units are set up in different environments to evaluate the performance of the UWB ranging. Static, kinematic, indoor and outdoor scenarios are investigated due to different expected magnitude of errors. Theoretically, the ranging error observed in an open static environment should be smallest. Moreover, the level or ranging error would be grown due to the existence of the NLOS situation and the movement of the units.

5.3.1 Indoor Static Test

The first test has been carried out in a laboratory room of the Nottingham Geospatial Building (NGB) to examine the positioning performance of the Thales UWB unit in a static scenario. The network consisted of Six BUs and one MU. The MU was placed on a table in the centre of the room, and six BUs were distributed around the perimeter of the room at different heights. All UWB units stood still during the test, and the distribution diagram is shown in Fig.5.4.

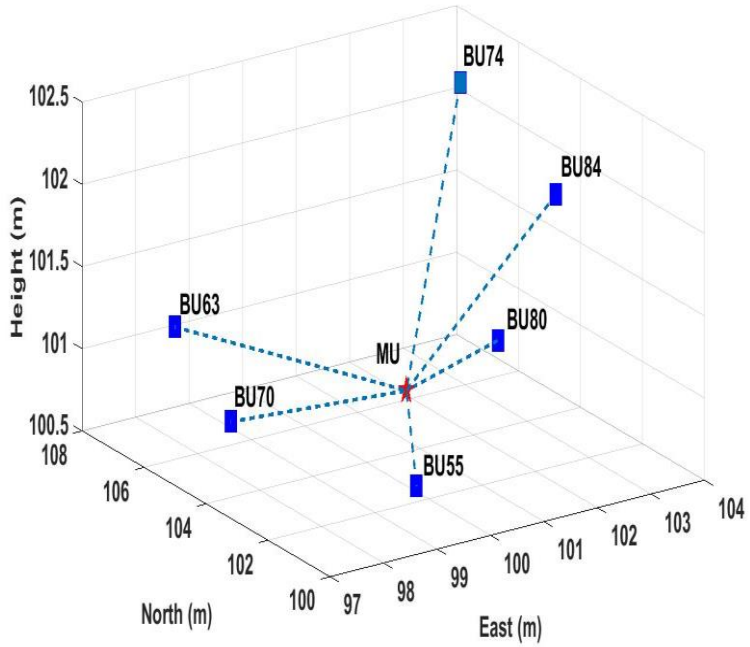


Fig.5.4 UWB System Setup in Static Test

Each BU location was pre-measured by a Leica TS30 Robotic Total Station (RTS) which can offer millimetre level accuracy. The precise coordinates were assigned to six BUs to form a temporary local coordinate system. The MU was placed in the middle of the network to measure ranging to each BU, and its ground truth of position was also obtained from the total station. Thus, the actual distance between the MU and each BU can be calculated based on known coordinates as shown in Table 5.1.

Table 5.1 The BU and MU Coordinates in Static Test

Unit Number	East (m)	North (m)	Height (m)	Distance to the MU (m)
BU55	99.31	101.18	100.73	3.02
BU63	97.85	106.48	101.24	3.85
BU70	97.72	104.45	100.89	3.01
BU74	103.83	107.59	102.10	5.03
BU80	102.99	104.93	100.89	2.55
BU84	102.94	102.96	102.01	2.69
MU	100.67	103.87	100.90	

The UWB ranging observations from the MU to each BU were logged on a laptop for 7 minutes and compared to the exact distances. To collect as much as possible UWB ranging observations, the sampling rate was set as approximate 4 Hz. The reason we called it "approximate" is that when the Thales UWB unit cannot provide exact 4 Hz, instead, the output sampling rate will fluctuate around 4 Hz depending on the communication. As shown in Fig.5.5, 60% of epoch the Thales UWB unit gave the 4 Hz output during the test.

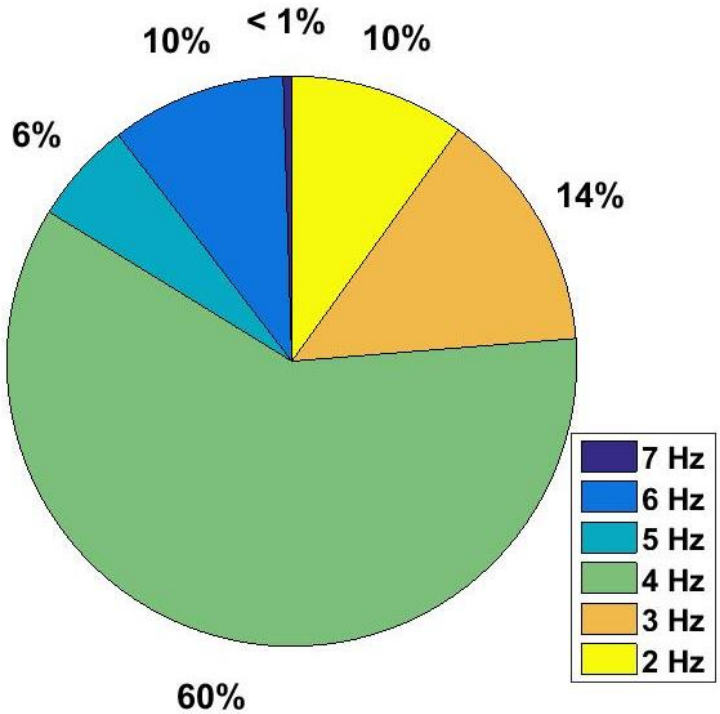


Fig.5.5 UWB Ranging Sampling Rate in Static Test

Before comparing to the ground truth, the logged UWB ranging observations are pre-processed by averaging the received ranging in each second. Then the difference between resampled 1 Hz ranging and exact distance is regarded as the ranging error and plotted in Fig.5.6. The severe missing data on the ranging observation of BU55 was caused by the wrong configuration of the Thales UWB unit and this problem has been found and corrected in the future data collection. In addition, the few spikes may be caused by the NLOS situation of people passing around because the test was conducted in a lab.

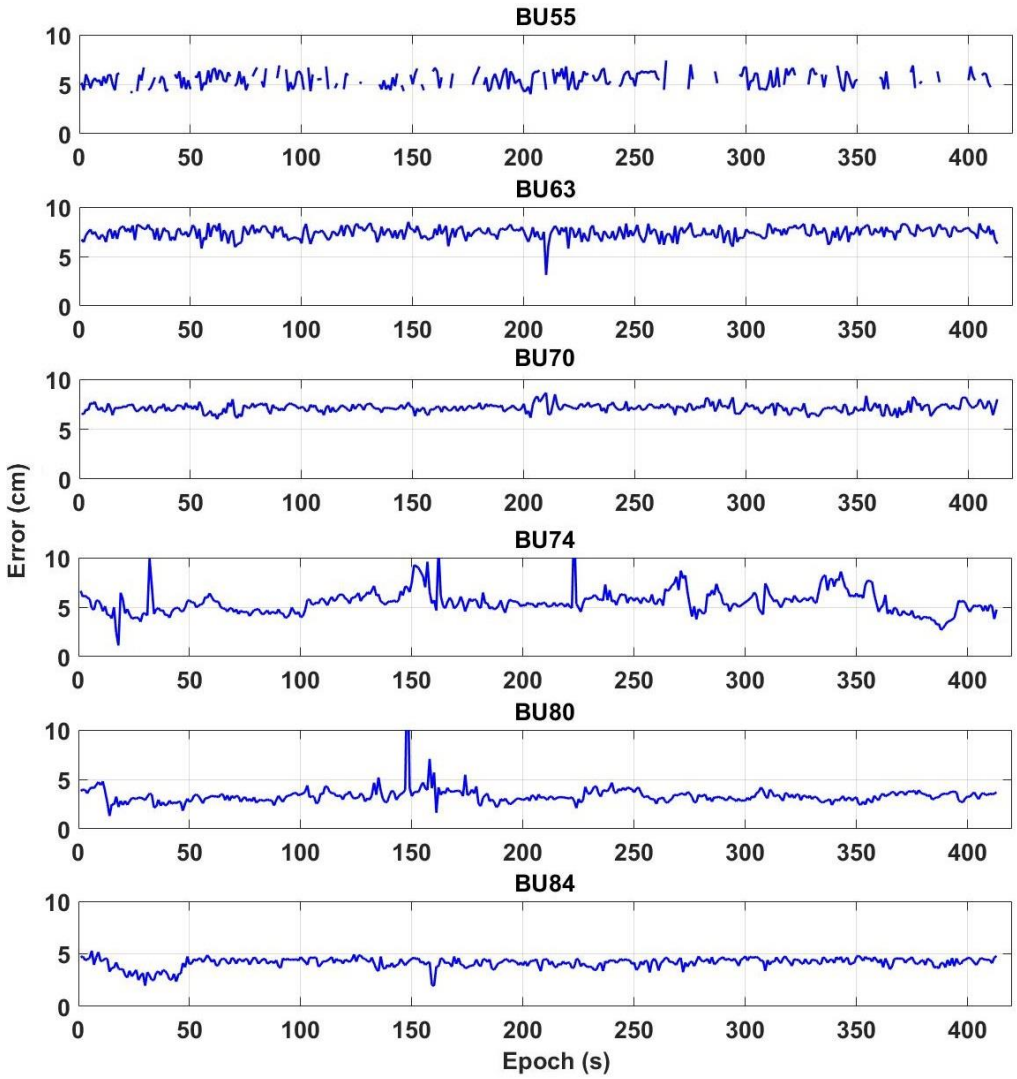


Fig.5.6 UWB Ranging Error in Static Test

Although there are few outliers, the Thales UWB unit generally provides very accurate ranging in the static test with the units setup in a good geometry. The

UWB units can provide approximately 5 cm accuracy with 1 cm precision, and the detailed statistics are listed in Table 5.2.

Table 5.2 UWB Ranging Error in Static Test

MU to BU Number	Accuracy (cm)	Precision (cm)	1 σ Percentage	2 σ Percentage
BU55	5.6	0.8	55.9%	99.3%
BU63	7.4	0.8	70.2%	97.6%
BU70	7.2	0.4	73.4%	93.9%
BU74	5.6	2.0	77.2%	95.4%
BU80	3.5	1.2	93.0%	98.5%
BU84	4.2	0.6	79.9%	94.7%

The static test proves the ability of the Thales UWB unit to provide very accurate ranging in an ideal environment. However, the ranging information is intended to apply in vehicle positioning where the unit is in a dynamic scenario. It is anticipated that the ranging accuracy may drop when the MU is moving as its relative position to other units will keep changing. The ranging performance in a dynamic mode will be investigated in the next section.

5.3.2 Outdoor Dynamic Test

The dynamic test was conducted in an open environment in the middle of a piece of grass field as shown in Fig.5.7. The test aimed to evaluate how much the dynamic condition and measuring distance affect the UWB ranging performance and whether the ranging performance is improved in an open environment. A full network of four BUs and one MU was set up where four BUs and MU26 are spread evenly and placed still on the tripod. Moreover, another MU, MU74, was carried to move freely within the network coverage area.



Fig.5.7 Setup Environment in Dynamic Test

As same as the static test, the accurate coordinates of five stationary units were pre-measured by the Leica TS30 to provide ground truth as listed in Table 5.3. It is worth noting that the size of the network is much bigger than the size of indoor static test where the distances between static units were about fivefold to that in the indoor static test.

Table 5.3 The Stationary BU and MU Coordinates in Dynamic Test

Unit Number	East (m)	North (m)	Height (m)	Distance to the MU (m)
MU26	1099.23	1027.94	101.88	
BU80	1106.03	1045.55	102.07	18.88
BU84	1072.53	1020.13	101.95	27.82
BU89	1106.84	1017.09	101.66	13.26
BU97	1079.12	1047.48	101.95	28.04

In addition, MU74 was tied up on the top of a pole with a 360 °reflective prism, which was tracked by a Leica TS30 robotic total station in real-time. As claimed in the data sheet of Leica TS30 RTS that it can achieve 3 mm kinematic accuracy with a 360 °tracking prism (Leica, 2016a). With millimetre level accuracy provided by the total station, the accurate coordinate of MU74 can be recorded and then the performance of the UWB dynamic ranging

observations can be assessed. A laptop was synchronised to the GPS time and connected to the stationary MU, MU26, to store the ranging observation.

The dynamic test lasted about 16 minutes, and the sampling rate was set as 1 Hz. The ranging errors of MU26 to the stationary BUs and the moving MU74 are drawn below in Fig.5.8 and Fig.5.9. It is evident that the ranging observation on BU80 is less than other ranging observations. That was caused by the bad connection between the unit and external battery which led data missing of 45 out of 993 epochs. Moreover, there was also 1 epoch data missing on BU89 and BU97's ranging observations, respectively.

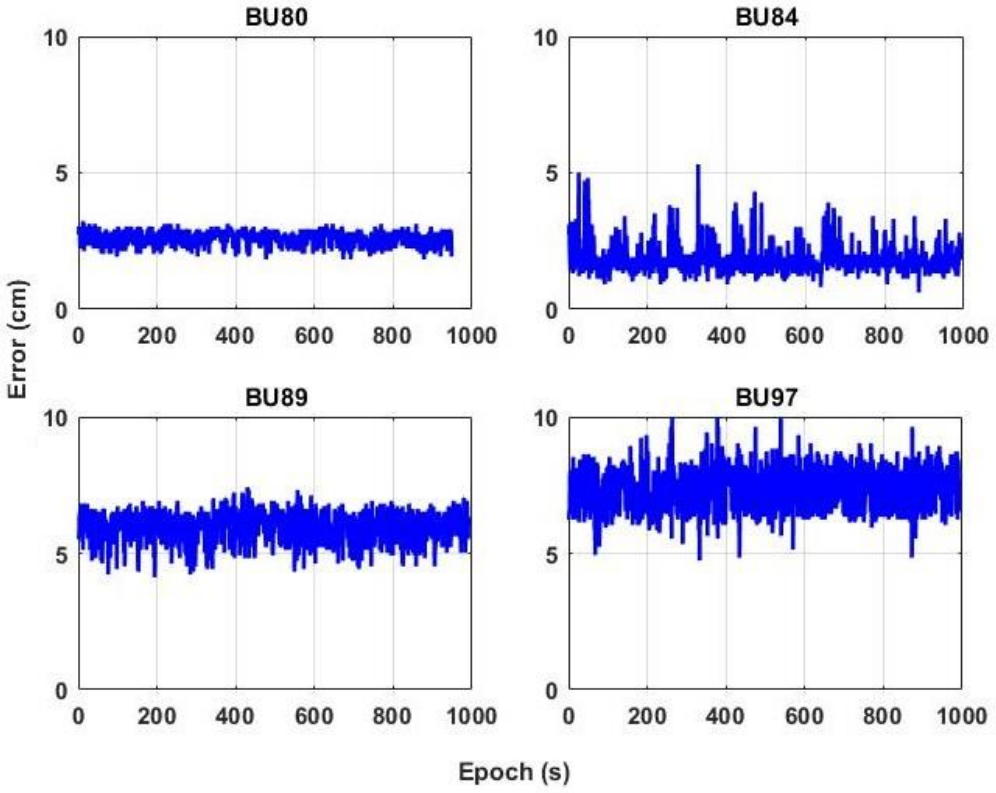


Fig.5.8 UWB Ranging Error in Open Environment

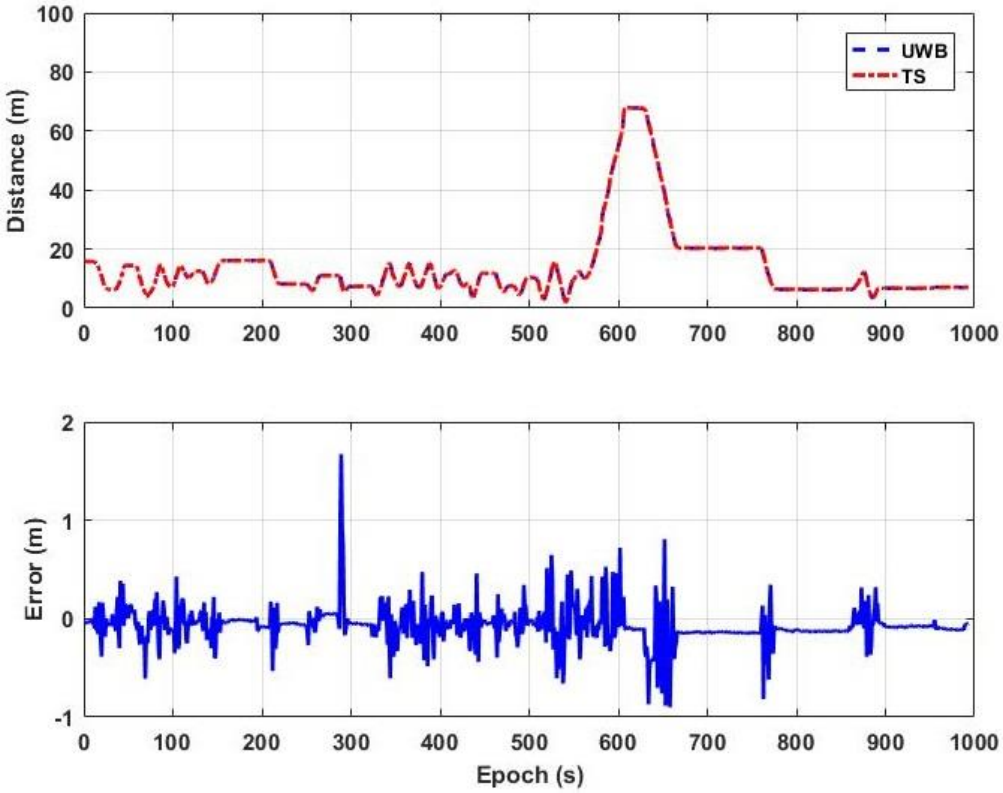


Fig.5.9 UWB Ranging Error under the Dynamic Condition

As listed in Table 5.4, the static ranging error in the outdoor open environment can maintain centimetre level, and the precision is better than 1 cm. To compare with the results in the indoor environment, the accuracy in the outdoor open environment is generally higher and more precise even though the measuring distance is much longer. The reason could be that there is less multipath in an open environment than the indoor environment.

On the other hand, the UWB ranging accuracy of the moving unit (between MU74 and MU26) is degraded than that of the static unit due to the movement of MU74. It can be found in Fig.5.9 that the ranging error in dynamic condition is larger than that in a static condition, but decimetre level accuracy can still be maintained. Throughout the 16 minutes dynamic test, the UWB ranging observations matched well with the distance calculated from total station observation and only a few large errors occurred which went over 1 metre at around epoch 300.

Table 5.4 UWB Ranging Error in Dynamic Test

MU to Unit Number	Accuracy (cm)	Precision (cm)	1 σ Percentage	2 σ Percentage
MU26	19.4	18.2	82.3%	94.7%
BU80	2.6	0.3	67.1%	95.9%
BU84	1.9	0.5	81.1%	95.0%
BU89	6.0	0.6	67.4%	96.0%
BU97	7.4	0.9	57.4%	97.8%

The dynamic test shows that the Thales UWB unit can offer 20 cm accuracy ranging observations under the dynamic condition and 0.2 metres is also chosen for the parameter to form the measurement noise matrix R as discussed in Section 4.3.3.2. In consideration of the V2X application scenario in which may contain multipath effect from surrounding construction and other transportation participants, the further dynamic test was performed to investigate the influence of multipath environment.

5.3.3 Locomotive Test

The locomotive test proceeded on the roof of the NGB in Jubilee Campus of the University of Nottingham. Seven UWB units and two sets of GPS device were used throughout the test. Specifically, five UWB units were placed on the tripod and distributed on the roof as the static BUs while other two units were carried by the locomotive and a person to moving along the track. An RTS was put on the top of a pillar to measure the precise coordinates of BUs before the test, and BUs' coordinates are listed in Table 5.5. The track is in an "8" shape and 120 m long with 20 cm width. As depicted in Fig.5.10, the solid blue line indicates the track and red pentagrams show the location of BUs. BU21 and BU22 were placed outside the track at the far corner while BU14 and BU23 were put near the middle part of the track and BU85 was placed in the inner loop of the track.

Table 5.5 The Static BU Coordinates in Locomotive Test

Unit Number	Easting (m)	Northing (m)	Height (m)
BU14	454931.224	339713.109	42.587
BU21	454915.295	339698.101	42.376
BU22	454950.217	339714.979	42.701
BU23	454939.832	339702.265	42.690
BU85	454924.088	339708.183	42.736

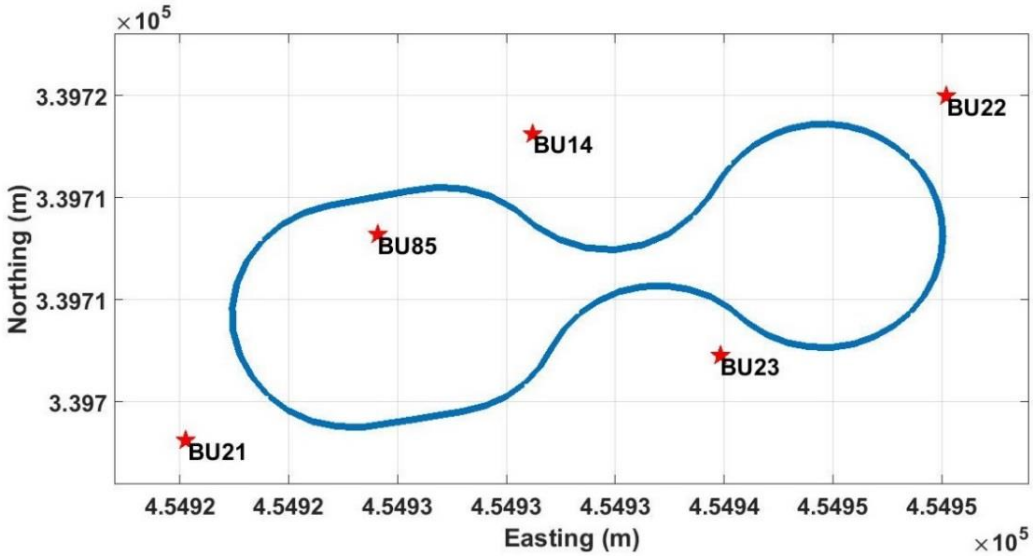


Fig.5.10 BUs Distribution in Locomotive Test

As revealed in Fig.5.11 and Fig.5.12, the roof of the NGB is in an open sky environment. However, it should be noticed that the metal fence and the ventilating duct around the circumference of the roof and seven metal pillars in the midline of the track may lead to multipath effect. The locomotive and a person carried MU26 and MU92 respectively to move along the track, and each UWB MU was wired together with a set of Leica GS10 receiver and AS10 antenna to provide the ground truth of the MUs' precise locations as shown in Fig.5.13. The level-arm between each group of GNSS antenna and UWB MU was pre-measured by measuring tape, and the few centimetre differences in horizontal and vertical directions were compensated when computing the ranging accuracy. Leica Viva GS10 receiver claims that 8 mm + 1 ppm (horizontal) and 15 mm + 1 ppm (vertical) kinematic accuracy can be achieved with post processing (Leica, 2016b). A laptop was connected to the

UWB MU which is put on the locomotive to record the ranging observations. In total, six ranging observations should be stored at each epoch, and one of them has been made between two moving MUs.



Fig.5.11 Setup Environment in Locomotive Test

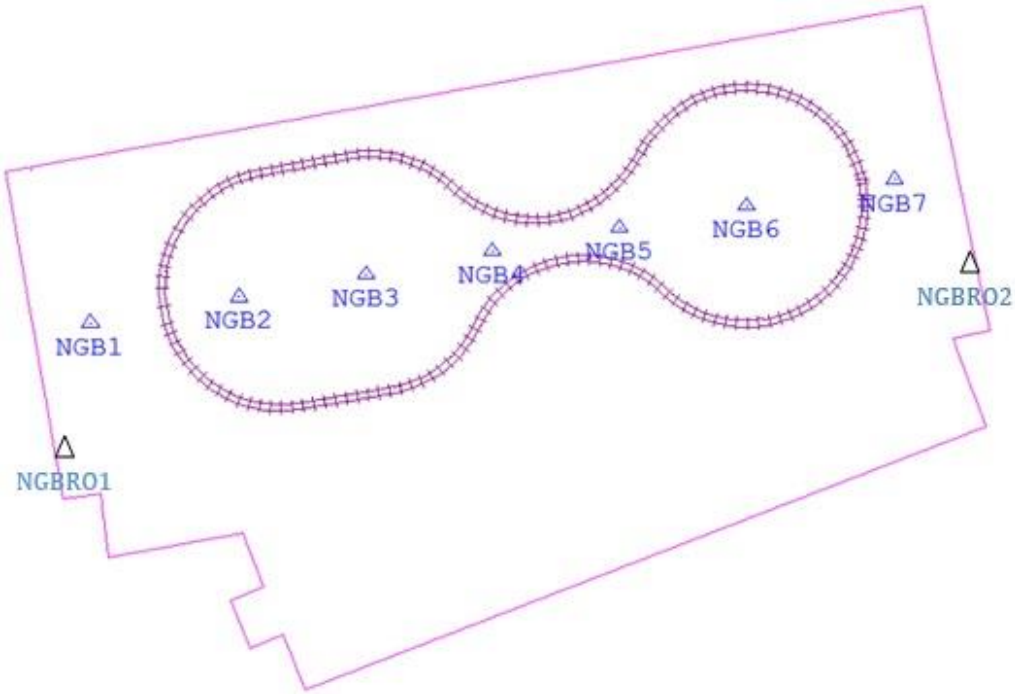


Fig.5.12 The Plan of the Roof of NGB



Fig.5.13 Two MU Carried by the Locomotive and a Person in Locomotive Test

There were three purposes for conducting the locomotive test: 1. to assess the UWB ranging performance in a multipath contaminated environment; 2. to evaluate the UWB ranging performance when both transmitting and receiving units are in a dynamic condition; 3. to investigate the influence of the measuring distance on the ranging accuracy. During the test, UWB MU26 and GPS devices Leica04 were assembled on the locomotive while UWB MU92 was wired together with GPS devices Leica08. The locomotive was run on the track in a counter-clockwise direction as well as the person carried another set of equipment and walk around the track. The locomotive ran for about 16 laps which were equivalent to a 20 minutes data collection. The MU92 was connected to the permanent power and put alongside the track due to the dead battery in the second half of locomotive test. The sampling rates of GPS receiver and UWB unit are all set as 1 Hz.

As illustrated in Fig.5.14, the blue line and red line indicate UWB ranging measured by MU26 and GPS computed ranging respectively and the UWB

ranging overall matches the ground truth, i.e. GPS computed ranging. The maximal distance between MU26 and other units is about 40 metres measured from BU21 and BU22 while the rangings to other three stationary units, BU14, BU23 and BU85, fluctuate around 20 metres. In addition, the ranging observation between MU26 and MU92 changes irregularly until approximate epoch 800 because MU92 was freely moving on the roof. Moreover, then a clear pattern can be recognised from epoch 800 to the end of the test due to the stop of MU92.

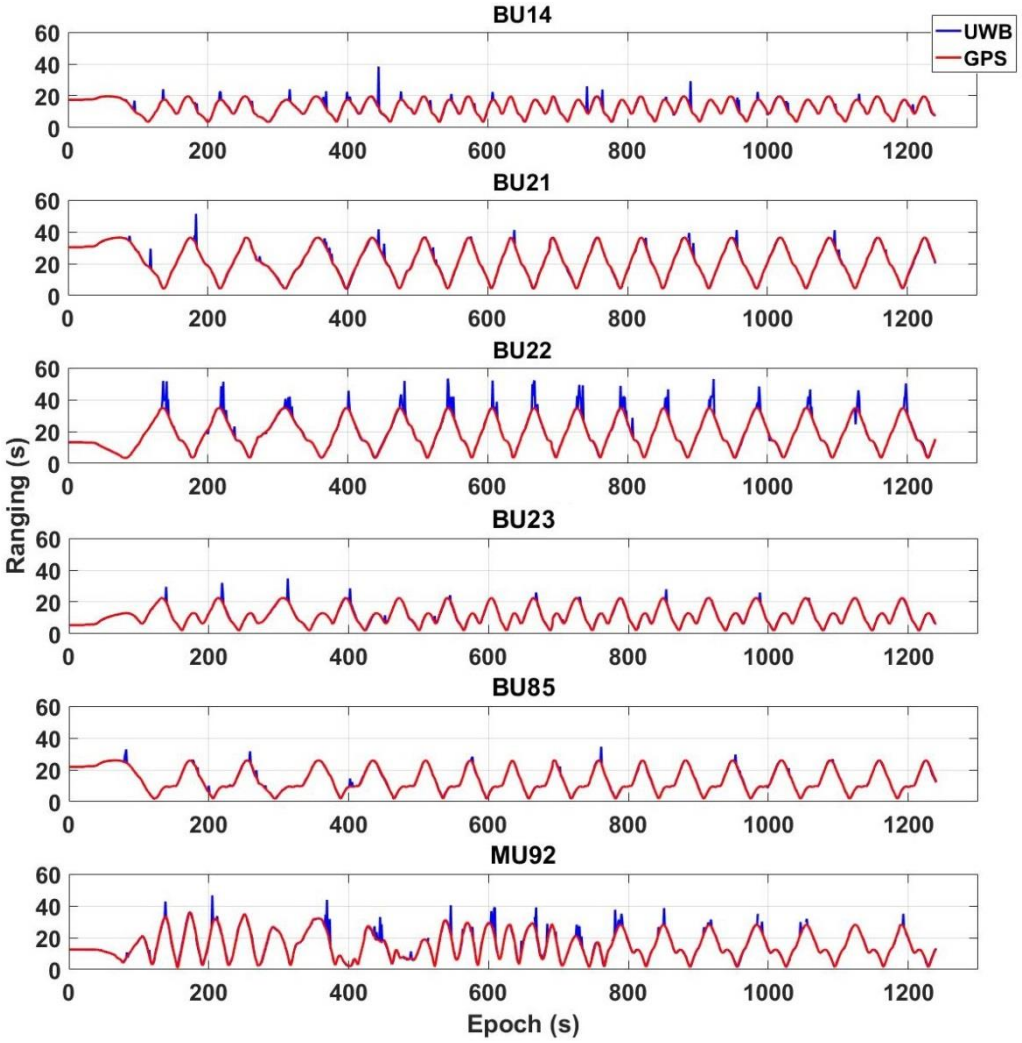


Fig.5.14 The Comparison between Raw UWB Ranging and Ground Truth in Locomotive Test

It is also can be found in Fig.5.14 that several outliers (blue spikes) appear during the test which mainly occur at the peaks of the ranging observations.

Fig.5.15 and Fig.5.16 demonstrate the raw UWB ranging error of locomotive test result and the corresponding histogram. It is clear that the majority of error centralises at zero although several outliers exist. The rangings of BU23 and BU85 have a smaller magnitude of an outlier that around 10 metres whereas the outliers of other four units jump over 20 metres.

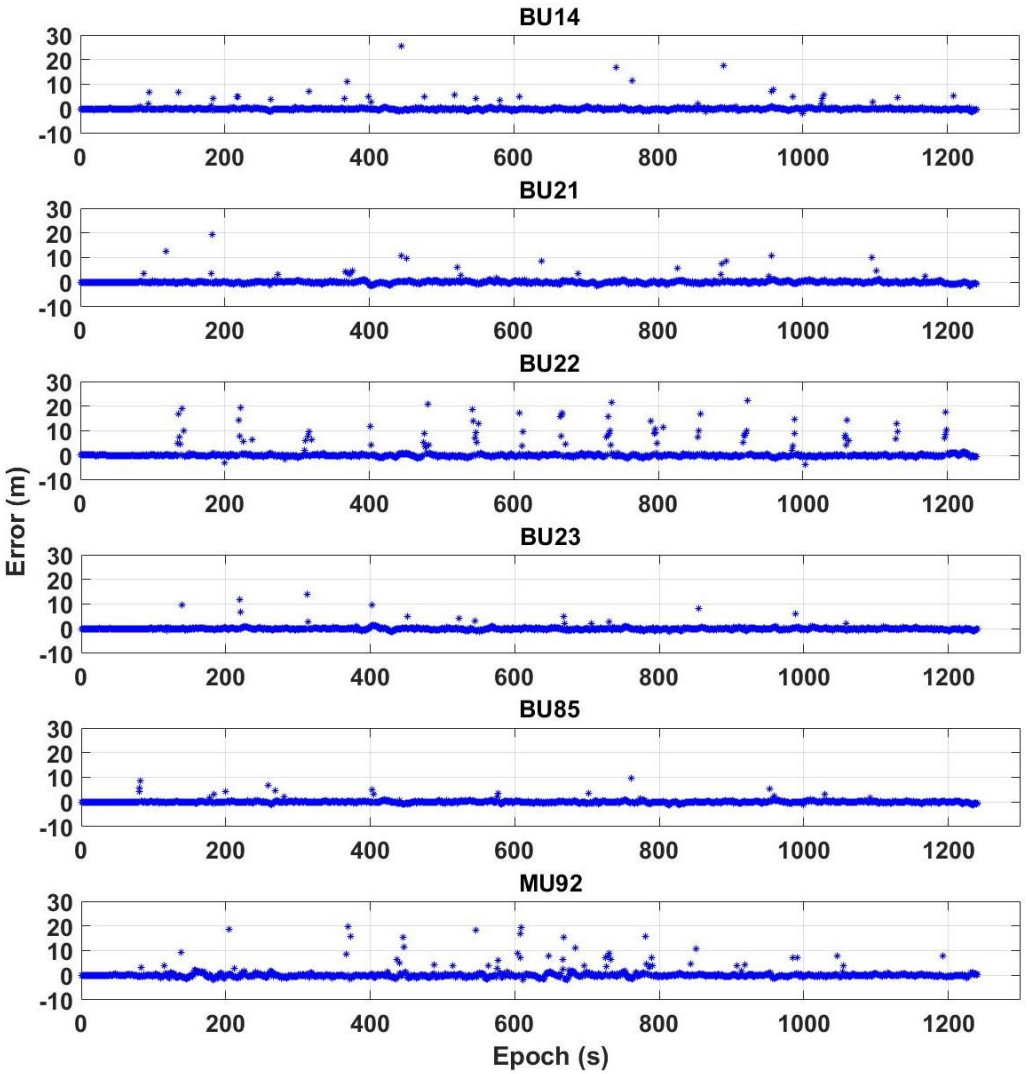


Fig.5.15 Raw UWB Ranging Error in Locomotive Test

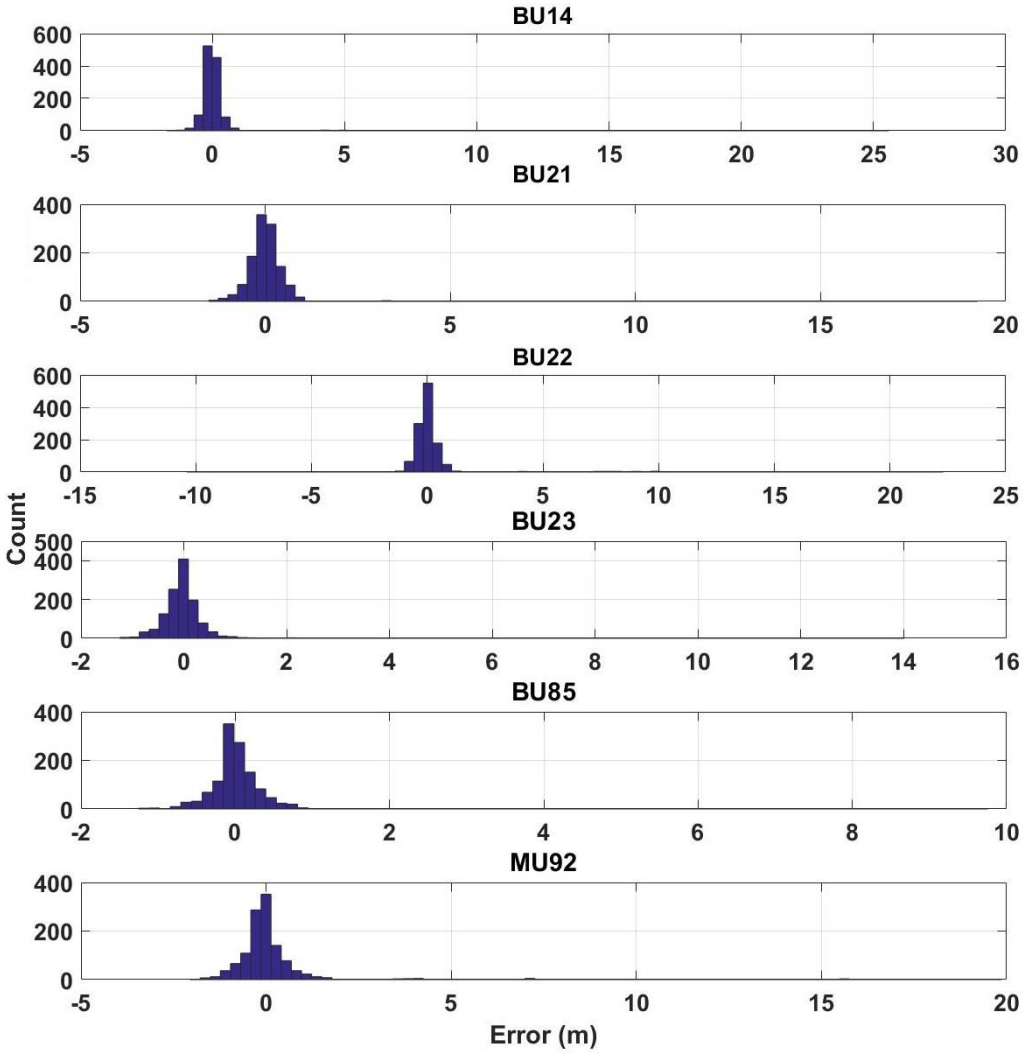


Fig.5.16 The Histogram of Raw UWB Ranging Error in Locomotive Test

The error that exceeds 1 metre is deemed as an outlier for locomotive test and plotted in Fig.5.17. Red pentagrams and diamonds indicate the location of five static BUs and seven metal pillars. The figure reveals the location where the outliers are observed by MU26, and different colour of circles indicate the outlier generated by different BUs. The ranging error between MU26 and MU92 is not represented here because the moving MU92 gives different position every epoch. It is clear that most of the outliers are situated at the northeast and south-west corners of the track where BU22 and BU21 were located nearby. This maybe because that both BU22 and BU21 were close to the corner of the metal fence where could introduce more multipath effect on the ranging observation.

Apart from those two corners, the pillars that align in the midline of the track can cause the Non-Line-of-Sight (NLOS) ranging observations which result in outliers. Every ranging dataset is involved in NLOS-caused outlier, for examples, five outliers of BU21 ranging (red circle) near BU85 may be caused by the obstruction of pillar NGB2; five outliers of BU21 ranging (red circle) on the north side of the middle part of the track and three outliers of BU14 ranging (blue circle) on the south side of the middle part of the track may be caused by the obstruction of pillar NGB4; two outliers of BU85 ranging (green circle) at the southeast of the track, three outliers of BU23 ranging (purple circle) on the north side of the middle part of the track and five outliers of BU22 ranging (yellow circle) on the south side of the middle part of the track may be caused by the obstruction of pillar NGB5. It also can be found that the majority of BU21 and BU22's outliers are spread at the northeast and south-west corners respectively where are most easily obstructed by pillar NGB2 to NGB6. Another evidence can demonstrate the effect of NLOS is that there is quite few outlier at the northeast corner of the track where the sight of MU26 should not be blocked by any BUs or pillars.

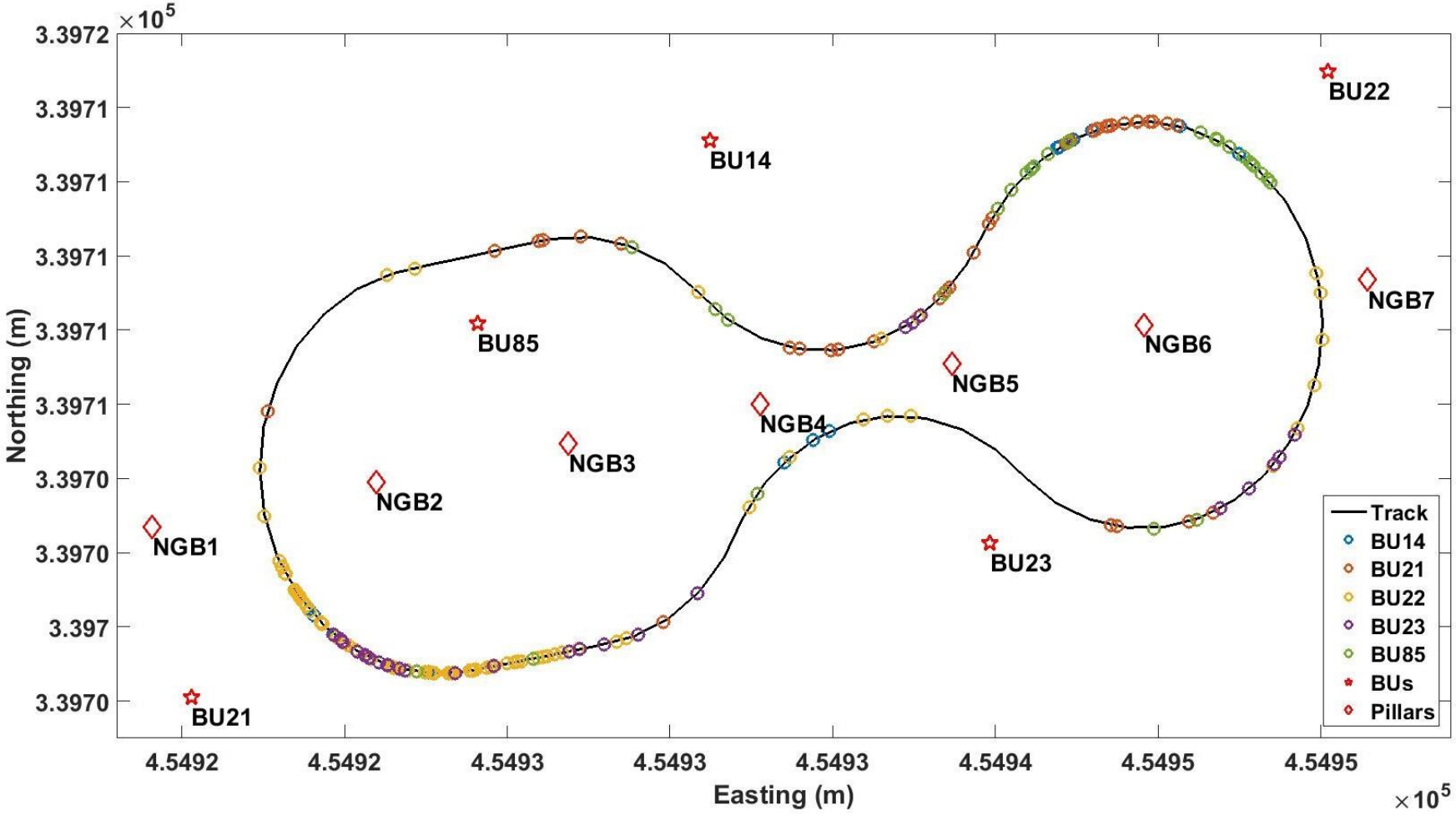


Fig.5.17 The Outlier Distribution in Locomotive Test

The outliers are excluded in order to evaluate the reasonable UWB ranging performance. Fig.5.18 demonstrates UWB ranging error after outlier excluding of locomotive test, and detailed statistic result is listed in Table 5.6. As mentioned earlier that MU92 was moving around at the beginning of the test for a time length of approximately 800 seconds and followed by about 400 seconds static period. The test lasted for 1240 seconds, and the availabilities of five BUs ranging datasets are all higher than 99% as well as the MU ranging dataset drops slightly to 98% in both parts. Regarding the availability of MU92 ranging, the static period gives a litter better result than the kinematic period. It can be seen that the ranging data collection is not affected by the dual-moving situation. Most of the outlier percentages of each unit account for less than 5 percent of the corresponding received data. As an exceptional case, the ranging dataset of BU22 contains more outliers, i.e. 7.6 percent of available data, than other static BUs and even higher than the moving unit MU92. The reason is BU22 was closer to the metal fence than other UWB units which make the ranging suffering from worse multipath effect. The ranging error of locomotive test generally stays around 30 cm, except the ranging error of MU92 which gets worse to 40 cm. On the other hand, the precision of locomotive test follows the pattern in accuracy and shows similar values to the accuracy. Owing to the dual-moving situation of MU92, its ranging error will be separately discussed in the following paragraphs. Comparing the rest of ranging error with the result of the dynamic test, UWB ranging can still offer decimetre level accuracy and precision, but they are about 1.5 times as much as the figures in dynamic test discussed in the last section which is caused by the multipath effect.

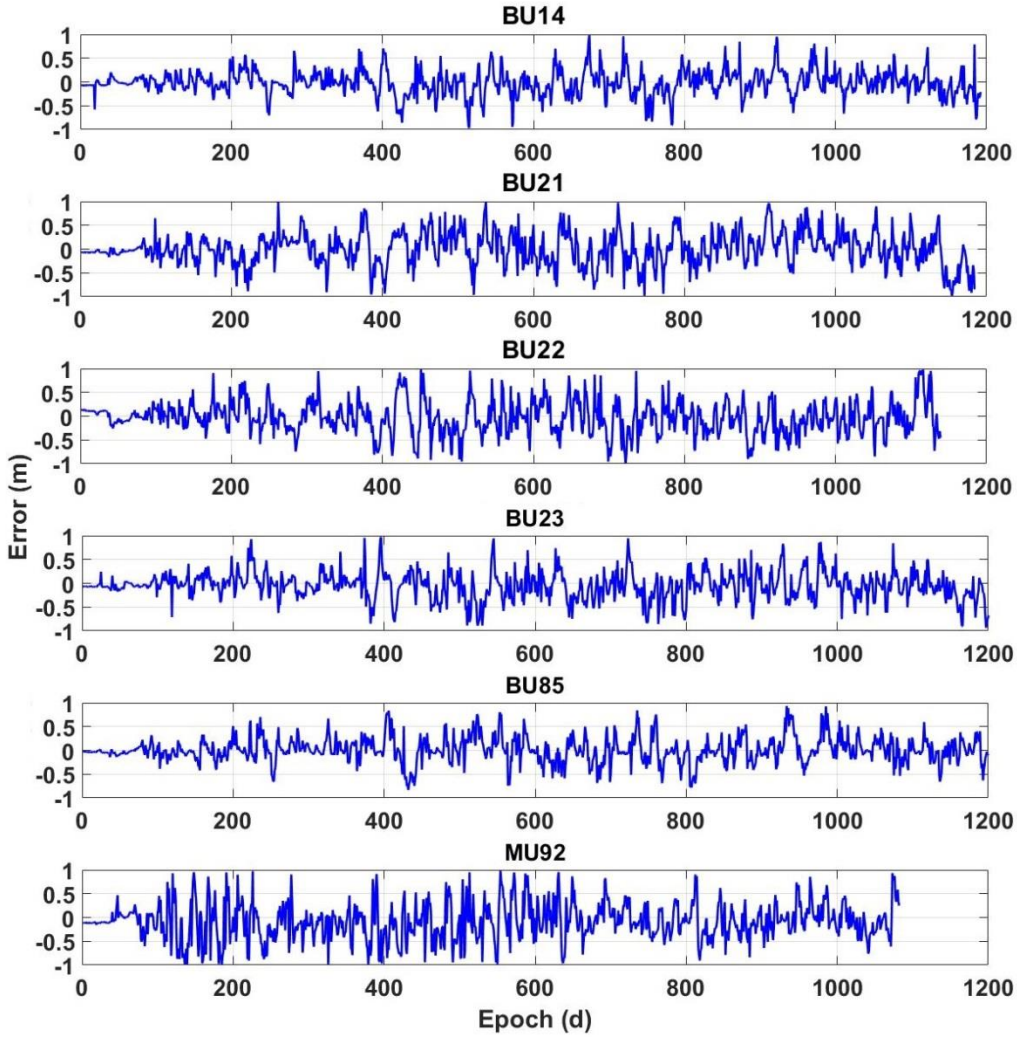


Fig.5.18 UWB Ranging Error (Outlier Excluded) in Locomotive Test

Table 5.6 UWB Ranging Error (Outlier Excluded) in Locomotive Test

Unit Number	BU14	BU21	BU22	BU23	BU85	MU92
Availability	99.2%	99.4%	99.4%	99.5%	99.9%	98.6%
Outlier Exclusion	3.1%	4%	7.6%	2.5%	2.3%	11.5%
Accuracy (cm)	27.1	35.3	34.9	32.4	30.1	39.7
Precision (cm)	27	35.4	34.8	32.1	29.6	38.7
1σ Percentage	71.3%	67.8%	64.2%	69.5%	72.5%	57.6%
2σ Percentage	90.7%	90.2%	86.0%	90.2%	90.9%	80.9%

Due to the strict screening criterion of outliers, less than 90 percentages of collected MU92 ranging observation remains which are not enough to evaluate the UWB ranging performance. To better understand the ranging error of

MU92, the screening criterion of outliers is extended to 2 metres and two periods that MU92 was moving and static are analysed individually. The MU92 ranging error and its distribution are illustrated in Fig.5.19. It can be seen in the above figure that the absolute values of several errors exceed 1 metre which can also be found on the short bars located between the absolute value of 1 metre and 2 metres in Fig.5.19 (bottom). As previously mentioned, MU92 has stopped at around epoch 800, and it is indicated by a red vertical line in Fig.5.19 (top). Comparing two periods in Fig.5.19 (top) divided by the red vertical line, the first half of the ranging error of MU92 is noisier than the second half. The specific figures that how much the first half is worse than the second half will be given further.

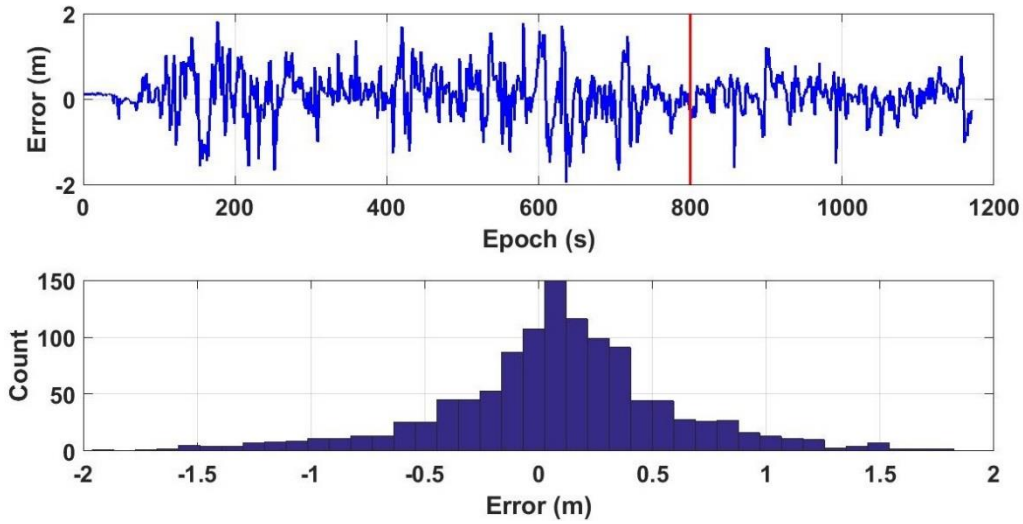


Fig.5.19 UWB MU92 Ranging Error (Outlier Excluded) in Locomotive Test and Its Corresponding Histogram

Table **5.7** shows the comparison of the statistic results of two split periods between two outlier screening criteria. As same as the previous test result, similar figures are shown in accuracy and precision. The statement derived from Fig.5.19 has been testified that the accuracy of MU92 in kinematic is worse than that in the static case under both outlier screening criteria.

Comparing the results between two outlier screening criteria, they show similar accuracies of a litter higher than 30 cm in the static case which also accord with the accuracy levels of other five BUs. The major difference comes from the accuracies in kinematic case. Specifically, it is 60.2 cm under 2 metres criterion against 32.9 cm under 1 metre criterion. The reason can be found from the outlier exclusion rates that the number of excluded outlier increases by approximately two times when the screening criterion becomes tight. Equivalently, 10.7 percentages of available ranging observation contains absolute error between 1 metre and 2 metres.

The accuracy of MU92 based on 2 metres outlier screening criterion is contrasted with the previous test results to quantify the influences of multipath and move status. Choosing the BUs and the single moving MU92 ranging accuracies in the locomotive test as the control group, i.e., the scenario that only one UWB unit out of transmitting and receiving unit pair is moving with multipath effect, the kinematic MU92 ranging error is almost double that in the control group. It could address that the dual-moving situation brings near to 30 cm accuracy degradation than the single moving situation. Further comparing to the accuracy of MU26 in dynamic test discussed in Section 5.3.2, i.e., the scenario that the single moving mode without multipath effect, the kinematic MU92 ranging error is about threefold to the figure of the control group. Overall, the dual-moving situation and multipath do make things worse that 40 cm deterioration in ranging accuracy and precision is witnessed than the single moving and multipath-free scenario.

Table 5.7 UWB MU92 Ranging Error (Outlier Excluded) in Locomotive Test

Screening Criteria	Move Status	Outlier Exclusion	Accuracy (cm)	Precision (cm)	1σ Percentage	2σ Percentage
2 metres	**Kinematic**	4.7%	60.2	59.2	67.9%	88.1%
	Static	3.3%	36.6	36.3	72.8%	92.4%
1 metre	**Kinematic**	15.4%	43.7	42.1	68.6%	91.2%
	Static	5.0%	32.9	32.6	58.8%	80.0%

It can be noticed in Table 5.6 and

Table **5.7** that systematic errors were involved in UWB ranging observations due to the non-zero means of rangings. Since limited technical information can be found from Thales website and insufficient output can be provided from the Thales UWB unit, it was difficult to figure out the exact source of that systematic error of Thales UWB units. Alternatively, the compensation that consists of the scale factor and the bias for each unit can be extracted from collected ranging observation. A more thorough derivation of the equations of ranging errors and the characterisation of the ranging error magnitudes can be found in (MacGougan et al., 2009). The UWB ranging errors can be well fit by a first order line, and the actual distance can be expressed as follows:

$$r = d_{U_a} - c_{U_a} = (1 - k_{U_a}) d_{U_a} - b_{U_a} \qquad 5.1$$

Where d_{U_a} and c_{U_a} are the ranging observation and the ranging compensation for UWB unit a. k_{U_a} is the scale factor which determines the error that is proportional to the measuring distance for unit a. b_{U_a} is the consistent bias of ranging observation for unit a.

Fig.5.20 shows the raw ranging errors versus measuring distances derived from GPS for six UWB units in the locomotive test. The blue circle and red line indicate the ranging error and linear fit of each unit respectively. The outliers larger than 1 metres have been removed and only the period of the single moving MU92 ranging is represented. Note that the maximal distance in the test is about 37 metres. The figure cannot tell a very obvious correlation between ranging error when the measuring distance for each unit is in a short distance. However, there is a hint that the right end of the linear fit is a bit higher than 0 and this is worth leading the further discussion.

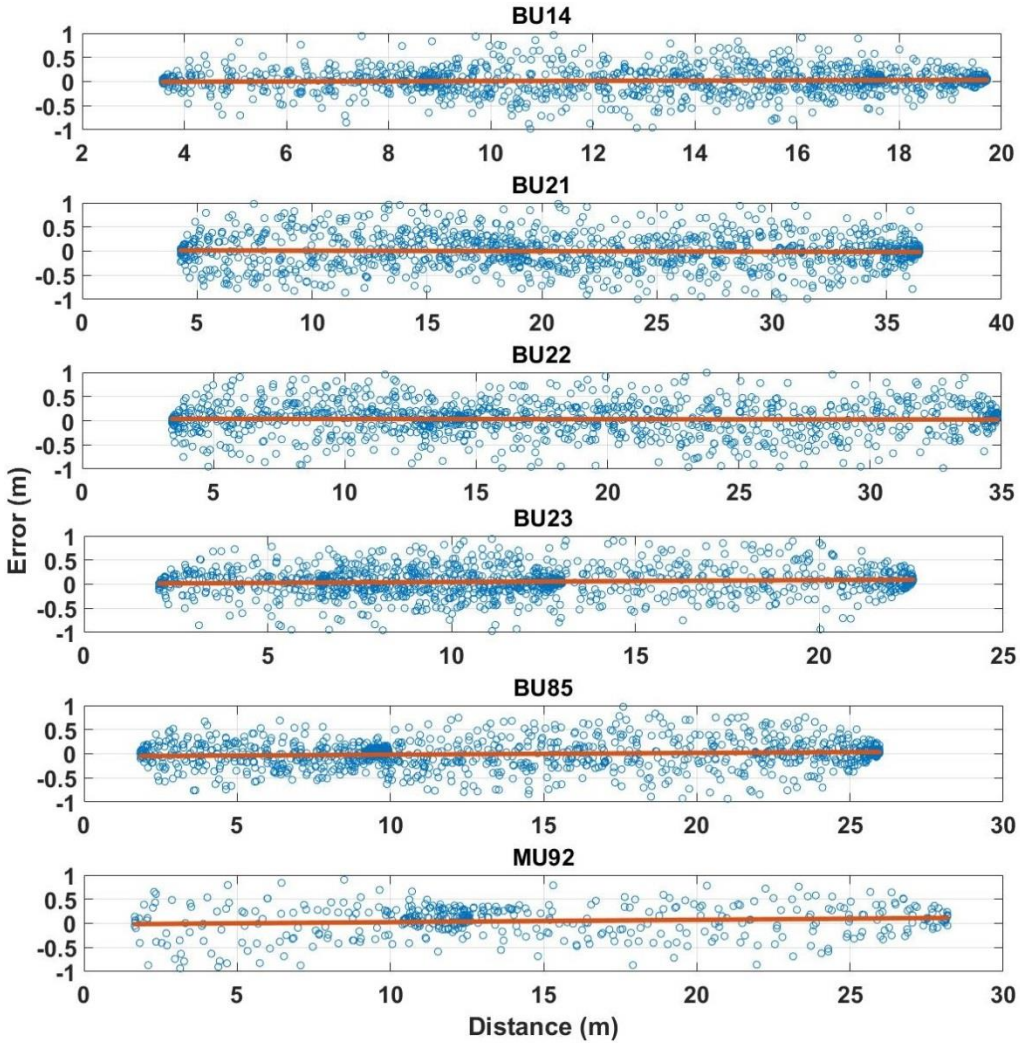


Fig.5.20 Raw Ranging Error (Outlier Excluded) with Linear Fit in Locomotive Test

In the V2X applications, the distance between two vehicles or between a vehicle and an RSU could be hundreds metre away. Therefore, the details of the fitting parameter, namely, the scale factor and bias, need to be paid more attentions. The scale factor and bias of each unit are listed in Table 5.8 as below. Surprisingly, the scale factors of BU21 and BU22 show unreasonable negative value. It could be because the rangings of BU21 and BU22 are easiest to be obstructed by the pillar due to their locations. Then, it could either lead to outliers in NLOS situation or result in multipath contamination in LOS situation. It also can be referred to Table 5.6 that the ranging accuracies of BU21 and BU22 are the worst out of five BUs.

Table 5.8 Scale factor and Bias of Each Unit in Locomotive Test

Unit Number	Scale Factor (ppm)	Bias (cm)	Compensation Max (cm)	Compensation Min (cm)
BU14	2349	-1.3	3.4	-0.4
BU21	-1050	2.0	1.6	-1.8
BU22	-466	4.0	3.8	2.4
BU23	3853	0.8	9.5	1.6
BU85	3516	-5.4	3.8	-4.7
MU92	4848	-2.4	11.3	-1.6

The scale factors vary between 2000 ppm and 5000 ppm and the biases changes between -5 cm to 11 cm among the UWB units. Based on this test, the compensation of each unit has shown non-negligible benefit under the short measuring distance. The maximal compensation is up to 11 cm which is about one-third of the ranging accuracy. Furthermore, it could correct huge error when the measuring distance gets longer. Taking BU23 as an example, imagine two UWB units are 200 metres away to one another. The error caused by scale factor and bias will be as big as 65 cm which is more than twice of the accuracy.

Abandoning the ranging observations of BU21 and BU22 due to abnormal compensation parameter, the histograms of remaining four ranging observations are depicted in Fig.5.21 and Fig.5.22. The width of bins are set as 10 cm, and the red curve illustrates the fitted normal distribution. The contrast between two figures shows a slight improvement that the mean shifts to zero and the red curve fits better to a normal distribution.

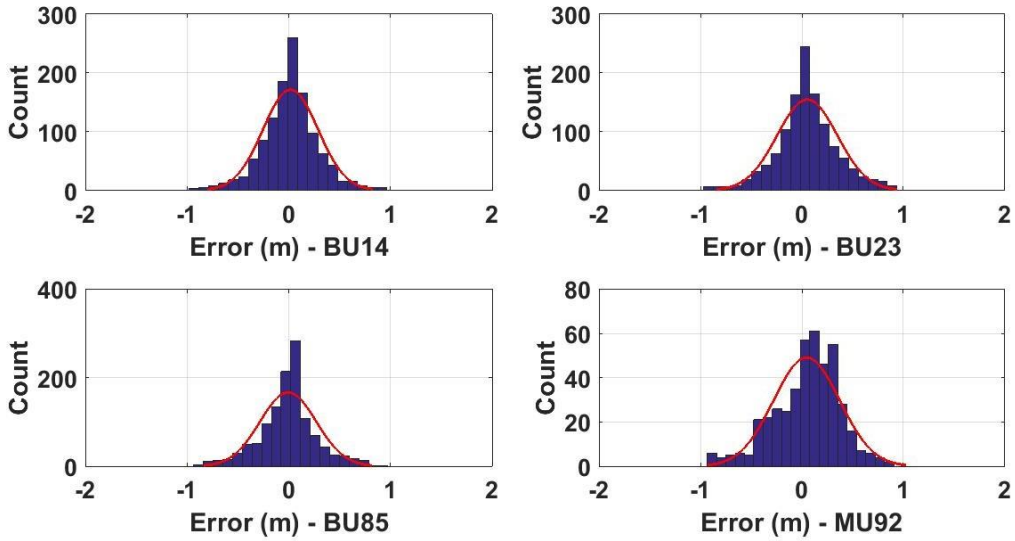


Fig.5.21 Ranging Errors Histogram (Outlier Excluded) without Linear Fit Scale Factor and Bias Compensation

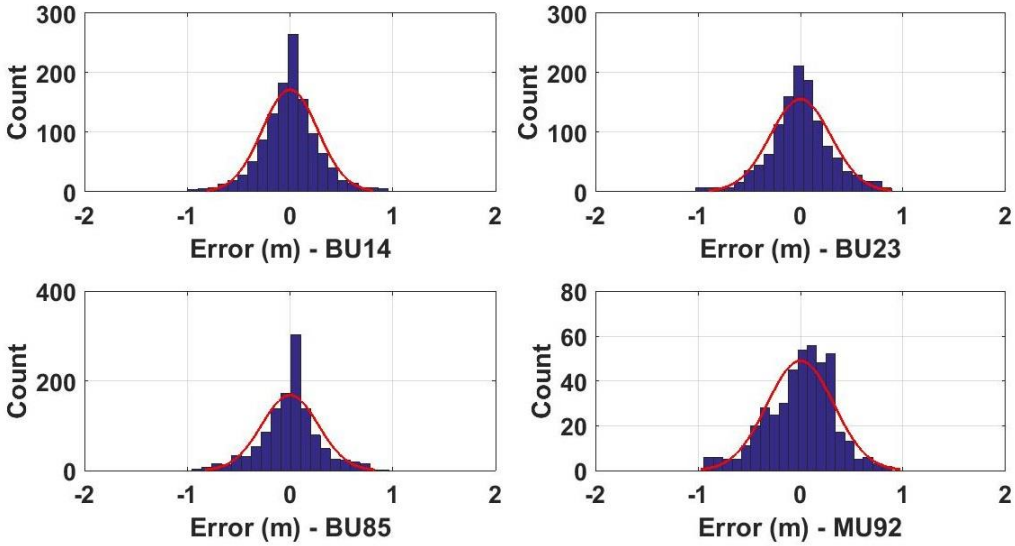


Fig.5.22 Ranging Error Histogram (Outlier Excluded) with Linear Fit Scale Factor and Bias Compensation

To find out the correlation between measuring distance and error in the dual-moving situation, the outlier screening criterion is broadened to 2 metres. Fig.5.23 demonstrate raw ranging error and its corresponding distribution before linear fit compensation. It can be found from the left figure in Fig.5.23 that there is a clear pattern that the longer the measuring distance, the bigger the ranging error is. The error correlated to measuring distance could be 40 cm at 35 m, and there is an around 10 cm bias at 0. Regarding the linear fit to raw ranging error, the scale factor and bias are 12192 ppm and -8.1 cm respectively.

The reason of getting a bigger magnitude of compensation parameter than those in the single moving situation could probably be UWB MU92 was carried by a person so that the antenna orientation of MU92 may differ from the antenna orientations of BUs. Thales UWB unit manual suggests that (Thales, 2010): "Although the antenna is nominally omnidirectional, it does have a null vertically above and below the unit. The BUs should generally be mounted in the same orientations as the MU, so as to match polarisations."

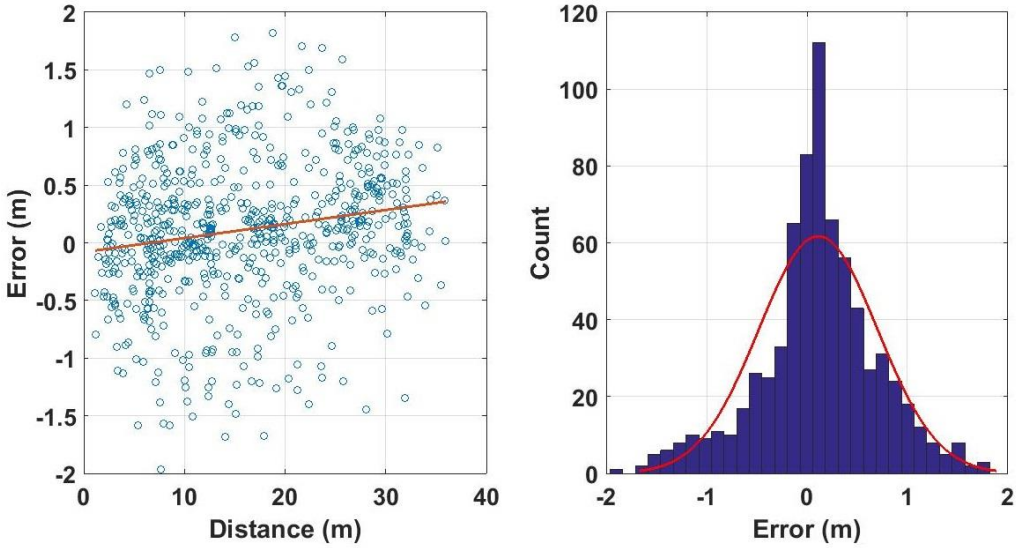


Fig.5.23 Raw Ranging Error (Outlier Excluded) in Dual-moving Situation Versus Reference Distance and with Linear Fit (Left); Raw Ranging Error with Normal Distribution Fit (Right)

Applying for the linear fit compensation, the corrected ranging error and corresponding distribution are represented in Fig.5.24. It can be seen from the left figure that the measuring distance dependent error has been completely removed and well fitted with a horizontal red line on zero. It can also be found from the right figure that the bars slightly shift to the left and the middle bars stay at zero, and the whole histogram fits better to a normal distribution indicated in red curve. Comparing to the raw ranging error, the mean of the corrected ranging error mean diminishes from 11 cm to 0 cm, and the accuracy and precision have been improved by 2 cm.

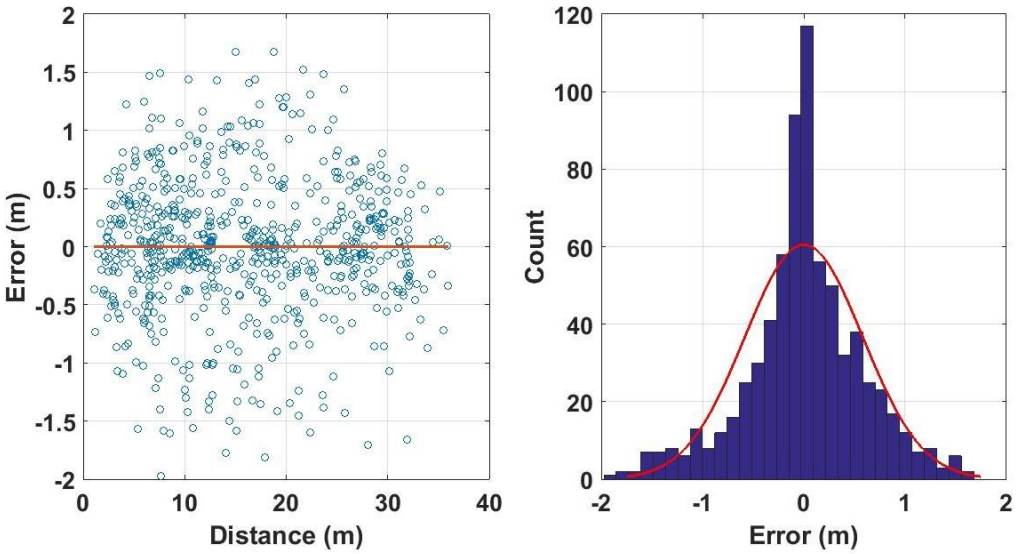


Fig.5.24 Ranging Error (Outlier Excluded) in Dual-moving Situation Versus Reference Distance and with Compensation (Left); Compensated Ranging Error with Normal Distribution Fit

5.4 UWB Positioning Assessment

To evaluate the positioning performance produced purely by UWB ranging observations, three datasets collected from a static test, a dynamic test and a locomotive test are used as the inputs of the proposed positioning method. For all tests, the coordinate systems were established within the European Terrestrial Reference System 1989 (ETRS89) coordinate system, so the X, Y and Z axes followed the directions defined in the ETRS89 system. The software Grid InQuestII was used for coordinate conversion between Ordnance Survey Great Britain 1936 (OSGB36) and ETRS89 systems. The X, Y, and Z directions in ETRS89 correspond to the northing, easting, and up directions respectively.

5.4.1 Indoor Static Positioning

Applying the LSE method, Fig.5.25 reveals the three directional (3D) positioning accuracies in the static test within a temporary local coordinate system formed by six Base Units (BUs). The accuracies in the X and Z directions are overall stable except there is a spike at about epoch 148. On the other hand, the accuracy in the Y direction is quite noisy throughout the test. As shown in the first row of Fig.5.26, the existence of the spike is attributed by

an outlier on the UWB ranging observation of BU80 that is bigger than 20 cm. Meanwhile, the reason of the noise is associated with the change in the number of ranging observations as shown in the second row in Fig.5.26. As mentioned in Section 5.3.1, the ranging observations of BU55 cannot always be recorded due to the limit of unit specification of up to five ranging transaction at each time. It can be found that the accuracy in the Y direction gets worse when the number of ranging observations drops to 5. The changes of the number of ranging observations lead to fluctuations in the accuracy of the Y direction.

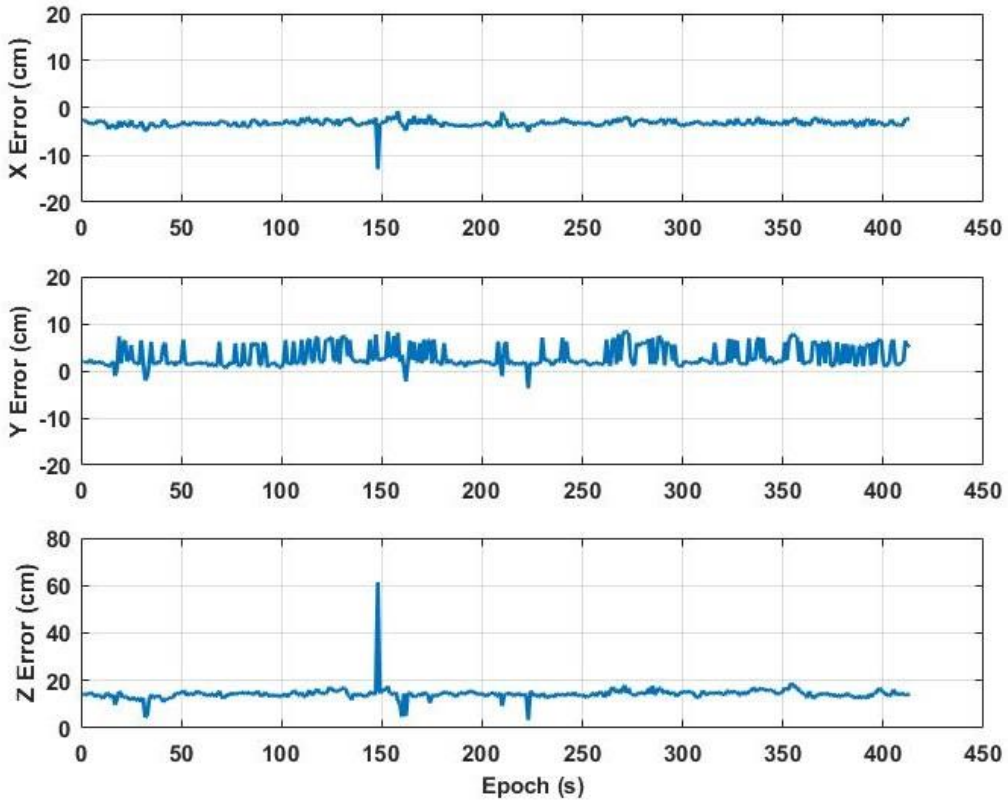


Fig.5.25 UWB Positioning Accuracy in a Static Test (6 BUs)

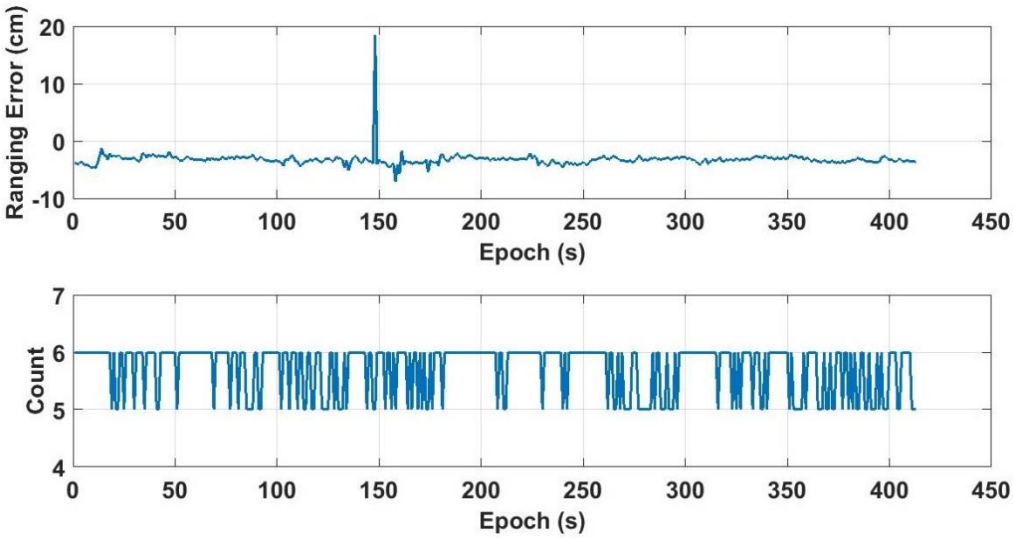


Fig.5.26 Ranging Error of BU80 and Number of BUs for Positioning

Discarding the ranging observations of BU55, Fig.5.27 reveals the 3D positioning accuracies in the static test within a temporary local coordinate system formed by five BUs. To compare with Fig.5.25, the zigzag noise in the Y direction disappears. Instead, a few more small spikes that are less than 10 cm emerge on the accuracies in the Y and Z directions.

Fig.**5**.**28** shows the ranging errors of five BUs (each colour indicates a different BU) which also explains where the small spikes come from. With the comparison between Fig.5.27 and

Fig.**5**.**28** epoch by epoch, it turns out that a small spike in the position solution corresponds to ranging error.

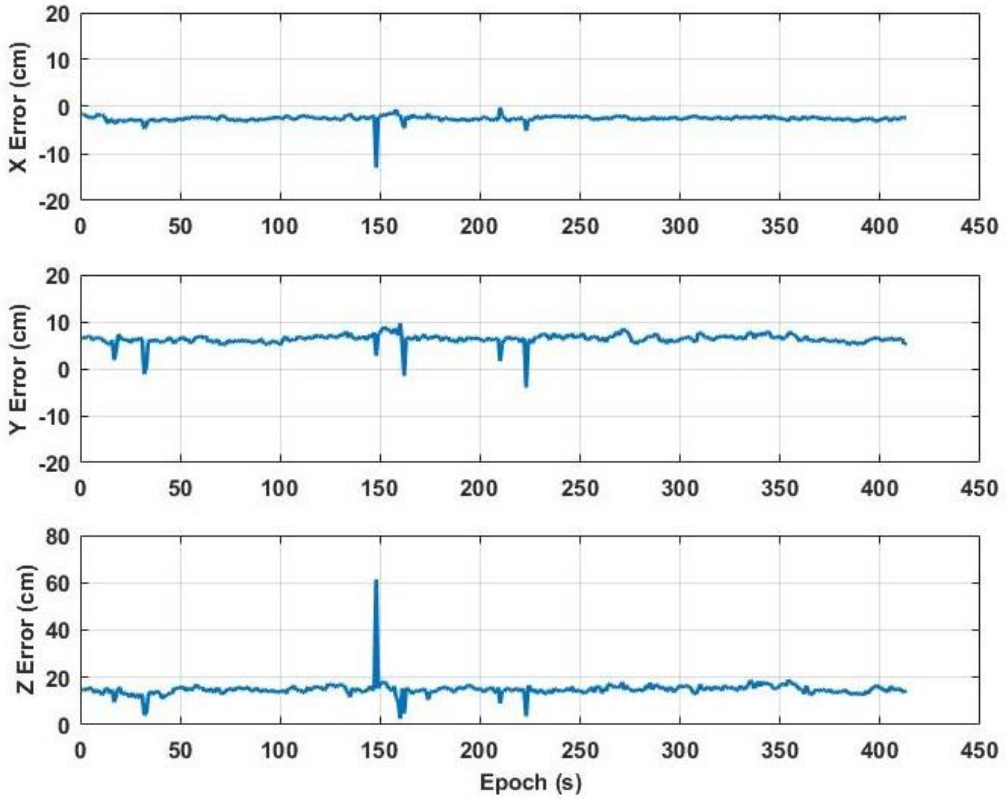


Fig.5.27 UWB Positioning Accuracy in the Static Test (5 BUs)

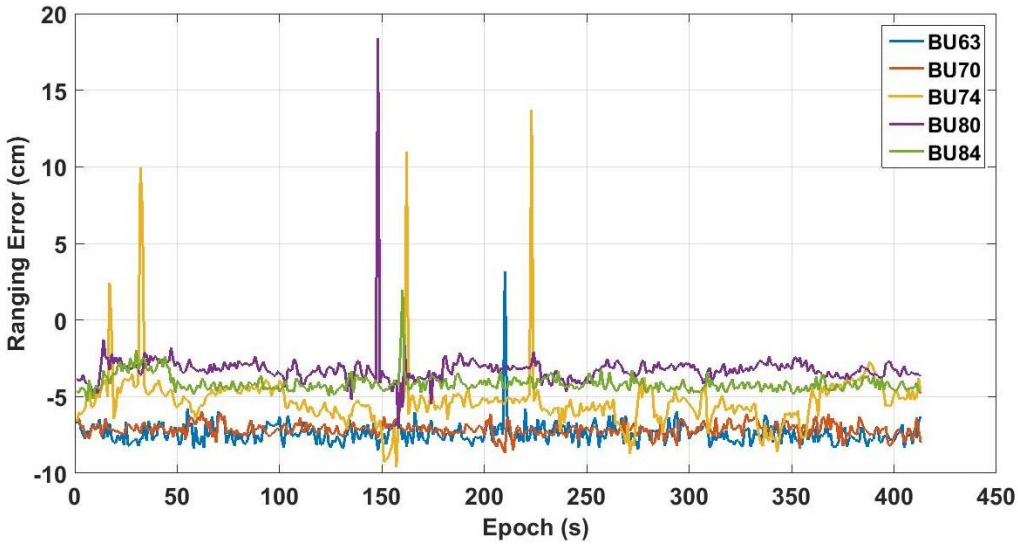


Fig.5.28 Combined 5 Ranging Errors in the Static Test

The detailed statistic of UWB static positioning performance in the indoor static test is listed in Table 5.9. The accuracies in the X and Y directions maintain around few centimetres, and the accuracy in the Z direction achieves 15 cm that is approximately threefold of those in the X and Y directions. That is not surprisingly to get a worse vertical accuracy than the horizontal accuracy

because the DOP value in the Z direction is clearly higher than the DOP values in the horizontal plane. As shown in

Fig.**5**.**29**, the red and blue lines indicate DOP values for the six applied observations and the five applied observations respectively. It can be found that there are no big differences in XDOP and ZDOP, but the YDOP is improved by applying one more ranging observation. This can also lead to the fact that the accuracy in the Y direction is better when the six ranging observations are used although the precision drops a bit due to an unstable geometry as shown in the middle figure. In general, the static positioning accuracy produced from UWB ranging observations can achieve better than 10 cm in 2D and better than 20 cm 3D accuracy using five ranging observations. Moreover, adding one additional ranging observation can lead to 27.5% and 7.2% improvements in 2D and 3D accuracies respectively.

Table 5.9 UWB Static Positioning Performance in the Indoor Static Test

Number of BUs		**X**	**Y**	**Z**	**2D**	**3D**
5	**Mean DOP**	0.6	0.9	2.4	1.1	2.7
	Accuracy (cm)	2.6	6.4	15.1	6.9	16.7
	Precision (cm)	0.7	1.1	2.9	0.8	2.9
6	**Mean DOP**	0.6	0.7	2.4	0.9	2.6
	Accuracy (cm)	3.3	3.8	14.6	5.0	15.5
	Precision (cm)	0.8	2.3	2.8	1.5	2.9
Accuracy Improvement (%)		-27	41	3	28	7

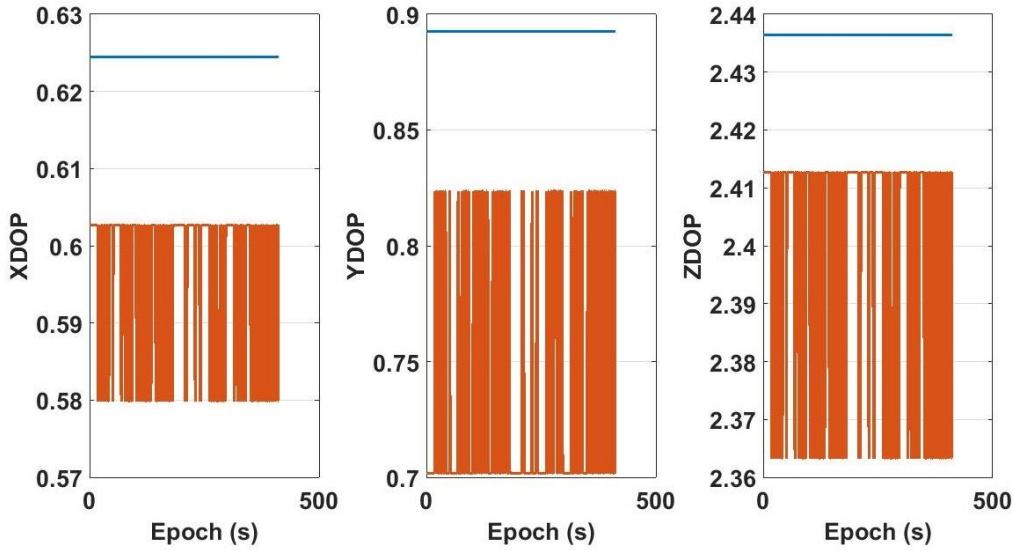


Fig.5.29 DOP Comparison between six and five Ranging Observations in the Static Test

5.4.2 Outdoor Static Positioning Based on Dynamic Ranging Observations

Applying the LSE method,

Fig.**5.30** demonstrates the 3D positioning accuracies in an outdoor dynamic test within a temporary local coordinate system formed by five BUs. The accuracies in the X and Y directions keep at a centimetre level whereas the accuracy in the Z direction is at a metre level. As described in Section 5.3.2, four static BUs and one moving MU have been used throughout the test which led to four static and one dynamic ranging observations.

Fig.**5.31** shows five ranging errors in different colours during the test where the dynamic ranging is worse than the static ranging. From the comparison between

Fig.**5.30** and

Fig.**5.31**, it is easy to link the degradation of positioning accuracy to the increase of the MU74 ranging error. For instance, the spike occurs at about epoch 300 in three directions can be attributed to a big MU74 ranging error over 1.5 metres, and the fluctuation in the Y and Z directional accuracies after epoch 600 is caused by the deterioration of the MU74 ranging observations.

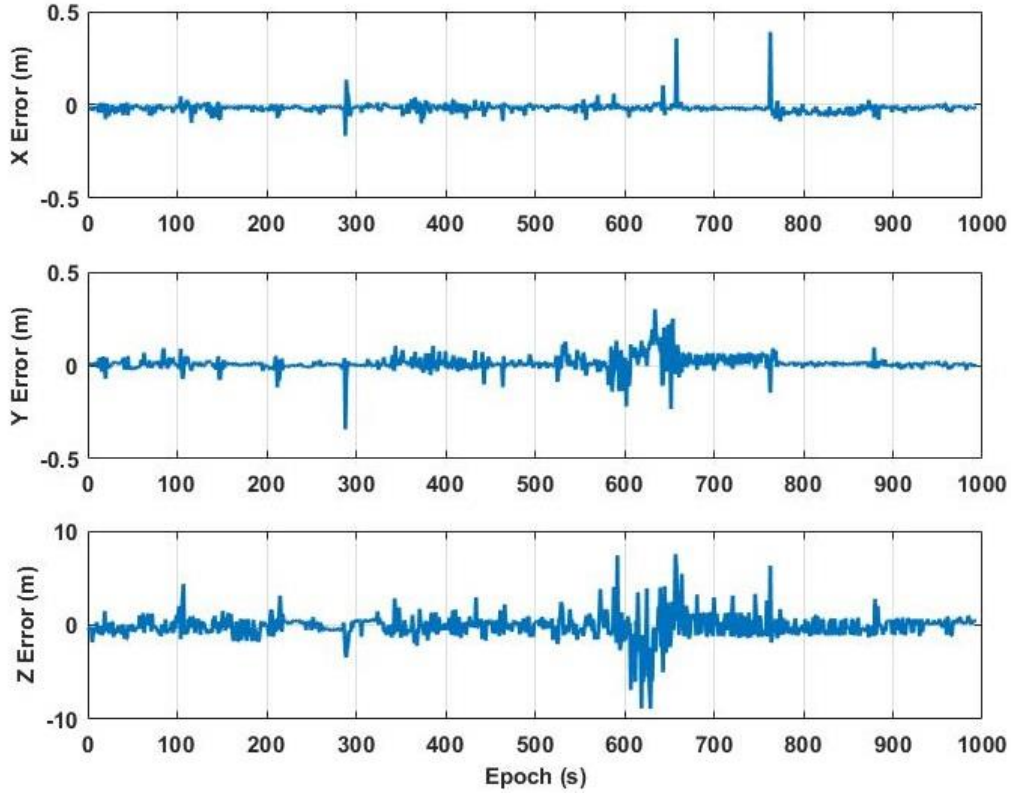


Fig.5.30 UWB Static Positioning Accuracy Using the Dynamic Ranging Observations (5 BUs)

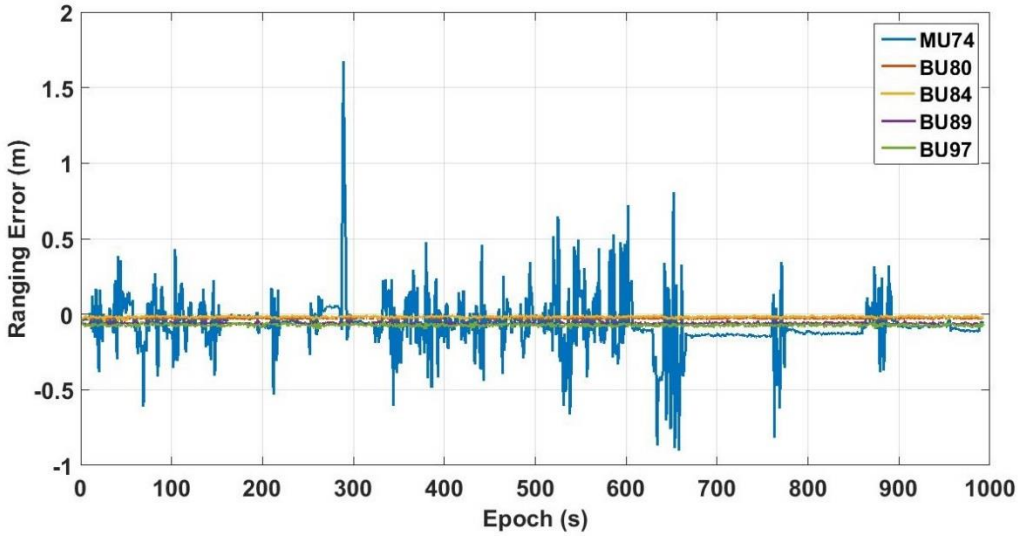


Fig.5.31 Combined 5 Ranging Errors in the Dynamic Test

To identify the impacts of MU74 ranging observations, the position of MU26 is computed again without the input of MU74 ranging observations.

Fig.**5**.**32** illustrates the positioning accuracies in three directions based on 4 static ranging observations. To compare with

Fig.**5**.**30**, the positioning accuracy of four raging input has similar level accuracy in the X and Y directions with the positioning accuracy with five ranging inputs even one less ranging observation is used, but the Z-directional accuracy is got worse with lots of errors of almost 10 metres.

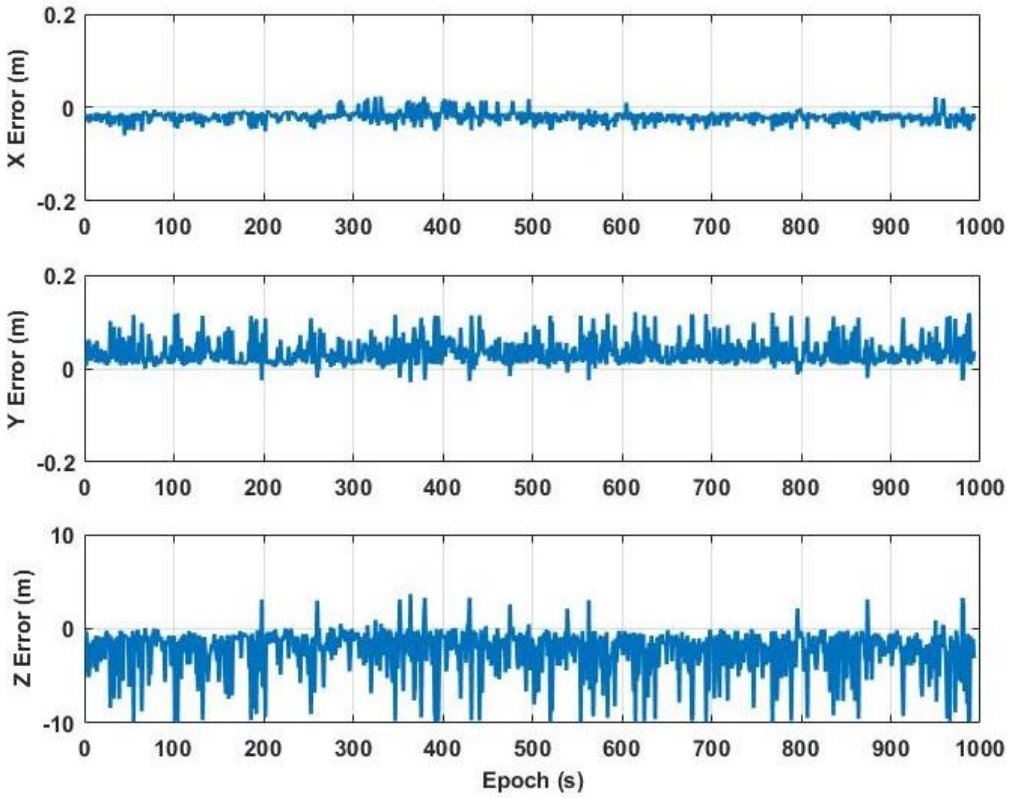


Fig.5.32 UWB Static Positioning Accuracy (4 BUs)

It can be found from above discussion that the positioning accuracy can be affected when the dynamic ranging observations of MU74 are used in the LSE positioning calculation. On the other hand, the involvement of MU74 ranging observations does improve the positioning accuracy in the Z direction. To wisely make use of MU74 ranging observation, the Weighted Least Squares Estimation (WLSE) method is applied, and the three directional positioning accuracies are shown in

Fig.**5**.**33**. It can be seen by comparing to

Fig.**5**.**30** that most of the spikes are removed, and the accuracy in the Z direction is especially improved although the fluctuation after epoch 600 still exists in the Y and Z directions.

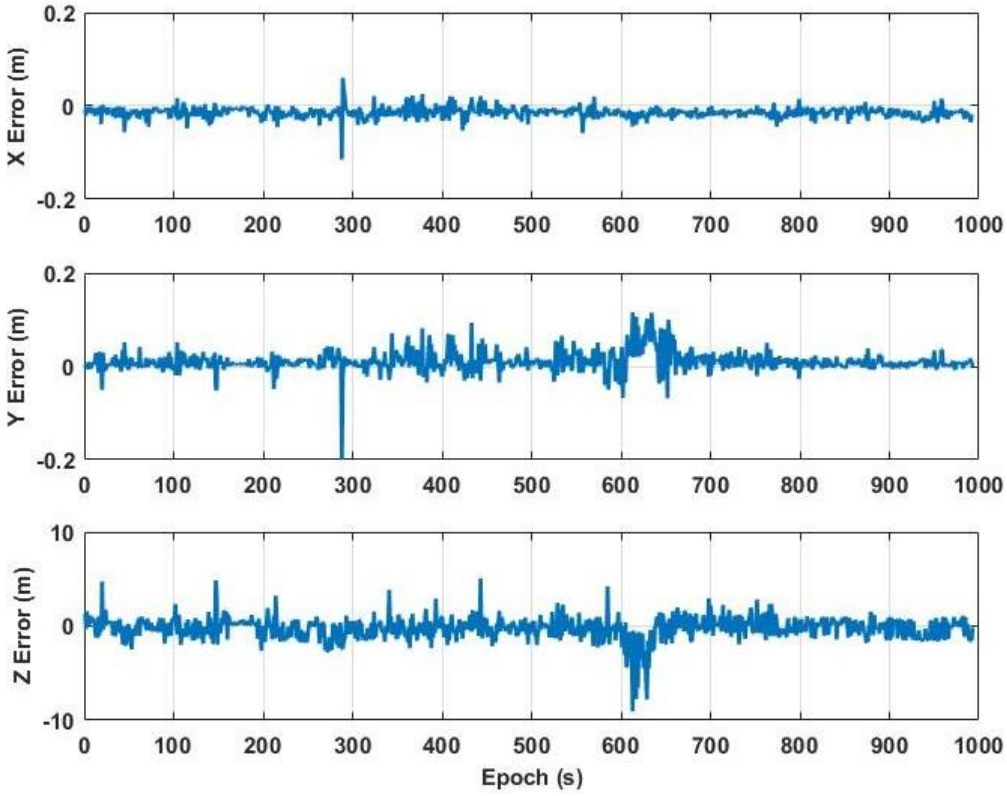


Fig.5.33 UWB Static Positioning Accuracy Using Dynamic Ranging Observations (5 BUs and Applying WLSE Method)

The detailed statistic of UWB static positioning performance in the outdoor dynamic test is listed in Table 5.10. The accuracies in the X and Y directions achieve few centimetres, and the accuracy in the Z direction is worse than 1 metre. The reason of the significant error in the Z direction is the small height difference among BUs. Referring to Table 5.3, the maximal difference in the Z direction is less than 1 metre whereas the maximal differences in X and Y direction are more than 30 metres. This gives rise to small XDOP and YDOP values and an extreme high ZDOP value.

As shown in

Fig.**5**.**34**, the red and blue lines represent the DOP values in three directions in the dynamic test using five-unit and four-unit cases respectively. By utilising less ranging observations, the XDOP does not change a lot and maintain around 0.8. The YDOP increases a bit from 0.8 to 1.3. However, the ZDOP dramatically deteriorates and jumps to 100. Moreover, an extreme value occurs at epoch 800 on the blue line because there were only three available ranging observations. As same as reflected in Table 5.10, the comparison between five- and four-ranging observations cases shows that the XDOP and YDOP remain similar and the ZDOP increases from 25 to 100. Regardless of the Z-directional accuracy due to a poor geometry, the horizontal positioning accuracy, as well as the precision using four units, is slightly higher than that of five units. It can be concluded that the horizontal positioning accuracy will not be further improved by employing additional ranging observations if the existing ranging accuracy is high and the geometry is good. On the other hand, the vertical positioning can perform better by adding additional ranging observations (even contains relative big errors) if the geometry is not good.

To take maximal advantage from additional ranging observations contained higher errors, the WLSE can help to balance the positioning accuracy improvement and impact of ranging errors. The ratio between dynamic and static ranging observations is weighted as 1 to 4 based on the ranging accuracies in Table 5.4. In the case of WLSE with 5 units, the accuracies and precisions in three directions are the highest out of three cases, i.e. about 2 cm in the X and Y direction and 1.2 metres in the Z direction. In general, the accuracy in the Z direction degrades to metre level due to the bad geometry in the Z direction. On the other hand, the horizontal accuracy is 3 cm that is higher than that in the indoor static test. It can be found that the higher ranging accuracy leads to higher a positioning accuracy and a better geometry. Also, the WLSE method can be utilised to maximise the benefit of additional ranging observation.

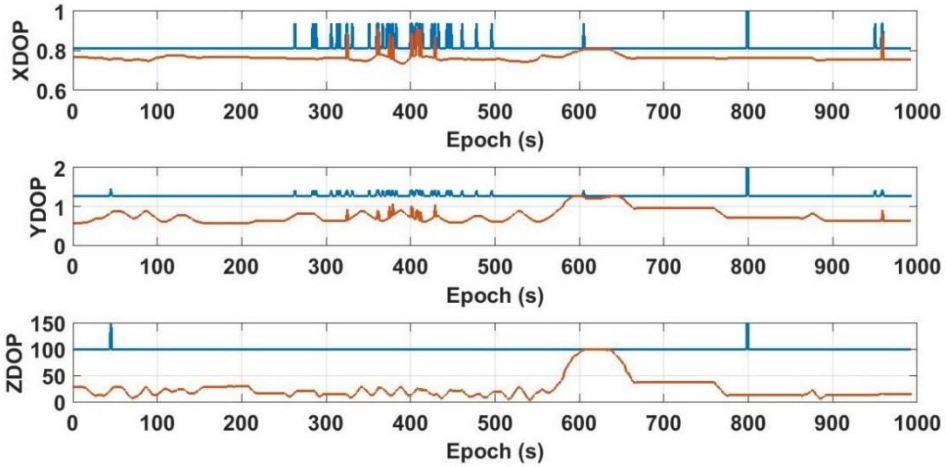


Fig.5.34 DOP Comparison between Five- and Four-Unit Scenarios in the Dynamic Test

Table 5.10 UWB Static Positioning Performance in the Outdoor Dynamic Test

Method	Number of Units		X	Y	Z	2D	3D
LSE	4	Mean DOP	0.8	1.3	100.0	1.5	100.0
		Accuracy (cm)	2.3	4.3	326.4	4.9	326.5
		Precision (cm)	1.2	2.7	235.9	2.6	226.4
LSE	5	Mean DOP	0.8	0.8	25.3	1.1	25.3
		Accuracy (cm)	3.2	4.3	126.8	5.3	126.9
		Precision (cm)	2.7	4.1	126.2	3.9	95.6
Accuracy Improvement (%)			-39	0	61	-8	61
WLSE	5	Mean DOP	0.8	0.8	25.3	1.1	25.3
		Accuracy (cm)	1.8	2.4	121.5	3.0	121.6
		Precision (cm)	1.1	2.1	119.4	1.8	87.2
Accuracy Improvement (%)			44	44	4	43	4

5.4.3 Kinematic Positioning Based on Dynamic Ranging Observations

Firstly, standard KF method is applied to solve the kinematic positioning problem based on six ranging observations.

Fig.**5.35** shows the positioning accuracy in a locomotive test. The red line indicates the height positioning result derived from GPS post-processing

whereas the blue line is the result given by the KF method. It can be found that the locomotive is relatively stable in the height direction and a severe error occurs which is bigger than 20 metres. The significant errors are mainly attributed to a bad geometry and the outliers of ranging observations. According to the height information recorded in Table 5.5, the heights of the five BUs differ within 40 cm. By including MU92, the maximal height difference among units can be extended to 80 cm as shown in the upper figure of

Fig.**5**.**36**. The high ZDOP value is obtained and shown in the lower figure of

Fig.**5**.**36**. Throughout the test, lots of ZDOP values are greater than 20. The impact of the outlier contained in ranging observations will be discussed in the following part of horizontal positioning accuracy.

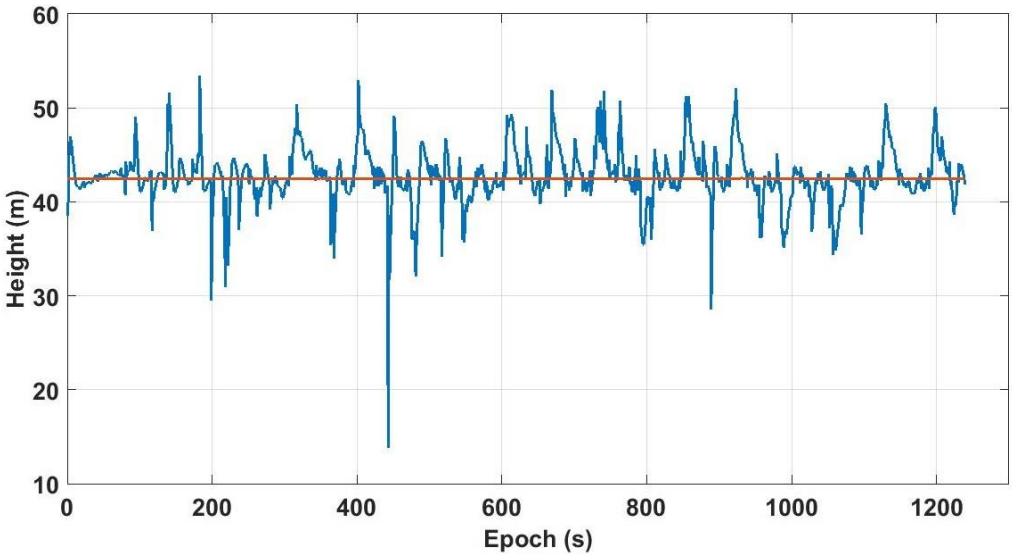


Fig.5.35 Positioning Result in Height Direction (Applying Standard KF Method) in the Locomotive Test

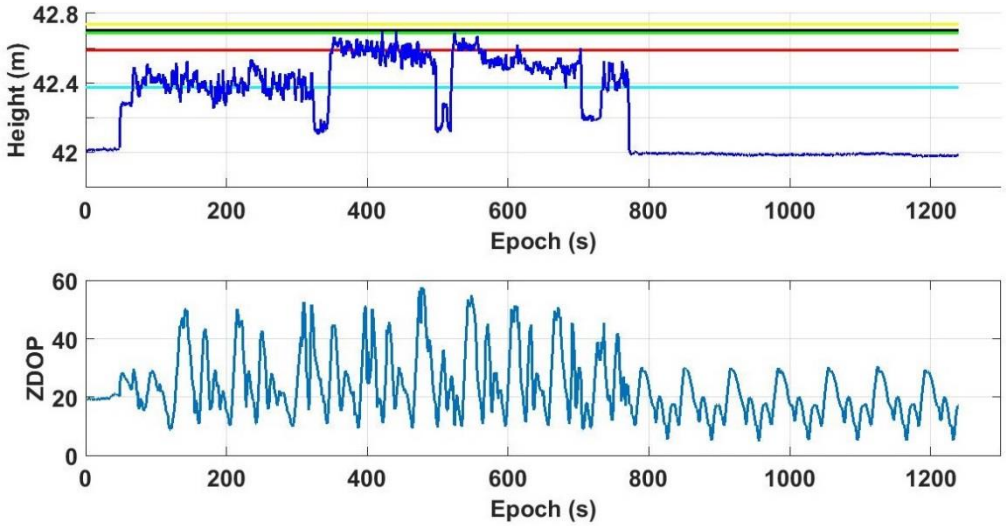


Fig.5.36 Measured Heights of 4 BUs and MU26 against the ZDOP Values in the Locomotive Test

Due to the limitation of BUs geometry, the height positioning performance is not focused in this section. The position in easting and northing directions computed based on the standard KF method is demonstrated by the blue line in

Fig.**5**.**37**, and the GPS post-processing positioning result is given in red line, and the corresponding errors in both directions are drawn in

Fig.**5**.**38**. It can be found that most of the big errors, larger than 5 metres, occur when the locomotive is changing direction. The first reason is the severe outliers contained in ranging observations as shown in

Fig.**5**.**39**. Due to the presence of outliers, the KF measurement model cannot generate precise positions based on the inaccurate ranging observations. On the other hand, the second reason is the real dynamic model of the locomotive does not fit the selected Constant Velocity model during turning. As discussed in Section 4.3.3, the Constant Velocity model assumes the object moves at a steady speed, but the turning makes a sudden change in velocity. Thus, the KF predicts the object keeps heading in the previous direction at next epoch which differs from the true heading. In a nutshell, both the measurement and dynamic models cannot work properly when the locomotive is turning whereas the dynamic model can alleviate the impact of inaccurate solution from measurement model when the locomotive keeps running in the same direction.

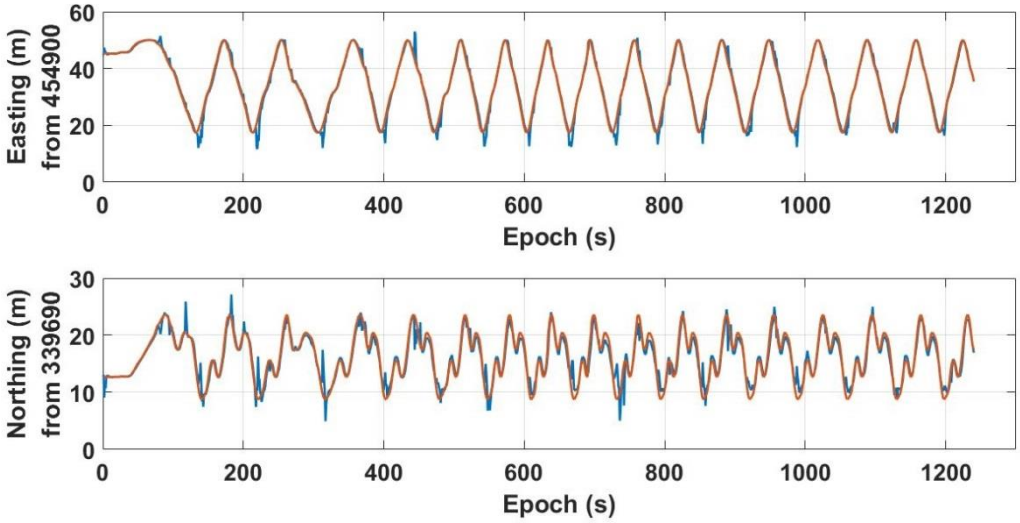


Fig.5.37 Positioning Result in Easting and Northing Directions (Applying Standard KF Method) in Locomotive Test

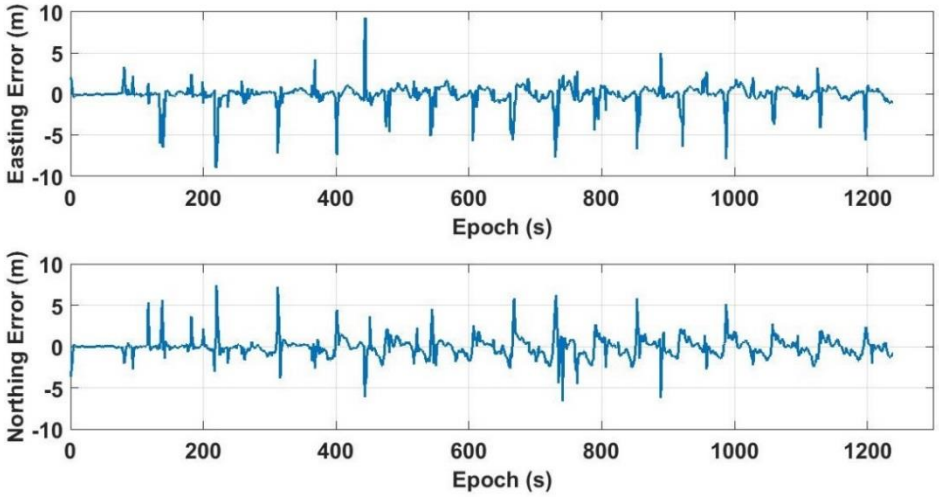


Fig.5.38 Position Error in Easting and Northing Directions (Applying Standard KF Method) in Locomotive Test

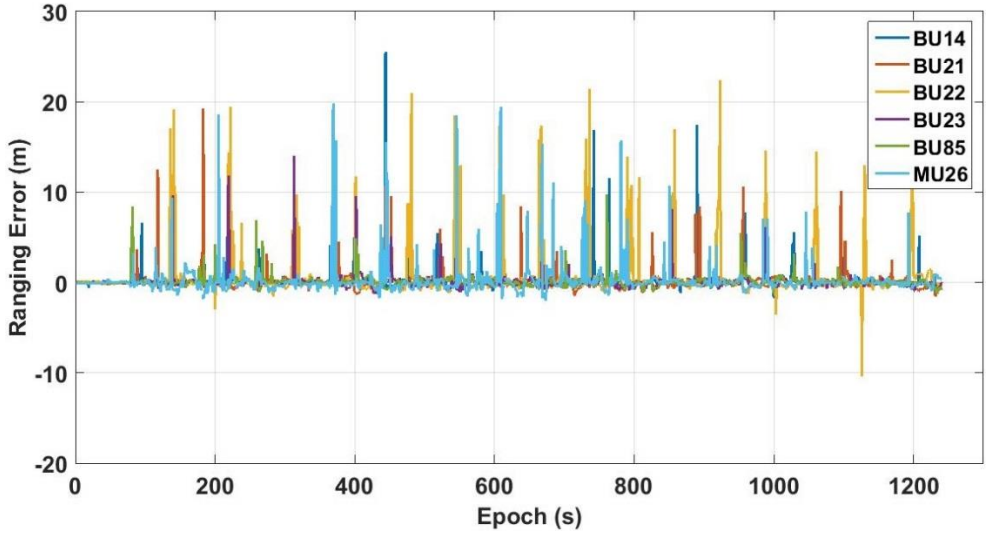


Fig.5.39 Combined 6 Ranging Errors in the Locomotive Test

Regarding the first reason discussed above, the RKF method is applied to produce accurate position to minimise the impact of ranging outliers. The horizontal position computed from RKF method is demonstrated by the blue line in Fig.5.40, and the GPS post-processing positioning result is given in red line. The corresponding errors in both directions are drawn in Fig.5.41. Comparing to standard KF method, the RKF method shrinks the impact of outliers and the errors in both easting and northing directions are not larger than 2 metres.

It can be found that the easting accuracy is better than northing accuracy which is attributed to the lower XDOP value. Fig.5.42 reveals the XDOP and YDOP in the locomotive test in blue line and red line respectively[19]. During the test, the XDOP maintains below 1 while the YDOP is not bigger than 2. As can be testified in Table 5.5, the BUs are distributed in easting direction by 35 metres which are about twice of the distance of 17 m in northing direction. It can easily find the one-to-one correspondence between the errors in the Y direction and YDOP values.

In addition, the position error in northing direction is also caused by the inaccurate dynamic model and ranging outliers. A sample lap in the locomotive test (from epoch 604 to 664) is randomly picked to show the position error in Fig.5.43. The red circle and blue circle indicate the ground-truth GPS position and the calculated position based on UWB ranging observations respectively. It can be found that the drift only happens on the west side of the trajectory. Specifically, the locomotive was running in a counter-clockwise direction, and it suffers from the severe ranging outliers in the beginning as shown earlier in Fig.5.39. Although the RKF method effectively controls the impact of ranging outliers, the maximum position error can still reach to 2 metres. At the end of the trajectory, the motion direction of the locomotive alters from a straight line

[19] The XDOP, YDOP and ZDOP discussed in this section are actually the Easting DOP, Northing DOP and Up DOP.

to a left turn which results in the drift of calculated position. With the similar geometry condition, the position error more likely increases when the locomotive does a relatively sharp steering. For example, the position error on the east side of the trajectory does not get larger because the locomotive manoeuvres a smoother turn even the DOP value is high.

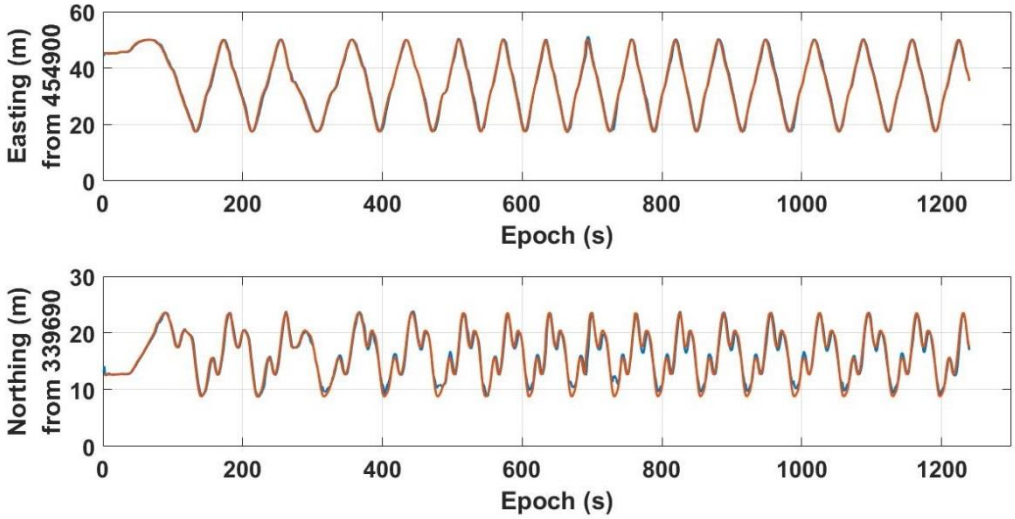


Fig.5.40 Positioning Result in Easting and Northing Directions (Applying Robust KF Method) in the Locomotive Test

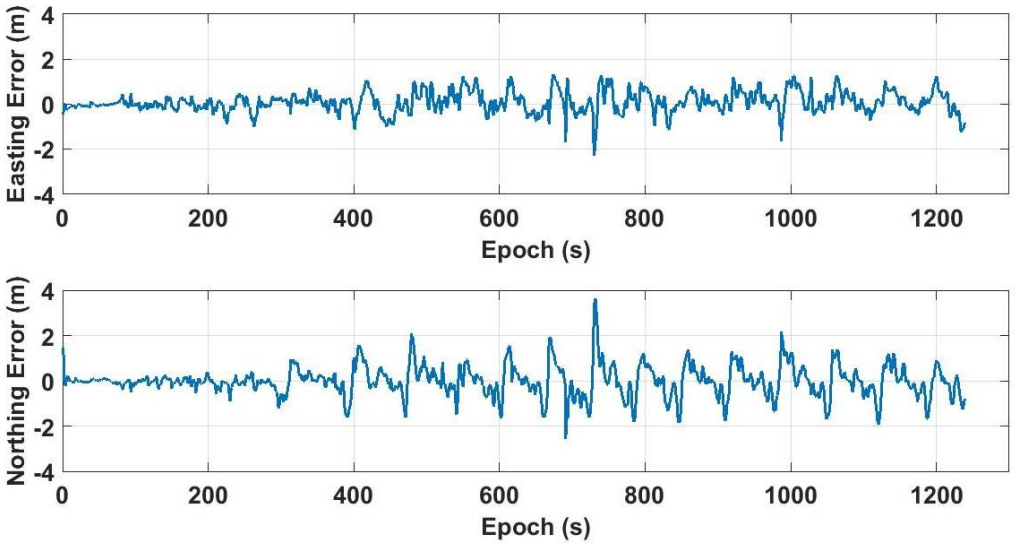


Fig.5.41 Position Error in Easting and Northing Directions (Applying Robust KF Method) in the Locomotive Test

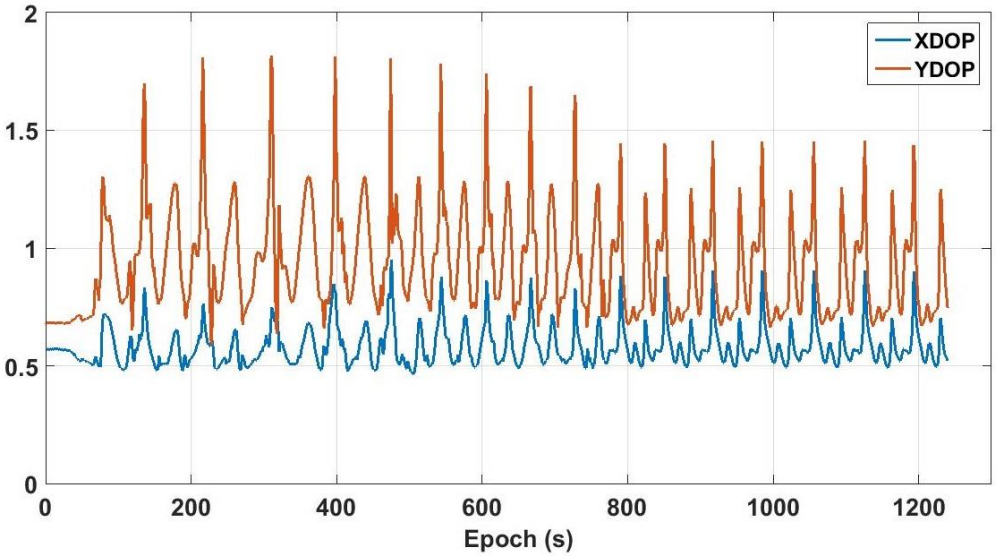


Fig.5.42 XDOP and YDOP in the Locomotive Test

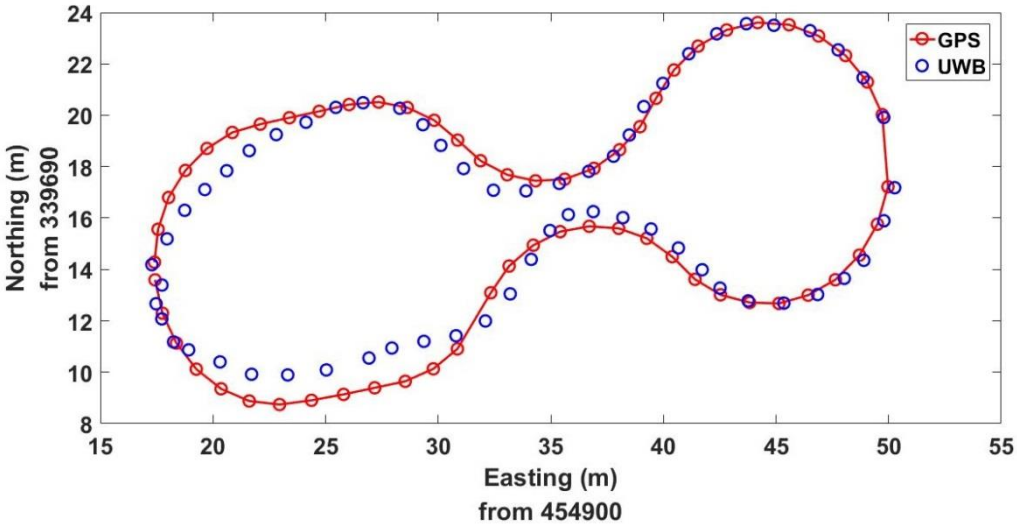


Fig.5.43 A Sample Lap Position Error in Locomotive Test

Another interesting point is the accuracies in both directions are becoming worse after about epoch 400. The error fluctuates in a regular pattern due to the continuous movement of the locomotive along the track. The increase of error is because the locomotive speeds up after epoch 400. Fig.5.44 shows the velocity of the locomotive throughout the test. The velocity is derived through differentiating the GPS post-processing position. As illustrated in Fig.5.36 that there are only small changes in height during the test, the velocity mainly reflects the horizontal velocity. It can be seen that the velocity of the locomotive gradually accelerates from the beginning of the test and maintain a stable speed of approximately 1.2 m/s after epoch 400. The four spikes

between epoch 600 and epoch 800 are due to the data missing. It can be found by linking to Fig.5.41 that the position error gets bigger when the locomotive is running at a relatively high speed. Operating at a relatively low speed, the inaccurate state update of the locomotive can be balanced by the measurement update. On the contrary, the state difference between two epochs is bigger, and the inaccurate estimate of the state model will lead the final solution to a wrong way.

Overall, the significant position error due to the ranging outliers are eliminated with the RKF method. Hence, the measurement model can provide more precise position estimate in the update phase. However, the error brought by inaccurate dynamic model and bad geometry cannot be corrected because of limited observation input.

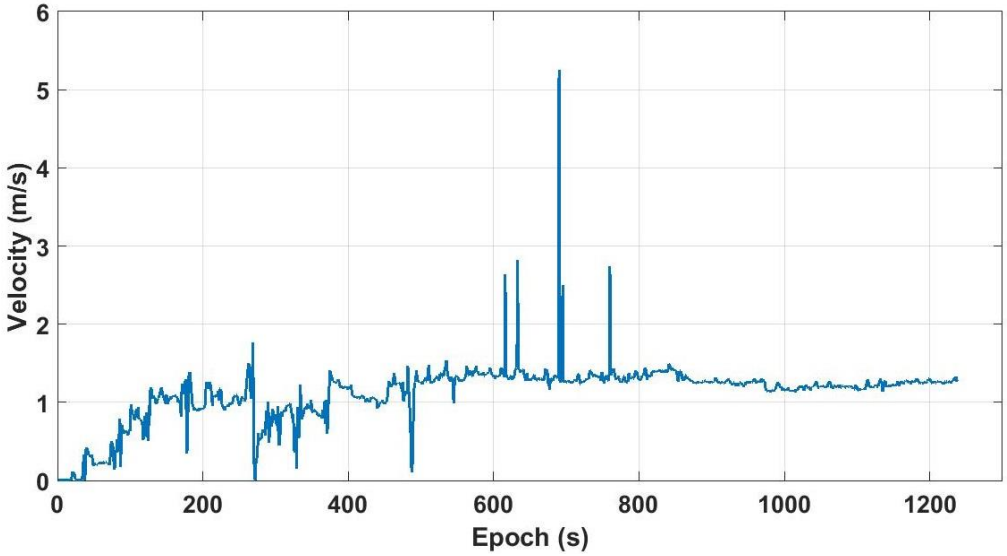


Fig.5.44 Velocity of the Target Unit in the Locomotive Test

To clearly see the improvement of RKF method, the detailed statistic of UWB kinematic positioning performance by using two methods in the locomotive test is listed below in Table 5.11. Applying standard KF method, the accuracies in easting and northing directions are both higher than 1 metre, and the height accuracy is about 3 metres because of the existence of ranging outliers. By

utilising the RKF method, the easting accuracy and northing accuracy can achieve around 60 cm while the height accuracy is improved to near 2 metres. With a better BUs distribution, the easting accuracy had some room to be promoted than the northing accuracy. By comparison, the easting accuracy has the largest improvement of 64% meanwhile the northing accuracy is improved by 43%. Due to the small height distinction of BUs, the height accuracy only has a limited improvement of 28 percentages. Overall, the RKF method improves the horizontal accuracy and 3D accuracy by 62% and 35%, respectively. Moreover, the RKF method is useful to eliminate the ranging outliers induced error which can be demonstrated by the lessening of extreme value compared to that of the KF method result.

Table 5.11 UWB Kinematic Positioning Performance in the Locomotive Test

Method		**E**	**N**	**H**	**2D**	**3D**
Standard KF	**Accuracy (m)**	1.31	1.21	2.93	1.78	3.43
	Precision (m)	1.31	1.21	2.91	1.36	2.43
	Max (m)	9.34	7.42	28.65	10.88	30.65
Robust KF	**Accuracy (m)**	0.48	0.69	2.12	0.84	2.28
	Precision (m)	0.47	0.69	2.10	0.52	1.59
	Max (m)	2.27	3.65	7.84	4.16	8.76
Accuracy Improvement (%)		64	43	28	62	35

5.5 Summary

This chapter has comprehensively assessed the Thales UWB ranging and positioning performances by conducting an indoor test, an outdoor dynamic test and a roof locomotive test. Three tests are designed to evaluate the overall performance of Thales UWB in different environments, namely, static multipath contaminated scenario, dynamic open scenario and dual-moving multipath contaminated scenario. Then the result has shown that Thales UWB ranging could offer centimetre level accuracy in a perfect environment and static situation. On the other hand, the ranging accuracy can be deteriorated to

60 cm due to the effect of NLOS and dual-moving situations. Also, the result has testified that the multipath effect and NLOS situation do make ranging performance worse. Furthermore, the correlation between ranging error and measuring distance has been found out, and the corresponding correction is modelled for future tests. At the end of this chapter, the corresponding UWB-only positioning performance based on ranging observations collected in these three tests is assessed by applying WLSE, standard KF and RKF introduced in Chapter 4. The centimetre level and decimetre level accuracies have been achieved for the static and kinematic case respectively. Furthermore, the effect of UWB ranging outliers has been effectively eliminated by applying the RKF method.

Chapter 6 Robust Cooperative Positioning with DD Code Pseudo-range and UWB Ranging Integration Supported by V2X Communication

6.1 Overview

Chapter 5 has discussed and evaluated the UWB ranging and positioning performances in different environments and dynamic modes. The units are capable of providing centimetre level accuracy in a favourable environment and can overall maintain at a sub-metre level ranging accuracy even in a multipath contaminated environment in dynamic mode. In this chapter, the positioning improvement by integrating UWB ranging observations with DD code pseudo-range positioning will be discussed. In the beginning, the roof trial is carried out to examine the proposed Robust Cooperative Positioning (RCP) solution, and the overall assessment of the performance of the proposed method will be followed. In the end, a simulative dataset has also been generated for further evaluation of proposed RCP solutions.

6.2 Robust Cooperative Positioning Based on DGPS/UWB Integration

This section will evaluate the performance of DGPS/UWB based cooperative positioning scheme by conducting a trial where the V2X communication environment was assumed to be established to allow the position-related information exchange. As same as the test configuration in Section 5.4, the coordinate system was established within the European Terrestrial Reference System 1989 (ETRS89) coordinate system, so the X, Y and Z axes followed the directions defined in the ETRS89 system.

6.2.1 Data Collection of the Roof Trial

The roof trial has been conducted on the roof of the Nottingham Geospatial Building (NGB) in the Jubilee Campus of the University of Nottingham. The

integration system consisted of a reference station, four Leica GNSS receivers (GS10) and six UWB units. Specifically, a chock-ring antenna was put on the pillar NGB2 to act as a reference station to provide GPS corrections as shown in the left figure in Fig.6.1. Two UWB units, BU51 and BU70, were set up as static BUs in the ETRS89 system with precise coordinates which were pre-measured by a Leica RTS (TS30) and the coordinates of static BUs and GPS reference station are listed in Table 6.1. Based on the lessons learnt from the previous locomotive test discussed in Section 5.3.1, the static BUs were not placed at the corner of the roof in order to avoid the impact of multipath. Two static BUs were located on the NGB7 pillar near to the east side of the roof and the north edge of the roof respectively. The remaining four units were separately tied together with a set of Leica GS10 receivers and AS10 antennas to provide ground truth trajectory as shown in the right figure in Fig.6.1. Particularly, BU26 and BU55 were configured as the moving BU to broadcast its GPS RTK position via simulated V2X communication as well as MU89 and MU80 were set as the MU to record ranging observations and receive position information from assumed surrounding transportation participants. All of those four device sets were carried by three people and the locomotive to move along the track.

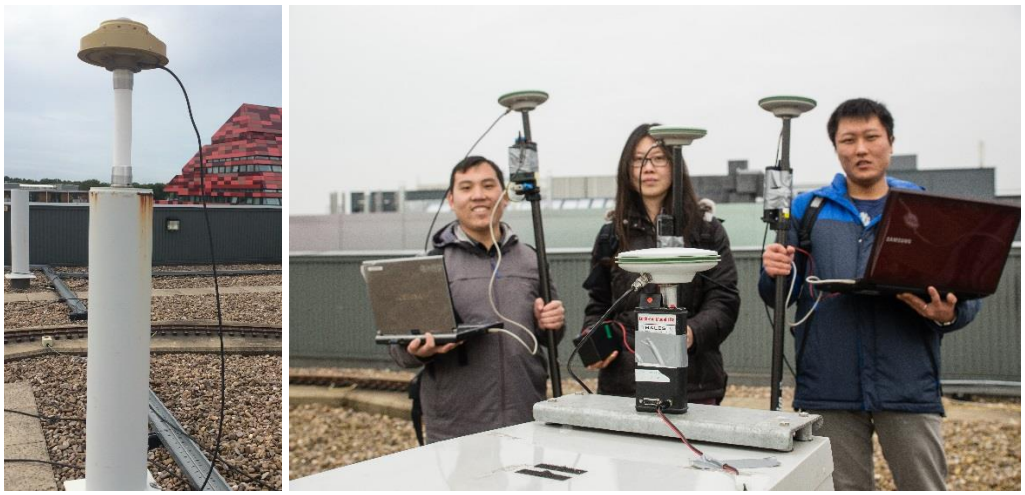


Fig.6.1 The GPS Reference Station and the Bundles of UWB and GPS Units

Table 6.1 Coordinates of the Static BUs and GPS Reference Station

Unit Number	Easting (m)	Northing (m)	Height (m)
BU51	454934.428	339712.632	42.395
BU70	454951.437	339709.354	42.683
Reference Station	454920.971	339703.908	42.682

The trial lasted more than 30 minutes which included a 10 minute static period in the beginning and around 20 minutes kinematic data collection. To calibrate the GPS antenna and the UWB unit precisely, the GPS antenna and UWB unit were fixed on a pole a known lever-arm and was held vertically as stable as possible especially for the units carried by people. As the UWB ranging observations are time stamped by the laptop system time, and the laptop was synchronised to the GPS time to collect 1 Hz UWB ranging before the test. Before starting the tests, we assume that all UWB units were equipped with the V2X communication devices within the reachable communication range of normally 500 m to share position information. The sampling rate of GPS receivers was also configured as 1 Hz to match the UWB ranging observations. Two MUs (users) and two moving BUs (reference vehicles) moved along the track to simulate the transportation participants that were running in a V2X communication environment where is able to exchange raw UWB and GPS observations and calculated positions. Although the proposed method processes the data epoch by epoch which enables the real-time processing, all UWB and GPS observations were collected separately for post-processing and analysis. Thus, a system consisted of two target vehicles, two surrounding transportation participants and two static RSUs were set up and an overview of the system deployment is displayed in Fig.6.2.

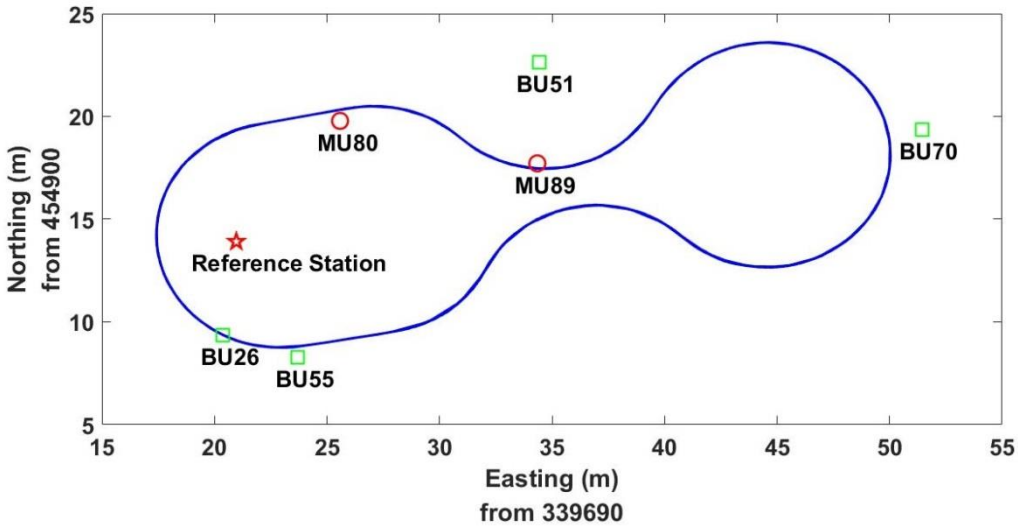


Fig.6.2 System Deployment in the Roof Trial

6.2.2 UWB Ranging Observations Assessment of the Roof Trial

Due to the connection problem and bad battery of MU80 it had unfortunately recorded very limited ranging observations. Therefore, only MU89's ranging observations had been stored and analysed. As shown in Fig.6.3, the blue line and red line indicate UWB raw ranging observations measured by MU89 and GPS-derived ground truth distance respectively. The UWB ranging generally matches the ground truth and the zero metre ranging observations in blue denote loss of data during the trial. Most of the time, the UWB ranging reflected the correct distance, but the outliers did exist. The maximal value of four distances was not larger than 40 metres, but the ranging outlier went to almost 100 metres, particularly on the ranging of MU89-BU55. It can be seen that the ranging observations of BU26, BU51 and BU70 contained a reasonable number of outliers whereas the ranging of BU55 was jeopardised by the outliers. The reason for outlier presence is explored and found out that about half of them are caused by NLOS situation. That also explains why there were very few outliers during the first 10 minutes as five UWB units had clear LOS among one another when they stood still. The reason for the rest of outliers may attribute to the hardware failure since those units have been damaged in the previous cow-tracking project and have not been properly fixed.

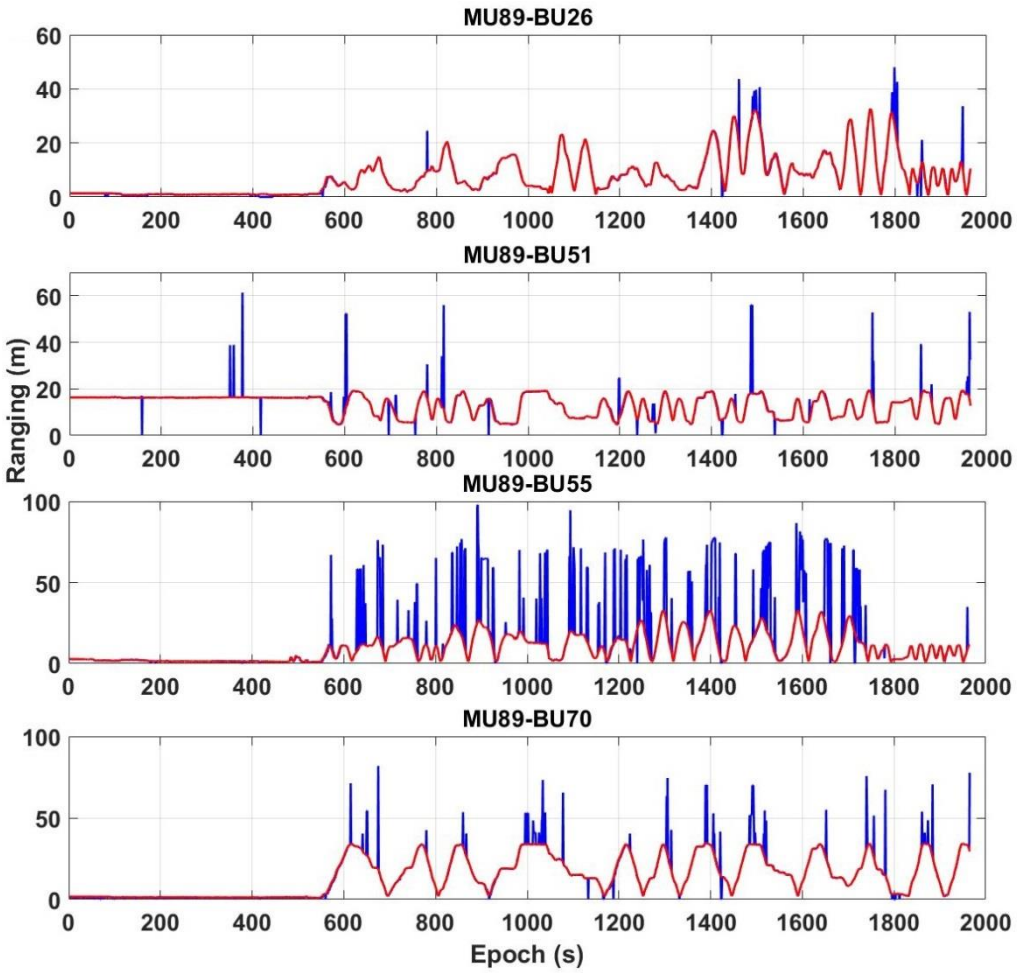


Fig.6.3 Comparison between UWB Raw Ranging Observations and Ground Truth Distances in the Roof Trial

Fig.6.4 gives four examples of NLOS induced outlier for each individual ranging observation. In each subfigure, the seven black diamonds and two blue pentagrams denote the metal pillars and the static BUs. The four solid circles indicate the positions of two moving BUs and two MUs and the red line shows the LOS between MU89 and a particular BU. It can be found that the ranging outlier occurs if the NLOS situation happens due to the obstruction from either a moving BU or a pillar. Moreover, another obstruction comes from the human body. As shown in Fig.6.1 that the height of the MUs or moving BU held by people is not higher than the height of people when they stand still. Although the whole pole was lifted as high as possible, the human body may obstruct the LOS between the MU and BUs during walking. Also, the BU55 was held at a lower height, and further increases the possibility of NLOS situation. As the

solid circle only show the position of the units, it is difficult to verify whether the people stand there to block the way without the precise position of people.

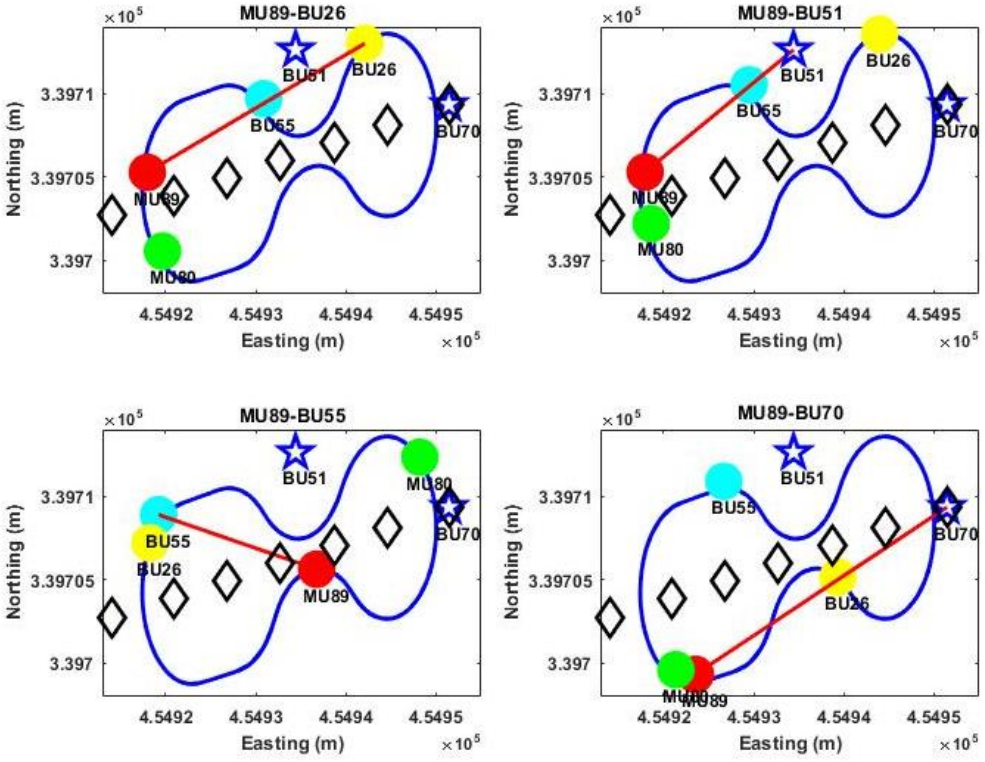


Fig.6.4 Examples of NLOS Situations Induced Ranging Outliers in the Roof Trial

Table 6.2 lists the detailed statistic of the UWB ranging performance in the roof trial. For all four ranging observations, the availability is not lower than 98% except the BU26 is 0.2% short. The outliers larger than 4 metres are removed from the statistic, and the outlier percentage is obtain from the ratio between the number of outliers and the number of received observations. It shows that BU26 and BU51 have less than 2 percentages outlier; BU70 has 3.2 percentages outlier, and BU55 has the highest 10.0% of outliers. By comparison the outlier percentages of two static BUs, BU70 is almost double of BU51. That is because BU70 was put at the east end of the field and the moving BUs and MUs moved relatively narrower in a north-south direction which led to a more limited angle of view to BU70 and higher possibility of blockage of BU70. The ranging accuracies are overall better than 40 cm after excluding the outliers. Comparing to the results of the locomotive test, the

participation of more people brings more opportunities of NLOS which leads to the slight drop in ranging availability. Regarding the outlier percentage, the better distribution of static BUs helps to reduce the frequency of occurrence of the outlier. Finally, the ranging accuracy still maintains the similar level of around 30 cm even a little looser outlier screening criterion has been applied.

Table 6.2 UWB Ranging Evaluation (Outlier Removed) in the Roof Trial

Total Epoch (1965 s)	**BU26**	**BU51**	**BU55**	**BU70**
Received Observation	1921	1956	1949	1936
Availability (%)	97.8	99.5	99.2	98.5
Number of Outlier	15	33	194	61
Outlier Percentage (%)	0.8	1.7	10.0	3.2
Accuracy (cm) (Outlier Removed)	28.6	26.1	39.2	37.1
Precision (cm) (Outlier Removed)	28.3	26.1	39.3	32.2

6.2.3 Positioning Performance Evaluation of the Roof Trial Applied the RCP Method

To deal with a large amount of ranging outliers, the proposed Robust Cooperative Positioning (RCP) method has been applied to provide the position. The position in three directions computed based on the RCP method is demonstrated by the blue line in Fig.6.5, and the GPS post-processing position is given in red line. Fig.6.6 shows the errors in three directions corresponding to Fig.6.5. With the utilisation of the RCP method, the impact of ranging outlier has been significantly mitigated. There are only a few fluctuations throughout the trial which lead to the errors of few metres in both easting and northing directions whereas the height errors are up to 10 metres.

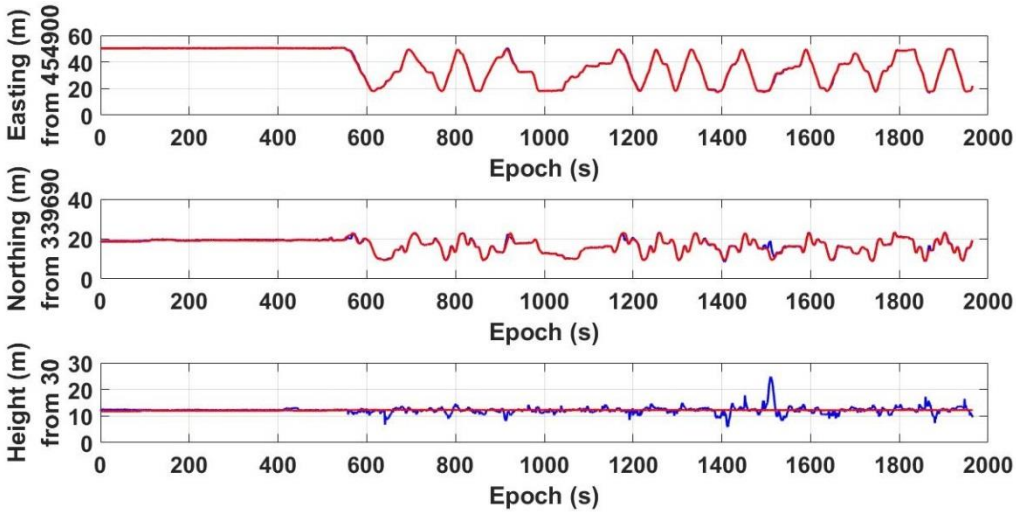


Fig.6.5 Positioning Result in Three Directions Based on the Pure UWB Ranging Observations in the Roof Trial (Applying the RCP Method)

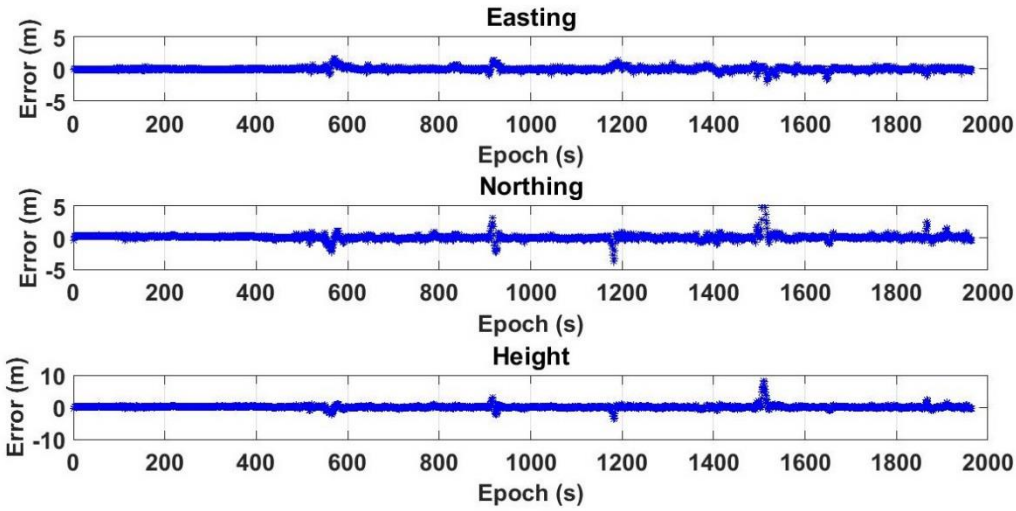


Fig.6.6 Position Errors in Three Directions Based on the Pure UWB Ranging Observations in the Roof Trial (Applying the RCP Method)

As shown in the upper row in Fig.6.7, four BUs were not distributed widely in height where the biggest height difference among four BUs was less than 1 metre. The heights of BU51 (in black) and BU70 (in green) stay the same, and the height of BU26 (in red) is relatively keeping constant at 41.8 metres since it was attached to the top of the locomotive and moved on a plane track. Moreover, BU55 (in blue) was held by a person and its height changes between 42.4 metres and 42.7 metres. To compare with the ZDOP values as shown in Fig.5.36 because the experimental environment was similar as in the locomotive test, the ZDOP value in the roof trial is generally better as shown in

the lower row in Fig.6.7. The ZDOP in the roof trial is generally lower than 20 except several extreme values caused by the loss of ranging observations.

In addition, the XDOP and YDOP values shown in Fig.6.8 are completely degraded by contrasting to the results in Fig.5.42. Lots of spikes occur in both XDOP and YDOP values. It is because four BUs in total were used in the trial and the bad geometry took place when MU89 received less than four ranging observations. Due to the space limitation of the roof, the BUs can move more widely in an east-west direction which results in the smaller YDOP value than XDOP value[20].

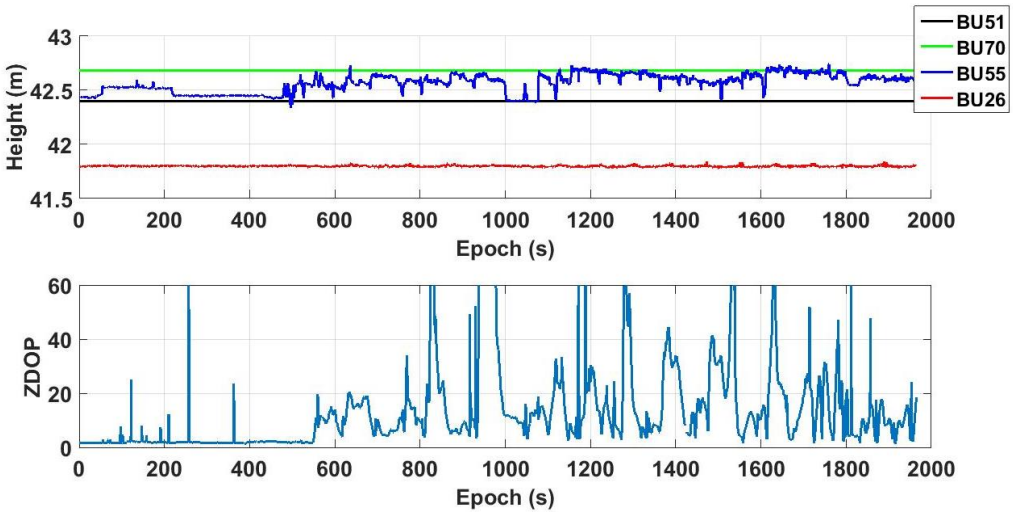


Fig.6.7 BUs Height Changes and ZDOP in the Roof Trial

[20] It should be noticed that the X and Y directions correspond to the northing and easting directions after the coordinate conversion from Cartesian XYZ coordinate to the local ENU coordinate.

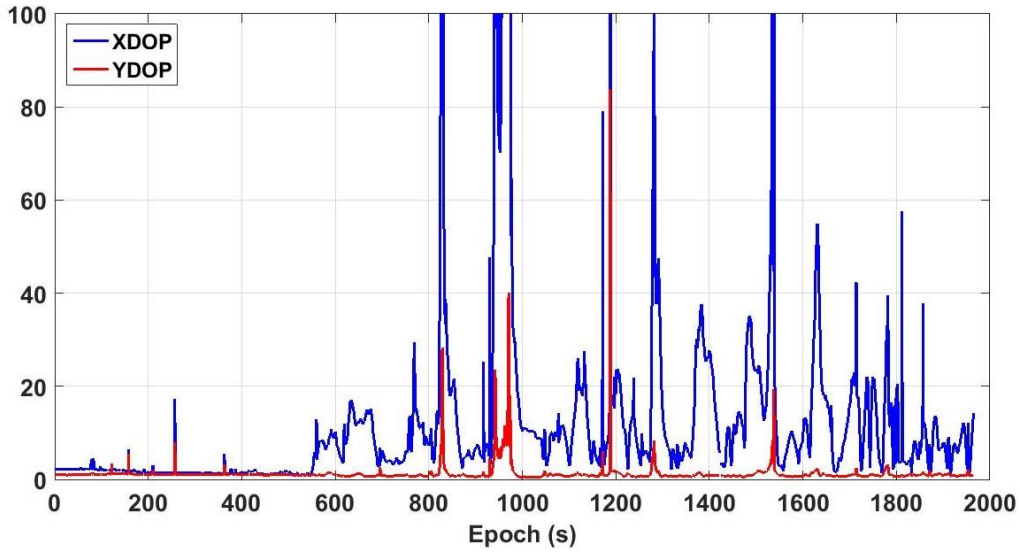


Fig.6.8 XDOP and YDOP in the Roof Trial

Table 6.3 lists the pure UWB positioning performance based on the RCP method in the roof trial, and the result is split into static and kinematic periods. With four UWB ranging observations, the static positioning accuracies are 11 cm, 26 cm and 37 cm in three directions respectively. To compare with the static positioning results as discussed in Section 5.4.2, the easting and northing accuracies and precisions in the roof trial drop from a centimetre level to a decimetre level. It is because of the less available number of BUs and a bad geometry where two moving BUs and MU89 stayed next to each other. On the other hand, the height accuracy and precision in the roof trial are much improved due to the larger height distinction among BUs.

As for the kinematic case, the easting accuracy is 33 cm that is two times better than the northing accuracy of 67 cm. By contrast to the result in Table 5.11, the easting accuracy is increased by 15 cm while the northing accuracy keeps at the similar level of 69 cm even less number of BUs were deployed and higher DOP value is obtained. Although many severe outliers existed which resulted in the bigger extreme values, the overall improvement could owe to the better choice of the BUs' locations where is not so close to the corner of the metal fence so that the overall ranging accuracy is improved by relieving multipath effects. Furthermore, the improvement is also achieved in the height accuracy

which is 60 cm. Basing on four UWB ranging observations, the overall kinematic accuracy and precision can achieve 75 cm and 64 cm in 2D and 1.7 metres and 1.33 metres in 3D respectively.

Table 6.3 Pure UWB Positioning Performance in the Roof Trial (Applying the RCP Method)

Motion State		**E**	**N**	**H**	**2D**	**3D**
Static (before epoch 550)	**Accuracy (m)**	0.11	0.26	0.37	0.29	0.46
	Precision (m)	0.07	0.15	0.18	0.12	0.17
	Max (m)	0.66	0.98	1.13	1.00	1.15
Kinematic (after epoch 550)	**Accuracy (m)**	0.33	0.67	1.53	0.75	1.70
	Precision (m)	0.32	0.66	1.53	0.64	1.33
	Max (m)	1.94	8.36	12.51	8.37	14.92

As shown in Fig.6.9, the positions in three directions computed based on pure DD code pseudo-range and the combination of DD code pseudo-range and UWB ranging using the RCP method are demonstrated as blue and red lines respectively. It can be found that the errors in both cases are smaller than 2 metres. The position error of pure DD code pseudo-range case changes smoothly based on the good satellite geometry. Fig.6.10 is the sky plot for the roof trial and the short red lines, and yellow pentagrams indicate the satellite trajectories and the ending position of the satellites respectively. It can be seen that there were eight visible GPS satellites during the trial and they spread evenly in easting and northing directions.

On the other hand, the positions of the combination case have few small spikes. Specifically, the spikes in both easting and northing directions around the epoch 600 occurred when MU89 started to move. Moreover, both the spike in easting direction at around epoch 900 and the spike in northing direction near to epoch 1200 are due to MU89 heading in the opposite direction. It can be concluded that the significant errors often occurred when the motion direction of the target suddenly changes. The reason that additional observations bring in

bigger errors is the covariance matrix of the measurement noise R is enlarged caused by outliers (referring to Eq. 4.27), and then the Kalman gain K is decreased in order to reduce the weight of the estimate of the measurement model. Meanwhile, the estimate of the state model becomes inaccurate due to the sudden change of the motion direction. Therefore, the final estimate of the RCP method is inclined to the estimate of the state model which results in a bigger error. Overall speaking, the position accuracies in three directions are improved by introducing the UWB ranging observations.

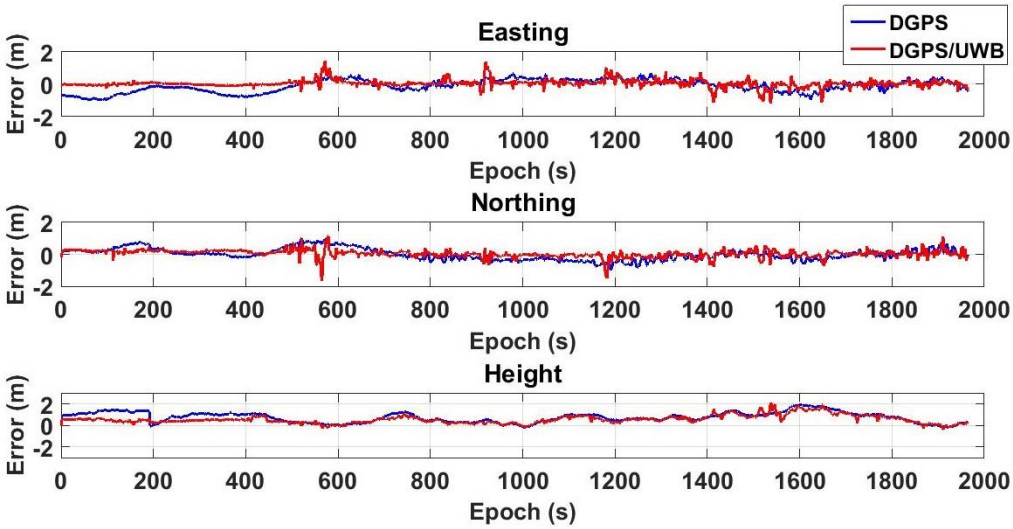


Fig.6.9 The Positioning Result Comparison between Pure DD Code Pseudo-range and DD Code Pseudo-range/UWB Ranging Combination in the Roof Trial (Applying the RCP Method)

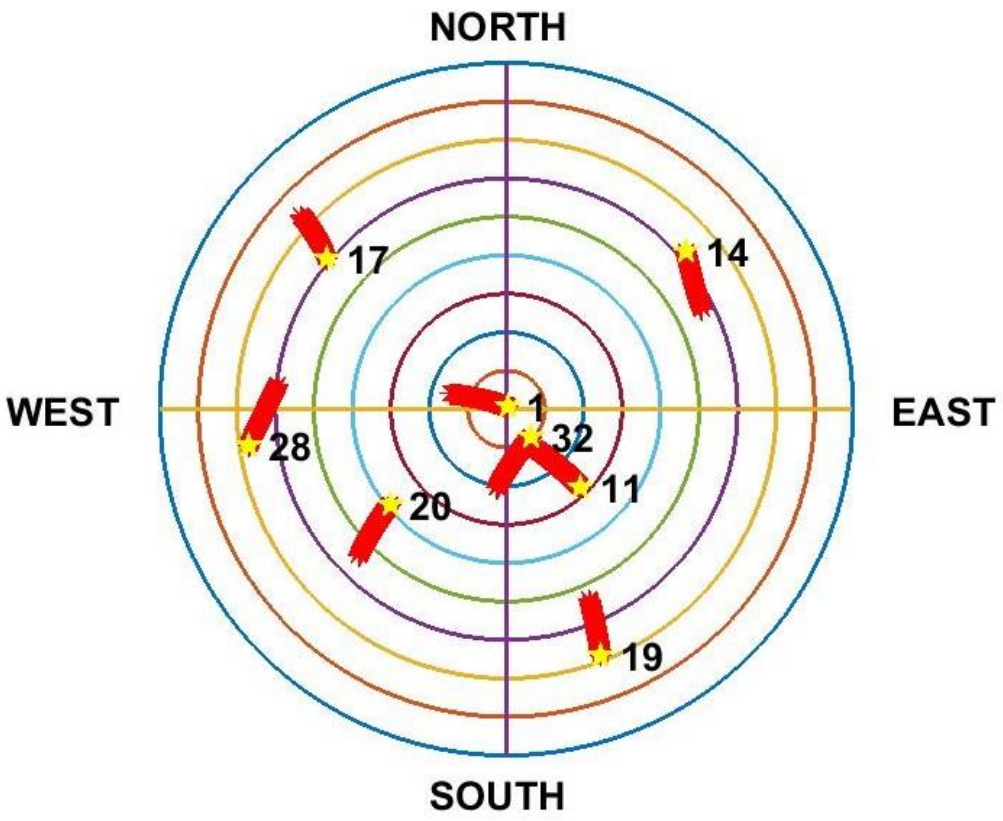


Fig.6.10 The GPS Sky Plot for the Roof Trial

The employment of UWB ranging observations not only augments the number of observations but also improves the observation geometry of the target MU. Fig.6.11 presents the available GPS satellite and UWB BUs during the roof trial. In total, 8 GPS satellites were always available, and 4 UWB BUs were functional properly most of the time though one of BUs snapped at several epochs and all other four BUs were missed out at 2 epochs. As shown in Fig.6.12, the blue and the red lines denote the DOP values of the pure DGPS case and the combination case respectively. It can be found that the DOP values of the pure DGPS case are lower than 0.8 in three directions because of good geometry. By adding UWB ranging observations, the DOP values are even better in the combination case. The XDOP and YDOP are lower than 0.6 and ZDOP fluctuates around 0.6.

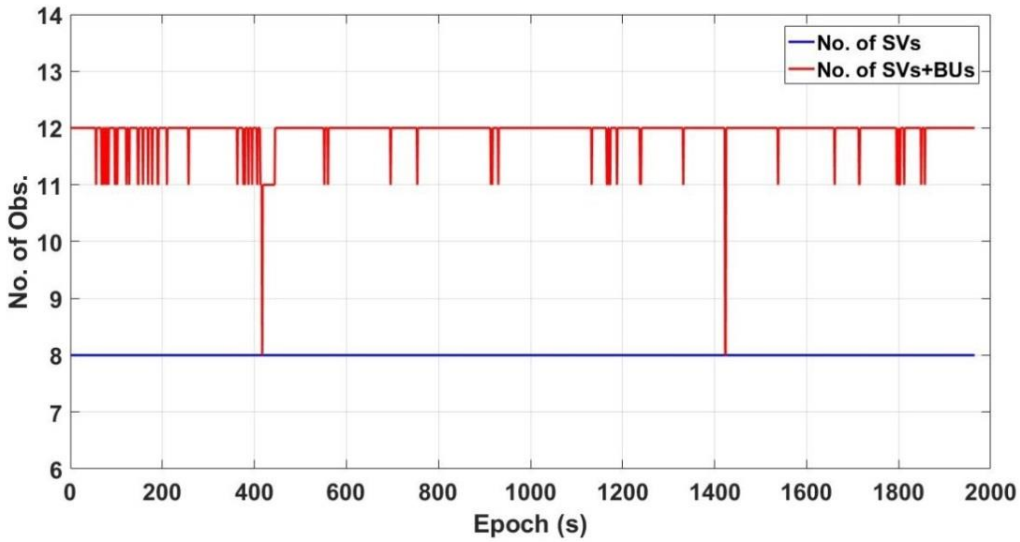


Fig.6.11 The Numbers of SVs and BUs in the Roof Trial

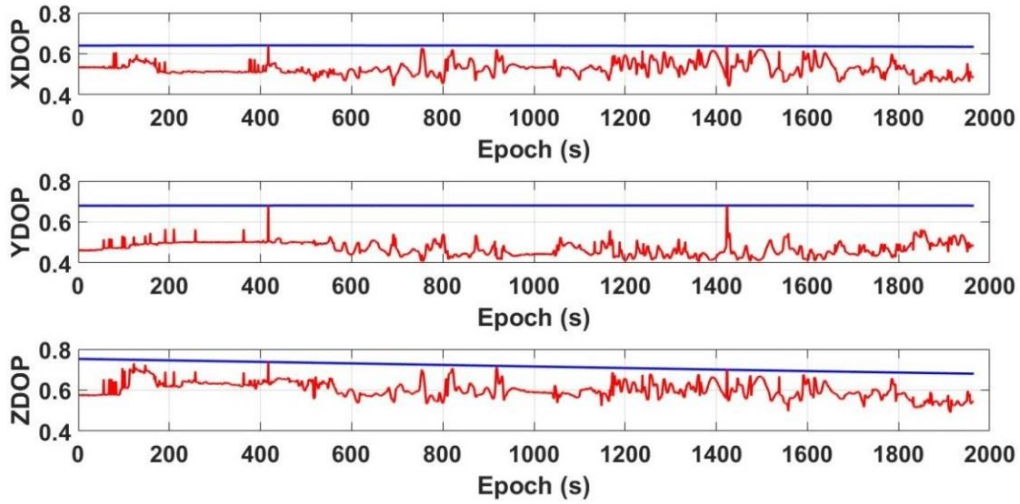


Fig.6.12 The DOP Comparison between Pure DD Code Pseudo-range and DD Code Pseudo-range/UWB Ranging Combination in the Roof Trial

With the application of the RCP method, the details of the positioning performance comparison between the pure DD code pseudo-range and DD code pseudo-range/UWB ranging combination in the roof trial is listed below in Table 6.4, and the positioning results are split into static and kinematic periods. Regarding the DOP values in the static period, the mean DOP values in the pure DGPS case are good enough and stay around 0.7 in all three directions, and they keep the same in the kinematic period as there was no high building around the NGB to obstruct the GPS satellites. By using extra UWB BUs, the DOP values become lower in three directions. In both static and kinematic periods, the XDOP, YDOP and ZDOP are improved by about 19, 28

and 15 percentages respectively. The reason is same as the earlier discussion that the UWB BUs moved more widely in an east-west direction.

From the accuracy and precision perspective, the pure DD code pseudo-range can provide slightly bigger than 30 cm accuracy and precision in easting and northing directions no matter the target MU is static or moving, except the static easting accuracy is almost 60 cm for some unknown reasons. The height accuracy is about 90 cm with better than a half metre precision. With the augmentations of UWB ranging observations, the static positioning performance is better than that of kinematic and the improvement of the static case is also higher than the kinematic case. One of the reasons is the static ranging accuracy is higher than the kinematic ranging accuracy. Another reason is there was seldom ranging outliers when the units are static comparing to the kinematic scenario. The static easting, northing and height accuracies are 8 cm, 23 cm and 48 cm with 86%, 38% and 52% improvements respectively by adding UWB ranging observations. On the other hand, the kinematic positioning performance is worse than the static results. The easting, northing and height accuracies of the combination case are 28 cm, 24 cm and 74 cm respectively while there is about 10 percentages improvement in easting and height directions and the biggest improvement of 29 percentages in northing direction. It should also be noticed that the maximum values are getting bigger after introducing the UWB ranging observations which is led by the existence of outliers. Based on 7 DD code pseudo-range and 4 UWB ranging observations, the proposed RCP method can overall offer better than 30 cm 2D static accuracy and 50 cm 3D static accuracy as well as 40 cm 2D kinematic accuracy and 90 cm 3D kinematic accuracy under the influence of severe UWB ranging outliers.

Table 6.4 The Positioning Performance Comparison between Pure DD Code Pseudo-range and DD code pseudo-range/UWB Ranging Combination in the Roof Trial (Applying the RCP Method)

Motion State	Case		E	N	H	2D	3D
Static (before epoch 550)	Pure DGPS	Mean DOP	0.64	0.68	0.74	0.93	1.19
		Accuracy (m)	0.57	0.37	0.99	0.68	1.19
		Precision (m)	0.30	0.28	0.39	0.22	0.35
		Max (m)	1.02	0.98	1.47	1.07	1.79
	DGPS & UWB	Mean DOP	0.52	0.49	0.63	0.72	0.96
		Accuracy (m)	0.08	0.23	0.48	0.25	0.54
		Precision (m)	0.08	0.12	0.15	0.11	0.14
		Max (m)	0.50	0.93	0.95	0.94	0.97
DOP Improvement (%)			19	28	15	23	19
Accuracy Improvement (%)			86	38	52	63	55
Kinematic (after epoch 550)	Pure DGPS	Mean DOP	0.64	0.68	0.71	0.93	1.17
		Accuracy (m)	0.30	0.34	0.84	0.46	0.95
		Precision (m)	0.30	0.33	0.49	0.21	0.40
		Max (m)	0.94	0.99	1.94	1.07	2.14
	DGPS & UWB	Mean DOP	0.53	0.46	0.59	0.70	0.92
		Accuracy (m)	0.28	0.24	0.74	0.36	0.82
		Precision (m)	0.27	0.24	0.44	0.26	0.41
		Max (m)	1.44	1.62	2.15	1.91	2.46
DOP Improvement (%)			17	32	17	25	21
Accuracy Improvement (%)			7	29	12	22	14

6.3 Positioning Performance Assessment Using Simulated UWB Ranging Observations

Although the effect of severe outliers of UWB ranging observations has been greatly diminished by the proposed RCP method, the full potential of UWB ranging observations cannot be effectively exploited. To evaluate the maximal advantage that the augmentation of UWB ranging observations can bring, the simulated UWB ranging observations are generated based on the error distribution of collected real UWB ranging observations. This simulated UWB

ranging observation will be further integrated with the real GPS pseudo-range observations gathered in the roof test to be processed through the proposed RCP method. Since quite a few UWB ranging outliers can be found in the static scenario as shown in Fig.6.3 and the research is interested in transportation application, only the kinematic scenario is considered, and the UWB kinematic ranging observations are simulated. To preprocess the original collection of UWB ranging observations after epoch 550, all the ranging errors bigger than 1 metre are removed. The simulated ranging observations are created based on the real error distribution of each individual remaining real data. Fig.6.13 demonstrates the collected and simulated ranging observations of individual BU in the blue bar and red bar respectively. Also, 1416 ranging observations are entirely generated by each unit, and the simulated ranging observations accord well with the collected ranging observations. It can be seen that most of the ranging observations centralised at zero except there is a small shift in MU89-BU70 ranging observation.

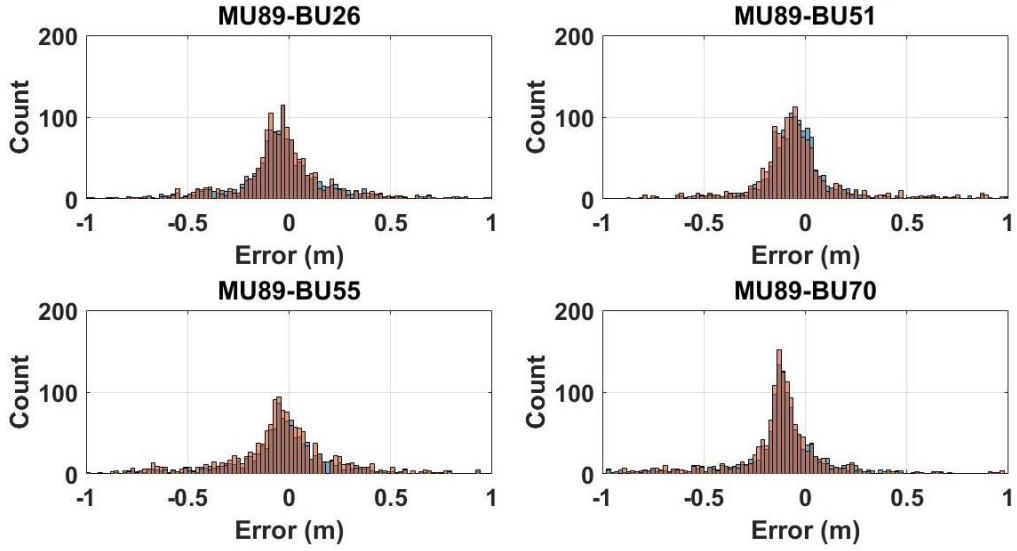


Fig.6.13 The Histogram of Collected and Simulated Kinematic Ranging Observation

To comprehensively evaluate the performance of the proposed RCP method and the maximal benefit of the introduction of UWB ranging observations, different scenarios are considered relying on the data collection of the roof trial. In this section, the trial setup and environment are exactly same as the roof trial

discussed above in Section 6.2.1. Regarding the dataset has been used, the raw GPS observation is remained and the only difference comes from the replacement of raw UWB ranging observation with simulated UWB ranging observation. In all simulated scenarios, two static BUs and two moving BUs in total were used to act as the RSUs and surrounding vehicles respectively. We assume that all neighbouring vehicles and the RSUs are equipped with a UWB unit to produce ranging observations and a DSRC device for communication with the target vehicle. In addition, the neighbouring vehicles are equipped with a set of dual-frequency GPS receivers and antennas to provide precise positions and share pseudo-range observations. Also, a GPS reference station is operating in this area to broadcast the DGPS corrections. Moreover, the target vehicle is equipped with a set of single-frequency GPS receiver and antenna, a UWB MU and a DSRC device. The four hypothetical scenarios are described in following sections.

6.3.1 The Robustness Assessment of the Proposed RCP Method (Scenario 1)

As the raw UWB ranging observations contain too many outliers, it is difficult to show the specific capability of the proposed RCP method to deal with a particular outlier. To assess the advantage of the proposed RCP method, the outliers will be purposely added onto the simulated UWB ranging observation. In addition, the position of the target vehicle will be generated in the GPS partially obstructed environment (the GPS cut-off angle is set as 40 degrees) because too many redundant DD code pseudo-ranges would relief the effect of outlier observations without using robust estimation approach. Therefore, a simulative outlier of 20 metres is added onto the simulated UWB ranging observation MU89-BU70 every 60 seconds and the KF module in the RCP method is swapped between the standard KF and the RKF.

The position errors in three directions based on two approaches have been shown in Fig.6.14 and Fig.6.15. It can be found that the standard KF cannot deal with the simulative outliers and the position errors in three directions

increase whenever the outlier exists. Moreover, the effect of outlier mainly emerges in easting direction. This is because the outlier is added on ranging MU89-BU70 where BU70 was placed on the east end of the test field and then the added outlier would push the calculated position to the west. On the other hand, the RKF method completely eliminated the impact of outliers and had smaller position errors with 15 cm, 26 cm and 93 cm accuracy in easting, northing and height directions.

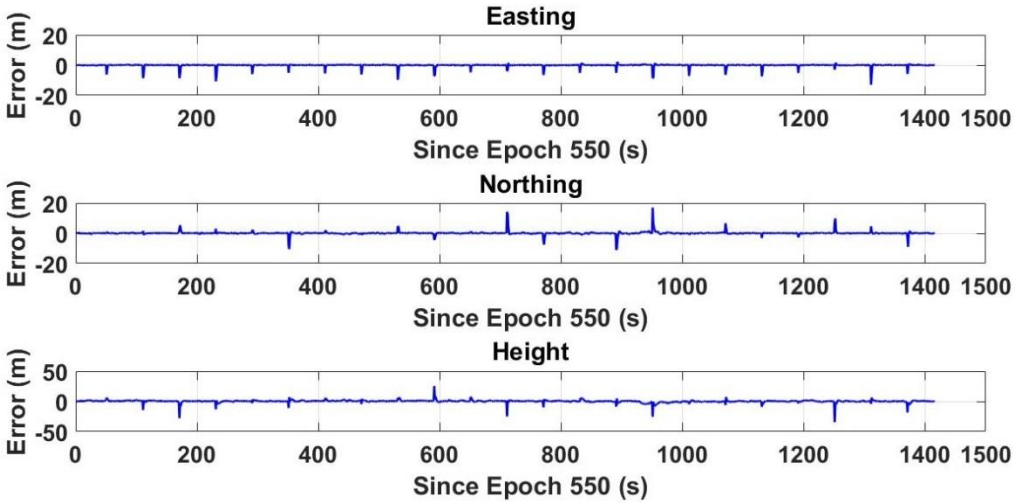


Fig.6.14 Position Error Based on Selected GPS Pseudo-range and Contaminated UWB Ranging Observations Using Standard KF Method

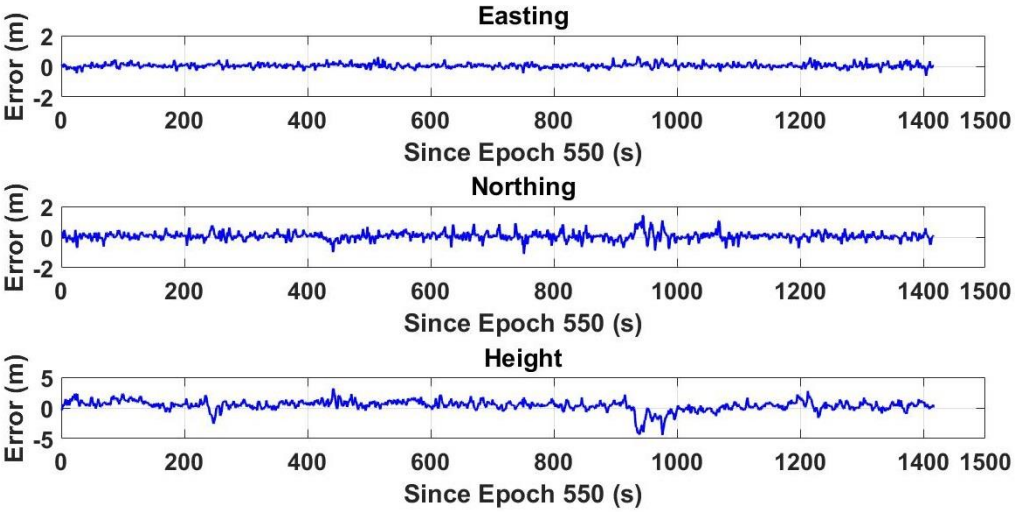


Fig.6.15 Position Error Based on Selected GPS Pseudo-range and Contaminated UWB Ranging Observations Using RKF Method

6.3.2 The Urban Canyon Scenario (Scenario 2)

Assume the target vehicle (MU89) is driven into an urban canyon where is within the coverage area of a GPS reference station (NGB2). Also, two RSUs are deployed at the known locations along the road and other two surrounding vehicles are driven in the communication range. The GPS satellite visibility of the target vehicle is obstructed with 40 degrees cut-off angle and different numbers of UWB ranging observations are augmented.

As shown in Fig.6.16, 4 GPS satellites are still available with the cut-off angle of 40 degrees during the test, i.e. 3 DD code pseudo-range observations. To evaluate the improvement based on a different number of UWB ranging observations can contribute the positioning performance, the positioning Cumulative Distribution Function (CDF) in three directions are estimated and shown in Fig.6.17. Different colour indicates the different number of UWB ranging observations that have been introduced to the DD code pseudo-range observation. The cyan line denotes the positioning result based on to pure DD code pseudo-range which means there are no redundant observations. The red line represents the positioning result based on 3 DD code pseudo-range and 4 UWB ranging observations. It can be found that introduction of UWB could effectively improve the position accuracies in all three directions and the easting accuracy is the highest due to the BUs' distribution as discussed earlier. Furthermore, the improvement in position accuracy clearly reduced when two UWB ranging observations have been added. With four UWB ranging observations, the position errors in three directions are lower than 1 metre.

Table **6.5** lists the full positioning performance using different numbers of simulated UWB ranging observations. Without the UWB ranging observation, the easting accuracy is about 0.9 m, and northing accuracy is doubled as 1.8 m, while the height accuracy is 4.5 m. By adding two UWB ranging observations, the horizontal accuracy is improved to decimetre level as 0.64 m and the 3D accuracy as 1.65 m. Employing all available UWB ranging observations, the accuracies can achieve 16 cm, 26 cm and 93 cm in easting, northing and height

directions respectively and the precisions also reach to the similar level. The accuracy improvement in the table is all calculated by comparing to the accuracy without add UWB ranging. It can tell that the 2D and 3D accuracies are significantly improved by 68.2% and 66.3% respectively by adding the two UWB rangings. Any extra UWB rangings beyond two only can give around 15 percentages improvement, and the maximal 2D and 3D accuracy improvements can be achieved in 84.6% and 80.0% respectively by adding four UWB rangings.

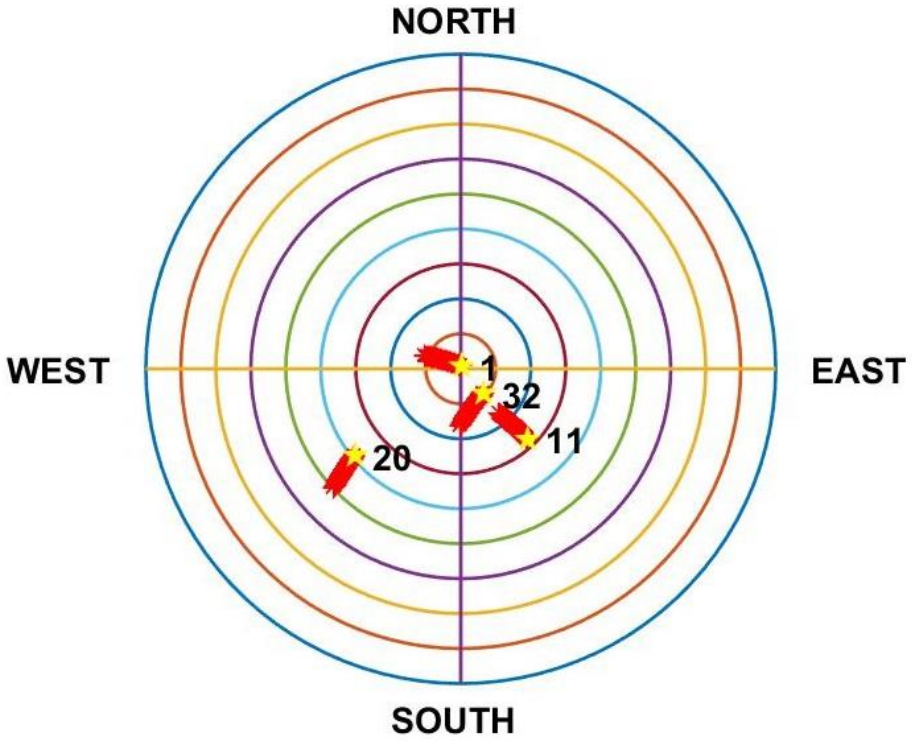


Fig.6.16 The GPS Sky Plot with Cut-off Angle of 40 Degrees

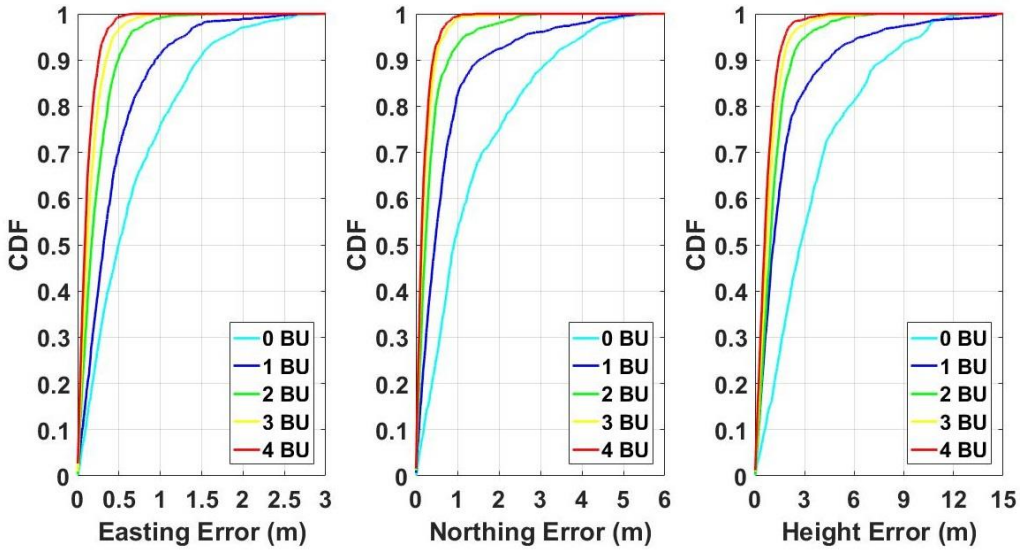


Fig.6.17 Positioning CDF Using Different Numbers of Simulated UWB Ranging Observations with Three DD Code Pseudo-range Observations

Table 6.5 The Positioning Performance Comparison Using Different Numbers of Simulated UWB Ranging Observations with Three DD Code Pseudo-range Observations

Number of Added Ranging		**E**	**N**	**H**	**2D**	**3D**
0	**Accuracy (m)**	0.87	1.81	4.47	2.01	4.90
	Precision (m)	0.80	1.43	4.15	1.25	2.97
1	**Accuracy (m)**	0.59	1.12	2.93	1.26	3.19
	Precision (m)	0.59	1.04	2.93	0.90	2.39
Accuracy Improvement (%)		32.2	38.1	34.5	37.3	34.9
2	**Accuracy (m)**	0.31	0.56	1.52	0.64	1.65
	Precision (m)	0.31	0.52	1.49	0.43	1.04
Accuracy Improvement (%)		64.4	69.1	66.0	68.2	66.3
3	**Accuracy (m)**	0.21	0.32	1.15	0.38	1.21
	Precision (m)	0.21	0.31	1.09	0.24	0.75
Accuracy Improvement (%)		75.9	82.3	74.3	81.1	75.3
4	**Accuracy (m)**	0.16	0.26	0.93	0.31	0.98
	Precision (m)	0.15	0.26	0.84	0.19	0.59
Accuracy Improvement (%)		81.6	85.6	79.2	84.6	80.0

6.3.3 The Approaching Tunnel Scenario (Scenario 3)

Assume the target vehicle (MU89) is approaching a tunnel where two RSUs are deployed at the known locations, and other two vehicles are also driven towards to the tunnel. When the target vehicle is getting closer to the tunnel, the number of visible GPS satellite will keep dropping until no GPS observation is available.

To exploit the influence that the reducing numbers of the DD code pseudo-range observations could bring in the positioning performance using four simulated UWB ranging observations, the positioning Cumulative Distribution Function (CDF) in three directions is shown in Fig.6.18. Different colour indicates the various numbers of DD code pseudo-range observations that have been combined with the simulated UWB ranging observation. The blue line indicates the positioning result based on pure UWB simulated ranging observations whereas the red line denotes the positioning results using additional three DD code pseudo-range observations. The positioning performance does not degrade a lot when the GPS satellites are all obstructed, except in the height performance. This is because the UWB can offer more accurate ranging observations than GPS and therefore obtains an accurate position with a small number of observations. Table 6.6 tells the details of the positioning performance using different numbers of DD code pseudo-range observations. Without three DD code pseudo-range observations, the positioning accuracy and precision only drop 4 cm and 9 cm in easting and northing directions while a high degradation of a half metre in height direction. It can be found that the accuracy improved (compared to the UWB-only positioning result, i.e. no DD code pseudo-range observations) up to 22.5% in 2D and 33.3% in 3D respectively by integrating three GPS DD code pseudo-range observations.

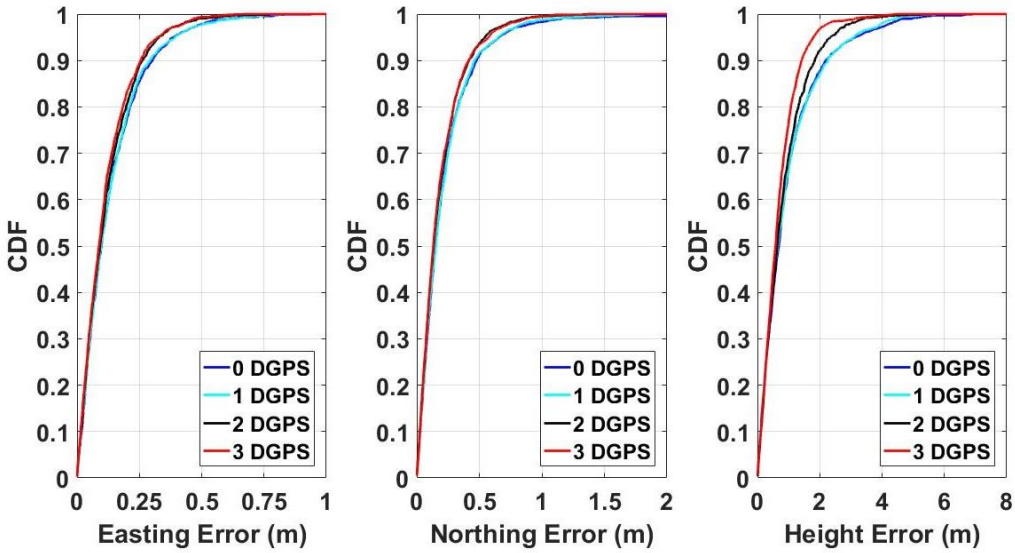


Fig.6.18 Positioning CDF Using Different Numbers of DD Code Pseudo-range Observations with Four Simulated UWB Ranging Observations

Table 6.6 The Positioning Performance Comparison Using Different Numbers of DD Code Pseudo-range Observations with Four Simulated UWB Ranging Observations

Number of DD code pseudo-range		**E**	**N**	**H**	**2D**	**3D**
0	**Accuracy (m)**	0.19	0.35	1.41	0.40	1.47
	Precision (m)	0.17	0.35	1.41	0.28	1.02
1	**Accuracy (m)**	0.18	0.31	1.36	0.36	1.41
	Precision (m)	0.17	0.30	1.36	0.23	0.96
Accuracy Improvement (%)		5.3	11.4	3.5	10.0	4.1
2	**Accuracy (m)**	0.16	0.26	1.13	0.31	1.17
	Precision (m)	0.16	0.26	1.11	0.19	0.74
Accuracy Improvement (%)		15.8	25.7	19.9	22.5	20.4
3	**Accuracy (m)**	0.16	0.26	0.93	0.31	0.98
	Precision (m)	0.15	0.26	0.84	0.19	0.59
Accuracy Improvement (%)		15.8	25.7	34.0	22.5	33.3

6.3.4 Mobile Reference Station (Scenario 4)

In the case of communication link down to receive DGPS corrections from the GPS reference station or NRTK facilities, the Mobile Reference Station (MRS) offers an alternative way to continue offering the DGPS solution. Based on the V2X communication, the target vehicle is able to talk to the surrounding vehicle which equips with dual-frequency GPS receiver and antenna. This surrounding vehicle would act as an MRS and generate the correction like information, which includes the RTK solution of its position and raw GPS pseudo-range and that information will be transmitted to the target vehicle to enable the DGPS solution.

Fig.6.19 and Fig.6.20 demonstrate the position errors using different MRS (MRS02 and MRS04), based on three DD code pseudo-range and four simulated UWB ranging observations. The position error based on pure DD code pseudo-range is shown in blue line, and the red line represents the position error based on the combination of three DD code pseudo-range and four simulate UWB ranging observations. It can be found that the position errors in both cases are relatively stable and fluctuate around zero. Table 6.7 gives the statistics of the positioning performance using MRS02 and MRS04. It can be seen that the horizontal position accuracies in both cases have been improved by 49% and 43% respectively, with a smaller improvement in the height direction. To compare with the result in Section 6.3.3, the position accuracy achieves at the same level of 30 cm in the horizontal plane and even better in height direction. This maybe the MRS stays at a similar height as the target vehicle. Therefore they can experience the similar level of error from the external environment which can be better differenced in DGPS procedure.

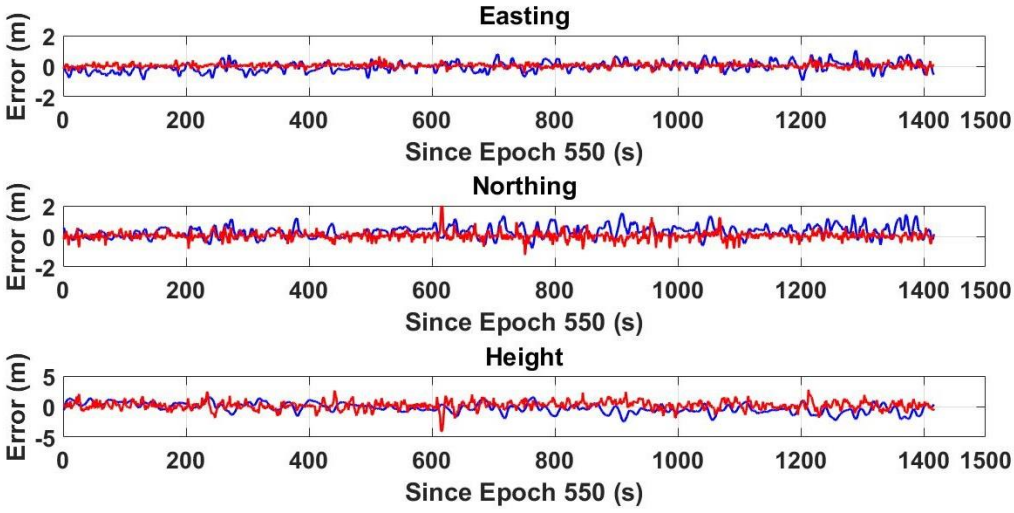


Fig.6.19 Position Error Comparison with or without Simulated UWB Ranging Observations Based on the MRS02

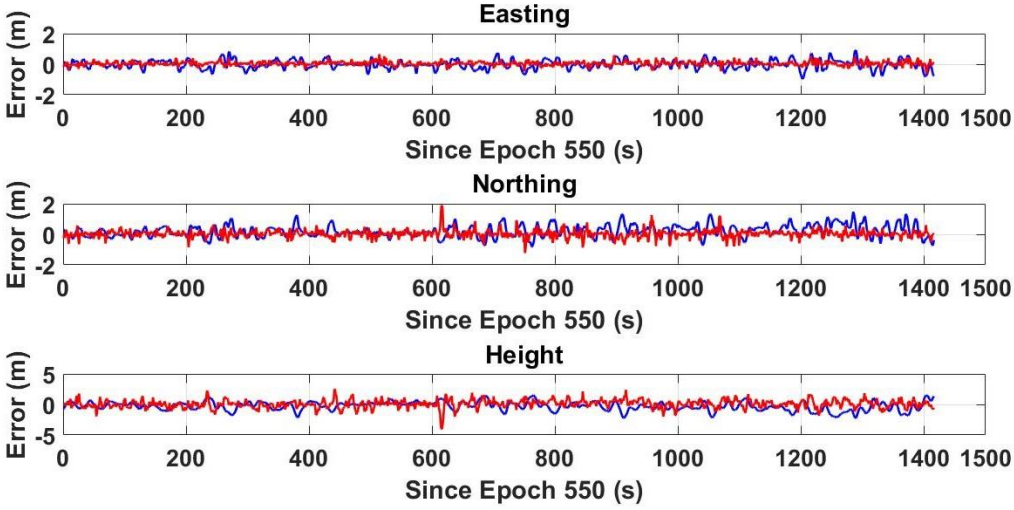


Fig.6.20 Position Error Comparison with or without UWB Simulated Ranging Observations Based on the MRS04

Table 6.7 The Positioning Performance Comparison with or without Simulated UWB Ranging Observations Using Different MRS

			E	N	H	2D	3D
MRS02	**Without UWB**	**Accuracy (m)**	0.32	0.49	0.81	0.59	1.00
		Precision (m)	0.32	0.38	0.78	0.27	0.48
	With UWB	**Accuracy (m)**	0.15	0.26	0.71	0.30	0.77
		Precision (m)	0.14	0.26	0.69	0.19	0.47
Accuracy Improvement (%)			53	47	12	49	23
MRS04	**Without UWB**	**Accuracy (m)**	0.29	0.44	0.76	0.53	0.93
		Precision (m)	0.29	0.39	0.71	0.27	0.51
	With	**Accuracy (m)**	0.15	0.26	0.68	0.30	0.74

	UWB	**Precision (m)**	0.14	0.26	0.68	0.19	0.45
Accuracy Improvement (%)			48	41	11	43	20

6.4 Summary

In this chapter, the roof trial has been conducted to assess the performance of the proposed RCP method. With the assumption of the existence of the V2X communication, the DD code pseudo-range and UWB ranging observations have been cooperatively integrated together to provide about 30 cm horizontal accuracy and 80 cm 3D accuracy. To fully exploit the benefit of integrating UWB ranging observations, the simulated ranging observations have been generated basing on the collected raw data in order to get rid of the impact of UWB ranging outliers. Finally, four scenarios are considered to assess the advantages of UWB ranging observations in GPS hostile environment and the concept of the Mobile Reference Station (MRS) has been proposed.

Chapter 7 Conclusions and Recommendations

The developments of modern ITS road applications can significantly benefit the current transportation situation by enhancing safety, reducing emission and improving mobility. However, the problems encountered in vehicle positioning in GNSS hostile environment, such as urban canyon and tunnel, restrict the maximisation of these benefits since GNSS are still the most common vehicle positioning technology. To provide continuous and reliable positioning solution in such environments, multi-sensor integration and cooperative positioning approaches have been increasingly paid attentions. While the V2X communication technology is becoming a standard on-board module in the near future, how to effectively and efficiently utilise this technology and what information should be transmitted are two questions that need to be answered urgently for various V2X applications. Also, the combination of GNSS and other integrated sensors can more cost-effectively provide satisfied positioning solution should be considered because the extra cost must be affordable for mass market applications. This thesis proposes a Robust Cooperative Positioning (RCP) solution that tightly integrates DD code pseudo-range and UWB ranging observations supported by assumed V2X communication and can provide a decimetre level accuracy at an acceptable cost.

7.1 Conclusions

This research tackled one of the CAV challenges that vehicle positioning in GNSS hostile environment and developed a new RCP solution to improve positioning performance. To refer the objectives of the research, the outcomes and findings can be summarised as follows:

- The review of ITS-related literature clarified two emerging mainstream technologies, namely, Connected Vehicle (CV) and Autonomous Vehicle (AV), to support modern ITS road applications, i.e. the V2X applications. However, there are plenty of challenges to realise such applications. From the perspective of technical difficulty, the GNSS alone solution cannot always provide a reliable position solution due to

its inherent LOS requirement, particularly when the signal is obstructed in the environments such as an urban canyon. Regarding the non-technical aspect, the high cost of complementary sensors and the public acceptance of sharing their locations should be considered and balanced when talking about any V2X applications. Currently, the standardisation of required positioning performance does not follow the flourish and development of a variety of V2X applications. Although a premature standard or specification on required positioning performance for such V2X applications may limit the development of those technologies, few preliminary standards are believed to guide the maximisation of CAV technology benefit. So international and national societies or governments should take actions on standards formulation which academia has given some examples of required positioning performance classification. Regarding the positioning accuracy, the road level, lane level and where in the lane level accuracy have been proposed to categorise the V2X applications. On the other hand, the positioning-related communication performance requirement has also been considered.

- Positioning technology is one of the underlying technologies for the V2X applications, and multi-sensor integration is considered to improve positioning performance to support the V2X applications. In consideration of accuracy, cost-effectiveness, coverage, and many other factors, GNSS technology will still be the mainstream positioning technology applied in transportation applications because of its global coverage, 24/7 availability and free of charge. However, extra sensors are needed to compensate GNSS in the environments such as an urban canyon and a tunnel where GNSS signal is obstructed. The selection criteria of other positioning sensor include cost, coverage, accuracy, etc. The UWB positioning technique is selected to integrate with GPS in this thesis due to its independently positioning capability, fine positioning accuracy, sufficient effective range and resilience on multipath.
- The evaluation of UWB ranging observations demonstrated that the capability of UWB unit to offer good ranging performance. In

particular, the ranging accuracy and precision can achieve few centimetres in a perfect environment and static situation as shown in the indoor static test in Table 5.2. On the other hand, the accuracy and precision can still maintain 20 to 40 cm accuracy due to the influence of multipath and kinematic situation as discussed in the outdoor dynamic and locomotive tests in Table 5.4 and Table 5.6. The main reason caused UWB ranging outlier (even bigger than the magnitude of the actual measuring distance) has been proved to be the NLOS situation, although the penetration capability of UWB signal has been declared in many manufacture technical reports. Also, the correlation between ranging error and exact measuring distance has been analysed and modelled. The derived scale factor and bias should be handled carefully as they will show bigger difference under longer measuring distance in a real traffic situation. Moreover, the investigation of UWB positioning technology showed the viability of providing position solution on its own which means the possibility to take over or compensate GNSS when GNSS signal is obstructed. The primary performance metrics used to evaluate the proposed Robust Cooperative Positioning (RCP) method are the positioning accuracy and precision. The positioning result of UWB alone solution showed that the positioning accuracy mainly depended on ranging error rather than DOP, e.g., four UWB ranging observations with bigger error induced low positioning accuracy even there was a small DOP value. The static positioning accuracy and precision of UWB alone solution are better than 10 cm and 20 cm in 2D and 3D respectively in Table 5.9. The existence of NLOS situation deteriorates the kinematic positioning accuracy and precision to metre level. However, the accuracy and precision could achieve sub-metre level if the RKF method is adopted as demonstrated in the locomotive test as shown in Table 5.11.

- The RCP method is proposed in this thesis to integrate UWB ranging and DD code pseudo-range and control the influence of outlier observations by adopting the Robust Kalman Filter (RKF). The roof trial has been conducted to assess the proposed RCP method, and the results showed that additional UWB ranging observations enhanced the

observation geometry and further improved the 2D accuracy by 22% from 46 cm to 36 cm while 14 percentage improvement in 3D accuracy from 95 cm to 82 cm in the kinematic period within a pleasant GPS signal environment in Table 6.4. Although the plenty of outliers have been involved by adding UWB ranging observations, the positioning result has not been affected due to the use of RKF module in the proposed RCP method.

- The positioning result of the simulated UWB outlier dataset has demonstrated that the simulated outlier does not affect the positioning result because the proposed RCP method can effectively minimise the influence of the simulated outlier. In the simulative dataset of the urban canyon scenario, the RCP method could improve the 2D accuracy by 68.2% from 2.01 metres to 0.62 metres by adding two extra UWB ranging observations under the simulated GPS obstruction (only four visible GPS satellites) and more than 90% easting and northing errors maintain at sub-metre level ("where in the lane" requirement). Moreover, the 2D accuracy could improve to 31 cm and the overall 3D accuracy can achieve a sub-metre level as well if four additional UWB rangings are utilised. Furthermore, the simulative dataset of the approaching tunnel scenario tells that three integrated DD code pseudo-range observations can only contribute up to 22.5% and 33.3% in 2D accuracy and 3D accuracy respectively as the UWB alone positioning accuracy has already achieved to 0.40 metres and 1.47 metres. In another word, an additional UWB ranging observation can bring more improvement in accuracy than an additional GPS DD code pseudo-range observation because UWB can provide more accurate ranging observation than a GPS DD code pseudo-range observation. Finally, it is demonstrated in the Mobile Reference Station (MRS) scenario that the MRS could lead to the better positioning accuracy and precision, particularly in height direction, compared to the traditional static reference station DGPS solution. Specifically, the 2D and 3D MRS positioning accuracies are around 55 cm and 1 metre respectively based on three GPS DD code pseudo-range observations whereas the traditional static reference station solution provides 2.01 metres in 2D

accuracy and 4.90 metres in 3D accuracy based on the same number of GPS DD code pseudo-range observation.

7.2 Recommendations and Future Work

Based on the development of the proposed RCP solution and the analysis of practical and simulative experimental results, there are few limitations of this work and possibly future work listed below:

- Since Thales has abandoned its UWB research interest, an alternative UWB manufacture or other ranging sensors should be considered. The high sampling rate (10 Hz) is necessary for modern ITS road applications. However, the Thales UWB unit used in this research cannot provide data collection time in decimal level though it is capable to output 5 Hz ranging observations. Therefore, a ranging sensor that can provide precise decimal time tag will facilitate the multi-sensors synchronisation. What is more, the communication capability in this research is simulated by assumed DSRC device, so the communication latency was not considered. The communication latency will affect the positioning performance, and this factor must be evaluated when a real V2X communication device is employed.
- Although low susceptibility to multipath and the penetration capability of UWB signal has been declared in many manufacture technical reports, the evaluation of UWB ranging observations tells an opposite story. The UWB ranging accuracy still can be degraded by multipath and the NLOS induced outlier may bring lots of trouble for positioning, particularly when there are continuous outliers. Therefore, further investigation regarding the performance of UWB ranging in multipath and NLOS environment should be carefully carried out. In addition, Constant Velocity state model is currently chosen for the proposed RCP method, and it does lead to non-negligible errors. The integration of a low-cost Inertial Measurement Unit (IMU) is believed to deal with those problems.
- This research aims to cope with the positioning problem of traffic applications and the data mainly collected from a moving locomotive

whose speed was lower than 2 m/s. This may not completely reflect the real dynamic situation, so the data collected in real traffic environment is desired to assess whether the UWB ranging performance drops in high velocity.

- In this research, the position of MRS is provided by assumed RTK solution which is at centimetre level accuracy. In the future work, the MRS concept may extend to the real-time DGPS solution which is normal around few metres accuracy. Therefore, the degradation of final positioning performance will occur by using a relatively inaccurate MRS coordinate and the impact level of MRS position error should be evaluated.
- To avoid diversity of data sources, only GPS data and data inherent in the DSRC signal are incorporated into CP techniques. However, the trend of using GNSS for positioning and navigation is to consider multi-constellation GNSS for increasing the satellite availability and signal diversity in order to improve positioning performance. The assessment showed that the improvement of adding additional observations would be very limited when it already have enough number of quality input. Thus, it is worth noting that wisely selecting input, instead of, using all of the available data should be considered for computation efficiency.

References

5GPPP. 2015. 5G Automotive Vision. 5G Infrastructure Public Private Parternship. Available: https://5g-ppp.eu/wp-content/uploads/2014/02/5G-PPP-White-Paper-on-Automotive-Vertical-Sectors.pdf

AKOS, D., LUO, M., PULLEN, S. & ENGE, P. 2001. Ultra-wideband and GPS: can they co-exist? *GPS World.* 12 (9)**,** pp. 59.

ALAM, N. & DEMPSTER, A. G. 2013. Cooperative positioning for vehicular networks: facts and future. *IEEE Transactions on Intelligent Transportation Systems.* 14 (4)**,** pp. 1708-1717.

ALIEIEV, R., KWOCZEK, A. & HEHN, T. Automotive requirements for future mobile networks. 2015 IEEE MTT-S International Conference on Microwaves for Intelligent Mobility (ICMIM), 27-29 April 2015 Heidelberg, Germany. pp. 1-4.

AMIRLOO ABOLFATHI, E. 2015. *Integrating vision derived bearing measurements with differential GPS for Vehicle-to-Vehicle relative navigation.* University of Calgary.

ANDERSON, D. S., DROCELLA, E. F., JONES, S. K. & SETTLE, M. A. 2001. Assessment of compatibility between ultrawideband (UWB) systems and global positioning system (GPS) receivers. U.S. DEPARTMENT OF COMMERCE National Telecommunications and Information Administration Available: https://www.ntia.doc.gov/files/ntia/publications/ntia_special_publication_01_47_2.pdf

ANDERSON, J. M., NIDHI, K., STANLEY, K. D., SORENSEN, P., SAMARAS, C. & OLUWATOLA, O. A. 2014. *Autonomous vehicle technology: A guide for policymakers*, Rand Corporation.

ANDREWS, S. & COPS, M. 2009. Final report: Vehicle infrastructure integration proof of concept executive summary–Vehicle. Research and Innovative Technology Administration (RITA). Available: https://ntl.bts.gov/lib/31000/31000/31079/14443_files/14443.pdf

ANGRISANO, A. 2010. *GNSS/INS integration methods.* PhD thesis, University of Calgary, Canada.

AUDI. 2015. *Audi piloted driving* [Online]. Available: http://www.audi.com/content/com/brand/en/vorsprung_durch_technik/content/2014/10/piloted-driving.html [Accessed 15 Nov 2015].

BALLESTER-GURPIDE, I., HERRÁIZ-MONSECO, E., MIGUEL, A., ROMAY-MERINO, M. & BEECH, T. Future GNSS constellation performances inside urban environments. Proceedings of the 13th International Technical Meeting of the Satellite Division of The Institute of Navigation (ION GPS 2000), 19-22 September 2000 Salt Lake City, UT, USA. pp. 2436-2445.

BALLINGALL, S. 2013. Vehicle positioning for C-ITS in Australia (background document). Austroads Ltd. Available: https://www.onlinepublications.austroads.com.au/items/AP-R431-13

BAR-SHALOM, Y., LI, X. R. & KIRUBARAJAN, T. 2001. *Estimation with applications to tracking and navigation: theory algorithms and software*, John Wiley & Sons.

BARBARESSO, J., CORDAHI, G., GARCIA, D., HILL, C., JENDZEJEC, A. & WRIGHT, K. 2014. USDOT's Intelligent Transportation Systems (ITS) ITS strategic plan 2015-2019. Intelligent Transportation Systems Joint Program Office (ITS JPO). Available: http://www.its.dot.gov/strategicplan/

BARRETT, T. W. 2001. History of ultra wideband communications and radar, Partl UWB Communications. *Microwave Journal.* 44 (2)**,** pp. 20-43.

BARTH, M. & BORIBOONSOMSIN, K. 2009. Traffic congestion and greenhouse gases. *ACCESS Magazine.* 1 (35)**,** pp. 2-9.

BASNAYAKE, C. 2011. Road talk: interoperability considerations for V2X GNSS receivers. *GPS world.* 22 (3)**,** pp. 36-42.

BASNAYAKE, C., WILLIAMS, T., ALVES, P. & LACHAPELLE, G. R. 2010. Can GNSS drive V2X? *GPS World.* 21 (10)**,** pp. 35-43.

BELL, M. C. 2006. Environmental factors in intelligent transport systems. *IEE Proceedings - Intelligent Transport Systems.* 153 (2)**,** pp. 113-128.

BERTOZZI, M., BROGGI, A., COATI, A. & FEDRIGA, R. I. 2013. A 13,000 km intercontinental trip with driverless vehicles: the VIAC experiment. *IEEE Intelligent Transportation Systems Magazine.* 5 (1)**,** pp. 28-41.

BLOBEL, V. 2005. *Linear least squares* [Online]. University of Hamburg. Available: http://www.desy.de/~blobel/blobel_leastsq.pdf [Accessed 11 April 2016].

BMW. 2015a. *BMW ConnectedDrive connectivity technologies* [Online]. Available: http://www.bmw.com/com/en/insights/technology/connecteddrive/2013/connectivity_technologies/index.html [Accessed 30 Dec 2015].

BMW. 2015b. *Traffic jam assistant* [Online]. Available: http://www.bmw.com/com/en/newvehicles/x/x5/2013/showroom/driver_assistance/traffic_jam_assistant.html [Accessed 18 Nov 2015].

BOEING. 2016. *Boeing, U.S. Air Force complete GPS IIF constellation* [Online]. Available: http://boeing.mediaroom.com/2016-02-05-Boeing-U-S-Air-Force-Complete-GPS-IIF-Constellation [Accessed 27 Sept 2016].

BONNOR, N. 2012. A brief history of global navigation satellite systems. *Journal of Navigation.* 65 (01)**,** pp. 1-14.

BORRE, K. 2003. The GPS easy suite–Matlab code for the GPS newcomer. *GPS Solutions.* 7 (1)**,** pp. 47-51.

BROGGI, A., BUZZONI, M., DEBATTISTI, S., GRISLERI, P., LAGHI, M. C., MEDICI, P. & VERSARI, P. 2013. Extensive tests of autonomous driving technologies. *IEEE Transactions on Intelligent Transportation Systems.* 14 (3)**,** pp. 1403-1415.

BROWN, R. G. & HWANG, P. Y. 2012. *Introduction to random signals and applied Kalman filtering: with MATLAB exercises and solutions*, John Wiley & Sons.

BUNCH, J., SHAH, V., BURNIER, C., HICKS, D., HATCHER, G., GREER, L., BALL, W. & FENDER, K. 2012. Review of existing literature and deployment tracking surveys: decision factors influencing its adoption. Research and Innovative Technology Administration. Available: https://ntl.bts.gov/lib/45000/45600/45616/FHWA-JPO-12-043_v2_Final_508.pdf

CAMPBELL, M., EGERSTEDT, M., HOW, J. P. & MURRAY, R. M. 2010. Autonomous driving in urban environments: approaches, lessons and challenges. *Philosophical Transactions of the Royal Society of London A: Mathematical, Physical and Engineering Sciences.* 368 (1928)**,** pp. 4649-4672.

CEBR. 2014. The future economic and environmental costs of gridlock in 2030: An assessment of the direct and indirect economic and environmental costs of idling in road traffic congestion to households in the UK, France, Germany and the USA. Cebr. Available: http://ibtta.org/sites/default/files/documents/MAF/Costs-of-Congestion-INRIX-Cebr-Report%20(3).pdf

CHAPLAIN, C. T., BARKAKATI, N., GALLEGOS, A., LEE, J., RICHEY, K., TALLON, J., AHEARN, M. P., ANDERSON, P., BOOTH, B. & BOTHWELL, B. 2015. GPS: actions needed to address ground system development problems and user equipment production readiness. United States Government Accountability Office. Available: https://www.gao.gov/products/GAO-15-657

CHEN, K. & MILES, J. C. 2004. *ITS handbook 2004: recommendations from the world road association (PIARC)*, Artech House.

CHEON, S. 2003. An overview of automated highway systems (AHS) and the social and institutional challenges they face. University of California Transportation Center. Available: http://escholarship.org/uc/item/8j86h0cj

CHINA SATELLITE NAVIGATION OFFICE. 2015. *System introduction to BeiDou (in Chinese)* [Online]. Available: http://www.beidou.gov.cn/xtjs.html [Accessed 08 Oct 2015].

CHIU, D. S. & O'KEEFE, K. P. Seamless outdoor-to-indoor pedestrian navigation using GPS and UWB. Proceedings of the 21st International Technical Meeting of the Satellite Division of the Institute of Navigation (ION GNSS 2008), 16-19 September 2008 Savannah, GA, USA. Citeseer, pp. 322-333.

CHUI, C. K. & CHEN, G. 2008. *Kalman filtering: with real-time applications*, Springer Science & Business Media.

COAST GUARD NAVIGATION CENTER, U. S. 2016. *GPS constellation status for 09/27/2016* [Online]. Available: http://www.navcen.uscg.gov/?Do=constellationStatus [Accessed 27 Sept 2016].

CSNO. 2013. BeiDou navigation satellite system signal in space interface control document open service signal. China Satellite Navigation Office. Available: http://www.beidou.gov.cn/attach/2013/12/26/20131226b8a6182fa73a4ab3a5f107f762283712.pdf

DELPHI. 2015. *Delphi Drive* [Online]. Available: http://www.delphi.com/delphi-drive [Accessed 16 Nov 2015].

DRANE, C. R. & RIZOS, C. 1998. *Positioning systems in intelligent transportation systems*, Artech House, Inc.

EC. 1999. Communication from the Commission of 10 February 1999 - "Galileo - Involving Europe in a new generation of satellite navigation services" COM (1999) 54.

EC. 2009. setting emission performance standards for new passenger cars as part of the Community's integrated approach to reduce CO2 emissions from light-duty vehicles. No 443/2009.

EC. 2014. *Satellite applications for emergency handling, traffic alerts, road safety and incident prevention* [Online]. Available: https://ec.europa.eu/programmes/horizon2020/en/news/satellite-applications-emergency-handling-traffic-alerts-road-safety-and-incident-prevention [Accessed 19 Sept 2016].

EC. 2016. *Galileo satellite launches* [Online]. Available: http://ec.europa.eu/growth/sectors/space/galileo/launches/ [Accessed 27 Sept 2016].

EDDINGTON, R. 2006. *The Eddington Transport Study-The case for action-Sir Rod Eddington's advice to Government-December 2006*, the Controller of Her Majesty's Stationery Office

EEA. 2015. *New cars' CO2 emissions well below Europe's 2015 target* [Online]. European Environment Agency. Available: http://www.eea.europa.eu/highlights/new-cars2019-co2-emissions-well [Accessed 26 Oct 2015].

ESA. 2015a. 2015 GNSS market report. Available: http://www.gsa.europa.eu/2015-gnss-market-report

ESA. 2015b. *First result of Galileo* [Online]. Available: http://www.esa.int/Our_Activities/Navigation/The_future_-_Galileo/First_results [Accessed 07 Oct 2015].

ETSC 1999. *Intelligent transport systems and road safety,* Brussels, European Transport Safety Council.

ETSI. 2004. Electromagnetic compatibility and Radio spectrum Matters (ERM);Road Transport and Traffic Telematics (RTTT); Dedicated Short Range Communication (DSRC) transmission equipment (500 kbit/s / 250 kbit/s) operating in the 5,8 GHz Industrial, Scientific and Medical (ISM) band; Part 1: General characteristics and test methods for Road Side Units (RSU) and On-Board Units (OBU). ETSI EN 300 674-2-2 V1.2.1.

ETSI. 2008. Electromagnetic compatibility and Radio spectrum Matters (ERM); Short Range Devices (SRD) using Ultra WideBand (UWB) technology; Location Tracking equipment operating in the frequency range from 6 GHz to 8,5 GHz; Part 1: Technical characteristics and test methods. ETSI EN 302 500-1 V1.2.1.

ETSI 2014a. Intelligent Transport Systems (ITS); Vehicular communications; basic set of applications; part 2: specification of cooperative awareness basic service.

ETSI 2014b. Intelligent Transport Systems (ITS); Vehicular communications; basic set of applications; part 3: specifications of decentralized environmental notification basic service.

EU. 2010. Directive on the framework for the deployment of Intelligent Transport Systems in the field of road transport and for interfaces with other modes of transport. Directive 2010/40/EU.

EU 2012. *Towards low carbon transport in EU*, European Union.

EUROPEAN GNSS SERVICE CENTRE. 2017. *Constellation information of Galileo* [Online]. Available: https://www.gsc-europa.eu/system-status/Constellation-Information [Accessed 10 Jan 2017].

EZELL, S. 2010. Explaining international IT application leadership: intelligent transportation systems. The Information Technology and Innovation Foundation. Available: http://www.itif.org/files/2010-1-27-ITS_Leadership.pdf

FARAGHER, R. 2012. Understanding the basis of the Kalman filter via a simple and intuitive derivation. *IEEE Signal Processing Magazine.* 29 (5)**,** pp. 128-132.

FCC. 1999. Amendment of Parts 2 and 90 of the Commission's Rules to Allocate the 5.850-5.925 GHz Band to the Mobile Service for Dedicated Short Range Communications of Intelligent Transportation Services FCC-99-305.

FCC. 2002. Revision of Part 15 of the Commission's Rules Regarding Ultra-Wideband Transmission Systems. FCC-02-48.

FCC. 2004. Amendment of the Commission's Rules Regarding Dedicated Short-Range Communication Services in the 5.850-5.925 GHz Band (5.9 GHz Band), Amendment of Parts 2 and 90 of the Commission's Rules to Allocate the 5.850- 5.925 GHz Band to the Mobile Service for Dedicated Short Range Communications of Intelligent Transportation Services. FCC-03-324.

FCC. 2013. Revision of Part 15 of the Commission's Rules to Permit Unlicensed National Information Infrastructure (U-NII) Devices in the 5 GHz Band. FCC-13-22

FEDERAL SPACE AGENCY. 2016. *GLONASS constellation status, 27.09.2016* [Online]. Federal Space Agency Information-analytical centre. Available: https://www.glonass-iac.ru/en/GLONASS/ [Accessed 27 Sept 2016].

GAO, P., HENSLEY, R. & ZIELKE, A. 2014a. A road map to the future for the auto industry. *McKinsey Quarterly.* 2014 (4)**,** pp. 43-53.

GAO, Y., LIU, S., ATIA, M. & NOURELDIN, A. 2015. INS/GPS/LiDAR Integrated Navigation System for Urban and Indoor Environments Using Hybrid Scan Matching Algorithm. *Sensors.* 15 (9)**,** pp. 23286-23302.

GAO, Y., MENG, X., HANCOCK, C. M., STEPHENSON, S. & ZHANG, Q. UWB/GNSS-based Cooperative Positioning Method for V2X Applications. Proceedings of the 27th International Technical Meeting of The Satellite Division of the Institute of Navigation (ION GNSS+ 2014), 8-12 September 2014b Tampa, FL, USA. pp. 3212-3221.

GARELLO, R., LO PRESTI, L., CORAZZA, G. & SAMSON, J. 2012. Peer-to-peer cooperative positioning part I: GNSS aided acquisition. *InsideGNSS.* 7 (2)**,** pp. 55-63.

GASSER, T. M., ARZT, C., AYOUBI, M., BARTELS, A., BÜRKLE, L., EIER, J., FLEMISCH, F., HÄCKER, D., HESSE, T., HUBER, W., LOTZ, C., MAURER, M., RUTH-SCHUMACHER, S., SCHWARZ, J. & VOGT, W. 2013. Legal consequences of an increase in vehicle automation : Consolidated final report of the project group ; Part 1. BASt. Available: http://bast.opus.hbz-nrw.de/volltexte/2013/723/pdf/Legal_consequences_of_an_increase_in_vehicle_automation.pdf

GASSER, T. M. & WESTHOFF, D. 2012. *BASt-study: definitions of automation and legal issues in Germany* [Online]. Transportation Research Board. Available: http://onlinepubs.trb.org/onlinepubs/conferences/2012/Automation/presentations/Gasser.pdf [Accessed 09 May 2017].

GHAVAMI, M., MICHAEL, L. & KOHNO, R. 2004. *Ultra wideband signals and systems in communication engineering*, John Wiley & Sons.

GHILANI, C. D. & WOLF, P. R. 2010. *Adjustment computations: spatial data analysis*, John Wiley & Sons.

GIBBONS, G. 2012. *Munich summit charts progress of GPS, GLONASS, Galileo, Beidou GNSSes - Speakers describe budgets, launches, and modernization* [Online]. Available: http://www.insidegnss.com/node/2981 [Accessed 27 Sept 2016].

GIGL, T., JANSSEN, G. J. M., DIZDAREVIC, V., WITRISAL, K. & IRAHHAUTEN, Z. Analysis of a UWB Indoor Positioning System Based on Received Signal Strength. 2007 4th Workshop on Positioning, Navigation and Communication, 22 March 2007 Hannover, Germany. pp. 97-101.

GM. 2015a. *Emerging technology: driving safety, efficiency and independence* [Online]. Available: http://www.gm.com/vision/design_technology/emerging_technology.html [Accessed 18 Nov 2015].

GM. 2015b. *GM vehicles & onstar: connecting you to what matters* [Online]. Available: http://www.gm.com/vision/design_technology/onstar_safe_connected.html [Accessed 30 Dec 2015].

GONZALEZ, J., BLANCO, J. L., GALINDO, C., ORTIZ-DE-GALISTEO, A., FERNANDEZ-MADRIGAL, J. A., MORENO, F. A. & MARTINEZ, J. L. Combination of UWB and GPS for indoor-outdoor vehicle localization. 2007 IEEE International Symposium on Intelligent Signal Processing, 3-5 October 2007 Alcala de Henares, Spain. pp. 1-6.

GOODWIN, P. 2004. The economic costs of road traffic congestion. ESRC Transport Studies Unit, University College London. Available: http://discovery.ucl.ac.uk/1259/1/2004_25.pdf

GOOGLE. 2015. Google self-driving car project monthly report October 2015. Available: https://static.googleusercontent.com/media/www.google.com/en//selfdrivingcar/files/reports/report-1015.pdf

GREJNER-BRZEZINSKA, D. A., TOTH, C. K., MOORE, T., RAQUET, J. F., MILLER, M. M. & KEALY, A. 2016. Multisensor navigation systems: a remedy for GNSS vulnerabilities? *Proceedings of the IEEE.* 104 (6)**,** pp. 1339-1353.

GROVES, P. D. 2011. Shadow matching: a new GNSS positioning technique for urban canyons. *Journal of Navigation.* 64 (03)**,** pp. 417-430.

GROVES, P. D. 2013. *Principles of GNSS, inertial, and multisensor integrated navigation systems*, Artech house.

GSA. 2016. European GNSS (Galileo) open service signal-in-space interface control document. European GNSS Agency. Available: https://www.gsc-europa.eu/system/files/galileo_documents/Galileo-OS-SIS-ICD.pdf

GSMA. 2012. 2025 every car connected: forecasting the growth and opportunity. GSMA. Available: http://www.gsma.com/iot/wp-content/uploads/2012/03/gsma2025everycarconnected.pdf

GSMA. 2013. Connected car forecast: global connected car market to grow threefold within five years. GSMA. Available: http://www.gsma.com/iot/wp-content/uploads/2013/06/cl_ma_forecast_06_13.pdf

GSMA. 2015a. The mobile economy 2015. Available: http://www.gsmamobileeconomy.com/GSMA_Global_Mobile_Economy_Report_2015.pdf

GSMA. 2015b. Mobilizing Intelligent Transportation Systems (ITS). GSMA. Available: http://www.gsma.com/connectedliving/wp-content/uploads/2015/09/ITS-report-new.pdf

GUTIERREZ, P. 2012. Brussels view: remembrance of things past. can China and Europe get over a failed GNSS partnership? *InsideGNSS.* 7 (4)**,** pp. 24-26.

HÄMÄLÄINEN, M., HOVINEN, V., TESI, R., IINATTI, J. H. & LATVA-AHO, M. 2002. On the UWB system coexistence with GSM900, UMTS/WCDMA, and GPS. *IEEE Journal on Selected Areas in Communications.* 20 (9)**,** pp. 1712-1721.

HAMALAINEN, M., IINATTI, J., HOVINEN, V. & LATVA-AHO, M. In-band interference of three kinds of UWB signals in GPS L1 band and GSM900 uplink band. 12th IEEE International Symposium on Personal, Indoor and Mobile Radio Communications. PIMRC 2001. Proceedings (Cat. No.01TH8598), 30 September-3 October 2001 San Diego, CA, USA. pp. 76-80.

HARTMAN, K. & STRASSER, J. 2005. Saving lives through advanced vehicle safety technology: Intelligent vehicle initiative final report. Federal Highway Administration. Available: https://ntl.bts.gov/lib/jpodocs/repts_pr/14153_files/ivi.pdf

HENDRICKS, D., FELL, J. & FREEDMAN, M. 2001. *The relative frequency of unsafe driving acts in serious traffic crashes*, National Highway Traffic Safety Administration Washington, DC.

HIRAMATSU, K., SATOH, K. & MATSUKAWA, F. Estimation of the number of fatal accidents reduced by Advanced Safety Vehicle (ASV) Technologies. MOBILITY FOR EVERYONE. 4TH WORLD CONGRESS ON INTELLIGENT TRANSPORT SYSTEMS, 21-24 October 1997 BERLIN. pp. PAPER NO. 4026.

HIRT, W. The European UWB Radio Regulatory and Standards Framework: Overview and Implications. 2007 IEEE International Conference on Ultra-Wideband, 24-26 September 2007 Singapore. pp. 733-738.

HITCHCOCK, G., CONLAN, B., KAY, D., BRANNIGAN, C. & NEWMAN, D. 2014. Air quality and road transport: impacts and solutions. Available: http://www.racfoundation.org/assets/rac_foundation/content/downloadables/racf_ricardo_aea_air_quality_report_hitchcock_et_al_june_2014.pdf

HODGE, V. J. & AUSTIN, J. 2004. A survey of outlier detection methodologies. *Artificial Intelligence Review.* 22 (2)**,** pp. 85-126.

HOFMANN-WELLENHOF, B., LICHTENEGGER, H. & WASLE, E. 2007. *GNSS–global navigation satellite systems: GPS, GLONASS, Galileo, and more*, Springer Science & Business Media.

HUBER, P. J. 1964. Robust estimation of a location parameter. *The Annals of Mathematical Statistics.* 35 (1), pp. 73-101.

HUBER, P. J. 2011. *Robust statistics*, Springer.

ICAO. 1999. Manual on Required Navigation Performance (RNP). International Civil Aviation Organization. Available: http://www.wing.com.ua/images/stories/library/ovd/9613.pdf

IMECHE. 2012. Intelligent transport intelligent society. Institution of Mechanical Engineers. Available: http://www.imeche.org/docs/default-source/knowledge/IMechE_Intelligent_Transport_Intelligent_Society.pdf?sfvrsn=0

ISOLA, A., HÄMÄLÄINEN, M., IINATTI, J. & AIROS, E. UWB coexistence with GPS and aggregate UWB noise rise in the selected radio bands. Military Communications Conference, 2007. MILCOM 2007. IEEE, 29-31 October 2007 Orlando, FL, USA. IEEE, pp. 1-7.

ITS AMERICA. 2011. Sizing the U.S. and North American Intelligent Transportation Systems Market: Market Data Analysis of ITS Revenues and Employment. Intelligent Transportation Society of America. Available: http://www.itsa.org/images/MDA/itsa%20mda%20report%20final.pdf

ITS JPO. 2015. *DSRC: the future of safer driving* [Online]. Available: http://www.its.dot.gov/factsheets/dsrc_factsheet.htm [Accessed 26 Dec 2015].

JEAN-CHARLES, P. & ANDREW, W. 2015. Study of Intelligent Transport Systems for reducing CO2 emissions for passenger cars. ERTICO-ITS Europe. Available: http://erticonetwork.com/wp-content/uploads/2015/09/ITS4rCO2-Report-Final-2015-09-10-submitted.pdf

JI, S., CHEN, W., DING, X., CHEN, Y., ZHAO, C. & HU, C. 2010. Potential benefits of GPS/GLONASS/GALILEO integration in an urban canyon–Hong Kong. *Journal of Navigation.* 63 (04), pp. 681-693.

JIANG, T., PETROVIC, S., AYYER, U., TOLANI, A. & HUSAIN, S. 2015. Self-driving cars: disruptive or incremental? *Applied Innovation Review.* (1), pp. 3-22.

JIANG, Y., PETOVELLO, M., O'KEEFE, K. & BASNAYAKE, C. Augmentation of carrier-phase DGPS with UWB ranges for relative vehicle positioning. Proceedings of the 25th International Technical Meeting of The Satellite Division of the Institute of Navigation (ION GNSS 2012), 17-21 September 2012 Nashville, TN, USA. pp. 1568-1579.

JOHNSON, J. & DEWBERRY, B. Ultra-wideband aiding of GPS for quick deployment of anchors in a GPS-denied ad-hoc sensor tracking and communications system. Proceedings of the 24th International Technical Meeting of The Satellite Division of the Institute of Navigation (ION GNSS 2011), 20-23 September 2011 Portland, OR, USA. pp. 3959 - 3966.

KALMAN, R. E. 1960. A new approach to linear filtering and prediction problems. *Journal of Basic Engineering.* 82 (1), pp. 35-45.

KAPLAN, E. & HEGARTY, C. 2005. *Understanding GPS: principles and applications*, Artech house.

KARAGIANNIS, G., ALTINTAS, O., EKICI, E., HEIJENK, G., JARUPAN, B., LIN, K. & WEIL, T. 2011. Vehicular networking: a survey and tutorial on requirements, architectures, challenges, standards and solutions. *IEEE Communications Surveys & Tutorials.* 13 (4), pp. 584-616.

KIM, A., KNISS, V., RITTER, G. & SLOAN, S. M. 2011. An approach to communications security for a communications data delivery system for V2V/V2I safety: technical description and identification of policy and institutional issues. Intelligent Transportation Systems Joint Program Office (ITS JPO). Available:

http://ntl.bts.gov/lib/43000/43500/43513/FHWA-JPO-11-130_FINAL_Comm_Security_Approach_11_07_11.pdf

KIM, P. & HUH, L. 2011. *Kalman filter for beginners: with MATLAB examples*, CreateSpace.

KLJAI, Z., P, KORPUT & AMIN, N. The challenge of cellular cooperative ITS services based on 5G communications technology. 2016 39th International Convention on Information and Communication Technology, Electronics and Microelectronics (MIPRO), 30 May-3 June 2016 Opatija, Croatia. pp. 587-594.

KOCH, K. & YANG, Y. 1998. Robust Kalman filter for rank deficient observation models. *Journal of Geodesy.* 72 (7-8)**,** pp. 436-441.

KPMG. 2013. Self-driving cars: are we ready? KPMG. Available: https://www.kpmg.com/US/en/IssuesAndInsights/ArticlesPublications/Documents/self-driving-cars-are-we-ready.pdf

KPMG. 2014. Infrastructure 100: world markets report. KPMG. Available: http://www.kpmg.com/Global/en/IssuesAndInsights/ArticlesPublications/infra100-world-markets/Documents/infrastructure-100-world-markets-report-v3.pdf

KPMG. 2015. Connected and autonomous vehicles: the UK economic opportunity. KPMG. Available: https://www.kpmg.com/BR/en/Estudos_Analises/artigosepublicacoes/Documents/Industrias/Connected-Autonomous-Vehicles-Study.pdf

KÜNZLI, N., KAISER, R., MEDINA, S., STUDNICKA, M., CHANEL, O., FILLIGER, P., HERRY, M., HORAK JR, F., PUYBONNIEUX-TEXIER, V., QUÉNEL, P., SCHNEIDER, J., SEETHALER, R., VERGNAUD, J. C. & SOMMER, H. 2000. Public-health impact of outdoor and traffic-related air pollution: a European assessment. *The Lancet.* 356 (9232)**,** pp. 795-801.

LACHAPELLE, G., RYAN, S., PETOVELLO, M. & STEPHEN, J. Augmentation of GPS/GLONASS for vehicular navigation under signal masking. Proceedings of the 10th International Technical Meeting of the Satellite Division of The Institute of Navigation (ION GPS 1997), 16-19 September 1997 Kansas City, MO, USA. pp. 1511-1519.

LANGLEY, R. B. 1999. Dilution of precision. *GPS world.* 10 (5)**,** pp. 52-59.

LE MARCHAND, O., BONNIFAIT, P., IBAÑEZ-GUZMÁN, J., BETAILLE, D. & PEYRET, F. 2009. Characterization of GPS multipath for passenger vehicles across urban environments. *ATTI dell'Istituto Italiano di Navigazione.* 2009**,** pp. 77-88.

LEICA. 2016a. *Leica TS30 robotic total station technical datasheet* [Online]. Available: http://hds.leica-geosystems.com/downloads123/zz/tps/TS30/brochures-datasheet/TS30_Technical_Data_en.pdf [Accessed 06 Jul 2016].

LEICA. 2016b. *Leica Viva GNSS GS10 Receiver Data Sheet* [Online]. Available: http://www.leica-geosystems.co.uk/downloads123/zz/gpsgis/Viva%20GNSS/brochures-datasheet/Leica_Viva_GNSS_GS10_receiver_DS_en.pdf [Accessed 01 Aug 2016].

LI, C., CHEN, J. & CHU, H. A double difference measuring method of pseudo-range precision using to the real environment. China Satellite Navigation Conference (CSNC) 2012 Proceedings, 15-19 May 2012 Guangzhou, China. Springer, pp. 607-615.

LI, X. R. & JILKOV, V. P. 2003. Survey of maneuvering target tracking. Part I. Dynamic models. *IEEE Transactions on Aerospace and Electronic Systems.* 39 (4)**,** pp. 1333-1364.

LIU, K. & LIM, H. B. Positioning accuracy improvement via distributed location estimate in cooperative vehicular networks. 2012 15th International IEEE

Conference on Intelligent Transportation Systems, 16-19 September 2012 Anchorage, AK, USA. IEEE, pp. 1549-1554.

LIU, Y., DION, F. & BISWAS, S. 2005. Dedicated short-range wireless communications for intelligent transportation system applications: State of the art. *Transportation Research Record: Journal of the Transportation Research Board.* 1910**,** pp. 29-37.

LOCKHEED MARTIN. 2015. *GPS III* [Online]. Available: http://www.lockheedmartin.com/us/products/gps.html [Accessed 03 Oct 2015].

LOS ANGELES AIR FORCE BASE, L. A. 2015. *Global Positioning System (GPS) IIR/IIR-M satellite* [Online]. Available: http://www.losangeles.af.mil/library/factsheets/factsheet.asp?id=18671 [Accessed 03 Oct 2015].

LOVAS, T., WIECZYNSKI, A., BACZYNSKA, M., PERSKI, A., KERTESZ, I., BERENYI, A., BARSI, A. & BEEHAREE, A. Positioning for next generation intelligent transport systems services in SafeTRIP. Proceedings of ASPRS 2011 Annual Conference, 1-5 May 2011 Milwaukee, WI, USA. pp.

LU, N., CHENG, N., ZHANG, N., SHEN, X. & MARK, J. W. 2014. Connected vehicles: Solutions and challenges. *IEEE Internet of Things Journal.* 1 (4)**,** pp. 289-299.

LUTIN, J. M., KORNHAUSER, A. L. & LERNER-LAM, E. 2013. The revolutionary development of self-driving vehicles and implications for the transportation engineering profession. *ITE Journal.* 83 (7)**,** pp. 28-32.

LYNNE, G. & MARCUS, M. 2014. Future of highways. Arup. Available: http://www.arup.com/Future_of_Highways.aspx

LYSKOV, D. 2013. *Directions 2014: new horizons of GLONASS* [Online]. GPS World. Available: http://gpsworld.com/directions-2014-new-horizons-of-glonass/ [Accessed 30 Apr 2017].

MACGOUGAN, G., O'KEEFE, K. & KLUKAS, R. 2009. Ultra-wideband ranging precision and accuracy. *Measurement Science and Technology.* 20 (9)**,** pp. 95-105.

MACGOUGAN, G., O'KEEFE, K. & KLUKAS, R. 2010. Tightly-coupled GPS/UWB integration. *Journal of Navigation.* 63 (01)**,** pp. 1-22.

MACGOUGAN, G., O'KEEFE, K. & CHIU, D. Multiple UWB range assisted GPS RTK in hostile environments. Proceedings of the 21st International Technical Meeting of the Satellite Division of The Institute of Navigation (ION GNSS 2008), 16-19 September 2008 Savannah, GA, USA. pp. 3020-3035.

MACGOUGAN, G. D. & KLUKAS, R. Method and apparatus for high precision GNSS/UWB surveying. Proceedings of the 22nd International Technical Meeting of The Satellite Division of the Institute of Navigation (ION GNSS 2009), 22-25 September 2009 Savannah, GA, USA. pp. 853-863.

MALYS, S. & SLATER, J. Maintenance and enhancement of the World Geodetic System 1984. Proceedings of the 7th International Technical Meeting of the Satellite Division of The Institute of Navigation (ION GPS 1994), 20-23 September 1994 Salt Lake City, UT, USA. pp. 17-24.

MENG, X. 2016. *£1.7m project will pave the way for smarter cities and driverless cars* [Online]. The University of Nottingham. Available: https://www.nottingham.ac.uk/news/pressreleases/2016/january/1.7m-project-will-pave-the-way-for-smarter-cities-and-driverless-cars.aspx [Accessed 28 Sept 2016].

MENG, X., GAO, Y., ZHAO, H. & RYDING, J. Comprehensive assessment of UWB for indoor positioning and navigation. European Navigation Conference 2012, 25-27 April 2012 Gdańsk, Poland. pp.

MERCEDES-BENZ. 2015. *DISTRONIC PLUS with steering assist* [Online]. Available: http://techcenter.mercedes-benz.com/en/distronic_plus_steering_assist/detail.html?#detail-section [Accessed 18 Nov 2015].

MISRA, P. & ENGE, P. 2006. *Global positioning system: signals, measurements and performance*, Lincoln, MA: Ganga-Jamuna Press.

MOORE, D. S. 2007. *The basic practice of statistics*, WH Freeman New York.

MULLER, M. 2009. WLAN 802.11 p measurements for Vehicle to Vehicle (V2V) DSRC. *Application note Rohde & Schwarz.* 1**,** pp. 1-25.

MURFIN, T. 2015. The almanac - orbit data and resources on active GNSS satellites. *GPS World.* 25 (8)**,** pp. 46-49.

NADIAH, N., RAHIM, A., KAMAL, S. & ETENG, A. Band-reject ultra-wideband antenna for WLAN and DSRC environments. 2014 International Symposium on Technology Management and Emerging Technologies (ISTMET), 27-29 May 2014 Bandung, Indonesia. IEEE, pp. 78-81.

NATIONAL COORDINATION OFFICE. 2015a. *GPS Applicaitons on Roads & Highways* [Online]. National Coordination Office for Space-Based Positioning, Navigation, and Timing. Available: http://www.gps.gov/applications/roads/ [Accessed 11 Oct 2015].

NATIONAL COORDINATION OFFICE. 2015b. *New Civil Signals* [Online]. National Coordination Office for Space-Based Positioning, Navigation, and Timing. Available: http://www.gps.gov/systems/gps/modernization/civilsignals/ [Accessed 11 Oct 2015].

NATIONAL COORDINATION OFFICE. 2016. *GPS Current and Future Satellite Generations* [Online]. National Coordination Office for Space-Based Positioning, Navigation, and Timing. Available: http://www.gps.gov/systems/gps/space/ [Accessed 27 Spet 2016].

NCC. 2016. *Electronic Displays and Real Time Info* [Online]. Nottingham City Council. Available: http://www.nottinghamcity.gov.uk/transport-parking-and-streets/public-transport/electronic-displays-and-real-time-info/ [Accessed 19 Sept 2016].

NHTSA. 2008. National motor vehicle crash causation survey report to congress. National Highway Traffic Safety Administration (NHTSA). Available: http://www-nrd.nhtsa.dot.gov/Pubs/811059.PDF

NHTSA. 2013. *Provides guidance to states permitting testing of emerging vehicle technology* [Online]. Available: http://www.nhtsa.gov/About+NHTSA/Press+Releases/U.S.+Department+of+Transportation+Releases+Policy+on+Automated+Vehicle+Development [Accessed 08 Nov 2015].

NHTSA. 2016. 2015 motor vehicle crashes: overview. National Highway Traffic Safety Administration (NHTSA). Available: https://crashstats.nhtsa.dot.gov/Api/Public/ViewPublication/812318

NIKIFOROS, Z., UWE, T. & PETER, M. 2015. CO2 emissions from new passenger cars in the EU: Car manufacturers' performance in 2014. The International Council on Clean Transporation.

NIKOOKAR, H. & PRASAD, R. 2009. *Introduction to ultra wideband for wireless communications*, Springer Science & Business Media.

NURMI, J., LOHAN, E. S., SAND, S. & HURSKAINEN, H. 2015. *GALILEO positioning technology*, Springer.

OCHIENG, W. Y., SAUER, K., WALSH, D., BRODIN, G., GRIFFIN, S. & DENNEY, M. 2003. GPS integrity and potential impact on aviation safety. *Journal of Navigation.* 56 (01)**,** pp. 51-65.

OECD. 2014. The cost of air pollution: health impacts of road transport. Organisation for Economic Co-operation and Development (OECD). Available: http://dx.doi.org/10.1787/9789264210448-en

OECD/ITF. 2016. Road safety annual report 2016. Organisation for Economic Co-operation and Development (OECD). Available: http://www.oecd-ilibrary.org/docserver/download/7516011e.pdf?expires=1474923256&id=id&accname=guest&checksum=CBD9DD19C30D906BCDA28E014B07DF15

OFFICE, C. 2017a. *Satellite positioning services to complement GPS* [Online]. Government of Japan. Available: http://qzss.go.jp/en/overview/services/sv04_pnt.html [Accessed 09 Apr 2017].

OFFICE, C. 2017b. *What is the Quasi-Zenith Satellite System (QZSS)?* [Online]. Government of Japan. Available: http://qzss.go.jp/en/overview/services/sv02_why.html [Accessed 07 Apr 2017].

OPPERMANN, I., HÄMÄLÄINEN, M. & IINATTI, J. 2004. *UWB: theory and applications*, John Wiley & Sons.

OZGUNER, U., ACARMAN, T. & REDMILL, K. A. 2011. *Autonomous ground vehicles*, Artech House.

PACE, S., FROST, G., LACHOW, I., FRELINGER, D. & FOSSUM, D. 1995. The global positioning system: assessing national policies. RAND Corporation. Available: https://www.rand.org/pubs/monograph_reports/MR614.html

PAPADIMITRATOS, P., DE LA FORTELLE, A., EVENSSEN, K., BRIGNOLO, R. & COSENZA, S. 2009. Vehicular communication systems: Enabling technologies, applications, and future outlook on intelligent transportation. *IEEE Communications Magazine.* 47 (11)**,** pp. 84-95.

PARK, C. & RAPPAPORT, T. S. 2007. Short-range wireless communications for next-generation networks: UWB, 60 GHz millimeter-wave WPAN, and ZigBee. *IEEE Wireless Communications.* 14 (4)**,** pp. 70-78.

PARLIAMENTARY OFFICE OF SCIENCE AND TECHNOLOGY. 2009. Intelligent transport systems. United Kingdom Parliamentary Office of Science and Technology. Available: file:///C:/Users/isxyg1/Downloads/POST-PN-322.pdf

PATRICK, O. 2015. Let's drive smartly! An introduction to intelligent transport systems. Michelin Challenge Bibendum. Available: https://community.michelinchallengebibendum.com/docs/DOC-4054

PAUL, G. 2013. How does non-line-of-sight reception differ from multipath interference. *InsideGNSS.* 8 (6)**,** pp. 40-44.

PERRETT, K. 1996. Review of the potential benefits of Road Transport Telematics. *TRL report; 220.* pp.

PETOVELLO, M. 2008. Quantifying the performance of navigation systems and standards for assisted-GNSS. *InsideGNSS.* 3 (6)**,** pp. 20-24.

PETOVELLO, M. 2013. What are the differences between least-squares and Kalman filtering - the cornerstones of any GNSS or integrated system? *InsideGNSS.* 8 (2)**,** pp. 32-37.

PETOVELLO, M. G. 2003. *Real-time integration of a tactical-grade IMU and GPS for high-accuracy positioning and navigation.* Ph.D, University of Calgary.

PETOVELLO, M. G., O'KEEFE, K., CHAN, B., SPILLER, S., PEDROSA, C., XIE, P. & BASNAYAKE, C. 2012. Demonstration of inter-vehicle UWB ranging to augment DGPS for improved relative positioning. *Journal of Global Positioning Systems.* 11 (1)**,** pp. 11-21.

PINA, M., GRACE, N., OXLEY, C. L., SLOAN, S., TALLON, A. C., THORNTON, P., CENTER, V., BLACK, T., EASTON, A. V. & HAMILTON, B. A. 2012. Transforming

transportation through connectivity: ITS strategic research plan, 2010-2014 (progress update, 2012). Intelligent Transportation Systems Joing Program Office (ITS JPO). Available: http://www.its.dot.gov/strategicplan/pdf/ITS%20Strategic%20Plan%20Update%202012.pdf

RICHTER, E., OBST, M., SCHUBERT, R. & WANIELIK, G. Cooperative relative localization using vehicle-to-vehicle communications. 12th International Conference on Information Fusion, 2009. FUSION'09. , 6-9 July 2009 Seattle, WA, USA. IEEE, pp. 126-131.

RISDE. 2008. GLONASS interface control document. Russian Institute of Space Device Engineering. Available: http://russianspacesystems.ru/wp-content/uploads/2016/08/ICD_GLONASS_eng_v5.1.pdf

RITA. 2009. ITS strategic research plan, 2010-2014 executive summary Research & Innovative Technologies Administration (RITA). Available: http://www.its.dot.gov/strategic_plan2010_2014/index.htm#top

SABEY, B. & TAYLOR, H. 1980. The known risks we run: the highway. *In:* SCHWING, R. & ALBERS, W., JR. (eds.) *Societal Risk Assessment.* Springer US.

SAE 2014. Taxonomy and definitions for terms related to on-road motor vehicle automated driving systems.

SAE 2016. Dedicated Short Range Communications (DSRC) Message Set Dictionary.

SAFETRIP. 2013. *Context and Concept of SafeTRIP* [Online]. Available: http://www.safetrip.eu/ [Accessed 19 Spet 2016].

SAHINOGLU, Z., GEZICI, S. & GUVENC, I. 2008. *Ultra-wideband Positioning Systems - Theoretical Limits, Ranging Algorithms, and Protocols*.

SANTERRE, R., PAN, L., CAI, C. & ZHU, J. 2014. Single point positioning using GPS, GLONASS and BeiDou satellites. *Positioning.* 5 (4)**,** pp. 107-114.

SATO, Y., MIYA, M., SHIMA, Y., SSAITO, M., TAKIGUCHI, J. & YAMASHITA, J. 2011. Improvement of positioning performance in urban canyons utilizing QZSS. The 24th International Technical Meeting of The Satellite Division of the Institute of Navigation (ION GNSS 2011), 20-23 September 2011 Portland, OR, USA. pp. 1212-1218.

SCHOETTLE, B. & SIVAK, M. 2014a. Public opinion about self-driving vehicles in China, India, Japan, the US, the UK, and Australia. Transportation Research Institute (UMTRI). Available: https://deepblue.lib.umich.edu/bitstream/handle/2027.42/109433/103139.pdf?sequence=1&isAllowed=y

SCHOETTLE, B. & SIVAK, M. 2014b. A survey of public opinion about autonomous and self-driving vehicles in the US, the UK, and Australia. Transportation Research Institute (UMTRI). Available: https://deepblue.lib.umich.edu/bitstream/handle/2027.42/108384/103024.pdf?sequence=1&isAllowed=y

SDG. 2008. A report to the northern way: congestion management using intelligent transport systems. Steer Davies Gleave Consultancy. Available: http://www.northernwaytransportcompact.com/downloads/Delivery%20Gaps/Strategic%20Road%20Network/Congestion_Management_using_ITS.pdf

SE CONSULT. 2009. The potential of Intelligent Transport Systems for reducing road transport related greenhouse gas emissions. SE Consult. Available: http://ec.europa.eu/enterprise/archives/e-business-watch/studies/special_topics/2009/documents/SR02-2009_ITS.pdf

SHAHEEN, S. A. & LIPMAN, T. E. 2007. Reducing greenhouse emissions and fuel consumption: sustainable approaches for surface transportation. *IATSS Research.* 31 (1)**,** pp. 6-20.

SHELDRICK, M. 2014. *NHTSA calls for V2V technology in models built after 2020* [Online]. Available: http://automotivedigest.com/2014/08/nhtsa-eyes-half-million-crashes-prevented-v2v-technology/ [Accessed 26 Sept 2016].

SHLADOVER, S. E. & TAN, S.-K. 2006. Analysis of vehicle positioning accuracy requirements for communication-based cooperative collision warning. *Journal of Intelligent Transportation Systems.* 10 (3)**,** pp. 131-140.

SILBERG, G., WALLACE, R., MATUSZAK, G., PLESSERS, J., BROWER, C. & SUBRAMANIAN, D. 2012. Self-driving cars: the next revolution. KPMG LLP & Center of Automotive Research. Available: https://faculty.washington.edu/jbs/itrans/self_driving_cars[1].pdf

SILL, S., CHRISTIE, B., DIEPHAUS, A., GARRETSON, D., SULLIVAN, K. & SLOAN, S. 2011. Intelligent Transportation Systems (ITS) Standards Program Strategic Plan for 2011-2014. Intelligent Transportation Systems Joint Program Office Research (ITS JPO). Available: http://www.its.dot.gov/standards_strategic_plan/stds_strat_plan.pdf

SINGH, S. 2015. Critical reasons for crashes investigated in the national motor vehicle crash causation survey. National Highway Traffic Safety Administration (NHTSA). Available: http://www-nrd.nhtsa.dot.gov/pubs/812115.pdf

SIVAK, M. & SCHOETTLE, B. 2015. Road safety with self-driving vehicles: general limitations and road sharing with conventional vehicles. The University of Michigan Transportation Research Institute. Available: http://deepblue.lib.umich.edu/handle/2027.42/111735

SMITH, B. W. 2015. Automated and autonomous driving: regulation under uncertainty. OECD/ITF. Available: http://www.internationaltransportforum.org/pub/pdf/15CPB_AutonomousDriving.pdf

SMMT. 2015. 2015 automotive sustainability report. The Society of Motor Manufacturers and Traders. Available: http://www.smmt.co.uk/wp-content/uploads/sites/2/SMMT-16th-Sustainability-Report-final.pdf

SOMMER, H., KÜNZLI, N., SEETHALER, R., CHANEL, O., HERRY, M., MASSON, S., VERGNAUD, J., FILLIGER, P., HORAK JR, F. & KAISER, R. 2000. *Economic evaluation of health impacts due to road traffic-related air pollution: an impact assessment project of Austria, France and Switzerland*, OECD Publishing.

STEPHENSON, S., MENG, X., MOORE, T., BAXENDALE, A. & EDWARDS, T. A fairy tale approach to cooperative vehicle positioning. Proceedings of the 2014 International Technical Meeting of The Institute of Navigation, 27-29 January 2014 San Diego, CA, USA. pp. 431-440.

SWISSCOM. 2015. *Swisscom reveals the first driverless car on Swiss roads* [Online]. Available: https://www.swisscom.ch/en/about/medien/press-releases/2015/05/20150512-MM-selbstfahrendes-Auto.html [Accessed 29 Nov 2015].

TAKASU, T., EBINUMA, T. & YASUDA, A. Effect of quasi zenith satellite (QZS) on GPS positioning. Proceedings of 2009 International Symposium on GPS/GNSS, 4-6 November 2009 Jeju, Korea. pp.

TAN, Y. K., LI, B., SCOTT, C. & DEMPSTER, A. Positioning techniques for fewer than four GPS satellites. European Navigation Conference 2009, 3-6 May 2009 Naples, Italy. pp.

TANG, S., KUBO, N., KAWANISHI, N., FURUKAWA, R., HASEGAWA, A. & TAKEUCHI, Y. 2015. Cooperative relative positioning for intelligent transportation system. *International Journal of Intelligent Transportation Systems Research.* 13 (3)**,** pp. 131-142.

TANIGAWA, M., HOL, J. D., DIJKSTRA, F., LUINGE, H. & SLYCKE, P. Augmentation of low-cost GPS/MEMS INS with UWB positioning system for seamless outdoor/indoor positioning. Proceedings of the 21st International Technical Meeting of the Satellite Division of The Institute of Navigation (ION GNSS 2008), 16-19 September 2004 Savannah, GA, USA. pp. 1804-1811.

TEXAS A&M TRANSPORTATION INSTITUTE & INRIX. 2015. 2015 urban mobility scorecard. Texas A&M Transportation Institute. Available: http://mobility.tamu.edu/ums/report/

THALES. 2010. Lock-on model LD2 user manual. Thales Research & Technology (UK) Ltd.

THEWINDOWSCLUB. 2016. *Check the accuracy of your system clock* [Online]. Available: http://www.thewindowsclub.com/check-accuracy-system-clock [Accessed 29 Jun 2016].

THOMPSON, B. & BUEHRER, R. M. Characterizing and improving the collaborative position location problem. 2012 9th Workshop on Positioning Navigation and Communication (WPNC), 15-16 March 2012 Dresden, Germany. IEEE, pp. 42-46.

TIME.IS. 2016. *compare your system time with an atomic clock* [Online]. Available: http://time.is/ [Accessed 29 Jun 2016].

TREAT, J., TUMBAS, N., MCDONALD, S., SHINAR, D., HUME, R., MAYER, R., STANSIFER, R. & CASTELLAN, N. 1979. Tri-level study of the causes of traffic accidents: Executive summary. Transportation Research Institute (UMTRI) Available: http://deepblue.lib.umich.edu/handle/2027.42/64993

TRL. 2013. *Managed Motorways Calibration and Optimisation (MMCALO)* [Online]. Transport Research Laboratory. Available: http://www.trl.co.uk/case-studies/intelligent-transport-systems/ [Accessed 19 Sept 2016].

TSAI, M.-F., WANG, P.-C., SHIEH, C.-K., HWANG, W.-S., CHILAMKURTI, N., RHO, S. & LEE, Y. S. 2015. Improving positioning accuracy for VANET in real city environments. *The Journal of Supercomputing.* 71 (6), pp. 1975-1995.

TSAKIRI, M., STEWART, M., FORWARD, T., SANDISON, D. & WALKER, J. 1998. Urban fleet monitoring with GPS and GLONASS. *Journal of Navigation.* 51 (03), pp. 382-393.

U.K. DFT 2013. *Action for roads: a network for the 21st century*, Department for Transport U.K.

U.K. DFT 2015a. *The pathway to driverless cars: a detailed review of regulations for automated vehicle technologies*.

U.K. DFT. 2015b. *UK to lead the way in testing driverless cars* [Online]. Available: https://www.gov.uk/government/news/uk-to-lead-the-way-in-testing-driverless-cars [Accessed 20 Sept 2016].

U.K. DFT. 2016a. *Driverless cars technology receives £20 million boost* [Online]. Available: https://www.gov.uk/government/news/driverless-cars-technology-receives-20-million-boost [Accessed 20 Sept 2016].

U.K. DFT. 2016b. Reported road casualties in Great Britain: main results 2015. Available: https://www.gov.uk/government/uploads/system/uploads/attachment_data/file/533293/rrcgb-main-results-2015.pdf

U.K. DFT. 2016c. Road traffic estimates: Great Britain 2015. Available: https://www.gov.uk/government/uploads/system/uploads/attachment_data/file/524261/annual-road-traffic-estimates-2015.pdf

U.K. DFT. 2016d. Vehicle licensing statistics: quarter 4 (Oct - Dec) 2015. Available: https://www.gov.uk/government/uploads/system/uploads/attachment_data/file/516429/vehicle-licensing-statistics-2015.pdf

U.S. CONGRESS. 2012. Middle class tax relief and job creation act Of 2012. Public Law 112-96.

U.S. DOT. 2010. Achieving the vision: From VII to IntelliDrive. ITS JPO & RITA. Available: http://www.its.dot.gov/research_docs/pdf/2From%20VII%20to%20IntelliDrive.pdf

U.S. DOT. 2014a. *Estimated annual DSRC site operations, maintenance and replacement costs range from $1950 -$3050* [Online]. Available: http://www.itscosts.its.dot.gov/ITS/benecost.nsf/SummID/SC2014-00329?OpenDocument&Query=Home [Accessed 31 Dec 2015].

U.S. DOT. 2014b. *Researchers identify that DSRC field infrastructure deployment costs can range from $13,000 to $21,000 per site, with average cost estimated at $17,600* [Online]. Available: http://www.itscosts.its.dot.gov/ITS/benecost.nsf/SummID/SC2014-00325?OpenDocument&Query=Home [Accessed 31 Dec 2015].

U.S. GAO. 2012. Mobile device location data: additional federal actions could help protect consumer privacy. U.S. Government Accountability Office. Available: http://www.gao.gov/assets/650/648044.pdf

U.S. GAO. 2013. Intelligent transportation systems: vehicle-to-vehicle technologies expected to offer safety benefits, but a variety of deployment challenges exist. Available: http://www.gao.gov/assets/660/658709.pdf

U.S. GAO. 2015. Intelligent transportation systems: vehicle-to-infrastructure technologies expected to offer benefits, but deployment challenges exist. Available: http://www.gao.gov/assets/680/672548.pdf

UN. 2010. Improving global road safety. United Nations. Available: http://daccess-dds-ny.un.org/doc/UNDOC/GEN/N09/477/13/PDF/N0947713.pdf?OpenElement

UNECE 2012. *Intelligent Transport Systems (ITS) for sustainable mobility*, United Nations Economic Commission for Europe.

URMSON, C., ANHALT, J., BAGNELL, D., BAKER, C., BITTNER, R., CLARK, M. N., DOLAN, J., DUGGINS, D., GALATALI, T., GEYER, C., GITTLEMAN, M., HARBAUGH, S., HEBERT, M., HOWARD, T. M., KOLSKI, S., KELLY, A., LIKHACHEV, M., MCNAUGHTON, M., MILLER, N., PETERSON, K., PILNICK, B., RAJKUMAR, R., RYBSKI, P., SALESKY, B., SEO, Y.-W., SINGH, S., SNIDER, J., STENTZ, A., WHITTAKER, W. R., WOLKOWICKI, Z., ZIGLAR, J., BAE, H., BROWN, T., DEMITRISH, D., LITKOUHI, B., NICKOLAOU, J., SADEKAR, V., ZHANG, W., STRUBLE, J., TAYLOR, M., DARMS, M. & FERGUSON, D. 2008. Autonomous driving in urban environments: Boss and the Urban Challenge. *Journal of Field Robotics.* 25 (8)**,** pp. 425-466.

VAN SLYKE, T. H. 2009. *Technical considerations for co-locating UWB and GPS radios.* Kansas State University.

VANAJAKSHI, L., RAMADURAI, G. & ANAND, A. 2010. Intelligent Transportation Systems - Synthesis Report on ITS including issues and challenges in India. Centre of Excellence in Urban Transport, IIT Madras. Available: https://coeut.iitm.ac.in/ITS_synthesis.pdf

VIERECKL, R., AHLEMANN, D., KOSTER, A. & JURSCH, S. 2015. Connected car study 2015: racing ahead with autonomous cars and digital innovation. PwC. Available: http://www.strategyand.pwc.com/reports/connected-car-2015-study

VIERECKL, R., ASSMANN, J. & RADÜGE, C. 2014. In the fast lane: The bright future of connected cars. PwC. Available: http://www.strategyand.pwc.com/reports/in-the-fast-lane

VISLAB. 2014. *Presentation of DEEVA* [Online]. Available: http://vislab.it/events/presentation-of-new-vehicle/ [Accessed 16 Nov 2015].

VOLVO. 2015. *Volvo Cars responsible for the actions of its self-driving cars* [Online]. Volvo Car Group. Available: http://www.volvocars.com/intl/about/our-innovation-brands/intellisafe/intellisafe-autopilot/news/volvo-cars-responsible-for-the-actions-of-its-self-driving-cars [Accessed 15 Nov 2015].

WAADT, A., WANG, S., KOCKS, C., BURNIC, A., XU, D., BRUCK, G. H. & JUNG, P. Positioning in multiband OFDM UWB utilizing received signal strength. 2010 7th Workshop on Positioning Navigation and Communication (WPNC), 11-12 March 2010 Dresden, Germany. IEEE, pp. 308-312.

WANG, D. 2015. *Cooperative V2X relative navigation using tight-Integration of DGPS and V2X UWB range and simulated bearing.* PhD, University of Calgary.

WANG, D., O'KEEFE, K. & PETOVELLO, M. Decentralized cooperative positioning for Vehicle-to-Vehicle (V2V) application using GPS integrated with UWB range. Proceedings of the ION 2013 Pacific PNT Meeting, 23-25 April 2013 Honolulu, Hawaii, USA. pp. 793-803.

WANG, J., GAO, Y., LI, Z., MENG, X. & HANCOCK, C. 2016. A tightly-coupled GPS/INS/UWB cooperative positioning sensors system supported by V2I communication. *Sensors.* 16 (7)**,** pp. 944-959.

WEBB, M. 2008. Smart 2020: Enabling the low carbon economy in the information age. The Climate Group. Available: http://www.smart2020.org/_assets/files/02_smart2020Report.pdf

WEINER, G. & SMITH, B. W. 2015. *Automated Driving: Legislative and Regulatory Action* [Online]. Available: http://cyberlaw.stanford.edu/wiki/index.php/Automated_Driving:_Legislative_and_Regulatory_Action#Enacted [Accessed 29 Nov 2015].

WHITNEY, C. S. P. 2016. *Directions 2017: GPS navigates the future* [Online]. GPS World. Available: http://gpsworld.com/2016-in-review-gps-navigates-the-future/ [Accessed 17 Mar 2017].

WHO. 2009. *Global status report on road safety: time for action* [Online]. World Health Organization. Available: http://apps.who.int/iris/bitstream/10665/44122/1/9789241563840_eng.pdf [Accessed 18 Nov 2015].

WIESER, A., GEBRE-EGZIABHER, D., LACHAPELLE, G. & PETOVELLO, M. 2007. Weighting GNSS observations and variations of GNSS/INS integration. *InsideGNSS.* 2 (1)**,** pp. 26-33.

WOOLF, N. 2016. *Tesla fatal autopilot crash: family may have grounds to sue, legal experts say* [Online]. Available: https://www.theguardian.com/technology/2016/jul/06/tesla-autopilot-crash-joshua-brown-family-potential-lawsuit [Accessed 26 Sept 2016].

WU, F., KUBO, N. & YASUDA, A. 2004. Performance evaluation of GPS augmentation using quasi-zenith satellite system. *IEEE Transactions on Aerospace and Electronic Systems.* 40 (4)**,** pp. 1249-1260.

YANG, Y. 1991. Robust bayesian estimation. *Bulletin géodésique.* 65 (3)**,** pp. 145-150.

YANG, Y. 1994. Robust estimation for dependent observations. *Manuscripta geodaetica.* 19 (1)**,** pp. 10-17.

YANG, Y., GAO, W.-G. & ZHANG, X.-D. 2010. Robust Kalman filtering with constraints: a case study for integrated navigation. *Journal of Geodesy.* 84 (6)**,** pp. 373-381.

YANG, Y., HE, H. & XU, G. 2001. Adaptively robust filtering for kinematic geodetic positioning. *Journal of Geodesy.* 75 (2-3)**,** pp. 109-116.

YANG, Y., SONG, L. & XU, T. 2002. Robust estimator for correlated observations based on bifactor equivalent weights. *Journal of Geodesy.* 76 (6)**,** pp. 353-358.

YAO, J., BALAEI, A. T., ALAM, N., EFATMANESHNIK, M., DEMPSTER, A. G. & HASSAN, M. Characterizing cooperative positioning in VANET. 2011 IEEE Wireless Communications and Networking Conference (WCNC), 28-31 March 2011a Cancun, Mexico. pp.

YAO, J., BALAEI, A. T., HASSAN, M., ALAM, N. & DEMPSTER, A. G. 2011b. Improving cooperative positioning for vehicular networks. *IEEE Transactions on Vehicular Technology.* 60 (6)**,** pp. 2810-2823.

YOUNGS, J. 2014. *2014 U.S. Automotive Emerging Technologies Study Results* [Online]. J.d. Power and Associates. Available: http://www.jdpower.com/cars/articles/jd-power-studies/2014-us-automotive-emerging-technologies-study-results [Accessed 05 Dec 2015].

YUANXI, Y., JING, T. & CHUNHAO, H. 2012. *COMPASS/BeiDou Coordinate and Time Reference Systems*, National Academies Press.

ZHANG, C., KUHN, M. J., MERKL, B. C., FATHY, A. E. & MAHFOUZ, M. R. 2010. Real-time noncoherent UWB positioning radar with millimeter range accuracy: Theory and experiment. *IEEE Transactions on Microwave Theory and Techniques.* 58 (1)**,** pp. 9-20.

ZHANG, P., SUN, F., XU, Y., ZOU, J., DAI, W. & MENG, X. A centering correction method for GNSS antenna diversity theory and implementation using a software receiver. Proceedings of the 2014 International Technical Meeting of The Institute of Navigation, 27-29 January 2014 San Diego, CA, USA. pp. 904-908.

ZHU, J. 1996. Robustness and the robust estimate. *Journal of Geodesy.* 70 (9)**,** pp. 586-590.

ZSEDROVITS, T., BAUER, P., ZARANDY, A., VANEK, B., BOKOR, J. & ROSKA, T. Error analysis of algorithms for camera rotation calculation in GPS/IMU/camera fusion for UAV sense and avoid systems. 2014 International Conference on Unmanned Aircraft Systems (ICUAS), 27-30 May 2014 Orlando, FL, USA. pp. 864-875.